

LOUGHBOROUGH
UNIVERSITY OF TECHNOLOGY
LIBRARY

AUTHOR

DAVIES, R

COPY NO.

023335/01

VOL NO.

CLASS MARK

ARCHIVES
COPY

FOR REFERENCE ONLY

THE PHYSICAL SEPARATION OF PARTICULATES

by

R. DAVIES

Submitted for the Degree of Doctor of Philosophy

of

Loughborough University of Technology

External Supervisor:-

D. T. Wasan
Illinois Institute
of Technology.

Director of Research
and Supervisor:-

Professor D. C. Freshwater
Department of Chemical
Engineering.

July 1975

© R. Davies

Loughborough University of Technology Library	
Date	24 Jan 76
Class	
Acc. No.	23335/01

THE PHYSICAL SEPARATION OF PARTICULATES

Synopsis

Particulates are present in the atmosphere as a result of both natural and man-made processes. Typical particulates include windblown soil, sea salt, sulphur, nitrogen and hydrocarbon complexes, ammonium sulphate and nitrate, carbonaceous matter, biological debris, metal oxides, trace metals, and extraterrestrial magnetic and radioactive compounds. Natural processes such as cloud formation, rainfall, and sedimentation cleanse the atmosphere of these particulates and, in so doing, form particle groups or agglomerates which can contain many unit particles. For the purpose of atmospheric research and, in particular, the physical tracing of pollution sources, particulates are a useful emission indicator. Consequently, if one wishes to use them effectively, it is necessary to separate the agglomerate into its independent particle units prior to analysis and identification. This is no simple matter, as the particles are held together by strong physical forces.

The purpose of this thesis is to investigate a method of separating particulates for physical tracer studies, but the atmospheric aerosol was considered too complex a model for the initial studies. A metal foundry emission was employed as a useful substitute as it closely resembled the atmospheric aerosol in its water-insoluble particulate fraction, which was the prime fraction of importance in physical tracer studies.

It was indicated that the separation of this fraction, predominantly metal oxides, could be separated in aqueous tetrasodium pyrophosphate solutions under the action of ultrasonic energy at high pressures.

Actual atmospheric samples were then taken downwind of a metal foundry and tested on the device. Though successful in separating the particulates, the method introduced contamination as a result of erosion during cavitation. This was eliminated by the use of a fluorinated hydrocarbon liquid in which contamination-free separation was finally attained. Separation efficiencies of over 85% were obtained and the recollected particles were shown to be in a well separated state for chemical and physical analysis.

One further advantage of the technique was that fluorohydrocarbons were inert to water-soluble particles, and so the method had potential for separating the total particulate fraction from an atmospheric aerosol. Though not investigated, this was reported as worthy of future study.

TABLE OF CONTENTS

	<u>Page No.</u>
Synopsis	i
Table of Contents	iii
1. Introduction	1
2. Literature Survey	14
2.1 General Introduction	14
2.2 Basic Concepts of Interparticle Forces	14
2.2.1 Introduction	14
2.2.2 Discrete Particles and Particulate Systems	16
2.2.3 Influence of Particle Size and Particle Size Distribution	18
2.2.4 Influence of Particle Shape	19
2.2.5 Influence of Surface Area and Surface Structure	21
2.2.6 Influence of Surface Energy and the Adsorption of Films	24
2.2.7 Influence of Multilayer Adsorption and Effect of Free Liquid	26
2.2.8 Plastic Deformation, Melting, and Sintering	29
2.2.9 Nature and Magnitude of Interparticle Forces	31
2.2.9.1 Physical Forces	32
2.2.9.2 Chemical Forces	33
2.2.9.3 Interaction of These Forces	34
2.2.10 Summary of Interparticle Force Concepts	40

2.3	Aerosols in the Atmosphere	41
2.3.1	Introduction	41
2.3.2	Sources of Particles in the Atmosphere	45
2.3.2.1	Soil Derived Particles	48
2.3.2.2	Sulphur Derived Aerosols	49
2.3.2.3	Nitrogen Derived Particles	52
2.3.2.4	Organic Matter and Hydrocarbons	54
2.3.2.5	Combustion Sources	56
2.3.2.6	Trace Metals and Other Inorganic Materials	58
2.3.2.7	Marine Aerosols	60
2.3.2.8	Other Sources	61
2.3.2.9	Summary	61
2.3.3	The Nature and Composition of Foundry Effluents	62
2.3.3.1	Introduction	62
2.3.3.2	Foundry Processes	63
2.3.3.3	Emission Rates from Foundries	69
2.3.3.4	Characteristics of Effluents from Foundries	69
2.3.3.5	Control of Foundry Emissions	71
2.3.3.6	Summary	75
2.3.4	Mechanisms of Removal of Particles from the Atmosphere	76
2.3.5	Summary of the Atmospheric Aerosol Literature and the Philosophy of the Separation Study	79
2.4	Methods of Conditioning and Separating Particles from Surfaces and from Agglomerates	84
2.4.1	Methods of Conditioning Particles and Surfaces	84

2.4.1.1	Introduction	84
2.4.1.2	Methods of Conditioning Metal Oxides in Liquid Media	84
2.4.1.3	Summary	94
2.4.2	Methods of Measuring the Force of Adhesion in Liquids by Separating Particles from Plane Surfaces	96
2.4.2.1	Introduction	96
2.4.2.2	Experimental Methods Used to Measure the Force of Adhesion	97
2.4.2.3	Summary	105
2.4.3	Methods of Separating Particles from Agglomerates	107
2.4.3.1	Introduction	107
2.4.3.2	Methods of Separating Agglomerates	107
2.4.3.3	Summary	114
2.5	Methods to Indicate the Degree of Separation Attained	115
2.5.1	Introduction	115
2.5.2	Suspension Turbidity and Mean Particle Size	116
2.5.3	Sedimentation Volume	116
2.5.4	Change in Mean Size and Size Distribu- tion	117
2.5.5	Zeta Potential	119
2.5.6	pH and Electrical Conductivity	120
2.5.7	Surface Active Agent Nature, Purity, and Critical Concentration	120
2.5.8	Particulate Samples	121
2.5.9	Summary	121
2.6	Conclusions and Scope of the Experimental Studies	122
2.6.1	Conclusions	122
2.6.2	Scope of Experimental Work	126

3. Experimental Results	129
3.1 Preliminary Experiments	129
3.1.1 Selection of Metal Oxide Powders	129
3.1.2 Preliminary Screening of Surface Conditioning Agents	131
3.1.3 The Measurement of the Force of Adhesion Between Metal Oxides and Surfaces	161
3.1.3.1 Introduction	161
3.1.3.2 Method of Approach	162
3.1.3.3 Experimental Measurements	176
3.1.3.3.1 Effect of Surface Roughness	176
3.1.3.3.2 Effect of Surface Composition	178
3.1.3.3.3 Effect of Temperature	179
3.1.3.3.4 Effect of Particle Size	179
3.1.3.3.5 Determination of the Force of Adhesion for Different Particle/Surface Combinations	180
3.1.3.4 Theoretical Calculation of the Force of Adhesion	185
3.1.3.5 Conclusion	188
3.1.4 Selection of the Potential Separation Devices Based on the Force Available for Application	189
3.1.5 Preliminary Screening of Separation Devices	194
3.1.6 Summary of Preliminary Experiments	217
3.2 Experimental Separation of Atmospheric Aerosols Taken Downwind of an Iron Foundry	220
3.2.1 Aerosol Sampling	220
3.2.2 Preparation of Test Samples	222

3.2.3	Study to Show the Effect of the Blender on the Removal of Particles from Filters and Glass Surfaces	225
3.2.4	Studies to Show the Effect of Power and Pressure Upon the Efficiency of Removing Particles from the Filter	227
3.2.5	Experimental Studies to Show the Effect of Power and Pressure on the Removal of Sedimented Particles from the Glass Petri Dish	231
3.2.6	Experimental Studies to Show the Effect of Sonic Power and Applied Pressure on the Separation of Particles Removed from Filter Surfaces	233
3.2.6.1	Collection and Presentation of Separated Particles	233
3.2.6.2	Measurement of Particle Size Distribution and the Separation Efficiency	234
3.2.6.3	Effect of Power on the Separation Efficiency	236
3.2.6.4	Effect of Pressure	237
3.2.7	Experimental Studies to Show the Effect of Sonic Power and Pressure on the Separation of Particles Extracted from Glass Surfaces	241
3.2.8	Experimental Studies to Show the Effect of Sonic Power and Pressure on the Removal of Particles from Filters in a 1 Percent Krytox® 157 in Freon® E-3 Solution	246
3.2.9	Experimental Studies to Show the Effect of Sonic Power and Pressure on the Separation Efficiency of Particles Removed from the Filter in a 1 Percent Krytox® 157 in Freon® E-3 Solution	248
3.2.10	Experimental Studies to Show the Effect of Sonic Power and Pressure on the Separation Efficiency of Particles Removed from the Glass Surface in a 1 Percent Krytox®157-Freon® E-3 Solution	253

3.3 Discussion of the Experimental Results	258
4. Summary and Conclusions of the Thesis	
4.1 Summary	
4.2 Conclusions	
5. Recommendations for Further Work	
5.1 Hydrogen-Bonding Series	
5.2 Cavitation	
5.3 Extended Fluorohydrocarbon Studies	
5.4 Studies with Water-Soluble Particles	
5.5 Studies with Other Emissions	
5.6 Studies with Atmospheric Aerosol	
6. Acknowledgements	
7. References	

LIST OF FIGURES

1. Schematic Diagram of the Cleaning Process by Clouds and Precipitation for Aerosols and Trace Gases	9
2. Potential Energy Curves for the Interaction of Two Charged Surfaces	36
3. Particle-Size and Agglomerate-Strength Regions in Which Various Binding Mechanisms Predominate	37
4. Influence of Electrolyte Concentration on the Total Potential Energy of Interaction of Two Spherical Particles	39
5. Particle Nomenclature	44
6. Summary of Aerosol Distributions Observed at the Ground, Primarily in Polluted Areas	46
7. Gray Iron Cupola	64
8. Three-Phase Electric Arc Furnace	67
9. Electrical Induction Furnace	67
10. Open Hearth Air Furnace	68
11. Particle-Size Distribution of Particulates Emitted from Uncontrolled Iron Foundry Cupolas	72
12. Particle Size Ranges for Dust from Cold and Hot Blast Cupolas	73
13. Cupola with Wet Scrubber Control Equipment	74
14. Experimental Flow Chart for Thesis	128
15. Electron Microscope Size Distributions of the Ferric Oxide, Titanium Dioxide, and the Alumina	130
16. Sedimentation Volume vs Hydrogen-Bonding Value for Titanium Dioxide	133
17. Sedimentation Volume vs Hydrogen-Bonding Value for Ferric Oxide	134
18. Sedimentation Volume vs Hydrogen-Bonding Value for Alumina	135
19. Sedimentation Volume vs Hydrogen-Bonding Value for Aluminum Metal	136
20. Sedimentation Volume vs Hydrogen-Bonding Value for Titanium Dioxide Using Specific Solvents	138

21.	Sedimentation Volume vs Hydrogen-Bonding Value for Ferric Oxide Using Specific Solvents	139
22.	Sedimentation Volume vs Hydrogen-Bonding Value for Alumina Using Specific Solvents	140
23.	Sedimentation Volume vs Hydrogen-Bonding Value for Aluminum Using Specific Solvents	141
24.	Relationship Between Sedimentation Volume and Hydrogen-Bonding Value for the Four Powders	142
25.	Relationships Between pH, Sedimentation Volume, and Zeta Potential for TiO_2	148
26.	Relationships Between pH, Sedimentation Volume, and Zeta Potential for Alumina	149
27.	Dispersion of Ferric Oxide in Aqueous Solutions of Phosphates and Silicates - Relationships Between pH, Mean Particle Size, and Zeta Potential	150
28.	Effect of Dilution on Titanium Dioxide Size Data	152
29.	Mean Particle Sizes of Titanium Dioxide in Various Solvents	159
30.	Sorvall SS-1 Rotor with Tube	164
31.	Plastic Insert	165
32.	Surface of Rough Stainless Steel (240 Grit)	167
33.	Surfaces of Medium Rough and Smooth Stainless Steel	167
34.	Surface Characterization of the Stainless Steel Screw Heads	169
35.	Apparatus for the Deposition of Particles onto the Surfaces of the Screw Heads	171
36.	Surface After Deposition Showing the Particle Distribution	173
37.	Effect of Particle Size	181
38.	Data of Krupp for Gold Spheres on Cellulose and Polyester in Aqueous Triphosphate Solution	183
39.	Force of Adhesion Data	184
40.	Calculated Force of Adhesion of Ferric Oxide to Surfaces Using Theoretical Models	187

41.	Completely Assembled Separation Unit	196
42.	Power Supply Calibration Curves of 1-in. Diameter Horn Done in Water at Room Temperature	199
43.	Power Supply Calibration Curves of 1/2-in. Diame- ter Horn Done in Water at Room Temperature	200
44.	Relationship Between Mean Particle Size, Blending Time, and Temperature	212
45.	Effect of Blender Speed on the Mean Size of an Alumina Slurry	214
46.	Photomicrographs of the Foundry Effluent Collected on Whatman No. 52 Filter Paper	223
47.	Photomicrographs of the Foundry Effluent Collected on the Glass Surface	224
48.	Effect of Blending on the Removal of Foundry Particles from a Filter	226
49.	Effect of Sonic Power on the Separation of Foundry Effluent Particles from Filters	228
50.	Effect of the Application of Pressure on the Separation of Foundry Effluents from Filters	230
51.	Effect of 100-Watt Power and 100-psi Pressure on the Removal of Foundry Particles from the Glass Surface	232
52.	Typical Field of Foundry Particles Separated in Aqueous Phosphate at 50 Watts at Atmospheric Pressure	238
53.	Typical Field of Foundry Particles Separated at 100 Watts at Atmospheric Pressure	239
54.	Size Distributions of Foundry Particles Sepa- rated at 100 Watts, 30°C, Atmospheric Pressure for Five Minutes in Aqueous Pyrophosphate Solution	240
55.	Size Analysis of Particles Separated from Filters at 100 Watts, 50 psi, 30°C, for Five Minutes in Aqueous Pyrophosphate Solution	242
56.	Nature of Foundry Particles Separated from Glass Surfaces Using Ultrasonics at 100 Watts at Atmospheric Pressure in Aqueous Phosphate Solution	243

57.	Size Distributions of Foundry Particles Removed from the Glass Surface at 100 Watts, 50 psi, 30°C, for Five Minutes in Aqueous Phosphate Solutions	245
58.	Filter Paper after Sonication in Freon®	247
59.	Field of View Showing the Degree of Separation of Foundry Particles Separated at 100 Watts and 50 psi in Krytox® 157-Freon® E-3 Solution	249
60.	Size Distributions of Particles Separated at 100 Watts and 50 psi in Krytox®-Freon® Solution	250
61.	Typical Field Showing the Degree of Separation of Foundry Particles at 100 Watts and 100 psi in Krytox®157-Freon® E-3 Solution	251
62.	Size Distributions of Foundry Particles Separated at 100 psi and 100 Watts in Krytox®-Freon® Solution	252
63.	Typical Field of Foundry Particles Separated from the Glass Surface at 100 Watts, 100 psi, in 1 Percent Krytox®-Freon® E-3 Solution	254
64.	Size Distributions of Foundry Particles Separated from the Glass Surface at 100 Watts, 100 psi, 30°C, for Five Minutes in Krytox®-Freon® Solution	255
65.	Typical Scanning Electron Micrographs of Separated Particles Viewed at 30,000X	272
66.	Distribution of Elemental Iron in the Chicago Metropolitan Area (Gatz ²³⁵)	276

THE PHYSICAL SEPARATION OF PARTICULATES

1. INTRODUCTION

In the last decade, there has been a growing awareness of man's past disregard for the condition of the earth on which he lives. Through the efforts of scientists and conservationists, the eyes of the world have been made to focus on the present and future effects of air and water pollution on world ecology. The potential dangers of ignoring the many and varied sources of pollution have been the subject of countless articles in newspapers and magazines, and their gloomy predictions for future life on this planet have stirred the minds of men, both in government and industry, to act before it is too late.

In recent years, action has been taken through newly formed committees and research organizations, which have been backed by new and vigorous legislation, designed to curb excessive pollution of the biosphere.^{1,2} To protect the biosphere, i.e., that portion of the environment where life is known to propagate, standards have been proposed, both for effluents discharged to rivers and streams, and for emissions discharged into the atmosphere.^{1,2} These have been enforced by river authorities and air pollution boards respectively. The enforcement of these laws has taken the form of legal action against the guilty parties, and it has resulted in fines and threatened close down of the plants that have continued to violate these laws.

As a result, industry and government have been forced to develop surveillance and monitoring groups to continually take data on discharges and emissions within their jurisdiction. To illustrate both the operation and the problems faced by these groups, let us consider air pollution control as a prime example.

National networks have been conceived and operated by governments in many countries to survey and monitor the total air pollution levels over large land masses. A typical example is the National Air Surveillance Network established by the United States Environmental Protection Agency. This is described by Lee & Goranson,³ and Lee.⁴ In such surveillance systems, both gaseous and particulate levels of pollution are monitored,⁵ but for the purpose of this thesis, emphasis is given to the factors affecting the production and monitoring of particulates only. Particulates are defined as all airborne solid and liquid matter, and include solid particles and liquid aerosols.⁶ The nature and sources of particulates in the atmosphere are very complex, and are described in some detail in Chapter 2. They are of specific interest to the environmental control engineer and the atmospheric physicist because 1) they are a cause of poor visibility, 2) they can be a health hazard, 3) they act as a transport vehicle for gaseous pollution, and, as some are catalytically and chemically active, 4) they promote atmospheric reactions.⁷ In addition, McLellan⁸ reports

that atmospheric particles from anthropogenic, i.e., man-made sources are a possible cause of the mean reduction in the earth's temperature over the past century.

The National Surveillance Network monitors particulates at some 200 urban and 300 nonurban sites in the United States,⁶ the particulate mass concentration being measured by the use of Anderson cascade impactors.³ This technique is criticized by Davies⁹ who points out that the method is effective only over the size range of 0.25-1.8 μ m, which does not include very fine particulates, e.g., Aitken nuclei or coarse particulates, e.g., dust. The data from these network stations are then fed into a National Control Centre where they are inserted into computer programs along with prevailing meteorological data. Diffusion models are finally employed to predict the concentration of each pollutant at any geographical location at any selected time.

The general potential of the national networks has recently initiated the development of global monitoring programs.^{10, 11, 12, 13} One of the prior obstacles to a systematic program on an international scale has been the differences in the methods of presenting the computer data,¹¹ but the National and International Environmental Monitoring program organized through the Smithsonian Institute has recently overcome this by using a standardized data format.¹¹ They specify 33 listed parameters of pollution in both air and water and Table 1 lists the

TABLE 1

POLLUTION PARAMETERS MEASURED IN WORLD PROGRAMS¹¹

<u>Parameter</u>	<u>Number of Worldwide Programs</u>
Airborne SO ₃	167
Suspended Particulate Matter	240
CO	71
CO ₂	74
Airborne NO _x	80
O ₃ , photochemical oxidants and reactive hydrocarbons	109
Hg	145
Pb	130
Cd	89
Halogenated Organics; D.D.T.	113
Petroleum Hydrocarbons	71
Algal, Fungal, and Bacterial Toxins	33
NO ₃ , NO ₂	150
NH ₃	102
B.O.D.	144
Dissolved Oxygen	188
pH	214
Coliform Bacteria	122
Selected Radionuclides	180
Soluble Salts of Alkali & Alkaline Earth Metals	185
Eutrophication Factors (P0 ₄)	129
Heavy Metals	144
Noise	8
Waste Heat	156

parameters and the number of worldwide programs supplying data. It is significant to note that the largest number of programs are concerned with particulate monitoring. The incentives to conduct a successful worldwide system of monitoring are obvious. Firstly, a government can forewarn both its population and other governments of any impending adverse conditions. Radioactive emissions from nuclear power stations, and the recent sulphur dioxide threat to Scandinavian forests from acid rainfall¹⁴ are two examples. Secondly, the offender can be located, forced to eliminate the emission, and possibly made to pay retribution for damages to the affected party. Thirdly, by considering the total diffusion model, the impacts of new plants and new factories can be predicted before construction, and the site giving the least adverse impact to the environment recommended.

Unfortunately, the national and global monitoring programs do have certain limitations at this time.

Firstly, the dispersion models are not accurate over large distances, as the data are affected by variables whose interactions are not well understood.⁸ McLellan⁸ suggests that they can be improved by the use of better meteorological data using satellite imaging, and by the use of more realistic dispersion modeling. For example, he reports that intense local pollution over urban areas often travels hundreds of miles without any large horizontal dispersion as the pollution is apparently carried

along isotropic surfaces into the stratosphere. In consequence, he suggests that further investigation into stratospheric and general recirculation models should be pursued.

Secondly, the accuracy of the data input to the model depends on a knowledge of the number of pollution sources, their composition and their pollutant concentrations. For successful model predictions, the impact of each stationary and mobile source of pollution has to be understood. Their classification by type, composition and pollutant concentration over a wide and sometimes seasonal time period has to be known. Naturally occurring background levels of each pollutant class also have to be recognized, and the effects of natural phenomena such as forest fires, volcanoes, and cyclonic storms upon the background levels taken into account. The emission factor,⁶ i.e., the statistical average of the rate at which pollutants are emitted from the burning or processing of a given quantity of material or on the basis of some other meaningful parameter, has to be measured for every conceivable natural and man-made source. The United States Environmental Protection Agency has already spent millions of dollars in contract research in an effort to do this, but despite years of study, they are only just beginning to have useful data at their disposal.

Thirdly, the data taken so far on particulates have used a sampling and collection system open to some criticism.⁹

It is size selective, i.e., it preferentially collects particles in the range 0.25 to 1.8 μ m. at the expense of larger and smaller particles, and collects data only at ground level. To understand the reason for selecting this method, we have to consider the alternatives. To effectively sample the atmosphere, one can visualize the use of countless aircraft, helicopters, or balloons fitted with sophisticated sampling devices to take samples at all altitudes and all points of the compass. This is without doubt the best approach, if one wishes to record the conditions as they really prevail at all parts of the atmosphere. However, this is prohibitive in cost, not only for industry, but also for most governments. Moreover, as we are primarily concerned with effects on the biosphere, and more specifically on the health and welfare of our population, we are more interested in the conditions and effects of pollution at ground level than at higher altitudes. Consequently, most monitoring networks, including the E.P.A., make the decision to locate their sampling stations, either directly on the ground or on towers and rooftops very close to it.^{3,4} In this way, they happily minimize sampling costs and simplify the sampling procedure.

Fourthly, and of most importance to this thesis, the particles collected by this system cannot be used directly to pinpoint any emission. This is because the particulate phase of the atmosphere is no longer in the same form at ground level as it was at higher altitudes. Interactions between particles, involving impaction, sedimentation and

diffusion, draw particles into small groups or aggregates which persist until they are removed from the atmosphere by natural processes.¹⁵ Cloud formation, rainfall, snowfall, and natural sedimentation cleanse the atmosphere of its particles, Figure 1.¹⁵ When particles fall on the earth and are collected by impactors or filters, they are observed as large groups, sometimes 10-100 times the magnitude of the smallest individual particle size in the atmosphere. However, for general pollution monitoring, this is often of no consequence because only the mass of particulates per volume of air is of interest.^{3,4,6} Further, these groups of particles are still chemically similar in composition to their individual components and, because of their increased size, are easier to collect and handle.

However, since Sherlock Holmes first plucked the hair from the clothing of a suspect and, by microscopic analysis, showed it to have originated from the victim, particles have been used as very efficient tracers in processes. Apart from the forensic applications, they have been used to monitor the amount of wear in hydraulic systems,¹⁶ and the source of contamination in pharmaceutical intravenous solutions.¹⁷ Street sweepings in urban areas have been shown to contain lead particulates and rubber tire dust from automobiles.¹⁸ Hence, analysis revealing this kind of dust in the unknown sample leads the analyst to suspect the sample origin to be urban. Particles by their permanent nature are the best and often the only

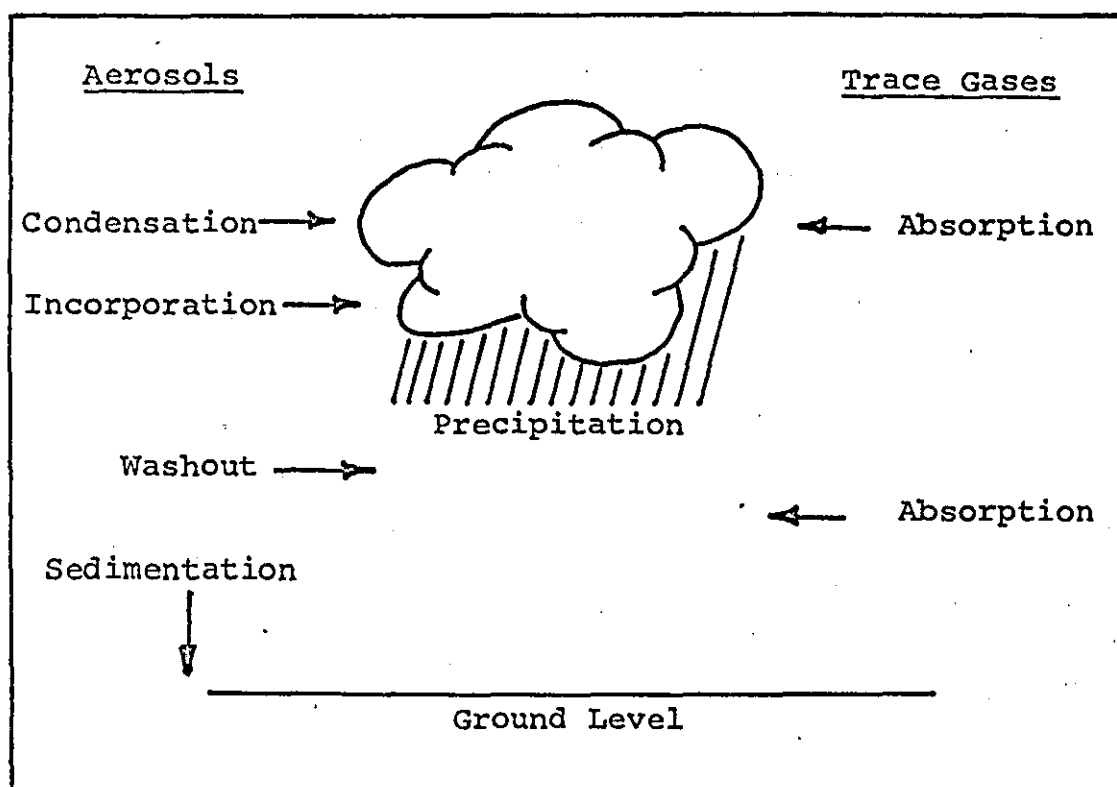


Fig. 1 - Schematic Diagram of the Cleaning Process by Clouds and Precipitation for Aerosols and Trace Gases

tracers that the pollution analyst has available to predict the source of any emission. Unfortunately, the groups of particles collected at ground level are usually unsuitable for tracer studies, as they consist of particles of all sizes and compositions adhering together by both physical and chemical binding forces. Those bound by physical forces are termed agglomerates and those by chemical forces are termed aggregates.¹⁹ Any toxic or noxious particulate material of value as a tracer is often buried inside the agglomerate structures, and it is only by separating the structure that the particle can be located and analyzed. Also such parameters as the physical size and shape of a particle can only be determined on the individual particle. However, for some studies the characteristics of the aggregate are also of interest. For example, it is conceivable that particles which have been subjected to high heat, coagulation and cooling could be found as aggregates with chemical bonding at their points of contact. The presence of such particles would, therefore, be indicative of an emission from this kind of process. Hence, it would be advantageous to be able to separate the agglomerated and aggregate sample collected at ground level into both its single particle and aggregate populations. Such a capability could enable the analyst to reconstruct the form of the tracer particle in the atmosphere, and possibly use its characteristics as a fingerprint of the source and nature of the process from which it has been emitted.

The separation of such agglomerated systems is no simple matter. Davies⁹ reports that the size distribution of atmospheric particulates lies between 10^{-3} and 10^2 micron. For particles of size greater than 10^1 micron, separation is relatively easy, as interparticle binding forces are low, and simple methods are available to separate them by size or species.²⁰ For particles of size less than one micron, high surface binding forces prevail, and separation is difficult.²⁰ Unfortunately, the largest number of particles in an atmospheric aerosol are submicron in size,⁹ which places them in this latter class. At present, there is no general method available to separate these particles. The microscopist tries arbitrary techniques to perform some separation, but in the submicron particle range, he is more often left with only a partial separation after his efforts. In consequence, there is a fundamental need to study this aspect of air pollution monitoring. A study should be performed to investigate methods of effectively separating particles from an agglomerated atmospheric aerosol, for the purpose of identifying a given particle species and measuring its concentration. Such a study should involve an investigation into the nature, composition, and structure of atmospheric aerosols both as found in the atmosphere and after collection at ground level. It should involve an investigation into the types of forces that bind such particles together into an agglomerated structure and should involve the definition and measurement of these forces. Finally, it

should involve the design and application of a method by which sufficient force can be applied to the atmospheric aerosol agglomerate to separate them into their individual and aggregate populations. It is the purpose of this thesis to study and develop a method to fulfill this need. Naturally, a complete study such as the one defined above is beyond the scope of one thesis, and so certain limitations have to be imposed on it.

Firstly, the composition of an atmospheric aerosol is shown, in Chapter 2, to be too complex to model with any accuracy. Consequently, it was decided to investigate an aerosol from a particular locality in this thesis. For convenience, the Chicago city air sampled downwind from a metals casting plant was employed. This was especially suitable in providing tracer particles of a particular and significant kind, i.e., inorganic metal oxides.

Secondly, the nature of the particle separation has to be specified. One can separate and classify particles by size, density, shape, mass, and species, but only one form of separation can be studied here.

As most particle size analysts are concerned with measuring the particle size distribution and the chemical compositions of the particles present, they desire a sample randomly dispersed on a substrate in such a manner that each individual discrete particle

and aggregate can be observed as having no points of contact with its neighboring particles. With such a system, physical and chemical measurements can be made and specifically referred to each individual particle, and in this way, its use as a tracer can be optimized. In this thesis, a method of separating and recollecting particles on a substrate in this form will be studied. Hence, separation will mean the physical separation of each particle from its neighbor, and the respective sizes, shapes, and species will be randomly spread over the recollection surface. Further, as most samples are analyzed by optical, transmission, and scanning-electron microscopy, a method of separation will be devised to handle small laboratory samples only.

In the following chapters of this thesis, a separation method is devised, designed, constructed, and tested for the separation of inorganic metal oxides from ambient air to meet these requirements. However, the method and procedure selected will be shown to be not only useful for inorganic oxides, but also useful for all types of atmospheric particles, including those which are water-soluble.

2. LITERATURE SURVEY

2.1 General Introduction

The purpose of this study is to devise a method whereby agglomerated atmospheric particles collected at ground level can be successfully separated into their discrete and aggregate particle populations. The study demands a knowledge of the types and structures of atmospheric aerosols, and it necessitates an understanding of the factors involved in their sampling, collection, and ultimate separation. To do this, the forces that bind agglomerates together have to be studied and measured so that a separation mechanism can be prescribed. The most suitable types and applications of energy, fluids, and surface active agents required to perform this task have to be investigated and, ideally, methods devised to recollect the separated particles in the same dispersed form as was present in the atmosphere. As much work has been done in these general fields of interest, the first task of such a program is to determine the state of the art in a wide series of topics. As a result, the literature survey cannot be fully comprehensive in all of them. However, a literature survey compiled on a recent U.S. Air Force contract can be used as a more complete reference.²¹

2.2 Basic Concepts of Interparticle Forces

2.2.1 Introduction

The science involved in the separation of particles from an agglomerated matrix is very complex. It incorporates

many facets of the basic sciences, each of which has an equally important role in the separation process. To understand the mechanism and energy involved in this process, one has to first appreciate the role played by each of the separate entities and then the way in which they interact.

To separate two particles in contact, one has to know the magnitude of the force binding them together and supply sufficient energy to overcome it. However, if one supplies energy considerably in excess, there is a danger that the original particles will be fractured and thus the resulting particles will not be truly representative. Once separated without fracture, one has to devise means to keep the particles apart, both prior to and after recollection. The binding force between two particles can be shown to be a function of such parameters as the particle size, the particle size distribution, the particle macroshape and rugosity, the total and external surface area, the nature and structure of the surface, the energy at the surface, the area of contact between the particles and their hardness and melting points.²² Once they have parted, the two particles can be kept apart by 1) collecting them on a surface in such a way that the interparticle distance is greater than that over which coagulation forces act, 2) adsorb ions onto their surfaces so that they repel each other, 3) change the rheology of the fluid in which they are suspended, so that they are mechanically held apart.²²

With this complex framework of interacting variables, it appears logical to introduce this portion of the literature survey by briefly discussing the importance and mode of interaction of each of the variables independently. The way in which they interact with one another can then be developed, so that at the conclusion of this section, the reader has a basic knowledge of particulate systems onto which the more specific and detailed parts of this literature survey can be built.

2.2.2 Discrete Particles and Particulate Systems

A "discrete particle" can be usefully described as a single unit of matter which can change in "size" only by the breakdown or fracture of chemical bonds within its structure. It may or may not be of uniform "density" throughout its mass, and its "shape" will be dependent on the method by which it is made.²¹ In other branches of science the word particle has a completely different meaning, but it is only the above definition that

will be used in the current research. The discrete particle can consist of a solid, a liquid or a gas, depending on the phase in which it is suspended.²³ Powders, dusts and slurries are examples of discrete solid particles; emulsions, sprays and mists are examples of discrete liquid particles; and foams and bubbles, present as "porosity", in ceramic and steel compacts are examples of discrete gaseous particles.²³ In the research conducted for this thesis, only the first category is of importance, i.e., the category involving discrete solid particles.

In the collection of discrete solid particles, we utilize a property of the particle which causes it to stick to a solid surface. When the particles (or, in fact, liquids or films) stick to a plane surface by purely physical bonding, the process is termed "adhesion".²² This property is not restricted to the sticking to plane surfaces. Discrete particles stick to each other irrespective of chemical composition, and this process is generally termed "cohesion".²² When chemically identical particles stick together by physical forces, the process can be termed "agglomeration". When chemically different particles stick together by physical forces, it can be termed "conglomeration".²¹ From both of these processes, a new particulate unit evolves. It is usually in the form of grouping of individual or discrete particles bound together by physical bonds. This unit can exist permanently in a fluid and behave as if it was a discrete particle of size similar to that of the unit itself. If the physically bonded particles are of the same chemical composition, the unit can be termed an "agglomerate",¹⁹ and if they are of different composition, it can be termed a "conglomerate".²¹ When the bonding between particles is not physical in nature, for example, in chemical reactions or sintering, the particulate unit can be termed as "aggregate".¹⁹ In this unit, the bonding is chemical, and the particles are joined together by necks of the same structural form as the particles themselves.

In future sections of this report, the terms "agglomerate", "conglomerate" and "aggregate" will be used as defined here. For simplicity, the adjective "discrete" will be omitted from the term "discrete particle" and the term "particle" will generally apply to all discrete systems. Its use up to this stage was simply to enable the definitions of multiparticle units to be clearly understood.

2.2.3 Influence of Particle Size and Particle Size Distribution

For many practical purposes, the particle has to be characterized by its size, shape, and "surface". For most solid particles, size is non-unique.²⁴ It depends entirely on the method by which it is measured, the experimental conditions prevailing at the time, and the instrument which is used to make the measurement. This is often operator dependent, and hence any unqualified statements indicating size are meaningless. The units of particle size can be centimeters, millimeters, microns, or angstroms. In most branches of particle technology, the term "micron" is used in which 1 micron (μm) is 10^{-4} cm. The angstrom (\AA) is also encountered and here 1 angstrom is 10^{-4} micron. The range of particles of interest in this thesis is generally from $10^{-3} \mu\text{m}$ - $10^2 \mu\text{m}$. Within any system involving discrete particles, a distribution of sizes is always present. "Particle size distributions" are usually measured, and data reported in terms of frequency, surface, volume or mass distributions.²⁵

The effect of particle size alone on interparticle forces is very variable. Corn,²⁶ Deryaguin and Zimon,²⁷ Kordecki and Orr,²⁸ and Böehme et al²⁹ all studied this for large particles and found little effect. No measurements were reported on submicron particles. In some instances, it was found that interparticle forces were directly proportional to size and in others they were inversely proportional to power functions of size.²² Each relationship was found to be dependent on the type of force acting,²² but this will be explained later when the types and magnitudes of forces are discussed.

2.2.4 Influence of Particle Shape

In general, shape can be subdivided into two categories: macro, and micro shape. Macro shape is a measure of the particle form, i.e., whether it is spherical, cuboidal, conical, etc., while micro shape or "rugosity" is a measure of surface roughness.³⁰ Both of these parameters can be measured, but again, qualification of the method employed to measure them has to be provided with shape measurement data if it is to be meaningful.³⁰ For the purpose of this research, the measurement of microshape or rugosity is most important. This is because the interparticle force between particles and a plane surface, and the cohesion between particles themselves, depends upon the area of contact between the bodies, which in turn depends upon the particle surface roughness.²² The effects of particle roughness were studied by Meldau,³¹ Zimon and Volkova,³² Böehme et al,²⁹ and Corn.^{33,34}

When ideally smooth surfaces are encountered, inter-particle forces are at a maximum on the surface of a particle. When the heights of the projections or asperities on the surface of a particle are an order of magnitude smaller than the particle diameter, the force of adhesion falls.²² However, when the height of the asperities is greater or equal to the particle diameter, the adhesion rises again.²² Zimon had grave doubts about the validity of previously published studies on the effect of surface roughness, because in most cases the surfaces were not characterized well enough.²² In addition to surface roughness, particle form was also shown to affect the force of adhesion,²² the minimum force occurring for particles of isometric shape, i.e., a sphere or regular polygon.

Spherical particles were shown to have lower forces of adhesion than plane particles, i.e., particles with their lengths and widths much greater than their thickness, e.g., Kaolin, bentonite, mica, graphite, and gypsum.²⁷

Fibrous or acicular particles, e.g., prisms and needles which have one dimension greatly exceeding all others, have even higher forces of adhesion.²²

The cleanliness of the surface was also shown to be important by McFarland and Tabor,³⁵ and Howe, et al.³⁶ The method of cleaning the surface affected the adhesion, and the way the particles were deposited did likewise.²² This

fact leads to the most important particle characteristic involved in interparticle force effects, the particle surface.

2.2.5 Influence of Surface Area and Surface Structure

The surface of a particle in a fluid is the boundary or interface between the two phases. The extent of this surface is a function of particle size and surface roughness. For a given weight of solid matter, the lower the particle size, and the rougher the particle surface, the greater the surface area. This "factor" is usually subdivided into two categories. These are the "external surface area" which is equivalent to the surface of all prominences on the particle plus the area of all indentations which are wider than they are deep, and the "internal surface area" which is that part of the surface contained in indentations deeper than they are wide.³⁷ At all points over the total surface, i.e., external and internal, there are unsatisfied bonds which give rise to a field of force around the particle.³⁷ This property is a specific feature of a surface which no other part of the particle exhibits. In order to appreciate how a surface attains this property, one has to understand some of the features involved in the structure of solids.

Solids can be subdivided into crystalline and noncrystalline substances.³⁷ The former have a high degree of order in their molecular structure, in which the crystal is built up in a pattern or space lattice. In contrast, a

noncrystalline solid has complete disorder within its structure. Four different kinds of lattice exist in a crystalline solid and these are termed "ionic", "homopolar", "molecular", and "metallic".³⁷ In ionic lattices, the constituent entities are ions, and the structure is held together by the attraction of unlike charges or "electrical forces".³⁸ Examples are sodium chloride, potassium bromide, etc. In homopolar lattices, the entities are neutral atoms, and the structure is held together by ordinary chemical valencies. An example is diamond. In a metallic lattice,³⁹ all electrons can be regarded as making up an assembly in which chemical valency bonds are formed between each atom and its neighbors in the lattice. In a molecular lattice, the entities are molecules which are held together by physical or "Van der Waals forces".^{39'} These arise from the interaction between electrons and adjacent molecules. An example is stearic acid.³⁹ In all cases, the forces holding lattices together are attractive, and their strengths increase in the order Van der Waals, electrostatic and valency forces, respectively. For the case of a perfect lattice, the forces can be calculated, and at the surface where unlinked bonds predominate, an estimate of the attractive force can be found. Unfortunately, perfect lattices are rare, and imperfect lattices are the general rule. Stone⁴⁰ and Gray⁴¹ discuss lattice defects and define two distinct kinds termed interstitial ion and ion vacancy defects. This means that at some point in the crystal, more ions are present than should be there

(if interstitial ion defects are present), and alternatively less ions are present than should be there (if ion vacancy defects are present). This gives rise to localized areas of high and low attraction at the surface of the particle. These kinds of defects give rise to the property of semiconductivity in solids.⁴² Stone⁴⁰ discusses a third defect due to nonstoichiometry in the lattice, which he categorizes into excess metal with anion vacancies, excess metal with interstitial cations, excess electronegative constituents with interstitial anions, and excess electronegative constituents with cation vacancies. The problem is complicated even further when the ion deficiencies are filled with ions of a different kind, i.e., when impurity ions are present in the lattice. This has a detrimental effect, if the impurity ion has a different valency, when the lattice structure is subjected to strain. Cottrell⁴³ and Reid⁴⁴ discuss the effect of lattice strain particularly for the cases when solids are deformed or dislocated. An analogy to this effect is faulting and folding of geological strata in the earth's crust. Differences in the size and nature of the ions are responsible for the degree of deformation, and it has been shown to be greater for anions than cations and to increase with the radius of the ion. One effect of deformation is the polarization of the structure, which is reflected in a change in the bond strength between the ions.³⁷ Thus, in some cases, a highly deformed ionic bond can behave like an unsymmetrical

homopolar one.³⁷ On these grounds, it is very difficult in practice to predict the strength and nature of the bond at the surface of any nonperfect lattice. However, irrespective of whether the strength of the surface bonds are predictable or not, some field of force will exist as a result of their presence. Thus, when a second particle is brought close to the first one in such a way that their fields of force overlap, attraction and eventual adhesion takes place.

2.2.6 Influence of Surface Energy and the Adsorption of Films

The force of adhesion will depend on the force of the field around the solid, and a measure of this is the "surface energy".³⁷ This is defined as the isothermal reversible work which requires to be done in creating 1cm^2 of new surface.³⁷ This, if a solid particle in the form of a 1 cm cube was pulled apart to make two equal halves, with plane forces and the operation was performed in a vacuum, the surface energy would be twice the free energy associated with each surface. If these two halves were placed in contact once again, perfect adhesion would take place with a gain in energy of the same magnitude. If the operation was performed in air or in the presence of a vapor, this would not occur. Instead, the unsatisfied surface bonds would attract molecules of moisture or vapor to the surfaces, and when the two halves were placed in contact once again, the gain in energy would be less.³⁷ In this case, the force of attraction between

the two surfaces of the clean solid has been replaced by the force of attraction between two adsorbed layers. In general, these have lower values of Van der Waals forces than the solid itself. Thus, the adsorption of surface films reduce the force of adhesion between two perfect surfaces.³⁷

If the experiment was now repeated in such a way the 1 cm cube was torn apart with a highly irregular interface between the two halves, each interface would be the perfect mate to the other, but the energy involved would be greatly different, as the surface area of the rough interface would be greater than 1 cm². With an irregular interface in a vacuum, it is possible that lattice distortion could then occur due to attraction between unsatisfied bonds in narrow cracks in the surface which could result in a change in the microshape.³⁷ In this way, the surface could be modified and it would no longer be the perfect mate for the other interface. In addition, in air or a vapor, the adsorption of films would be different in cracks than on prominences due to capillary condensation, and so when the two interfaces were brought together, the energy involved in the adhesion would be much lower than predicted.

This introduces much uncertainty into the estimation of interparticle forces on nonplanar surfaces, and even more uncertainty is introduced when one considers the effect of the surface defects and impurities discussed previously.

It was shown that areas of high and low attraction could be present even on plane surfaces, so that they certainly can be present and influence the uniformity of adsorption of surface films on irregular surfaces.³⁷ In this way, surface roughness, surface energy, surface purity, and surface structure cause the interparticle force to vary from point to point over a single particle surface, and the force between any two particles will depend on the specific surface location where contact will be made, and the actual contact area between the particles in question.²²

2.2.7 Influence of Multilayer Adsorption and Effect of Free Liquid

So far in this discussion, the adsorption of moisture or vapor onto surfaces has been restricted to surface films or monomolecular layers. In the presence of high humidity, multilayer adsorption can occur,^{45,46} and in the ultimate case, free water can form a "pendular bond" between particles. In this case, new forces are introduced termed "capillary forces" which bind the particles together strongly. If the pendular bond is an organic vapor or volatile component which has a low melting point, condensation can be followed by partial solidification and the pendular bond then acts like a cement or binder. In this case, the adhesive properties of the binder are added to those of the particles which, of course, is the prime objective with a wide range of adhesives manufactured by the chemical industries. In this case, the particles are cemented together into an aggregate-type structure, which is almost inseparable by physical dispersive techniques.

However, considering only the case for water at the present time, additional increases in concentration leads to a complete coverage of the particles by a layer of water, which may or may not "wet" the surface. If the forces of attraction at the solid surface are greater for the liquid than for the solid itself, wetting will occur spontaneously.⁴⁷ In contrast, if the forces of attraction at the surface of the solid particle are greater for another solid particle than for the liquid, then the liquid will not wet the particles, but agglomeration will be observed. This behavior is related to a parameter termed the "contact angle", i.e., the angle between the liquid interface and the solid surface.⁴⁷ If the angle is 0° , complete wetting occurs, while if the angle is 180° , no wetting takes place.⁴⁷ Hence, by using a liquid whose affinity for the solid is greater than the solid's affinity for itself, i.e., a liquid whose contact angle with the solid is 0° , one can replace the adhesion between particles by the adhesion between a particle and a liquid. In this way, particles can be separated or dispersed with a relatively low amount of energy.⁴⁷ This can be facilitated by proper selection of a pure liquid or by adding a "surface active substance" to the liquid itself. This substance has a high affinity for the surface, and is adsorbed there from solution. The interface or surface of the solid with the liquid is now converted to an interface of surfactant with the liquid, which leads to yet a further force involved in particle-particle interactions. It has been shown that

at a particle surface, there is a field of force due to the presence of unsatisfied bonds which, depending on the ion, can lead to a surface charge. If this surface is placed in contact with a liquid containing positive and negative ions, a "double layer" is developed between the ions localized in the surface of the solid and those in the region extending into the solution.^{47,48,49} When the particle is in motion, shear is developed between the double layer and the bulk solution. The potential difference between any point in the bulk solution and this shear plane is termed the "zeta potential".⁴⁷ This parameter can be used as a measure of the stabilizing potential of the double layer. Compression of this layer leads to a reduction in zeta potential and loss of stability, i.e., coagulation and flocculation take place. In other words, loss of stability means the net force acting between the particles is now attractive, whereas in stable systems, when the zeta potential is high, the net force is repulsive. In this way "double layer forces" are very important in particle separation phenomena in a liquid medium.

Liquid layers have yet another significant effect in adhesion between surfaces, which arises as a result of capillary condensation. With any two rough surfaces, the adhesion between them is a function of the areas of the surface in contact. With highly irregular surfaces, perhaps contact occurs at only one point, such as at the tip of a prominence in the surface. If it occurred at at the tips of two prominences, the contact area would be

radically changed if the valley between them was filled completely with liquid. In this case, contact would be made at the tips of the prominences and over the area of the liquid film. Thus, the overall contact area would be increased. A similar effect is obtained due to plastic deformation or surface melting.

2.2.8 Plastic Deformation, Melting, and Sintering

When two surfaces are brought into contact under conditions of known pressure, the extent of deformation of the solids at the point of contact depends on the area of the initial contact and the elasticity of the surfaces.⁵⁰ In general, the lower the value of Young's modulus of elasticity, the softer the material, the greater the deformation and, consequently, the greater the adhesion. In addition to elasticity, the deformation of a solid is a function of the applied pressure, and many materials can be made to adhere purely by the application of high pressures.⁵⁰ Examples can be found in the manufacture of cold welded compacts, in which scrupulously clean metal surfaces such as aluminum can be pressed together to form metal parts.³⁷ Scrupulously clean means freedom from oxide films, liquid films and dust, which adhere to the surface bonds and lower the adhesional energy of the surfaces. Welding is usually accomplished by the use of heat, which acts as a surface softener and promotes rapid deformability. Adhesion at high temperatures is termed "sintering" and in this process, surface melting and

subsequent deformability lead to surface bonding. However, sintering does begin below the melting point of most solids, and there is an actual temperature termed the "Tamman" temperature which is approximately half the value of the solid melting point in °K. At this temperature, the rate of sintering rapidly increases.⁵⁰ It is probable that at this temperature, the lattice defects, discussed earlier, are no longer rigidly bound in the lattice, and ion migration takes place at the surface. Thus, the structure and properties of the surface are modified by the release of impurities and defects, and this is usually demonstrated by an increase in the force of adhesion.³⁷ Deformability of this kind can also be induced by friction. As the areas of contact between particles are usually very small, very high local temperatures can be induced by the rubbing of one particle surface against another.⁵⁰ When this occurs, the very high pressures and temperatures induced at the points of contact result in the localized plastic flow of the softened surface. This continues until the total area of contact is such that the local pressure has fallen to the characteristic yield pressure of the softened material, and the temperature has fallen below the Tamman value.⁵⁰ Friction deformability can be reduced by the presence of adsorbed films between surfaces which, of course, is the principal mechanism involved in lubrication.⁵⁰ It should be noted that the multiparticle structures arising from the sintering of particles are aggregates and these cannot be separated by normal dispersion

techniques. If the energy is increased in order to separate such structures, one runs the risk of fracturing the discrete particles themselves.

2.2.9 Nature and Magnitude of Interparticle Forces

There are many types of forces that bind solid particles together. Some of them predominate under dry conditions, some predominate under conditions of high humidity, and others predominate when particles are suspended in a liquid. When a particle is in contact with either a plane surface or another particle, there is a total force of adhesion active between the surfaces. Krupp⁵¹ defines this as being equivalent to the force that must be applied perpendicular to the center of gravity of the particle in order to remove it from either the plane surface or the other particle in a fixed period of time. Zimon²² and Orr and Kordecki²⁸ suggest that as the forces at which particles are removed from surfaces vary widely due to the reasons discussed in 2.2.5, it is better to estimate the force of adhesion as being that value of force at which 50% of the number of particles are removed under the specific conditions of the experiment. This latter definition is used exclusively in this thesis.

The forces that are present between particles and surfaces fall into the following categories:

2.2.9.1 Physical Forces

a. Mechanical Forces of Attraction

These arise through the physical interlocking of surface protrusions.²² A perfect sphere on a smooth surface has negligible mechanical forces, whereas a dendritic particle on a rough surface could have high mechanical forces.

b. Van Der Waal Forces of Attraction

This force comprises of three parts, each of which donate to the total force.²² These parts are termed dispersion, induction, and orientation forces respectively. They arise through interactions between dipoles in the surfaces of particles, but Zimon²² reports that the dispersion forces dominate. These forces are attractive long range, relatively weak, and are nondirectional. The attraction energy V_A between two spherical particles is given by Kruyt⁴⁸ as

$$V_A = \frac{A r_1 r_2}{6(r_1 + r_2) H_0}$$

Where A = Hamaker constant, r_1 and r_2 are the radii of the particles, and H_0 is the shortest distance between the particles.

c. Electrical Forces of Attraction

These arise when particles contact a surface and there is a potential difference between them. The forces are proportional to $r^{2/3}$ where r is the radius of the particle.²²

d. Coulombic Forces of Attraction

These occur when particles are charged prior to contact by a high voltage field. The forces cause interaction over larger distances and are inversely proportional to r^2 .

e. Capillary Forces of Attraction

These arise when liquid bridges are present between particles and surfaces, and are sometimes referred to as pendular bonds. Within the liquid bridge, the force arises due to the presence of negative capillary pressure which draws the particles together.

f. Electrical Double Layer Forces of Repulsion

These arise due to multilayer adsorption of ions onto a particle surface when it is completely submerged in a liquid. These forces are discussed in 2.2.7. The energy of repulsion between two equal spheres due to these forces V_R was shown by Kruyt⁴⁸ to be:

$$V_R = \frac{\epsilon r^2 \psi_o^2}{a} \cdot e^{-K H_o}$$

Where ϵ = dielectric constant, K^{-1} = thickness of the double layer, H_o = closest distance between the two particles, ψ = surface potential, a = distance between the two particle centers, and r = particle radius.

2.2.9.2 Chemical Forces

a. Hydrogen Bond

This is a special type of dipole interaction in which two

electronegative atoms share a proton to produce a strong wider range force than the Van der Waals physical force. Though categorized as a chemical bond, it is better classified as a weak chemical bond.

b. Valence Forces of Attraction

Examples of these are covalent, metallic, and ionic bonds. These are short range and arise through electron exchange. These are formed at the points of contact when sintering or a solid bridging takes place, and are the types of bond that bind together aggregates at the points of contact of each individual particle.

2.2.9.3 Interaction of These Forces

It is significant to note that not all these forces are present at one time, and that the conditions of the fluid around the particles influence their effect. Only two forces are continually present both in dry or humid air and in liquids; namely, Van der Waals, and the mechanical forces of adhesion. In dry air, the electrical and coulombic forces are more common and can prevail up to 65% relative humidity.^{22,28} In liquids, the attractive electrostatic forces and capillary forces do not occur, and the dominant forces of interaction are the Van der Waals force of attraction and the electrical double layer force of repulsion.

The interaction between these two opposing forces in liquids is generally represented by the potential energy

diagram shown in Figure 2.^{21,47,48} The dotted lines represent V_R and V_A and the solid line the resultant of the two forces. At the primary minimum, strong flocculation takes place, and at the secondary minimum, mild flocculation occurs. However, at V_M , the maximum of the curve, separation or particle dispersion is facilitated.

To relate the importance of all these possible forces in particle separation, their magnitudes have to be compared. Rumpf²⁰ reported on the strength of granules and agglomerates, and presented a relationship between the tensile strength of the agglomerate and the particle diameter. This is shown in Figure 3. It is seen that the physical capillary force far exceeds the Van der Waals force in moist agglomerates, and the chemical forces far exceed both of them. In addition, Krupp⁵¹ estimated the differences between Van der Waals, double layer, hydrogen, covalent and ionic bond energies. He reported values of 0.1 eV for Van der Waals, 0.1 - 1 eV for hydrogen and double layer bonds, and 1 - 10 eV for ionic and covalent bonds.

Of prime importance, however, were the reports of Zimon²² which showed that the forces of adhesion between particles in liquid media were one-half that in air, and the energy required to detach particles in water was one-tenth that in air. Zimon and Deryaguin⁵² also reported data for the separation of 5-10 μ m particles of glass from steel to be 10^{-2} dynes in air, and 10^{-6} dynes in water. However,

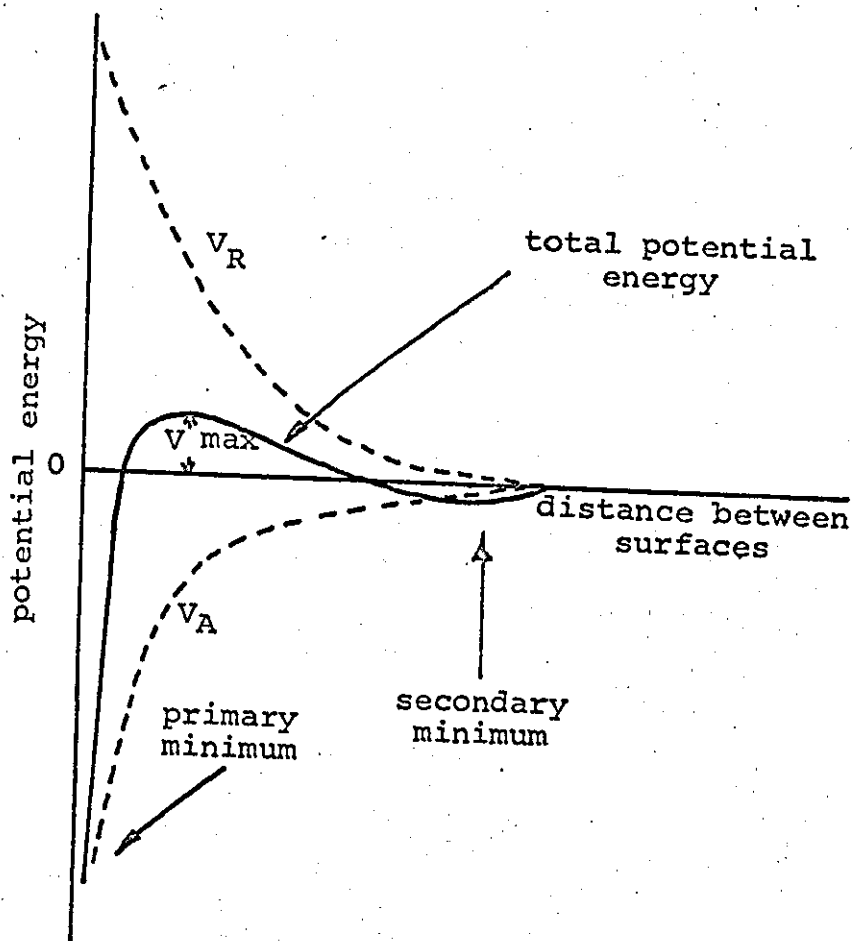


Fig. 2 - Potential Energy Curves for the Interaction of Two Charged Surfaces

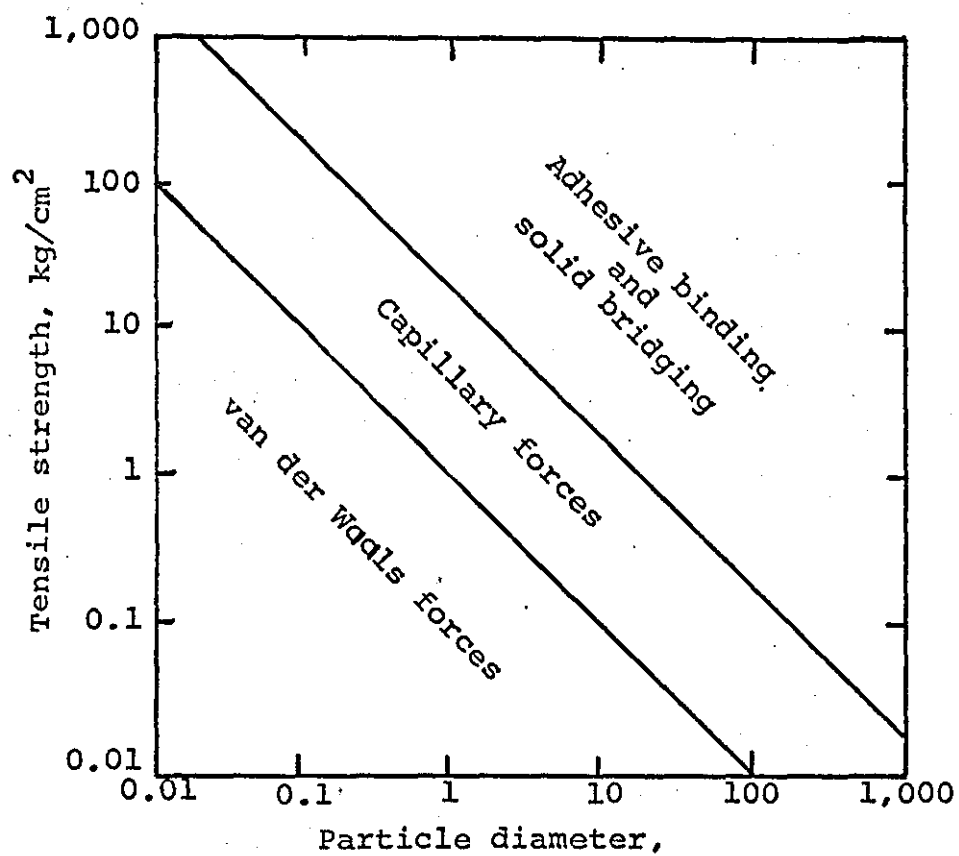


Fig. 3 - Particle-Size and Agglomerate-Strength Regions in Which Various Binding Mechanisms Predominate (Ref. 20)

Fuks, et al⁵³ reported that this was entirely dependent on the wettability of the surface and the pH of the liquid. He further stated that the electrolyte concentration and the valency of the ion in solution had a marked effect. Generally it was found that the minimum force of adhesion occurred in liquid media when the pH was at a maximum. Alkaline media tended to yield lower forces of adhesion than neutral or acid solutions. Adsorption of surface active agents was found to reduce the force of adhesion,⁵⁴ and polyphosphates had a similar effect.⁵⁵ However, these compounds were selective and had critical concentrations for different particle compositions and so had to be chosen carefully. They also showed differences between their temperature requirements. Generally, temperatures of 0-20°C were optimum for separating particles in pure liquids and electrolytes, but 60°C was optimum when surfactants were present.⁵⁵

In consequence, ionic liquids represent the easiest and the most potentially successful fluid for atmospheric aerosol particle separation. In Figure 2, the potential energy diagram for the interaction between the Van der Waals and the electrical double layer forces was depicted. When due consideration is now given to the correct choice of temperature, surfactant, pH, ionic strength, etc., this resultant force can be optimized.²¹ If $\frac{1}{K}$ represents the thickness of the double layer around a particle, then it can be seen from Figure 4 that the repulsive energy

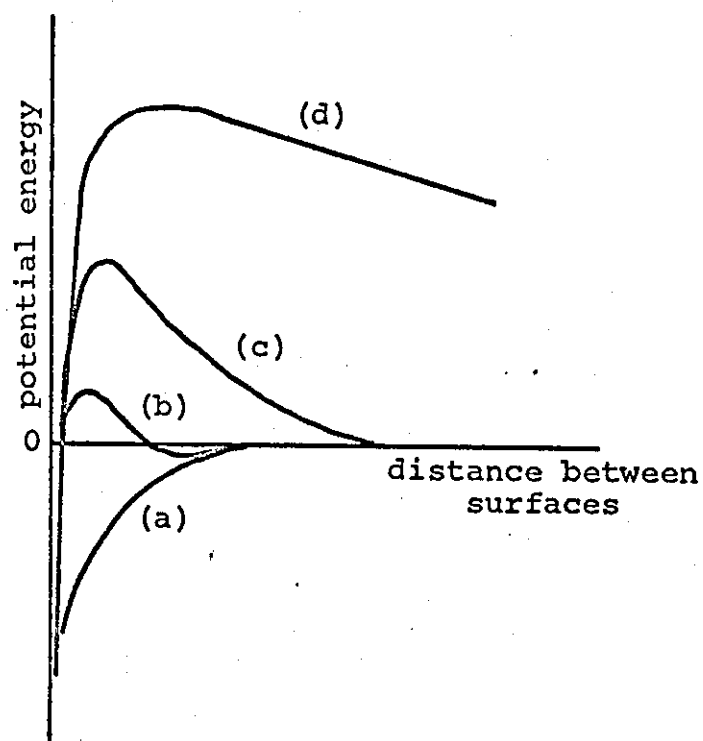


Fig. 4 - Influence of Electrolyte Concentration on the Total Potential Energy of Interaction of Two Spherical Particles of Radius 1000 Å in Aqueous Media.
 (a) $1/k = 10^{-7}$ cm, (b) $1/k = 10^{-6}$ cm,
 (c) $1/k = 10^{-5}$ cm, (d) $1/k = 10^{-4}$ cm.

becomes larger with increasing double layer thicknesses.⁴⁷ Wnek²¹ has shown that for spherical particles this resultant force can be theoretically predicted for all conditions of pH, dielectric constant, and ionic strength. By the correct choice of experimental conditions, he further could calculate the resulting repulsive forces and use them to predict interparticle force data.²¹ By equating both V_A and V_R for both aqueous and nonaqueous media, he was also able to predict that submicron particles could be more easily dispersed in aqueous systems than nonaqueous systems, but for particles of size larger than $1\mu m$, the reverse was true.

2.2.10 Summary of Interparticle Force Concepts

In summarizing the general literature reviewed so far, it is clear that the separation of particles is not easy due to the complex interactions between the possible forces of adhesion. It has been shown that particle size, shape, surface area, surface structure, surface cleanliness, surface energy, hardness, the presence of adsorbed films or ions all affect the resultant interparticle force. However, it has been further shown that though the physical and chemical properties of particles strongly influence this force, the mechanism of separation and its magnitude and number of interacting forces is always lower in ionic liquids than in air. This is primarily due to the presence and magnitude of the electrical double layer force of repulsion. Also, by the correct selection of pH,

ionic strength, temperature, and chemical additives, this repulsive force can be increased to an optimum value at which the probability of separation is high. Naturally, the magnitude of the force and the conditions necessary to reach this optimum value depend on the nature of the particles, and so the conditions have to be selected carefully for each particulate system. Therefore, it is quite clear that separation of particulates in liquids is the best approach, and certainly offers the greatest potential for success. In order to discover the feasibility of using this approach for separating atmospheric aerosols, it is necessary first to define the nature and composition of the particles found in the atmosphere. This is done in the following section.

2.3 Aerosols in the Atmosphere

2.3.1 Introduction

The nature of aerosols in the atmosphere has been the subject of several books and publications. Of significance are those of Junge,⁵⁶ Green and Lane,²³ Goldberg,⁵⁷ Robinson and Robbins,⁵⁸ Peterson and Junge,⁵⁹ Hidy and Brock,⁶⁰ Mitchell,⁶¹ Went,⁶² Shannon, et al,⁶³ Israel and Israel,⁶⁴ and Davies.⁶⁵

In these publications, it is shown that the air in all parts of the earth contains particulate matter. However, the concentration varies according to both the geographical surface location and the altitude above ground. For example, the polar regions contain very low particle concentrations

compared to urban areas, and the visible pollution above cities decreases with altitude as any air traveller will acknowledge. Aerosol particles found in the atmosphere can range briefly from airborne soil-derived dust such as grains of sand carried upwards in a sand storm to molecular particles produced by atmospheric reactions. Between these extremes of size, which range from millimeters to angstroms, atmospheric aerosols can be found from many various sources. Particles in the air can generally be categorized as dusts, smokes, and mists.²³

Dusts consist of solid particles suspended in air as the result of mechanical disintegration or aerodynamic dispersion of bulk particulates. Dusts generally have a very broad size distribution, and as a result, some particles tend to settle rapidly under the influence of gravity, while others remain suspended in air for days or weeks.²³ Smokes usually refer to suspensions of particles which are formed by volatilization and condensation, chemical reaction, and pulverization.²³ Smokes generally have particles less than 5 μm . in size. Mists result from the condensation of vapor and consist of droplets usually greater than 1 μm . in size. Cloud and fog droplets are examples of a mist, and these droplets very often carry dissolved components as well as insoluble particles.²³ Snow and rain forming in and descending through the atmosphere inevitably collect atmospheric aerosols and vapors before reaching the earth's surface.¹⁵

Nuclei are particles typically submicron in size, with condensation nuclei larger than about $0.2\mu\text{m}$ in diameter and Aitken nuclei less than $0.2\mu\text{m}$ in diameter. All natural cloud droplets start by vapor condensation on nuclei particles.⁶⁵

The terms haze and smog refer to combinations of the above types of aerosol particles and are often used to describe combinations of natural and man-made aerosols.⁶⁵

Aerosol size and property parameters are depicted in Figure 5 and show size ranges important for ions, light scattering, cloud physics, air chemistry, and routine air pollution measurements.⁶⁷

It is seen that the size spectrum varies from radii of 10^{-3} to $10^2\mu\text{m}$. Much has been learned about this size spectrum in recent years, and an interesting pattern of regularity in size distributions has been found. Generally, a large portion of the aerosol distribution function can be expressed as

$$n(r) = \text{constant } r^{-x}$$

Where r is the particle radius and $n(r)$ the number of particles in the range r to $r + dr$. x generally ranges between 3 and 5, and often maintains a value of 4 for particles of radius $\geq 0.1\mu\text{m}$.⁵⁶ The r^{-4} rule is interesting in that it requires that mass concentration of particles must be constant over the range of radius where it holds.

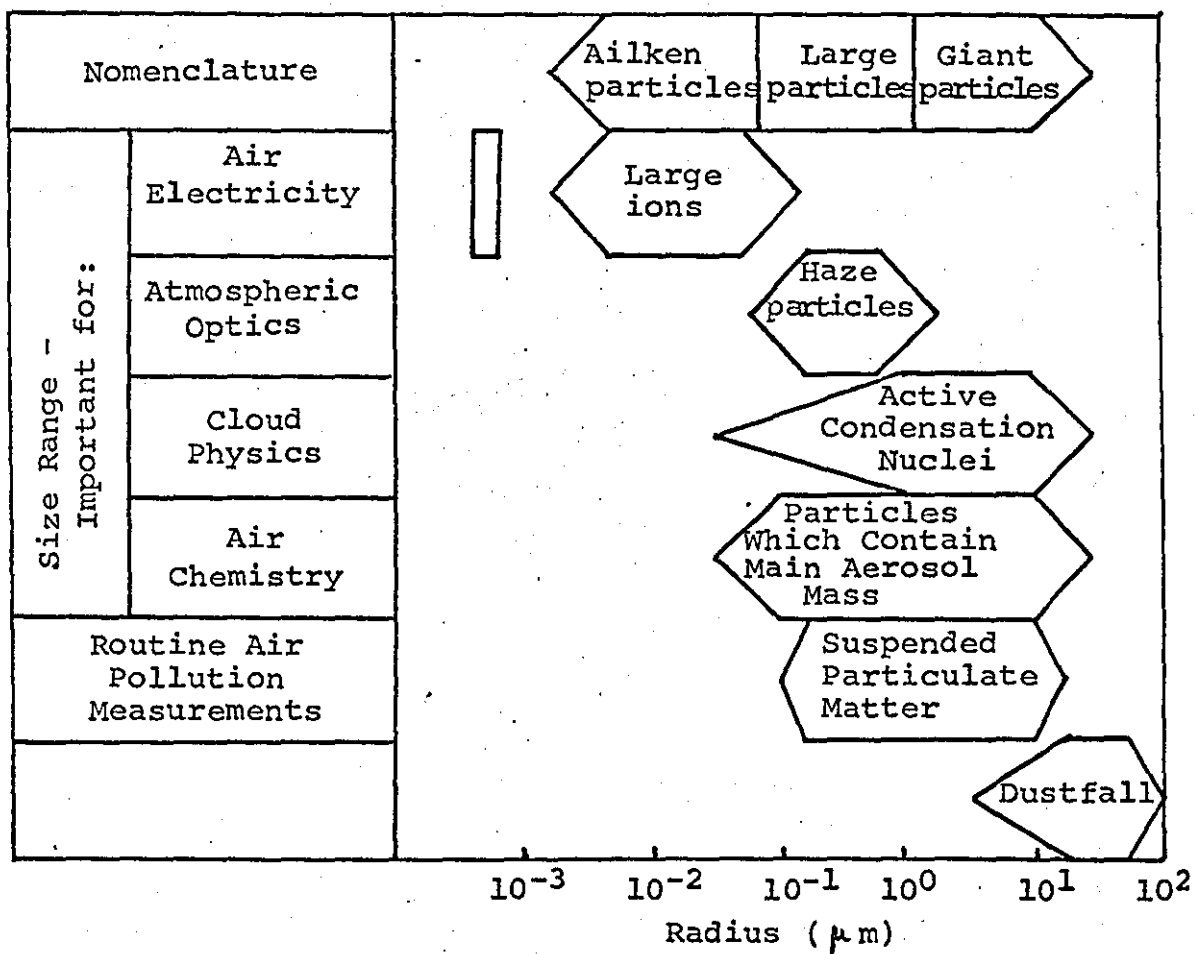


Fig. 5 - Particle Nomenclature (Ref. 67)

A typical plot of the data obtained by many workers was reported by Hidy,⁶² Figure 6. In trying to construct a useful model for the kinetics of the atmospheric aerosol spectrum, it was postulated that a steady state may be achieved in the atmosphere; hence, there should be a balance between particles entering the atmosphere and those leaving it if this postulate is true. This led to the concept of self-preserving size distributions and quasi stationary size distributions, which has caused much debate amongst aerosol physicists.^{9,56,62} Such a concept was recently shown to be incorrect by Davies²²⁸ who suggested that the reason the Junge distribution had been accepted for many years was a consequence of the difficulty of sampling aerosols accurately over a wide range of particle sizes. To better understand the formation and existence of atmospheric aerosols, the ways in which particles enter and leave the atmosphere have to be defined.

2.3.2 Sources of Particles in the Atmosphere

References 56 through 66 contain an abundance of data on particulate sources. McLellan⁸ summarized the data from these sources very conveniently in Table 2. From his table, it is seen that the particulate matter arising from man's activities can account for between 10% and 50% of all particulates present in the earth's atmosphere. Also, it can be seen that a total of between 6×10^8 and 2.6×10^9 metric tons of particulates are emitted from natural and man-made sources each year. These can be summarized in several categories:

1. Soil Derived Particles
2. Sulphur Derived Particles
3. Nitrogen Derived Particles

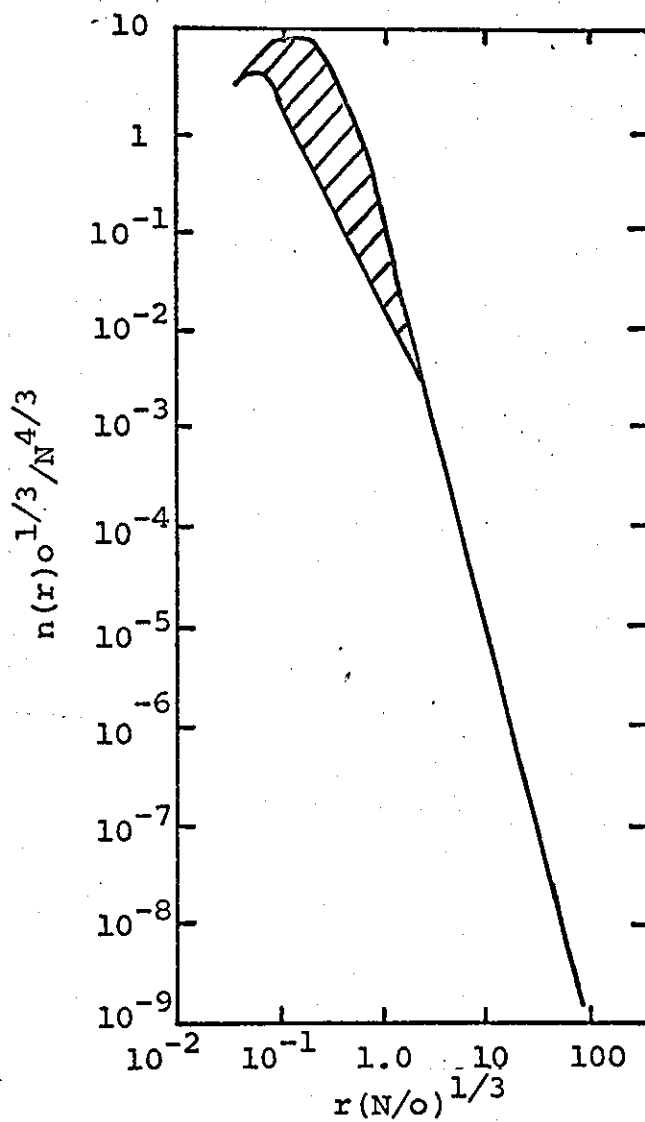


Fig. 6 - Summary of Aerosol Distributions Observed
at the Ground, Primarily in Polluted Areas

TABLE 2

ESTIMATES OF PARTICLES SMALLER THAN 20 μ m.
EMITTED TO OR FORMED IN THE ATMOSPHERE

<u>Atmospheric Particulates from Natural Sources</u>	<u>10⁶ Metre Tons/Yr</u>
1. Soil and Rock Debris	50-250
2. Forest Fires	1-50
3. Sea Salt	300
4. Volcanic Debris	25-150
5. Particles Formed from Gaseous Emissions	<u>345-1100</u>
	421-1850
 <u>Atmospheric Particulates from Man- Made and Man-Actuated Sources</u>	
1. Soil and Rock Debris	50-250
2. Slash Burning	2-100
3. Particulate Emissions	10-90
4. Particles Formed from Gaseous Emissions	<u>175-325</u>
	237-765

4. Organic Matter and Hydrocarbon Particles
5. Particles from Combustion Sources
6. Heavy Metal and Oxide Particles
7. Maritime Aerosols
8. Other Sources

These are not distinctly separate categories as atmospheric reactions occur between them. For example, heavy metals occur in soil derived aerosols, and sulphur derived aerosols in part arise from combustion sources. They are presented here in this simplified manner to give some construction to the discussion, and should only be regarded as a simplified guide.

2.3.2.1 Soil Derived Particles

Soil derived particles are present in the atmosphere as a result of the entrainment of soil, rock, and sand debris by surface winds. Peterson and Junge⁵⁹ suggested that this occurs as a consequence of natural phenomena, but it is aggravated by man-made factors. However, it is very difficult to determine the degree of influence of the man-made factor as they result as a consequence of historic or even prehistoric misuse of the land, e.g., overgrazing or deforestation.⁸ Sears⁷² discussed the varieties and types of airborne dusts and relates their origins or sources to dust storms in the past. Flanigan and DeLong⁷³ examined seventy soil derived particles from locations around the world and determined that their compositions were mainly clay, silica, and calcium carbonate. Dust

fall sampled southwest of the Canary Islands in 1962 was found to consist of silica, clay, and mica with 80% of the particles having diameters between 5 and 30 μ m. The Spanish Sahara was thought to be the origin of the dust. Continental dusts in the Pacific were examined by Prospero and Bonatti,⁷⁴ and by Ferguson, et al,⁷⁵ and again clay was the predominant mineral. The concentration and size of particles from this type of source was shown by Kashina⁷⁶ to depend on location and the wind velocities. During dust storms, the particle concentrations were high and varied with altitude. Prospero, et al⁷⁷ were able to trace dust in the Caribbean to an African dust storm of unusual energy which transported dust across the Atlantic in five days at 40 km/hour; dust concentrations of 2.2 microgram/m³ being measured at Barbados.

Essentially then, windblown aerosols in the atmosphere were found to be chemically similar to the soil from which they originated. They consisted of clay and silica and generally had sizes in excess of 5 μ m. Their size and concentration, however, depended on the wind velocity and the geographical sampling location.

2.3.2.2 Sulphur Derived Aerosols

The atmospheric aspects of the global sulphur cycle were reported by Friend.⁷⁸ Both natural and man-made sources were described, but Friend indicated the difficulty in assessing the former. Volcanoes, for example, constituted only 1% of the total sulphur sources, but were known

to emit large quantities of sulphate aerosols into the stratosphere.⁷⁹ The decomposition of organic matter in soil was also reported as a major source, particularly of H_2S ⁶⁴ but it was difficult to quantitatively estimate. Robinson and Robbins,⁵⁸ however, claimed that 142×10^6 tons of H_2S and sulphate originate from natural sources each year. Such quantities were claimed to represent 66% of the total sulphur emissions, the remaining 34% originating from man-made sources. This latter quantity was present primarily as a result of combustion from stationary and mobile sources. Sulphur dioxide emitted from coal and fuel oil combustion plus H_2S from these and other sources were shown to react in a complex manner in the presence of oxygen, ozone, and moisture to produce sulphuric acid.⁸⁰ Combination of this acid with ammonium salts rapidly gave rise to the presence of ammonium sulphate.⁸⁵

Earlier, Heard and Wiffen⁸¹ described the use of electron microscope analysis to detect ammonium sulphate, and Lodge and Frank⁸² identified both ammonium sulphate and sulphuric acid in the submicron atmospheric aerosol size fraction.

Dry crystals were found to have sizes in the 0.1 μm size range, though it was reported that they were originally collected as droplets of much larger size. This was substantiated by Dingle and Joshi⁹³ who found that ammonium sulphate crystallized out as stages of a cascade impactor after collection.

In addition to the sulphate aerosol, much literature has appeared on a second sulphur aerosol reaction which results in photochemical smog. Though discussed more fully later, it is mentioned here in context with sulphur derived aerosols. Good and Thynne⁸⁴ reported that SO_2 and oxygen undergo photochemical reactions with hydrocarbon to form $\text{R}\cdot\text{SO}_2$ and $\text{R}\cdot\text{O}_2$ radicals, which then undergo further rapid reactions to form particulates.⁸⁴ Many workers related the speed of SO_2 reactions to catalytic activity due to the presence of inorganic particulates.⁸⁶⁻⁸⁸ Urono et al⁸⁹ found that SO_2 in the presence of aluminum, calcium, chromium, iron, lead, and vanadium reacted within minutes even without ultraviolet light.

Sulphuric acid aerosols were found by Lodge and Pate⁹⁰ at all sampling sites in Panama, and they found a progression from ammonium sulphate to sulphuric acid with greater distance inland and greater altitudes. In contrast, Caribbean aerosols were characterized by the presence of ammonium sulphate and the absence of sulphuric acid. Junge and Scheich⁹¹ sampled air in London and three German cities and noted that the acid particles were generally smaller than $0.2\mu\text{m}$, but most of the mass of the aerosol was greater than this size. As for its concentration, Eggleton⁹² determined that the aerosol in the Tees area of England during June to October contained as high as 130 micrograms/metre³ of sulphate over a 24-hour period.

A more recent source of sulphur compounds was shown to arise from jet engine exhausts, primarily from commercial jet liners. McLellan⁸ estimated that 5.2×10^4 metric tons/year of sulphuric acid equivalent are emitted from this single source.

From the preceding data, it can be concluded that the major proportion of sulphur-derived aerosol exist as ammonium sulphate, photochemically created complexes and sulphuric acid. The two former sources are found as sub-micron particulates, while the latter appears as small droplets generally larger in size than 1 micron. These eventually react with ammonia in the atmosphere to produce submicron ammonium sulphate crystalline particulates.

2.3.2.3 Nitrogen Derived Particles

Nitrogen compounds are found in the atmosphere as nitrous oxide, nitric oxide, nitrogen dioxide, and ammonia.⁶⁴

Robinson and Robbins⁵⁸ estimated that 2.7×10^8 tons of ammonia alone are discharged into the atmosphere per year.

Pate⁹⁴ found a large concentration of ammonia, nitric oxide, and nitrogen dioxide in the remote forest of Brazil and Panama, suggesting that vegetation is a natural source.

Lodge and Pate⁹⁰ suggested that the oceans themselves were another source of natural ammonia emissions. The tendency of volcanoes to emit sulphates was discussed earlier in 2.3.2.2, and from this natural source, large quantities of sulphate were found combined with the ammonium ion.

Nitrous oxide is not known to produce particulates from natural sources or by reaction in the atmosphere as it is relatively inert,⁶⁴ but nitric oxide and nitrogen dioxide react readily. Nitrogen dioxide is produced naturally as a result of plant decay and electrical storms.⁶⁴

Forest fires are another natural source, Yamate¹¹⁶ estimating that 1.5×10^4 tons are emitted from USA forest fires per year. Robinson and Robbins⁵⁸ further estimate that natural emissions of nitrogen dioxide could be in the order of 700×10^6 tons from all sources.

Combustion of coal, fuel oil, and gasoline are the major man-made sources of the compounds, as 90% of nitrogen oxide emissions are derived from these origins.⁶⁴ Nitrogen oxides are particularly emitted from those high temperature combustion processes where the combustion gases are quenched rapidly enough to reduce the subsequent decomposition of NO .⁵⁸ It is interesting to note that of the total global emissions of nitrogen oxides, 95% occur in the northern hemisphere, showing the relevant geographical differences in combustion sources and population densities.⁵⁸ In the last two decades, interest in the importance of the atmospheric reactions of nitrogen oxides to form particulates has escalated. Reaction of nitrogen oxides with hydrocarbons, oxygen, and ozone in the presence of sunlight has been shown to produce peroxy-acetyl nitrate. This constitute the photochemical smog aerosol found in Los Angeles and other major cities. Stephens⁹⁵ has reviewed

the reactions involved in PAN formation, and has shown that the reactions yield submicron particulates. Condensation and precipitation reactions also occur, converting nitrogen oxides into the nitrate ion, which further react with free ammonia to form ammonium nitrate particulates. These again are a source of submicron particles in the atmosphere.

2.3.2.4 Organic Matter and Hydrocarbons

Went⁹⁶ estimated that 10^9 tons/year of volatile organic substances are released by natural vegetation throughout the world. Many of these compounds react in the atmosphere to form peroxides, ozonides, or free radicals, which are transformed into submicron particles by photolysis. Went⁹⁷ also reported that such organic matter as pinene vapor reacts with NO_2 in sunlight to form condensation nuclei, and Davies⁹ added that these were responsible for the haze in forested areas. He added that other compounds such as terpene, isoprene, mycene, and carotene are emitted from plants and have a similar potential for reaction. Terpene is also emitted from such diverse sources as plankton and algae, and is responsible for the familiar odor of pinewoods.⁹ Forest fires were claimed to be an additional source of organic particules, Yamate estimating that 6×10^5 tons of particulates arise from wood fires in the USA per year.¹¹⁶

Man-made combustion processes, on the other hand, were found to be the source of a wide variety of organic

pollutants including carcinogenic polycyclic aromatic hydrocarbons.⁹⁸ Man-made sources also accounted for the atmospheric levels of pesticides and in particular DDT in the US urban locations.¹⁰¹ Other compounds such as free amino acids, urea, polysaccharides, aldehydes, and acetic acid were found in rain and snowfall in Russia by Semenov, et al.⁹⁹ Of more importance, Robinson and Robbins⁵⁸ estimated that petroleum related sources accounted for some 88×10^6 tons of hydrocarbons/year. Gasoline usage was estimated to produce 34×10^6 tons/year, refinery operations 6.3×10^6 tons/year, and petroleum evaporation and transfer losses 7.8×10^6 tons/year. Hydrocarbons react with ozone, nitric oxide, and sunlight to form peroxyacetyl nitrate (PAN) or photochemical smog⁹⁵ and this has been extensively studied at urban centers in recent years.¹⁰²⁻¹⁰⁸ Polymerization and condensation reactions have also been found to occur, particularly with unsaturated compounds. These have been suspected as being a source of interparticle bonding; for example, olefin oxides are adsorbed on particle surfaces and polymerize at points of interparticle contact where catalytic activity is high. Semenov⁹⁹ reported that formaldehyde and urea undergo amine-aldehyde condensation reactions at points of particle contact enhancing interparticle adhesion.

A totally different organic species originates from biological sources. Junge¹⁰⁹ described the presence of populations of micro organisms in air, these being greater

than $1\mu\text{m}$ in size and originating from soil sources. In addition, Akermann¹¹⁰ showed the presence of fungi, which were thought to have originated from vegetation. Biological aerosols were thought to constitute as high as 50% of natural aerosols,¹¹¹ but the presence of such compounds as pollens and spores showed wide seasonal variations.¹¹² Finally, Wright, et al¹¹³ showed that under 500 ft altitude, 70% of the viable organisms in air were molds, 19-26% were bacteria, and the remainder were yeasts.

These findings showed that abundant numbers of particles were formed as a result of natural and man-made emissions of hydrocarbons and organic matter. In general, those particles formed by photolysis were submicron in size, those from biological sources had sizes in excess of $1\mu\text{m}$, and those from forest fires had sizes that ranged from the submicron to several centimeters.¹¹⁶

2.3.2.5 Combustion Sources

The combustion of fuel constitutes a major source of particulates emitted into the atmosphere. In 1970 alone, some 0.5 billion tons of coal, some 100 billion gallons of motor fuel, and nearly 60 million gallons of fuel oil were burned in the United States.¹¹⁴

Robinson and Robbins⁵⁸ estimated that the combustion of this fuel plus the combustion of waste in incinerators produced nearly 5×10^9 tons of particulates per year. Emissions from coal and waste sources were shown to fall

into two classes. The first was material from the fuel composition such as SO_2 , NO, and flyash. The second was material from the incomplete combustion of the fuel such as flue gases and soot. Incomplete combustion of coal in residential buildings and factories has yielded vast unknown quantities of fine soot into the atmosphere in past years, and the phrase "dark and satanic mills" was coined as a result of this following the industrial revolution. Carbonaceous material such as soot is emitted as fine carbon particulates of submicron size, but they tend to agglomerate readily to form larger groups of particulates. Flyash, in contrast, is much larger, e.g., it has an average size of $15\mu\text{m}$.⁶⁴ Secondary particulate formation by the reaction of SO_2 , NO_2 , O_3 , and hydrocarbons has already been described as a source of submicron particulates.

Motor vehicle emissions are estimated to yield 1.2×10^6 tons of particulates per year from traffic sources alone.⁶⁴

Internal combustion engines produce mists, smokes, and lead particulates, and the exhaust particulates amount to 5% by weight of the hydrocarbon emission.¹¹⁵ McLellan⁸ reported that aircraft engines release large quantities of carbon into the atmosphere and suggested that 0.1 gm/kgm of fuel is a good estimate. These particles had a size distribution in which 35% was less than $0.01\mu\text{m}$, 60% was less than $0.05\mu\text{m}$, and 99.9% less than $0.5\mu\text{m}$. In total, 5×10^4 tons/year comes from this source.

Emissions from natural gas combustion totaled some 1.9×10^7 tons/year, and those from incinerated wastes 12×10^6 tons/year.

Forest fires were found to emit huge quantities of particles, Yamate¹¹⁶ estimating 6×10^5 tons/year. Emissions from these sources were extremely variable as a result of the fire behaviour and nature.¹¹⁶ Consumable fuel and moisture had an effect, while terrain and wind velocity had minimal effects.¹¹⁶ Green vegetation was found to produce approximately three times the quantity of particulates as dead, dry materials, and the particulates produced ranged in the size from less than $0.1\mu\text{m}$ to large firebrands.¹¹⁶ Burning wood was shown to produce smoke with a mass mean diameter of $0.07\mu\text{m}$, whereas eucalyptus fires in Western Australia produced $0.1\mu\text{m}$ carbon particles and $50\mu\text{m}$ agglomerates of carbon and tar.¹¹⁶ It was difficult to assess the percentage of natural and man-made emissions from this source, but it was stated that man's influence in forest management contributed significantly large amounts of particulates to those from wild fires.¹¹⁶

Combustion sources also yield large quantities of particles in the form of trace metals, and these are now discussed.

2.3.2.6 Trace Metals and Other Inorganic Materials

Lee and Von Lehmden¹¹⁴ reported that trace metals are becoming of increasing importance to air pollution monitoring sources as a result of their hazard to health when inhaled. The major concentrations of trace metals were shown to be

present as iron, lead, zinc and magnesium, and the mass mean diameters of these ranged from 2.3-3.6 μ m, 0.2-1.4 μ m, 0.6-1.7 μ m and 4.5-7.2 μ m respectively. Primary sources of trace metals were summarized as fuel combustion, chemical industries' emissions, and windblown sources. Combustion, grinding, smelting, blending and other processes were also said to lead to aerosol generation.¹¹⁶ The current data indicated that specific heavy metals were concentrated in different size ranges; e.g., particles less than 1.5 μ m in diameter contained higher quantities of lead, cadmium, chromium and manganese, while those greater than 1.5 μ m contained higher concentrations of Al, Co, Cr, Cu, Fe, Mg, Mn, Sb, Se and Ti, whereas smelting operations yielded As, Ag, Be, Cd, Hg, Ni, Sr, V, Cu, Zn, Bi, Li, as additional elements. Fly ash was found to contain Al, B, Be, Cd, Cr, Cu, Fe, Mn, Ni, Pb and V.¹¹⁴

Lead concentrations were related to traffic sources, and Atkins noted that their concentrations in air were proportional to traffic flow in California.¹¹⁷ Sixty-five percent of the lead particulates in air, 30-1750 ft above well-travelled highways, were less than 2 μ m in size according to Daines,¹¹⁸ and such particles were suggested as potential tracers for automobile and man-made sources.⁸ Man-made mercury sources were typically power plants, chemical plants, pesticide plants and junkyards,¹¹⁹ but Kothny stated that most mercury entered the air as a result of evaporation from drying soil. Copper and sulphate ions appeared to be most common near

urban regions.¹²¹ Vanadium was abundant near oil combustion areas, and iron and manganese proliferated around cupola furnaces.¹²²

Windblown dust was suggested to be a source of Sc, Co, Mn, K, Cr, Rb, and Ce as well as a major source of Al, Ca, and Fe.¹²³ Volcanoes were also known to emit large quantities of trace metals and inorganic oxides into the air. In addition, extra terrestrial particles contributed a trace metal population of magnetic spherules of size 2-30 μ m, consisting of magnetite, and containing, according to Rosinski,¹²⁴ Al, Si, Ca, Ti, and Fe. A final class of trace metals was shown to originate from marine sources,⁶⁴ and the nature of these aerosols is now discussed.

2.3.2.7 Marine Aerosols

Israel⁶⁴ stated that the oceans were the largest natural aerosol source of worldwide extent, the primary constituent being sodium chloride. Particles are produced from spray and from fine bubbles which are expelled from the water surface. Particles are also generated from wave crests by the action of winds.

Robinson and Robins⁵⁸ estimated that 1×10^9 tons of maritime aerosols are produced per year, and this is one predominant constituent of atmospheric particles greater than 1 μ m in diameter. The aerosols contain sodium potassium chloride, bromide and iodide ions, but their size was said to depend greatly on humidity conditions in the air.⁹

2.3.2.8 Other Sources

Marchesani¹²⁵ et al summarized other minor sources of particles in the atmosphere and included rubber tire dust from vehicles, organic compounds from perfumes, smoke from cigarettes and cigars, vapors from aerosol spray cans, and others. Though apparently trivial, such sources add to the complexity of the atmospheric aerosol, and it is significant to note that a minor source such as aerosol spray cans has recently triggered international dispute over the effect of its fluorohydrocarbon constituents on the ozone layer of the atmosphere.

One further source not discussed so far is radioactive aerosols. These are present as a result of three major processes: exhalation of radioactive rare gases from the surface of the earth, production of radionuclides by cosmic rays, and production of artificial radionuclides by nuclear weapons tests.⁶⁴

The size spectrum of natural radioactive dust particles having activity was found to be less than $0.7\mu\text{m}$, and little or no activity is found in particles greater than $0.7\mu\text{m}$.⁵⁶ Junge confirmed that except after fresh injection of radioactive debris from weapons tests, particles had diameters between $0.1\mu\text{m}$ and $0.6\mu\text{m}$.⁵⁶

2.3.2.9 Summary

The eight preceding sections have attempted to convey some of the complexity of atmospheric aerosols. It is obvious from these sections that a typical aerosol does

not exist, as each aerosol found on earth is usually highly specific to the region where it is found. This fact enables certain particle types to be used as pollution tracers.

In summarizing the eight subsections, it is perhaps sufficient to say that on a worldwide basis 1.6 billion tons of particulates are put into the atmosphere each year by natural and man-made sources. Of these, approximately one-third are converted sulphates with lesser amounts of converted nitrates, hydrocarbons and carbonaceous matter. A large part comes from mineral and organic particles raised by wind from soil and ocean spray and from photochemical and chemical reactions. A large amount is derived from combustion sources, including fossil fuel and natural fires. Forest fires, volcanoes, extraterrestrial and vegetation sources contribute variable quantities of reactive gases, cellular and crystalline particles to the atmospheric aerosol. For the studies performed in this thesis, a simpler model of an aerosol has to be employed. In the introduction, the effluent from a metals casting plant or small foundry was proposed. To see how this type of emission compares to the complex atmospheric aerosol described previously, current literature on foundry effluents is now discussed.

2.3.3 The Nature and Composition of Foundry Effluents

2.3.3.1 Introduction

The art of iron founding consists of melting a mixture of pig iron, iron and scrap to obtain a melt of a desired

composition. This is then poured into a mold, usually of sand, and cooled to produce a component having a desired size or shape.¹²⁶⁻¹²⁸

Iron foundries range from primitive unmechanized hand operations to highly mechanized plants in which operators are assisted by electrical, mechanical and hydraulic equipment.¹²⁹ Various types of furnaces are employed. These include cupola, electric arc, electrically induced and reverberatory air furnaces. The iron melting process in foundries is the principal source of emissions. Secondary sources include materials handling, casting, shake-out systems, buffing and grinding operations, and coke ovens.¹²⁹ To understand the sources and compositions of these emissions, some time must be spent describing the types of furnaces and their charges in foundry processes.

2.3.3.2 Foundry Processes

The gray iron cupola in its simplest form is shown in Figure 7. This is a straight shaft furnace having a steel shell either lined with refractory or backed by a water curtain for temperature control.¹²⁶⁻¹³¹ A charging door located in the shaft of the cupola admits a charge consisting of coke, iron materials and flux. Tuyeres, located near the bottom of the cupola, admit air for combustion. Provision is made for removing slag and molten iron from openings below the tuyeres, the iron being tapped from the bottom level and the slag tapped

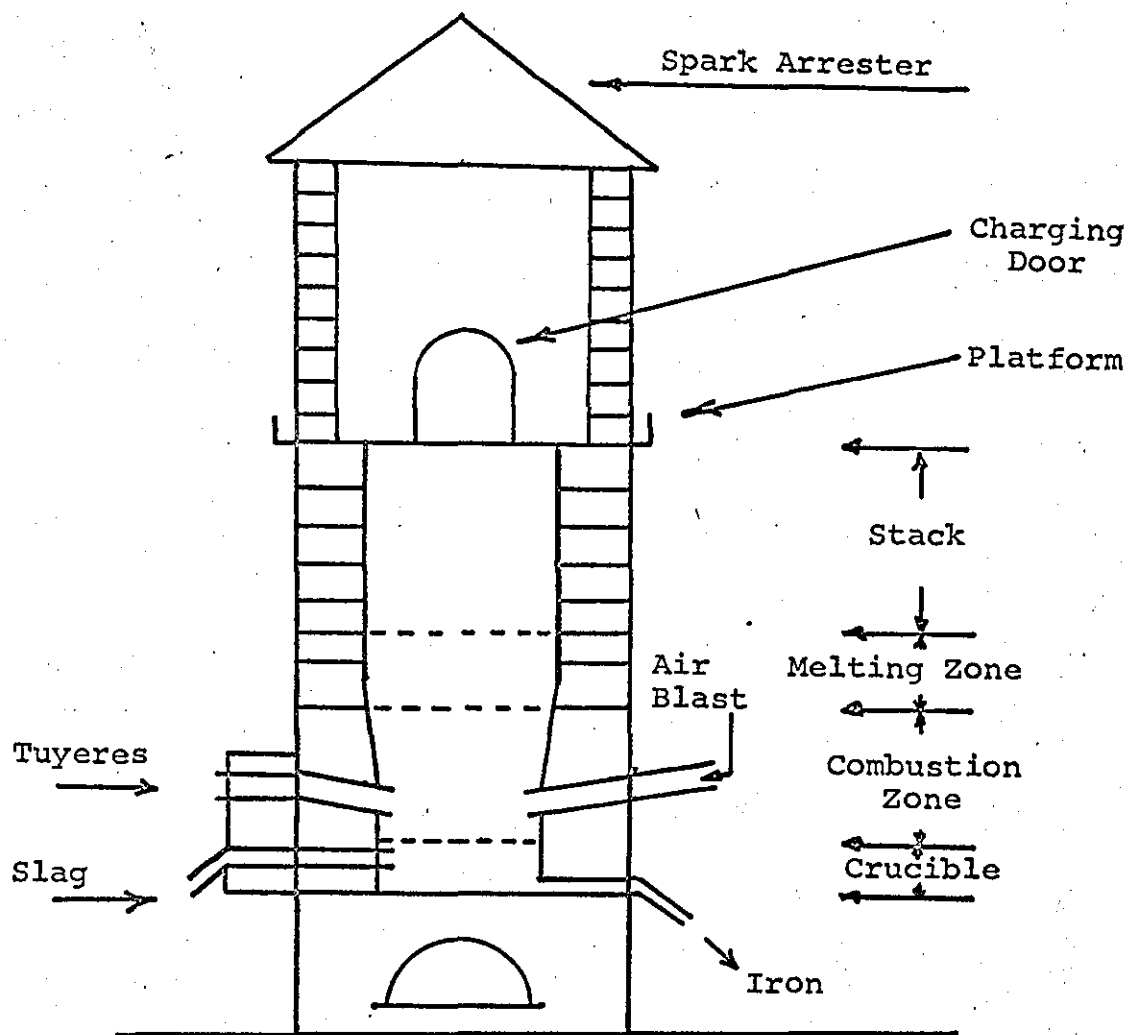


Fig. 7 - Gray Iron Cupola

off from above the iron. The various zones of the cupola furnace are shown in Figure 7.¹²⁶⁻¹²⁹

Physical processes, chemical reactions, and quality of scrap affect the emissions of dust and fumes from cupolas.¹²⁹ Physical processes include entrainment of coke, lime, oil, and grease particles. Nonuniform combustion results in oily emissions of black smoke, and the presence of fine metal chips can significantly influence metal fuming rates.¹²⁹ The quality and composition of emissions vary between cupolas and even at intervals between cupolas. This variation is caused by changes in the iron-to-coke ratios, air volumes/ton melted, and quality of scrap.¹²⁹ A charge containing limestone with a low degree of hardness and a large proportion of fines will produce a relatively high dust concentration in the waste gases.¹²⁹ The abrasion resistance and ash content of the coke also has an effect on the emission. Poor abrasion resistance and high ash contents produce effluents of higher and finer particle concentrations.

Electric arc furnaces are used to prepare special alloys of iron.¹³⁰ Here heat is generated by an arc formed between two electrodes. In the indirect arc furnace, the electrodes are placed above the charge and heat is transferred to the charge by radiation and from the surface lining.¹²⁶⁻¹²⁸ The furnace is shown in Figure 8 to consist of a horizontal body through the axis of which enter two graphite electrodes. The furnace is mounted on a base which rocks back and forth during the operation. It has the advantages that the quality of material

produced can be better, e.g., free of dirt and oils; higher degrees of superheat can be applied, and they can be easily maintained. For special alloys needing accurate control of compositions, these furnaces fulfill the need. They have a nonoxidizing atmosphere and can melt small scrap without high dust emissions. Emissions that do emerge are usually submicron metallic fumes. In the direct arc furnace the electrodes are simply placed in the molten metal.¹³⁰

Electrical induction furnaces, Figure 9, are used to prepare extremely pure metals.¹²⁶⁻¹³⁰ They consist of a crucible surrounded by a water-cooled coil of copper tubing through which a high frequency electric current is passed. This establishes an alternating magnetic field that, in turn, induces secondary currents in the metal. These heat the metal rapidly. The furnaces are available in two types, consisting of high frequency and low frequency respectively. The furnaces use extremely clean scrap and expose the metal to air for a minimum amount of time. Consequently, negligible amounts of emissions result. The ones that do emerge consist of metal oxides.¹²⁶⁻¹³⁰

Finally, air furnaces or acid hearth furnaces are used to produce malleable iron. A typical furnace is shown in Figure 10. In this type the heat is supplied by fuel oil or coal and the flames pass over and above the metal bed. The metal is protected from the flames by a layer

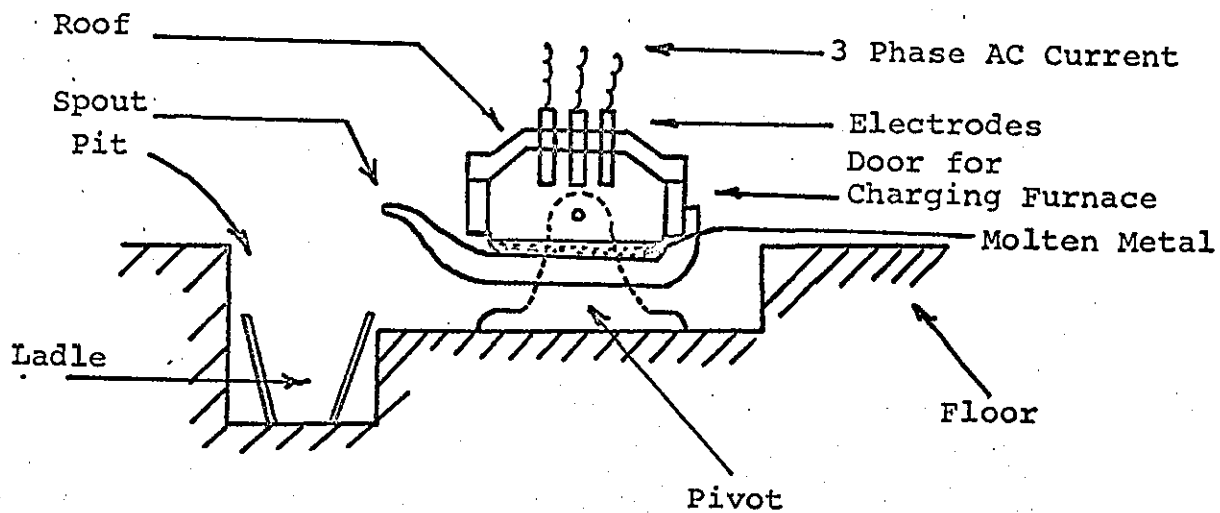


Fig. 8 - Three-Phase Electric Arc Furnace

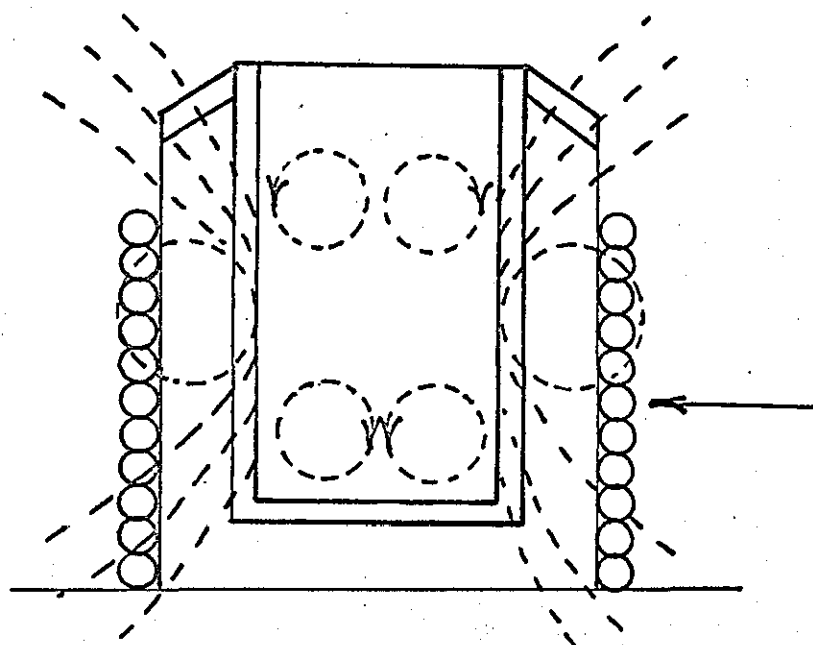


Fig. 9 - Electrical Induction Furnace

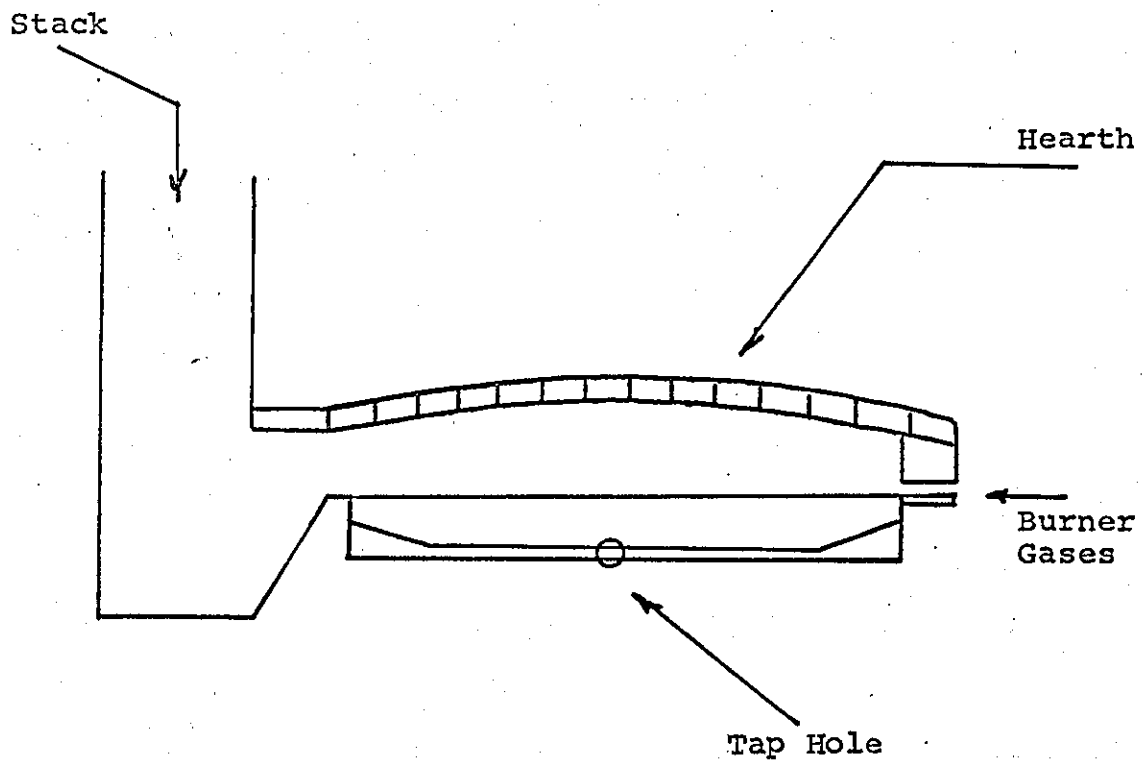


Fig. 10 - Open Hearth Air Furnace

of slag, and since the heat is independently supplied, the rate of heating, temperature and metal composition can be easily controlled.¹²⁶⁻¹²⁸ Emissions from this source are unspecified.¹²⁹

In addition to these processes, other sources of emissions are casting shake-out systems, buffing and grinding, coke ovens and sand molding. These emissions are small compared to cupola emissions, as will be seen in the following section.¹²⁹

2.3.3.3 Emission Rates from Foundries

Table 3 summarizes the data available on foundry sources. Though very scarce, the data compiled only really reflects cupola data. Other sources are expressed as being very inaccurate.^{129,132,133} Cupola emissions can be seen to be the dominant source. Sources from materials handling processes seem extraordinarily high, but as these are the only data available, they are quoted here.

2.3.3.4 Characteristics of Effluents from Foundries

The chemical and physical properties of foundry effluents are summarized in Table 4. Cupola dust dominates the emission, yielding 105,000 tons/year of the 143,000 tons emitted from foundries.¹²⁹ Particulates contain coke, flux, various metals, their oxides, and some sulphates. Silica content is high, particularly in the 0-10 μ m fraction. Of the metals portion, 60 percent are oxides of silica and iron, but significant amounts of zinc and

TABLE 3

EMISSION RATES FROM FOUNDRIES

<u>Source</u>	<u>Emission Factor Lbs. of Particulate Per Ton of Hot Metal</u>	<u>Emission Tons/Yr</u>
1. Furnaces		
a) Hot Blast Cupola	15	105,000
Cold Blast Cupola	23	
Electric Arc	5-10	
Induction	Negligent	
Air Reverberatory	-	
2. Materials Handling	5	37,000
3. Coke Ovens	0.3	1,000
4. Sand Molding	0.3	
		<hr/> 143,000

TABLE 4

CHARACTERISTICS OF FOUNDRY EFFLUENTS

<u>Source</u>	<u>Particle Size</u>	<u>Solids Loading</u> <u>Grams/Cu Ft</u>			
Open Cupola	2-30% < 5 μ m	0.3-15	SiO ₂	Cr ₂ O ₃	Ni
	2-35% < 10 μ m		CaO	Metals	Cu
	10-40% < 20 μ m		MgO	Carbon	Co
	20-60% < 50 μ m		Fe ₂ O ₃	H ₂ SO ₄	Ag
			MnO	Sn	
			Al ₂ O ₃	TiO ₂	
			PbO	Mb	
			ZnO	Zr	

lead oxides are also found. Other elements include manganese, chromium, tin, titanium, molybdenum, zirconium, nickel, copper, cobalt, and silver.^{132,134,135,137}

The range of particle sizes given in Table 4 covers 24 cupolas, and Figure 11 shows the extremes of this range and the arithmetic mean for uncontrolled cupolas. Under some conditions over 50 percent of the dust can be less than $1\mu\text{m}$, whereas in others less than 5 percent can be below $2\mu\text{m}$. Particle size distributions also vary in hot and cold cupolas (Figure 12). Sulphur emissions are usually low because the sulphur compounds in coke are 0.6 percent or less in concentration. SO_2 concentrations can vary between 25 and 250 ppm,¹³⁷ but when combined with moisture, sulphuric acid droplets form. These often corrode, surrounding equipment. Fluorine and hydrofluoric acid are also occasionally emitted.¹³⁴ Fine carbonaceous smokes are sometimes discharged, and metallic fumes can originate specifically from arc furnaces.

2.3.3.5 Control of Foundry Emissions

Control equipment for open cupolas, other furnaces, and miscellaneous dust sources in foundries is described in several publications.^{129, 132-136}

Electrostatic precipitation, wet scrubbers, and fabric filters have been employed for this purpose.¹²⁹ A typical system for a cupola employing a wet scrubber is shown in Figure 13.

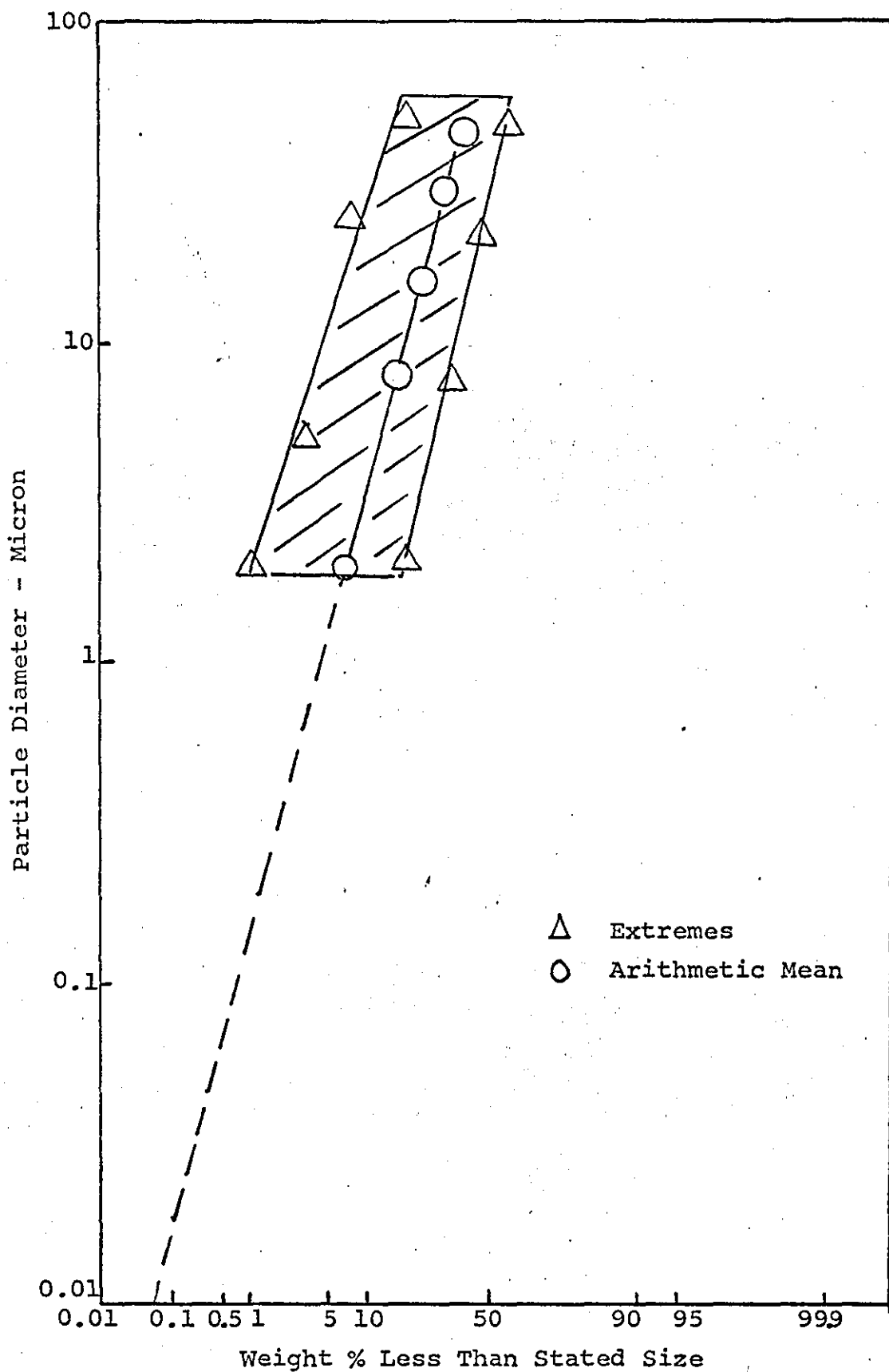


Fig. 11 - Particle-Size Distribution of Particulates
Emitted from Uncontrolled Iron Foundry Cupolas

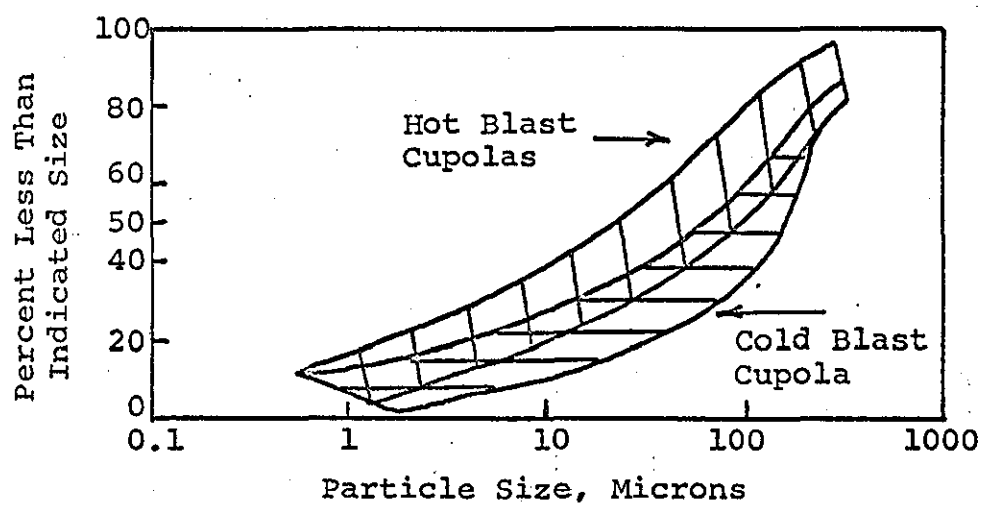


Fig. 12 - Particle Size Ranges for Dust from Cold and Hot Blast Cupolas

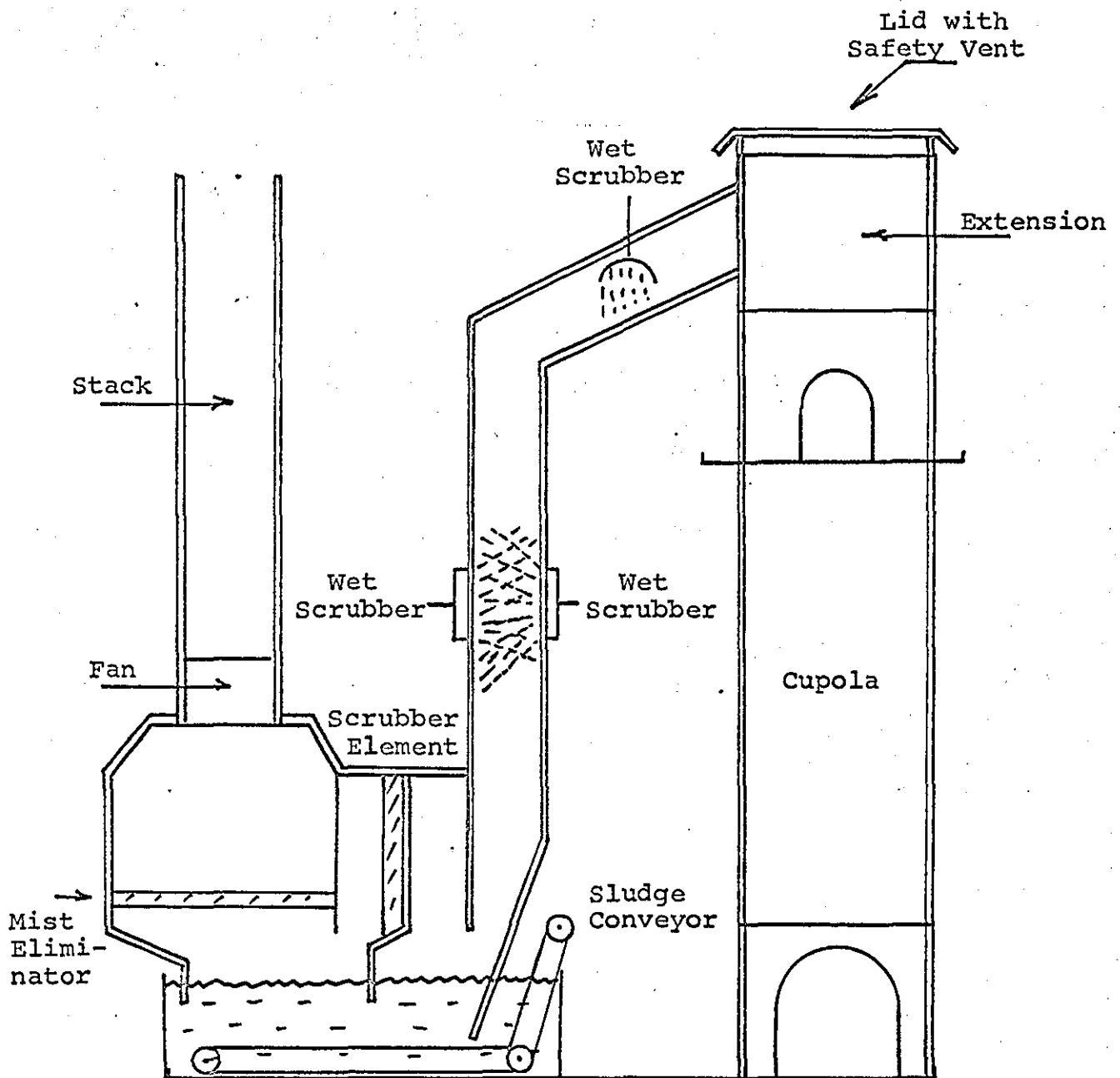


Fig.13 - Cupola with Wet Scrubber Control Equipment

More recent papers have discussed the performance and cost of this equipment¹³⁸⁻¹⁴¹ and have discussed the economics of replacing cupolas with arc furnaces.¹⁴⁰ As 75 percent of foundries in North America are small, e.g., employ fewer than 75 people, replacement of cupolas or implementation of costly control equipment would cause them to operate at a loss.¹⁴⁰ Consequently, in many instances, cheaper, less efficient control devices such as cyclones are used. These reduce the concentration of coarse particles but do not eliminate the emission.¹²⁹ Instead, an emission consisting predominantly of 0-10 μ m particulates is released.

2.3.3.6 Summary

A comparison of the nature of foundry effluents with the general concept of an atmospheric aerosol, discussed in 2.3.3, shows several striking similarities.

Firstly, the size distributions are comparable. Secondly, the presence of carbon, silica, alumina, iron oxides, sulphuric acid, and other trace metals is very similar in composition to the windblown dust, combustion product, and sulphuric acid portion of the atmospheric aerosol.

A marked dissimilarity occurs in that ammonium sulphate and nitrate, sodium and potassium halides, and hydrocarbon and organic complexes are virtually absent from foundry effluents.

However, if one simply considers the separation of particles of a permanent nature, e.g., water insoluble compounds, then the similarity between the foundry aerosol and a general urban atmospheric aerosol is fairly good.

Consequently, for such a limited separation system, the foundry effluent would be a good model to use.

2.3.4 Mechanisms of Removal of Particles from the Atmosphere

Aerosol suspensions are fundamentally unstable and cannot persist unless continuously or periodically reinforced to replace particles being removed by natural forces.⁶⁵

Gravity continuously acts on aerosols and results in sedimentation which increases as the particle size increases. Particles larger than about 1μ have terminal velocities of fall which exceed Brownian motion displacements. The reverse is true for submicron particles, and they would have exceedingly long airborne lifetimes except for other factors.²³

Particles in suspension also tend to agglomerate, and the rate of coagulation increases with increasing particle concentration. Since the number concentration of atmospheric aerosols reaches a maximum in the submicron range, growth of these small aerosol particles by coagulation is an ever present mechanism which would result in a decreasing number concentration except for a continual replenishment of submicron particles.⁵⁶ Thus, as the submicron particles collide with and attach to other particles,

whether submicron or larger, they eventually become either attached to an agglomerate of sufficient size to fall to the surface of the earth or are scavenged by snow, rain, or hail.¹⁵ Electrostatic charges on aerosol particles, unless unipolar, will enhance coagulation. Positive and negative ions produced by ionizing radiation in the air attach themselves to nearby particles to produce charged particles.⁵⁶

Thermal gradients in the air can result in particle migration (thermophoresis) toward a colder collecting surface, e.g., an evaporating droplet or a snowflake descending through warm air.²³ Vapor pressure gradients can result in particle migration (diffusiophoresis) in the direction of low vapor concentration.²³ Thus, vapor condensing on a drop will tend to transport particles to the drop surface unless balanced by a repelling thermophoretic force.²³

Air-suspended particles illuminated by sunlight can move in complex paths depending upon the light intensity, color, pressure of the air, particle size, shape, material, and on additional fields such as electric and magnetic.²³ Such motions induced by illumination are known as photophoresis. At sea level, particles below $0.1\mu\text{m}$ will be very photophoretic. Also, ferromagnetic particles will show magnetophotophoretic motion in the direction of the magnetic field of the earth.²³ The photophoretic or magnetophotophoretic velocity in sunlight at sea level is of the order of 10^{-2} cm/sec and can even result in

particles rising against gravity in the atmosphere under certain conditions.²³ Coagulation by these mechanisms leads to ultimate sedimentation.

Falling particulates, rain, and snow will accumulate additional particles during their descent through impaction and interception.^{68,69} The sampling of snow or rain can be an effective means of collecting particulates from the volume of air through which the rain or snow falls. Examination of particulates removed through the centuries by accumulated polar snows has revealed much information concerning atmospheric aerosols in ages past.

Atmospheric aerosols also interact with gases and vapors. Condensation nuclei tend to be hygroscopic such that a rise in humidity will cause particle growth. Condensation can start on hygroscopic nuclei at comparatively low humidities, as indicated by Houghton.⁷⁰ Hygroscopic gases, such as SO_3 and NH_3 , will also react with water vapor to produce droplets at low humidities. Vapors also adsorb on particle surfaces through physical adsorption, and reactions can be promoted or catalyzed by particles which contain active components. The inevitable presence of adsorbed or absorbed moisture on atmospheric particles leads to solution of soluble components and can result in recrystallization and mechanical binding of agglomerates through interparticle crystallization. Even in the absence of soluble components, adsorbed moisture will hold particles together through capillary force effects.

The presence of soil-derived aerosols containing transition elements also provides catalytic surfaces which could promote chemical reactions. These reactions could result in a still more tightly bound aggregate. It has become evident as well that many other reactions in the atmosphere, including the Los Angeles smog, occur preferentially on the surface of particles already in suspension, often coating them with a heavy layer of added material.⁷¹

These methods of interaction, which eventually result in their removal from the atmosphere, can be summarized in a number of categories. These are shown in Table 5.

Hidy⁶² presented a mathematical model to represent the formation and removal of particles in the atmosphere and suggested that in the absence of rain clouds, collisions due to Brownian motion, turbulence, and eddy diffusion dominate the coagulation phenomena and sedimentation terminates the existence of particles in the air. Thus, at ground level, settled or collected submicron particles are generally found in the agglomerated form; otherwise, it would be unlikely that they would have settled at all.

2.3.5 Summary of the Atmospheric Aerosol Literature and the Philosophy of the Separation Study

In the preceding atmospheric aerosol literature survey, the general size distribution, concentration, and composition of the particles usually present in air were

TABLE 5

REMOVAL MECHANISMS FOR ATMOSPHERIC AEROSOLS

1. Growth of Particles by Heterogeneous and Homogeneous Gas Reactions on the Surface of Particles and Their Ultimate Sedimentation
2. Diffusional or Convective Coagulation Followed by Sedimentation
3. Thermophoretic and Photophoretic Coagulation Followed by Sedimentation
4. Scavenging of Smaller Particles by Large Ones in Turbulent Velocity Gradients
5. Gravity Sedimentation
6. Impaction on Obstacles and Other Particles
7. Diffusional Deposition on Surfaces, e.g., Buildings
8. Washout Under Clouds
9. Rainout Inside Clouds
10. Electrical Charge Coagulation Followed by Sedimentation

discussed. There was evidence to suggest that most atmospheric aerosol size distributions measured displayed similarities in shape, which allowed their normalization on a universal curve. The hypothesis that the aerosols were self-preserving was reported and found to explain large portions of the curve, but some discrepancies were reported by Davies^{9,228} and Hidy⁶². The size distribution of particles present in the air was seen to contain large numbers of particles in the submicron size category, and the natural mechanisms that agglomerated them were found to be diffusion controlled. After coagulation, the particulate agglomerates were finally separated from the air by natural sedimentation and washout, and eventually reached ground level. Because of the wide variety of sizes and compositions present in the atmosphere, the composition of the settled agglomerates can be extremely variable. For example, the agglomerates can contain a mixture of particles of windblown soil, carbon, chemically reacted sulphates and nitrates, organo-complexes, sea salt, biological matter, and a variety of trace metals. Also, the discrete size distribution and composition distribution within each agglomerate can be postulated to be either wide or narrow, depending on both the composition of the air from which they came and the mechanism by which the agglomeration took place. For example, pure diffusional coagulation of sulphates could create an agglomerate consisting of all 0.1-1 μ m sulphate particulates, whereas coagulation by impaction or interception

caused by a large particle falling through a mixture of smaller ones could produce an agglomerate of size 0.1-100 μm having a variable composition. Hence, an atmospheric agglomerate can be extremely variable in size and composition and is too complex a model to use in any preliminary separation investigation. Instead, a simpler model is needed. In Chapter 1, the emission from a metals casting plant or small foundry was suggested as one alternative, and for this reason the foundry effluent literature was searched. The results showed that such a model was a good choice, for both physical and chemical tracer studies. These are defined as those studies in which the size, shape, and composition of the particles are used to fingerprint the emission. The results showed that the size distributions of the emission and the atmospheric aerosol were very similar, but that the number of chemical species present in the former was much less than in the latter. However, of extreme importance was the finding that the water-insoluble particulate fractions of both effluents were somewhat similar, and providing that this specific fraction was studied, the foundry effluent was an excellent model to use. In contrast, the water-soluble particulate fraction of the atmospheric aerosol containing such compounds as halides, sulphates, and nitrates was absent from the foundry effluent as were organo-complexes and biological matter. However, for the use of particles as physical tracers, these deficiencies in the model created no

disadvantage. Physical tracer studies demand the use of permanent particle structures, and water-soluble compounds which are humidity sensitive and prone to washout by rain are not suitable for this task. It should be emphasized, however, that such compounds would be extremely useful for chemical tracer analysis and cannot be overlooked in these instances.

By this logic, it was decided to use the foundry effluent as a model for the separation studies in this thesis, but only the separation of the water-insoluble particulates would be undertaken. As these were generally submicron in size and in the form of inorganic and trace metal oxides, separation of these compounds was to be given priority. The method found suitable for these materials would, however, be investigated for its potential on separating carbon and clay, the other common water-insoluble particulate components of the atmosphere. In addition, some consideration would finally be given to its modification for use with water-soluble compounds so that a method for separating the complete atmospheric aerosol could result. This latter phase will contain no experimental work, but it will be viewed as a projection for future work.

With such a specific study now defined, the final portion of the literature survey can be presented. Methods of separating inorganic oxides will be studied both for the purpose of measuring the interparticle force relationships

and separating and recollecting them for tracer studies. This will be preceded by a section in which the most suitable liquids, chemical additives, and chemical conditions for the conditioning or dispersing of metal oxides will be investigated. This will be directed towards finding the most suitable conditions for particle separation.

2.4 Methods of Conditioning and Separating Particles from Surfaces and from Agglomerates

2.4.1 Methods of Conditioning Particles and Surfaces

2.4.1.1 Introduction

This section first reviews the literature published on the methods of conditioning particles to reduce their interparticle attractive forces. Particular reference is given to the conditioning of water-insoluble inorganic metal oxides in aqueous media. When this has been done, the methods of measuring the resultant interparticle forces in liquid media are reviewed. Finally, the methods of separating particles from agglomerate structures are discussed, and those methods with the most potential for success with submicron particles are selected for use in the experimental studies.

2.4.1.2 Methods of Conditioning Metal Oxides in Liquid Media

In Sections 2.2.1 through 2.2.9, it was shown that the interparticle attractive forces were largely dependent on both the properties of the particles themselves and

the nature and properties of the liquid. The minimum interparticle forces were found to exist when the maximum electrical double layer repulsive force was acting. This was shown to be a function of the liquid pH, ionic strength, dielectric constant, and the nature of the ions adsorbed on the particle surface. The maximum repulsive force was, in fact, found to be acting when the above variables were optimized to produce the maximum double layer thickness and maximum surface charge around the particle. Hence, separation was much easier to perform when this maximum force was acting. The term "conditioning" of the particle then refers to the achievement of the optimum particle-liquid conditions necessary to produce the maximum double layer repulsive force. As this force is a function of the ions adsorbed on the particle and the thickness of their charge layer, the section will concentrate on defining those ions which adsorb readily and strongly on metal oxide surfaces and those conditions which produce the maximum charge from the resulting double layer. Wnek²¹ showed that the choice of media was different, depending on the particle size to be separated. Submicron particles were best separated in aqueous media where the ionic strength and dielectric constant were high. Particles larger than 1 μ m. were conversely best separated in nonpolar liquids where these values were low.

It was shown in the literature that the most important mechanism by which ions strongly adsorb onto metal oxides in water was hydrogen bonding.

Campbell, et al,¹⁴² described the types of bonding that could take place between ions and solid hydrophilic surfaces. In all aqueous dispersions, they found that there was a tendency to form hydrogen bonds between ions and the solid surface, but the main difficulties in investigating the presence of such bonds were due to a lack of knowledge of the reactivity of groups that were potentially hydrogen-bonding. They showed that hydrogens attached to oxygen and nitrogen were particularly prone to hydrogen bonding, even if the compounds were sulphonated. Sulphonation of a molecule with a consequent high degree of solvation in water did not impair its ability to form hydrogen bonds in aqueous solution. A hydrogen attached to a carbon formed hydrogen bonds much less readily, but it could be made to do so if activated by strongly electronegative groups, and such bonding, e.g., by a hydrogen in chloroform, was well known.

Similarly, a carbonyl oxygen could activate a hydrogen attached to a carbon atom, and it was suggested that by these means the aldehyde group and certain ester groups could act in water as proton donors towards nitrogen atoms in a second solute. Long, et al,¹⁴³ showed that the dimensions of forces at solid interfaces, e.g., the forces of adhesion between ions and surfaces, were of the same magnitude as those associated with hydrogen bonding. They studied the possibility of a monomolecular layer of water remaining on solid surfaces after vigorous heating

and showed some hydroxylation of steel surfaces still existed after heating to 800°C. They concluded that hydrogen bonding was a major component in the process of adhesion of ions to solid surfaces.

Although Long had proposed that hydrogen bonding was of major importance in the adhesion of ions to surfaces, Trudgian and Prihoda¹⁴⁴ suggested that the physico-chemical affinities of materials were responsible for many other properties of materials such as miscibility, solubility, compatibility, dispersion, and adhesion. To investigate this further, let us first consider the case of two pure solvents. Burrell¹⁴⁵ developed an integrated theory on miscibility, solubility, and compatibility of two or more solvents based on two parameters, the solubility parameter and the hydrogen bonding value. He showed that two solvents were miscible when their solubility parameters and hydrogen bonding values were similar. For the case of a resin or a polymer dissolving in a solvent, the same rule appeared to hold. Burrell then published tables of solubility parameters and put forward hydrogen bonding values for many solvents to aid in paint formulation. These hydrogen bonding values were determined by Gordy^{226,227} and Lieberman.¹⁴⁶ Lieberman assigned values of hydrogen bonding numbers to solvents which Burrell had placed in the groups of poorly, moderately, and strongly hydrogen-bonding solvents. These numbers were 0.3, 1.0, and 1.7 respectively. If in some

cases a polymer did not dissolve in a solvent of value 1.0 or 1.7, two solvents with these values could be mixed to provide solvent with an equivalent value of 1.3, e.g., when the polymer dissolved readily.

Thus, Lieberman was able to estimate the values of several other solvents by determining the solubility limits of selected polymers in mixtures of unknown solvents with those to which values had been assigned. In this way he was able to fit more precise hydrogen-bonding values to solvents, polymers, and resins and produce complex tables to improve those of Burrell. By plotting the square of these values against the solubility parameter, he was able to form solubility maps which graphically showed the solubility characteristics of typical polymers.

Trudgian and Prohoda¹⁴⁴ then published a paper in which they discussed the application of hydrogen-bonding parameters to predict not only solvent miscibility, compatibility, and solubility, but resin solubility and particle dispersion. They found that solvents such as ethyl alcohol, isopropyl alcohol, ethylene glycol, and n-butanol dispersed TiO_2 pigments better than any other solvents. After much searching to find the key to explain these results, they found that the hydrogen-bonding values of all four solvents were identical. Extending this to other pigments, they showed generally that hydrophilic inorganic pigments dispersed well in strongly hydrogen-bonding solvents, e.g., alcohols, and examples of typical

pigments were yellow oxide of iron, medium yellow chrome oxide, rutile titanium dioxide, and molybdate orange. Red iron oxide dispersed in moderately hydrogen-bonding solvents, e.g., ketones. Organic pigments, such as phthalocyanine blue and green and carbon black, dispersed best in moderately to weakly hydrogen-bonding solvents, e.g., esters, while dark "Bon-Red" pigment dispersed in weakly hydrogen-bonding n-nitropropane.

Hence, the hydrogen-bonding value of solvents could be used effectively to condition particles on surfaces in terms of their hydrogen-bonding tendencies. Strangely enough, no immediate notice was taken of this paper for several years, but in the polymer field, the concept of the solubility parameter was extended quite successfully.

Gardon¹⁴⁷ took the work of Lieberman further by investigating the correlation between solubility parameter, hydrogen-bonding value, and dipole moment. Crowley, Teague, and Lowe^{148,149} used these three parameters and resins, which predicted accurately the solvent type or mixture to use for any polymer. Similar work was done by Hansen,¹⁵⁰ but in his second paper,¹⁵¹ he extended this to pigments. He was able to show quite clearly that pigment dispersion in pure solvents could be predicted by the 3-D mapping system.

Lee¹⁵² introduced a fourth parameter of interest to the dispersion field when he studied the correlations between

the three parameters above and surface tension. Finally, Eissler, Zgol, and Stolp¹⁵³ studied sedimentation volumes of settled dispersions of zinc oxide and related them to the 3-D solubility parameters of the solvents used.

From these studies, it was seen that hydrogen bonding was the major mechanism of ion adsorption onto metal oxide surfaces in water, and it was indicated that the presence of hydroxyl groups on particle surfaces from strongly bonded water was the source of sites for effective hydrogen bonding to take place. This was confirmed by several experimental studies.

Every, et al,¹⁵⁴ studied the adsorption of methyl alcohol and water on rutile from hexane and showed a high value for the heat of wetting for both water and alcohol. Wade and Hackerman¹⁵⁵ studied the heat of wetting (ΔH) of hexane on rutile as well as water and methyl alcohol. They showed that ΔH increased slightly with increase in the degassing temperature, but that ΔH was very much less than the ΔH for alcohol and water. They attributed the high ΔH s with alcohol and water to the formation of hydrogen bonds between the surface hydroxyls and the alcohol and water molecules. With hexane no hydrogen bonding took place as the ΔH was small. This association of high heats of wetting with hydrogen bonding was also reported by Wade & Hackerman.^{156,237,238} Parfitt and Wiltshire¹⁵⁷ studied the adsorption of alternate members of a homologous series of aliphatic straight

chain primary alcohols on rutile. They studied ethanol and octadecanol from solution in p-xylene. A strong amount of each alcohol was adsorbed at relatively low concentrations which reached a minimum at hexanol and octanol, indicating the importance of water solvent interaction at the solid liquid interface.

Day and Parfitt¹⁵⁸ studied the adsorption of ethanol, n-octanol, and n-dodecanol on rutile from binary mixtures of p-xylene and n-heptane. Again they discussed hydrogen bonding and the interaction between the aromatic solvent and the hydroxyl groups which leads to competitive adsorption. The magnitude of this was shown to depend on the fraction of the surface covered by molecular water. The aliphatic solvent competed for the non-hydroxylated region which was again related to the water coverage. Thus, the hydroxylated surfaces of metal oxides were the sites at which hydrogen bonding took place. Ions that adsorbed by this mechanism could therefore be particularly useful as conditioning agents, providing that they produced a high surface charge. Such compounds as phosphates and silicates were found to do this in aqueous media.

Livanova, et al,¹⁵⁹ commented on the coagulation strengths of rutile suspension structures in the presence of impurities when treated with orthophosphate and metasilicate. Both ions stabilized rutile, but a pronounced effect was found with a dialyzed rutile when

surface impurities had been removed. Masaji, et al,¹⁶⁰ and Krupskii, et al,¹⁶¹ showed that phosphate ions can undergo specific adsorption regardless of the charge on the surface due to hydrogen bond formation. Ermolaeva, et al,¹⁶² showed that phosphoric acid could be adsorbed on TiO_2 to a degree that increased with the amount of electrolyte added. Such adsorption led to the production of high surface charge.

Dickman, et al,¹⁶³ and Kelley¹⁶⁴ commented that meta-silicate ions adsorbed similarly to phosphate and its stabilizing action was enhanced by the adsorption of strongly hydrated silicic acid from the hydrolysis of sodium metasilicate.

Some information on the mechanism of the phosphate hydrogen-bonding tendency was provided by Vissers¹⁶⁵ who studied the sorption of orthophosphate on the hydrated oxides of zirconium, hafnium, cerium, and thorium. The sorption of the phosphate ion was thought to be related in a stoichiometric manner to the surface hydroxyls. Models of the sorption process were suggested which assumed a tetrahedral phosphate molecule. From this model they indicated that the PO_4 ion was adsorbed with a stoichiometry of either 2 or 3 hydroxyl groups per sorbed PO_4 molecule. Low and Ramamurthy¹⁶⁶ investigated the adsorption of phosphorous compounds on oxides occurred by hydrogen bonding between the $-\text{PO}(\text{OH})$ group and the surface hydroxyls. When this group was present,

the hydrogen-bonding effects were very much greater than with carboxylic acids.

The ability of the phosphate ion to satisfy the hydrogen-bonding tendency of a solid surface was demonstrated by Eissler, et al.¹⁵³ They investigated two pigments - zinc oxide and phosphate-treated zinc oxide, and attempted to isolate the three effects of Hansen's three-dimensional solubility maps to study the important contributors. They measured sedimentation volumes as an indicator of dispersion on flocculation and found that for the untreated zinc oxide almost all the effect on sedimentation volume took place as the hydrogen-bonding tendency of the solvent was varied. With the treated pigment only, the polar parameter affected the sedimentation volume while the effect of the hydrogen-bonding tendency of the solvent was nil. Here the phosphate had clearly neutralized the hydrogen-bonding sites on the pigment surface.

In a similar way to TiO_2 , Wade and Hackerman showed high heats of immersion for Al_2O_3 and explained them in terms of hydrogen bonding.¹⁶⁸

The use of phosphates to disperse alumina was mentioned by Bakker and Bartok,¹⁶⁹ and they found the same type of reaction took place between the phosphate ion and the surface hydroxyls as demonstrated by TiO_2 . Again, like TiO_2 , the use of ions to neutralize the hydrogen-bonding tendency of the alumina surface was discussed by Peri.¹⁷⁰

He studied the effect of adsorbing fluoride on surface sites on alumina and showed that the effect of surface hydroxylation could be neutralized by fluorine treatment.

The adsorption of phosphate ions on red iron oxide was demonstrated by Tokiwa and Imamura,¹⁷¹ and once again the mechanism was one of hydrogen bonding. The tendency of the ferric oxide to require moderately hydrogen-bonding solvents was mentioned by Trudgian and Prihoda.¹⁴⁴ This is most probably due to the electronic configuration of the ferric oxide surface, which is less electronegative than either the alumina or the titanium dioxide.

Tokiwa and Imamura¹⁷¹ also showed that the nature of the phosphate was important. In studying the effect of various phosphate compositions on the surface charge on TiO_2 and Fe_2O_3 , they found experimentally that with pyrophosphates of general formula $\text{Na}_{2n}\text{P}_n\text{O}_{4n-1}$ the charge was at a maximum when $n = 3$. Wnek¹⁷² later calculated the surface charge produced by phosphates and found that, generally, as the oxygen species increased in the molecule, surface charge increased, but with increasing hydrogenation it became less. Thus, the nature of the phosphate adsorbed, effected the surface charge on the particle, and such compounds as pyrophosphates were particularly good conditioning agents for metal oxides.

2.4.1.3 Summary

The work reviewed in this section has indicated that hydrogen bonding is the most important bonding mechanism

between solid particles and adsorbed ions in aqueous suspensions. These bonds are strong and permanent, and hence any agent bound to the surface in this way will not be removed without considerable effort. Alcohols, monoamines, and carboxylic acids appeared to be effective conditioning agents. In addition, diamines, phosphates, and silicates were adsorbed using 2-3 surface hydroxyls per ion and formed stable surface coatings on most oxides. The oxides of silicon, titanium, aluminum, iron, hafnium, zirconium, thorium, cerium, and zinc were all shown to adsorb phosphate ions readily in aqueous media, and it appeared to be a general rule that all hydroxylated oxides in aqueous media were dispersed by phosphate treatments. However, it was shown that the composition of the phosphate had a marked effect upon the magnitude of the surface charge produced. Pyrophosphates were found to be particularly good conditioning agents, but their formulation had to be selected carefully if high surface charge values were to be obtained.

Also, the use of a hydrogen-bonding solvent series to predict the separation characteristics of particles appeared to be most encouraging, and could lead to a good method of classifying particulates according to their dispersibility and charge requirements.

2.4.2 Methods of Measuring the Force of Adhesion in Liquids by Separating Particles from Plane Surfaces

2.4.2.1 Introduction

Several methods have been employed to separate particles from substrates, some of which have been useful to measure the force of adhesion. Before each method is discussed, it must be emphasized again that the removal of identical particles from a surface is based on probability. If several identical particles are deposited on a surface, the force required to remove each one will be different. Complete separation of all particles will require a significant increase in the force field. As a result, it is common to report the force of adhesion data as a relationship between the number of particles removed from the surface under the influence of a specific force and the magnitude of the force. A value termed the "adhesion number" is expressed as the ratio of the number of particles remaining on the surface to the number initially there, after each force application. In some cases, however, detachment occurs in layers of particles, and this is discussed in detail by Zimon.²² Sometimes adhesion is expressed in the form of the number of rotations of a centrifuge, the frequency of oscillation of a vibrating plate, or the angle of rotation of a dusty plate. In estimating the force, it is realized that there is a minimum force under which the first few particles are removed and a maximum force under which the majority are removed. Orr and Kordecki²⁸ and Zimon²²

showed that it was better to estimate the force as being that value at which 50 percent by number are removed under the specific conditions and measuring method used in the experiment. This is now accepted as being the better method of relating adhesion measurements, but it is not without error.²²

2.4.2.2 Experimental Methods Used to Measure the Force of Adhesion

The following experimental methods have been used to measure the adhesion force of single particles on surfaces.

- a) Varying the slope of a surface
- b) Microbalance technique
- c) Pendulum method
- d) Centrifuge method
- e) Aerodynamic method
- f) Vibration method

Zimon²² reviewed the first method and pointed out that particles were dusted onto a surface at the bottom of a vessel which was rotated through specific angles until the particle separated from the surface. It was later modified by constructing a special cuvette mounted on a microscope.²² The method was used by Schubert and Wibowo¹⁷³ for large glass spheres in liquids, but it was generally found to be of little value for particles of size less than 20 μ m.

Corn⁵⁴² reported that microbalances were usually based on the use of quartz fibres which can take the form of a

cantilever, helical spring, or torsion balance. Electronic microbalances sensitive to $0.1 \mu\text{ gm}$ are commercially available, and Corn⁵⁴³ used a cantilever-type microbalance to study $5\text{-}90\mu\text{m}$ particles. The problem with the method was that single particles had to be attached to the balance spring of beam, and for submicron particles, this was impossible. However, one variation of this technique was used by Beischer¹⁷⁴ who allowed coagulating threads of individual Fe_2O_3 particles of $0.5\mu\text{m}$ diameter to break under their own weight. His work indicated that for submicron particles in air, the adhesive force was 0.5×10^{-4} dynes. This was not used in liquid media.

McFarlane and Tabor¹⁷⁵ used the pendulum method for measuring the force of adhesion between large particles. The particle was suspended on a vertical fiber in contact with the substrate. The substrate was then raised and tilted so that the angle between the fiber and the substrate increased. The angle between the fiber and plane at the moment of separation was then recorded. This method was restricted to air and was limited to large particles with high mass.

Of much greater value to the requirements of this thesis was the method of centrifugal separation.

Kordecki, et al,²⁸ used a centrifuge in studies of the adhesion of particles to a flat surface. Determinations

were made of the size distribution of the particles initially sprinkled on a slide and of the size distributions of those remaining after subjection in discrete steps to successively higher fields of force. The maximum acceleration applied was in excess of 8 g. At maximum acceleration, nearly all of the largest particles and a significant fraction of the smallest particles were removed.

"Boehme, Krupp, et al,^{29,176,177-183} used an ultracentrifuge capable of producing forces in excess of 10^6 g. Because they used a very narrow size range of particles, they plotted their results differently. They compared the percent of particles adhering versus the applied force (dynes) and found that the variation of force with particle size was small. Apparently the larger acceleration required for small particles was a consequence of their small mass. Also, these authors gathered some data on the influence of surface composition and texture on the adhesion of particles to the surface.

Deryagin, et al,¹⁸⁴ used centrifugal fields which provided up to 300,000 g, but they did not succeed in removing all 5μ diameter glass particles from a polished steel rotor.

On comparing the various possible errors, Zimon²² concluded that: "The main error in the centrifugal method is due to the different sizes of the particles in a specified fraction.

"In order to avoid errors associated with the rate of rotation, one must increase (or reduce) the revolutions of the centrifuge smoothly in order to eliminate the effects of inertial forces, holding the specified number of revolutions for several seconds. Further increasing the time of centrifuging has no effect on the detachment of dust particles in air. In centrifuging it is important to take proper precautions against vibrations of the body and heating of the centrifuge axis, since these effects may distort the results of measurements made on the force of detachment.

"In the practical use of this method for liquid media a number of special features have to be taken into consideration. The whole space in the cylinder (or cuvette) must be filled with liquid in order to prevent the liquid from moving in the course of centrifuging and thus eliminate the influence of side effects. Owing to the difficulty of hermetizing the cylinder (or cuvette) the number of revolutions of the centrifuge in the methods employed is no greater than 3000 and the detaching force no greater than 10^2 - 10^3 g. The time of centrifuging should be about 1 min, so that hydrodynamic factors associated with the way in which the dust-laden surface is situated in the liquid medium may be fully taken into account."

Because of its value in separating a wide range of particles, the centrifugal method of measuring the value of the detaching force has been the principal method used

in determining forces of adhesion. The advantages of the method lie in its simplicity and accessibility, and also in the reliability of the results and the rapidity of the measurements. In addition to this, a variety of conditions may be created in the centrifuge test tubes (humidity, temperature, pressure, etc.), which widens the experimental potentialities of the method. However, in order to obtain the integral adhesion curve several measurements have to be made with different numbers of revolutions.

Small particles (of under 10μ diameter) were found to stick so firmly to surfaces that forces corresponding to accelerations of the order of (10^3-10^4) g were incapable of overcoming the adhesive forces.¹⁸⁵ This explained the tendency to use ultracentrifuges for detaching small particles. However, an attempt at using an ultracentrifuge of the UTs-2-A type (produced by Mikrotechna of Prague) was unsuccessful. On rotating a sphere in the magnetic field of this centrifuge in vacuum, the sphere with the particles attached to it became heated. The heat melted particles consisting of fusible materials (for example, polymers),⁹⁸⁴ and this distorted the results of the measurement.

Of high significance to this thesis was the work reported by Davies, Ranade, and Werle.^{224,225} Typical inorganic oxide aerosol particles were employed and their forces of adhesion measured by the centrifugal method in aqueous phosphate solutions.

After the conditions of the experiments were controlled, useful data was taken on the force of adhesion of ferric oxide, carbon, and clay particles to substrates of stainless steel, ferric oxide, carbon, and silica.

The experiments were designed to investigate the effects of surface roughness, surface composition, particle size, particle composition, and temperature on the force of adhesion, and the experimental values were then compared to those calculated from theoretical models.

The results showed good agreement with theory and indicated that the molecular separation distance between the particle and the surface was in the order of 9 to 14 Å.

This agreed well with results reported in the literature.

For particles in contact, Bailey, et al,²²⁹ showed that a separation distance of 7 ± 2 Å was the most realistic.

The extensive data on ferric oxide agreed very well with this hypothesis, but the values on carbon and clay were not in such good agreement. This could be due to two factors. Firstly, insufficient experimental data was available on carbon and clay to conclusively measure the true force of adhesion. Secondly, the Hamaker constant used in the theoretical expression for clay was the value for silica, and this will introduce a second error. In addition, the theory assumed a spherical shape for the clay particles, which was not accurate. A shape factor should have been implemented into the theoretical expression to account for the plate-like nature of the clay,

but this was not done. Even with these errors, at 9 Å separation distances experimental values of 1.8×10^{-5} and 1×10^{-5} dynes for carbon and clay were measured compared to the theoretical values of 9×10^{-5} and 10×10^{-5} dynes.

The experimental data showed several interesting trends. Firstly, the effect of surface roughness appeared insignificant for particles less than $0.7 \mu\text{m}$ in size. Secondly, the force of adhesion between agglomerates was less than that for conglomerates. Thirdly, temperature had a highly significant effect on the force of adhesion, the force being much less at 60°C than at 25°C . Finally, the particle size distribution removed from the surfaces was very wide, spanning the full range of sizes originally deposited, but having a slightly coarser mean size than the initial distribution.

This work showed that the mathematical models did predict the force of adhesion between submicron particles fairly well. The theory was actually indicating a slightly higher force of adhesion than the experimental work suggested. This theoretical force was found to be about 10^{-4} dynes for 50 percent removal of particles and 10^{-3} dynes for the complete removal. Hence, any design of a separating unit based on these theoretical grounds should be more than adequate to experimentally separate submicron particles.

Another method that was used for submicron particles in air was the aerodynamic method. Unfortunately, the limitation of the aerodynamic method was found to reside in the difficulty of defining aerodynamic conditions in the vicinity of adhering particles. In the absence of a well-defined velocity field, results had to be expressed as efficiency of particle removal versus an air velocity characteristic of the particular system used. With a well-defined velocity field, it was possible to calculate, approximately, the air drag on particles at the time of their separation.

Though of no direct value to the current study, the aerodynamic method did produce some results which had a bearing on atmospheric particle separation.

From the experimental results obtained in the field, it was found that weathering processes continuously introduced changes in the collected surface layer of particles so that a simple relationship between the amount of contaminant resuspended and the wind speed only applied in some situations. As a result of weathering, a contaminant tends to become fixed at the site of deposition, and Corn and Stein¹⁸⁶ showed that for 1μ particles, only 20 percent of those that should have been removed were separated due to this effect. Therefore, particles collected from the atmosphere could have different outer particle forces dependent on the amount of weathering that had taken place. As a conclusion to this method, Fuks¹⁸⁷ considered

that for particles below 0.5μ complete dispersion has never been achieved by air jet methods and could not see that they would ever be of real value for this size range.

Finally, the use of the vibration method to measure the force of adhesion was reported by Zimon.²² It was found that the vibration method had been used only for determining the adhesive force of dust in air. For this purpose, either low-frequency (20-30 cps) or high-frequency (hundreds or thousands of cps) vibrations had been used.

With the high-frequency system, the sound vibrations, previously amplified, set in motion a dynamic diffuser to which the dust-laden plate was attached. The frequency of the oscillations was usually no greater than 2 kcs and the value of the detaching force reached 2500 g.

By varying the frequency of the vibrations, one could vary the detaching force over a wide range. In order to increase the range of detaching forces, one could use an ultrasonic system generating oscillations at a frequency of 10-20 kcs.¹⁸⁵ Here the value of the detaching force was $(10-24) \cdot 10^4$ g.

2.4.2.3 Summary

The various methods of measuring the force of adhesion between particles and surfaces have been discussed. For the separation of submicron particles in liquids, the

centrifugal method of Böehme, et al,²⁹ and Krupp¹⁷⁶ is considered the best approach. A modification of this method was employed by Davies Ranade and Werle^{224,225} to measure the force of adhesion of submicron inorganic oxides in aqueous phosphate solutions. It was shown that a force of 10^{-4} - 10^{-3} dynes was necessary to separate particles from various surfaces and that this force should be applied to agglomerate systems to separate them. In separating particles collected from the atmosphere, the effect of weathering was shown to be important, as particles were shown to be more tightly bound to surfaces after weathering had occurred.

2.4.3 Methods of Separating Particles from Agglomerates

2.4.3.1 Introduction

The methods of separating industrial powder agglomerates into discrete and aggregate populations were discussed by Parfitt.⁴⁷ The methods of ultrasonics, high- and low-speed shear, ball milling, and roll milling were used in liquid media, and fluid-energy milling was used in steam. For the separation of industrial powders, large quantities of agglomerated solids have to be dispersed or separated, and consequently, many of the devices used were designed for high solids throughputs. For the purpose of separating small quantities of solids with a minimum particle loss, as would be the case in this thesis, many of the techniques are inapplicable. However, a brief discussion of the methods is now given, and in the summary, the ones most suitable for trial in the experimental portion of this thesis are defined.

2.4.3.2 Methods of Separating Agglomerates

The first method discussed is ultrasonic. The mechanism of the action of ultrasound on a suspension is not fully understood. As a result of this, non-optimum conditions are often used. Ultrasound, depending on operating conditions, may have either a dispersing effect or a coagulant effect on a liquid suspension. Carlin¹⁸⁸ noted that the presence of gases and pressure influence the dispersing action, while the coagulating action depends on the frequency. Neduzhii¹⁸⁹ has presented an extensive review of

ultrasonic emulsification. Although the particles that we are concerned with are solid, this review is useful in selection of operating parameters for optimum operation.

Egorov¹⁹⁰ considered changes in the double layer at the particle-medium boundary in an ultrasonic field. The modification of the interfacial charge was the main cause of coagulant action of ultrasonic field on hydrophobic colloids. The effect of amplitude of the ultrasonic field was also studied. For amplitudes up to 120 \AA (at 400-2500 K Hz) dispersion is predominant. At higher amplitudes (up to 310 \AA) coagulation is prevalent, reaching a maximum at 180 \AA . Above 310 \AA dispersion was once again observed.

In addition to the factors discussed above, the temperature, pressure, and the duration of ultrasonic action have effects on the interaction of particles. Pohlman, et al,¹⁹¹ reported the effect of temperature on the clearing action of ultrasound. Higher temperature increased the clearing action, and 60°C appeared to be the optimum temperature to use.

Fridman¹⁹² made a first attempt to find a theoretical basis for the interaction between the cavitation bubbles and the particles in a suspension. This rather crude model suggests that above $2 \mu\text{m}$ dispersive action was brought about by the collapsing bubbles. Smaller particles tend to collect just beyond the boundary layer of the bubble and coagulate.

Experimental evidence from other studies, however, shows that dispersion of submicron particles was possible, indicating that the theoretical treatment of Fridman could not be generalized.

Brodov, et al,¹⁹³ report that during precipitation the particle size decreased from $> 1\mu\text{m}$ without ultrasound to $< 0.3\mu\text{m}$ in an ultrasonic field under atmospheric pressure. At a pressure of 24 atmospheres, the particle size further decreased to $0.08\text{--}0.1\mu\text{m}$. Holl¹⁹⁴ also noted that the dispersion was promoted at high pressures.

Sato and Yamane¹⁹⁵ fractionated a volcanic ash with the use of ultrasound. Most of the inorganic and organic complexes were separated from the aggregates easily. The clay minerals were less than $2\mu\text{m}$ diameter and other minerals containing Fe oxides and sand were less than $0.5\mu\text{m}$ in diameter.

Kaiser¹⁹⁶ found that ultrasonics were useful in the separation of carbon, calcium fluoride, and other compounds and found that separation in fluorinated hydrocarbons worked well.

Reports of other uses of ultrasound for dispersion were given by Agabalyants, et al,¹⁹⁷ who studied the dispersion of clay. It was found that the ultrasound again changed the structure of the suspension during the dispersion. The release of ion complexes from surfaces by ultrasound was also reported by Lowe and Parasher¹⁹⁸ who studied the dispersion of soils.

Various types of ultrasonic devices have been used for the separation of submicron particles. Hislop¹⁹⁹ reported two devices that utilize the ultrasonic energy most efficiently.

From this information it is seen that ultrasonic treatment at high pressure, e.g., 24 atmospheres and at 60°C, should separate the particles of interest. It can be applied over the particle size range required in aqueous media and can be applied to small volumes of sample. Contamination should be at a minimum providing clean-hood conditions are used in the sample preparation phase. No particles should be lost, and temperatures of 60°C will be easy to maintain.

In contrast to ultrasound, dispersion or separation of particles is achieved by mixing agglomerates in liquids using various types of machinery.

Cozzens²⁰⁰ studied the high-speed mixing of various powders and liquids in a planetary-type laboratory mixer fitted with an open planar blade. He found that the rate and degree of separation were increased by increasing the vehicle viscosity, particle concentration, and mixing speed, and that changes in the particle and vehicle nature drastically changed the rate and degree of separation. Other related work on high-speed dispersion was

reported by Guggenheim²⁰¹ and Schliesser, et al.²⁰²

These latter authors confirmed some of the findings of the previous authors when working with a flat paddle mixer with a four-blade impeller. This was similar to the laboratory Waring Blender. They showed that better dispersions were always obtained at higher pigment concentrations, while the rate of separation only depended on the energy input and indirectly on the mixer speed. Both Wade and Taylor²⁰³ and Ensminger²⁰³ reported that with very high-speed impellers, a low-viscosity vehicle was important. In spite of these series of experiments and reported mixing conditions, Dowling²⁰⁵ reported that under optimum conditions, formulation and geometry, high-speed mixers were not necessary, and in fact, the use of lower shear rate equipment could produce similar degrees of separation more economically. In support, a recent paper by Armstrong²⁰⁶ emphasized the usefulness of low peripheral speed impellers in the paint industry, and using a rotary saw-tooth variety he was able to show that high particle concentration and low liquid viscosity gave higher pigment yields/batch at a lower operating temperature than high-viscosity vehicles. This supported an earlier paper by Weisberg²⁰⁷ who had studied the influence of shear stress-shear rate profiles of a system on the rate and degree of dispersion of medium chrome yellow pigment. He used a smooth cylindrical impeller at slow speeds and showed that the rate of separation increased with the torque until turbulence set in.

In a system of proper rheology, ie., at a controlled Reynolds number with no turbulence, Weisberg reported that a cylindrical impeller provided a more efficient mode of power input than high-speed processes. Recent studies were performed by Daniel²⁰⁸ who used them for soft textured pigments.

The use of ball mills to disperse powders in liquids was reported by Daniels²⁰⁹ and Shurts²¹⁰. Fisher²¹¹ pointed out that the efficiency of ball milling was increased as the size of the ball was reduced; hence, the sand mill or sand grind was introduced in which the effective ball size was one sand grain. The operation of the sand mill was discussed by Bosse²¹² and by Brownlie²¹³ who studied TiO_2 pigments. Recent work on the efficiency of ball milling was reported by Vavra²¹⁴. One variation of the sand mill is the micromedia mill in which particles of compositions other than sand, e.g., glass beads, are used. It is patterned after a sand mill or wet attrition mill which has been used in the paint industry to de-agglomerate pigments and produce particles of size 0.3 to $1.5 \mu\text{m}$. Mölls and Hörnle²¹⁵ investigated this method and found that the size of media governs the minimum size of product. By selection of suitable conditions, a product as fine as $0.1 \mu\text{m}$ should be attainable.

In this type of mill the media, which may consist of sand or any variety of hard or resilient spheres, are set in motion by paddles or discs which stir them.

Agglomerates which find themselves between two media are subjected to a force, tending to break them up. The action is similar to ball milling, except that the impacts between media are much gentler and seldom result in breakage of ultimate particles, especially if the media are sufficiently small. Also, there is relative motion throughout the mill, and the rate of dispersion is greater than in ball milling because there are more impacts.

Notable comparisons of the techniques of sand milling, ball milling, and impeller dispersion were reported by Ensminger²⁰⁴ and Garrett and Hess.²¹⁶ These latter authors compared the three techniques with a fourth one - roller milling for TiO_2 and Fe_2O_3 pigments. They found that the ball mill, sand mill, high-speed impeller, and triple roll mill all gave good degrees of separation, and with TiO_2 , the degrees of separation were similar. The significant differences were shown in the rates of separation, which varied widely. The triple roll mill was superior to all the other three methods, and it dispersed the particles in one pass. The sand and ball mills were significantly slower, and the high-speed impeller was the slowest of all.

With red iron oxide, differences in the degree of separation were also found. The high-speed impeller never achieved the same degree of separation as the other three methods which, once again, were quite similar. As

before, the rates of separation were widely different, the triple roll mill being the fastest in achieving the best degree of separation. However, this was only true when a high liquid viscosity or a high solids concentration was employed. For an aqueous suspension having a low particle concentration, the triple roll mill is generally not as effective as an impeller or ultrasonic device.

2.4.3.3 Summary

From this literature review, three methods emerge with potential for separating submicron particles from agglomerate systems. Treatment with ultrasonics at high pressure has been reported as successful down to $0.08\ \mu\text{m}$. High-speed impeller mixing, ball milling, or micromedia milling have been successful for pigment dispersion. These methods should be investigated for their use in the separation of atmospheric particulates.

2.5 Methods to Indicate the Degree of Separation Attained

2.5.1 Introduction

This section is concerned with the techniques that are available as indicators to inform the analyst of both the degree of separation that has been attained by a specific separation process and the stability of the dispersion with respect to time.

The most common methods of assessing the degree of separation and the suspension stability are measurements of turbidity, size distribution, and sedimentation volume with respect to time. For highly concentrated suspensions, rheological properties such as the viscosity, shear strength, etc., are employed.

In this thesis the first two indicators are the most important, and only if higher particle concentrations are studied will other factors be considered. In addition to these measurements, it has been shown that a change in zeta potential, pH, electrical conductivity, and surface active agent concentration can induce instability in stable suspensions. Hence, measurements of these parameters have to be simultaneously recorded in any study to enable changes in a suspension to be explained and understood.

Hence, measurements that have to be made on each dispersion are ideally:

1. Suspension Turbidity and Mean Particle Size

2. Sedimentation Volume
3. Change in Mean Size and Size Distribution with Time
4. Zeta Potential
5. pH
6. Electrical Conductivity
7. Surface Active Agent Nature, Purity, and Critical Concentration

The methods that are available for these determinations are as follows:

2.5.2 Suspension Turbidity and Mean Particle Size

The use of light absorption to measure the turbidity and size characteristics of suspensions has formed the subject of much literature over the last twenty-five years.

Recent usage of turbidity to follow the degree of dispersion of pigments was reported by Koglin²³⁶ who measured the optimum concentration of pyrophosphate required to disperse zinc suspensions.

2.5.3 Sedimentation Volume

The use of sedimentation volume to assess the state of dispersion of pigments has been widespread. Examples of the method have been given by Weisberg,²¹⁷ Princen,²¹⁸ Tokiwa and Imamura,¹⁷¹ and Eissler, et al.¹⁵³ The method merely consists of shaking a known volume of powder with either a solvent or a surface active agent solution in a tube and then letting the suspension stand for a period of time. Frequent examination of the sediment in the

tube enables the sediment volume to be measured and a plot made of sediment volume versus time. At any one time, stable suspensions will show a negligible sedimentation volume, while unstable suspensions will show a large sedimentation volume. Weisberg²¹⁷ cautioned the analyst about placing too much value on this test to measure the degree of agglomeration. This was in direct conflict with the work of Dintenfass²¹⁹ who explained that the degree of agglomeration could be estimated from the sedimentation volume. Weisberg's caution was based on the effect of dielectric constant on agglomeration, and he advised persons using the method to check each sediment microscopically and not to place complete confidence on the sediment volume measurement. Similar work was reported by Yashiro.²²⁰ However, in most cases, Dintenfass' theory holds, and the method is considered a most convenient one for long-term studies.

2.5.4 Change in Mean Size and Size Distribution

In the introduction to this report, a powder was defined as a statistical group of discrete particles, agglomerates, and aggregates, and the difference between agglomerates and aggregates was defined in terms of the bonding strengths. An agglomerate was defined as a statistical group of discrete particles bound together by weak physical bonds, while an aggregate was defined as a statistical group of discrete particles bound together by strong chemical bonds. Dispersion techniques then

broke agglomerates down into discrete particles. leaving aggregates intact.

Hence, any improvement in a dispersion would always lead to the formation of a finer size distribution, and any coagulation or agglomeration of the suspension would produce a coarser size distribution. Thus, size analysis can be a useful tool to follow dispersion and agglomeration phenomena of suspensions. The determination of only the mean size of a suspension of particles is also useful as this will change with dispersion or agglomeration, but the full size distribution is better as it demonstrates the overall agglomerate sizes that are present at various times. The advantage of the former is speed of analysis, and that of the latter is more information.

Examples of the use of size analysis are given by Parfitt⁴⁷ and Matthews and Rhodes.

For submicron particles of uniform composition, the particle size distribution can be conveniently measured using centrifugal sedimentation.²⁴ The Joyce Loebel disc centrifuge is useful for this purpose, and its design and operation are given in reference 24.

For non-homogeneous submicron particles, such as will be found in atmospheric aerosol systems, electron or scanning electron microscopy has to be employed. Here the state of separation has to be estimated from the state

of the suspension after recollection on a fine filter. Such a technique was developed by Kaiser,¹⁹⁶ and will be used in this thesis. From photomicrographs of the recollected particulate system, the state of subdivision can be quantified by use of the separation efficiency factor. This is defined as:

$$\frac{\text{the number of discrete particles/10,000X field}}{\text{the number of discrete and non-discrete particles/10,000X field}} \times 100\%$$

To measure this parameter, photomicrographs of particles recollected on a 0.1 μ m Nuclepore filter are examined at 10,000X magnification on an S.E.M. The number of single particles/field are counted and their projected area diameters measured. These are termed "discrete particles". At the same time, the number of non-discrete particles, defined as those images in which two or more particles are in contact, are counted and sized. The separation efficiency factor can then be calculated.

2.5.5 Zeta Potential

The measurement of the mass transport, charge, and zeta potential of particles in suspension has been used by many authors to correlate suspension stability. Many of these are recorded by Parfitt⁴⁷ and no further references are necessary. There are several types of apparatus that are available to measure zeta-potential, and these were reviewed in a paper by Sennett and Olivier.²²² One of these units was later developed by these authors at the Freeport Kaolin Co., and the unit was licensed to the

Micromeritics Instrument Co. for manufacture. This unit has the advantage of being used over a concentration range of 1.5%-70% by weight. Another unit useful for low-particle concentrations was the Zeta-Meter, developed by Riddick.²²³

2.5.6 pH and Electrical Conductivity

There is no need to dwell on the types of measuring techniques for the determination of the pH and conductivity of suspensions. These are well-known in all branches of physical chemistry. In this thesis, a Beckman Zeromatic pH meter is used with a standard calomel and glass electrode system for pH, and a Fisher conductivity cell and meter are used for the electrical conductivity.

2.5.7 Surface Active Agent Nature, Purity, and Critical Concentration

The nature and purity of each surface active material can be obtained from the manufacturer, and where this is insufficiently pure, the material can be purified.

Each substance has to be diluted to known active strengths in aqueous media and stored as stock solutions.

The critical concentration of each substance on the submicron powders under study can be determined by plotting the adsorption isotherms in aqueous media or measuring the size distribution at various agent concentrations. Here critical concentration is defined as the minimum surfactant concentration which produces the best degree of dispersion. For surfactants at low concentrations, this

can be achieved by surface tension measurements or by the determination of conductivity.

2.5.8 Particulate Samples

For the purpose of the experimental program, powders and aerosols need to be sampled for analysis. Allen²⁴ describes the methods available for sampling powders, and in this thesis, a rotary sample divider was used exclusively. For sampling aerosols, particularly atmospheric aerosols, a wide choice of methods prevail.²³ However, many of these are intentionally size selective, which is a feature not required for this thesis. In this thesis a very wide range of sizes, including agglomerates, need to be sampled; hence, a simple method, such as high volume filtration, was considered the best choice. This was supported by a method involving sedimentation to specifically collect settled large agglomerates.

2.5.9 Summary

From this information, the state of subdivision achieved by the separation process can be quantitatively determined by monitoring the change in the size distribution for each change in the surface active agent concentration, the solution temperature, pressure, etc. For homogeneous powders, changes in the size distribution can be measured by use of the Joyce Loebel Disc Centrifuge, and for non-homogeneous powders, by the use of scanning electron microscopy. Parameters such as the sedimentation volume, the pH, the zeta-potential, the electrical conductivity, and the surfactant adsorption isotherm can provide additional information on the state of the suspension at the various parametric values.

2.6 Conclusions and Scope of the Experimental Studies

2.6.1 Conclusions

The literature has shown that particles collected from the atmosphere are in an agglomerated, conglomerated, and aggregated form. Each agglomerate, conglomerate, or aggregate can contain particles of many varied compositions and sizes. The forces that bind the discrete particles together in these systems have been found to be dependent upon the size, shape, surface, and chemical composition of the particles and upon their areas of contact, surface roughness, temperatures, and surface cleanliness. The forces acting can be mechanical, Van der Waals, capillary, electrical, or valency, and the ones acting at any one time are, in part, a function of the nature and conditions of the fluid in which they are suspended. For example, the magnitude of these forces is lower in liquids than in air, and the minimum force can be realized by absorbing a critical concentration of surface active agent onto the particle in a liquid, so that an electrical double layer force of repulsion is developed and maximized. The force of adhesion between the particles under these conditions can be measured in a variety of ways, the force between submicron particles being best measured by a centrifugal technique. It has been shown that the theoretical force of adhesion of submicron particles in aqueous phosphate media can range from 10^{-4} to 10^{-3} dynes for typical particles found in

the atmosphere, and a separation technique has to be capable of applying this force to the agglomerate system. To condition these particles so that the maximum repulsive force is in effect requires a knowledge of the chemical composition of the particles present.

Agglomerates from the atmosphere, found at ground level, can potentially contain a variety of particulate compounds with a wide particle size range. Particulates such as windblown soil, sea salt, sulphur, nitrogen, hydrocarbon and organic complexes, trace metals, metal oxides, ammonium sulphate and nitrate, sulphuric acid, biological and bacterial debris, carbonaceous combustion products, and extraterrestrial magnetic and radioactive compounds can all exist in the atmosphere and can be combined in the agglomerate. Submicron particles were particularly prevalent, but the agglomerate sizes are much larger than this.

For the fundamental studies in separation in this thesis, an atmospheric particulate sample of this kind was recognized as being too complex a system to use initially, and so a simpler but still relevant aerosol model was sought. An emission from a foundry or metals casting plant was found to be a good substitute as it was similar in size distribution but had fewer components than an atmospheric aerosol. Its chemical composition was similar to the atmospheric aerosol in that the water-insoluble particulate compounds were almost identical,

but it differed in that sea salt, ammonium sulphate and nitrate, sulphur, nitrogen and hydrocarbon complexes, and biological matter were absent. However, for the purpose of the thesis, this did not matter, as the use of particulates as useful tracers of pollution required that the particles be unaffected by rain and humidity. Hence, the water-insoluble particulate fraction was of most value. In examining this fraction, it was found that it consisted mainly of ferric oxide, aluminum oxide, titanium dioxide, zinc oxide, silica, carbon, and trace metals. A search was then made to locate potentially useful surface active agents to condition these compounds in liquid media.

It was found that organic solvents and aqueous phosphate and silicate solutions were particularly useful for sub-micron pigments and should be similarly useful for foundry effluent oxides. It, therefore, appeared that in such liquids, when the conditions were found for the maximum electrical double layer repulsion, it could be possible to devise a system to separate the particles into their discrete and aggregate particle populations. Such a method should also have the potential to separate the water-insoluble portion of atmospheric aerosols for tracer studies.

Separation methods utilizing ultrasound at high pressure and temperature, micromedia milling, and high-speed impeller mixing were selected as having the greatest

chance of success, and changes in the particle size distribution of the agglomerated particle system were thought to be the best way of measuring the degree of separation attained with each method. For submicron particles, the Joyce Loeb1 disc centrifuge and a scanning electron microscopy method of size analysis were selected to measure these changes. Other measurements, including pH, electrical conductivity, zeta-potential, sedimentation volume, surface active agent adsorption, isotherm and surface active agent nature, and concentration were also found to be important additional parameters that should be measured. Finally, the effect of weathering of particles was found to severely change the interparticle forces, so this effect had to be studied when actual atmospheric sampling took place.

From the above conclusions, the experimental scope of the thesis can now be defined, and this is done in the following section.

2.6.2 Scope of the Experimental Work

To achieve the objectives of this thesis, a systematic experimental program has to be designed. The scope of this experimental program can be subdivided into two parts.

First, a series of preliminary experiments will be conducted in which the potentially useful surfactants and separation methods will be screened for their suitability for use with submicron metal oxides. In these experiments, metal oxide powders of known physical properties and homogeneous chemical compositions will be used. This is necessary in order to conduct controlled experiments when investigating parametric effects. Using these conditions, the magnitude of the interparticle forces between metal oxides and surfaces will be measured using a centrifugal technique. This will indicate the amount of force that will have to be applied by any device to break down agglomerates. From these experiments, the best method for both conditioning and separating various metal oxides will be proposed.

Second, a series of final experiments will be conducted using this method, with actual samples taken from the atmosphere downwind from a metals casting plant. The samples will be collected in two ways to permit the effect of weathering to be studied. The resultant samples will be conditioned and separated by the selected technique and the efficiency of separation calculated for its different operating conditions of the device. From these experiments, both the efficiency of the device

and the conditions necessary for separating the inorganic oxides in foundry effluents will be established.

Finally, its potential for the separation of the more complex atmospheric aerosol will be estimated. This total program is outlined in Figure 14 as a flow chart, and this system will be followed in Chapter 3.

Preliminary Experiments with Powders

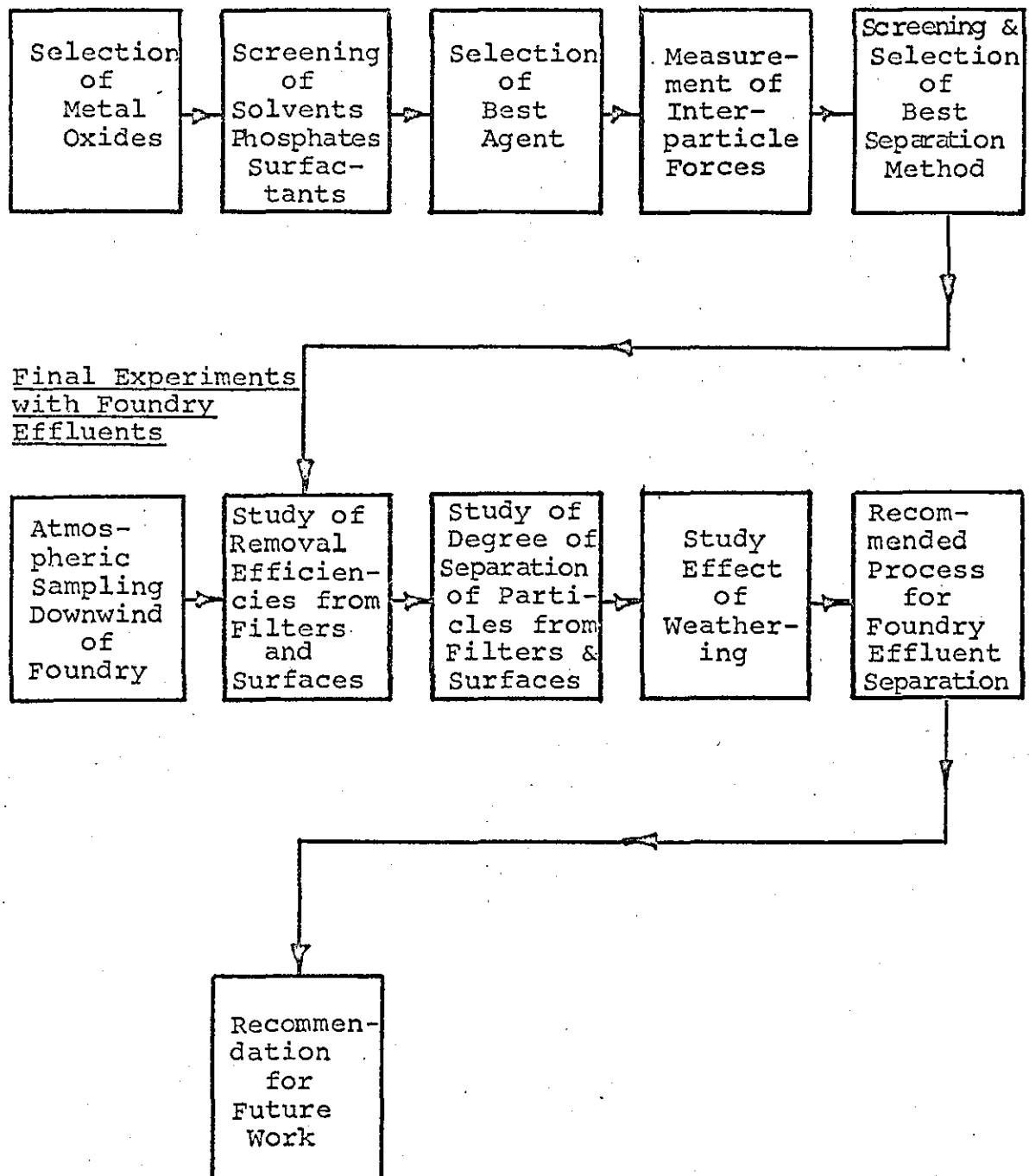


Fig. 14 - Experimental Flow Chart for Thesis

3. EXPERIMENTAL RESULTS

3.1 Preliminary Experiments

3.1.1 Selection of Metal Oxide Powders

In foundry effluents, the oxides of silicon, iron, titanium, zinc, aluminum, calcium, magnesium, manganese, lead, and chromium were found along with various metals. Not all of these materials can be studied in this thesis, so three were selected for the preliminary experiments. These were chosen because they were readily available, were well characterized, and were predominantly submicron in size. The powders chosen were titanium dioxide, alumina, and iron oxide. A flake metal pigment was also chosen to investigate the difference in the conditioning between one oxide and its metal.

The titanium dioxide was produced by the chloride process and was obtained as the pigment grade. The alumina was the α variety and was produced by milling in the presence of a hydrophilic grinding aid. Finally, the iron oxide was produced by calcining the sulphate and was obtained as the pigment grade. Their size distributions were obtained by electron microscopy and are shown in Figure 15.

The size distribution of the flake pigment is not shown as measurements varied so widely, dependent on the size analysis method. The average size was, however, estimated as a platelet of projected area diameter $5\mu\text{m}$ and thickness $0.3\mu\text{m}$.

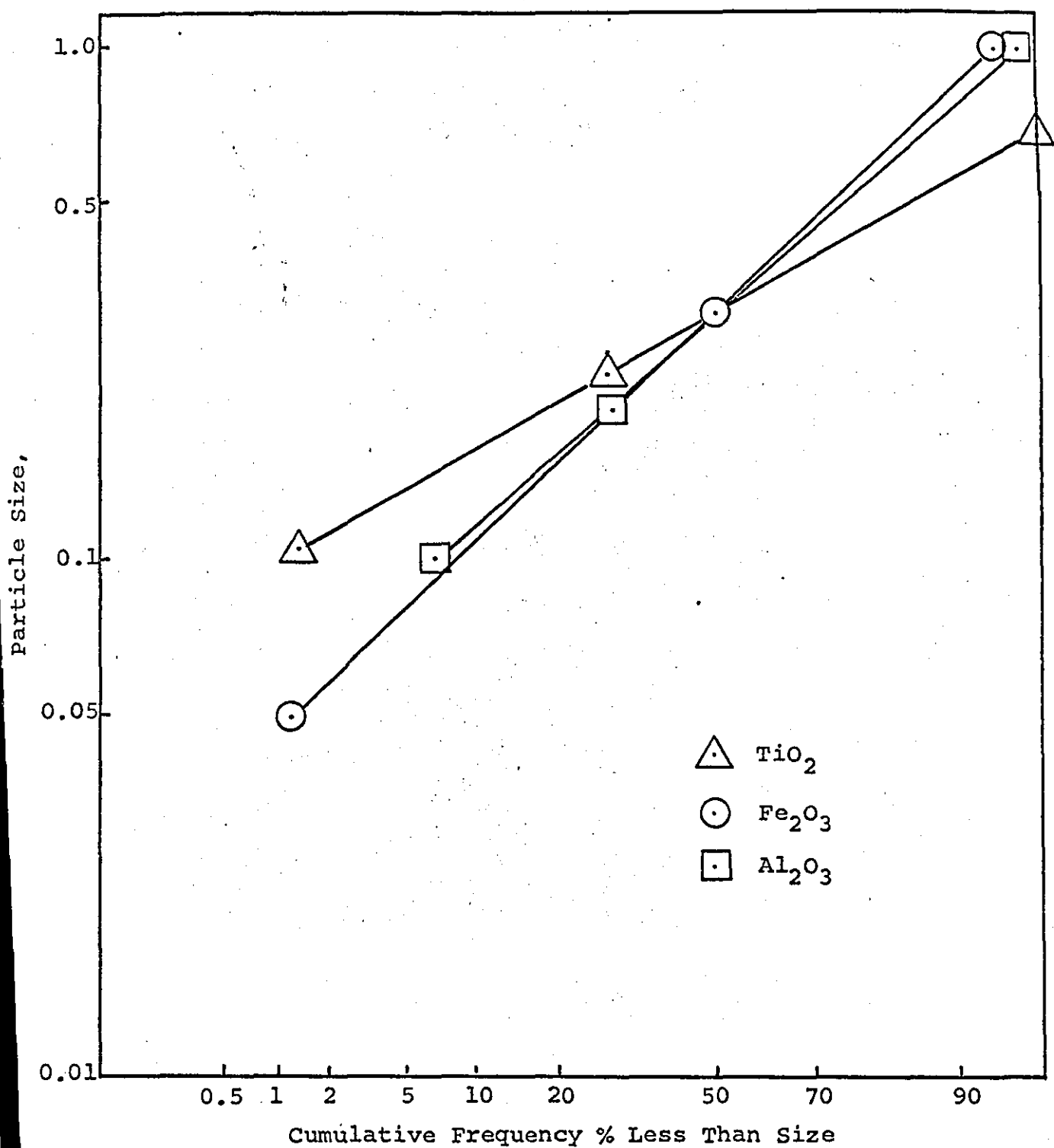


Fig. 15 - Electron Microscope Size Distributions of the Ferric Oxide, Titanium Dioxide, and the Alumina

3.1.2 Preliminary Screening of Surface Conditioning Agents

Three categories of surface conditioning agents were selected for study. These consisted of pure organic liquids, aqueous phosphate solutions, and aqueous surfactant solutions. The literature survey had indicated that the surfaces of inorganic oxides were hydroxylated and that bonding between these surfaces and molecules of surface agents occurred by hydrogen bonding. The first experiment tried was to create a hydrogen-bonding series similar to the one created by Trudgian and Prihoda¹⁴⁴ to investigate differences in the hydrogen-bonding demand of the four powders. This used pure organic liquids.

Lieberman¹⁴⁶ introduced hydrogen-bonding parameters and gave them arbitrary values of 0.3-1.7.

However, a more useful hydrogen-bonding value was introduced by Gordy.^{226,227} who used a spectroscopic technique and monitored absorption bands in the range 3.6-4.35 microns using deuterated methyl alcohol CH_3OD . The hydrogen-bonding effect was to shift the OD band to a lower frequency, and the frequency shift in wave numbers was proportional to the hydrogen-bonding strength. Ten wave numbers shift \approx 1 hydrogen bonding unit. His results showed organic solvents were largely proton acceptors, with their order being:

amines > ethers > ketones > esters > nitro compounds.

Benzene was used as the reference having a hydrogen bonding value of 0.

A typical solvent series as used by Trudgian and Prihoda¹⁴⁴ is shown in Table 6. This shows both Lieberman's and Gordy's values taken directly from their data and from later data by Hansen and Lee.¹⁵⁰⁻¹⁵³ These actual solvents were then used in this study to investigate the hydrogen-bonding tendencies of the four materials TiO_2 , Al_2O_3 , Fe_2O_3 , and Al metal. The preliminary screening studies were performed using sedimentation volume as a means of indicating particle dispersion - the lower the volume, the better the dispersion - the higher the volume, the more flocculated the dispersion. A suspension of 2 percent by volume was prepared in 40 mls of each solvent and ultrasonically dispersed at 100 watts for 60 seconds using a Branson sonifier at atmospheric pressure. This suspension was then poured into a sedimentation volume tube and allowed to settle. Typical curves of the Final Volume against Hydrogen-Bonding Value are given in Figures 16, 17, 18, and 19, showing the behavior in each solvent. With TiO_2 , the minima occurred with methanol and butyl carbitol over the range 13.0-18.9 hydrogen-bonding units. With ferric oxide, the minimum occurred with butyl carbitol only at a value of 13 units, showing a need for moderate hydrogen-bonding solvents.

The alumina showed a minimum with methyl isopropyl ketone at a value of 8 units, showing a preference for moderately low hydrogen-bonding solvents. Finally, the

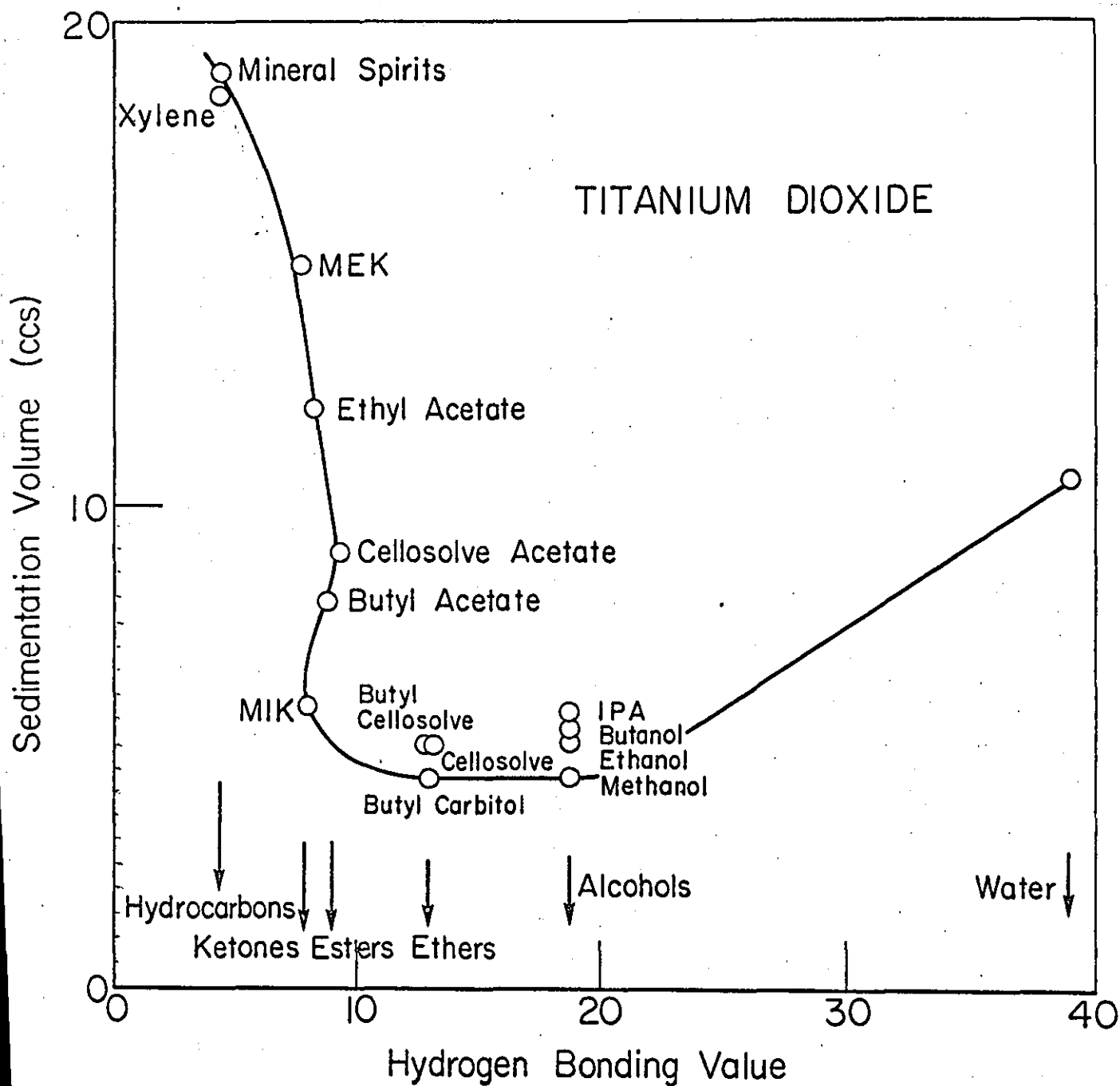


Figure 16

Sedimentation Volume Vs Hydrogen-Bonding
Value for Titanium Dioxide

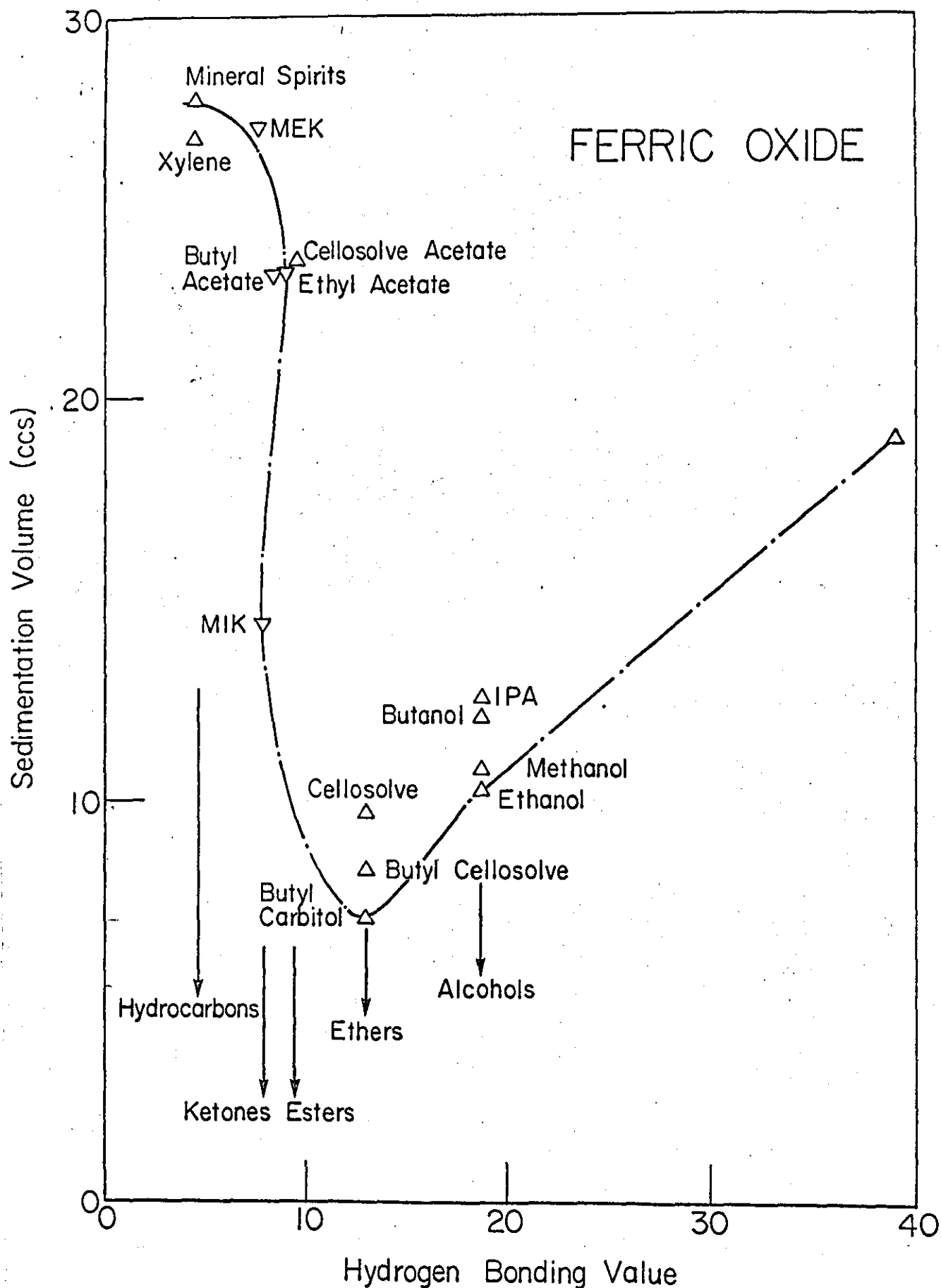


Figure 17
Sedimentation Volume Vs Hydrogen-Bonding
Value for Ferric Oxide

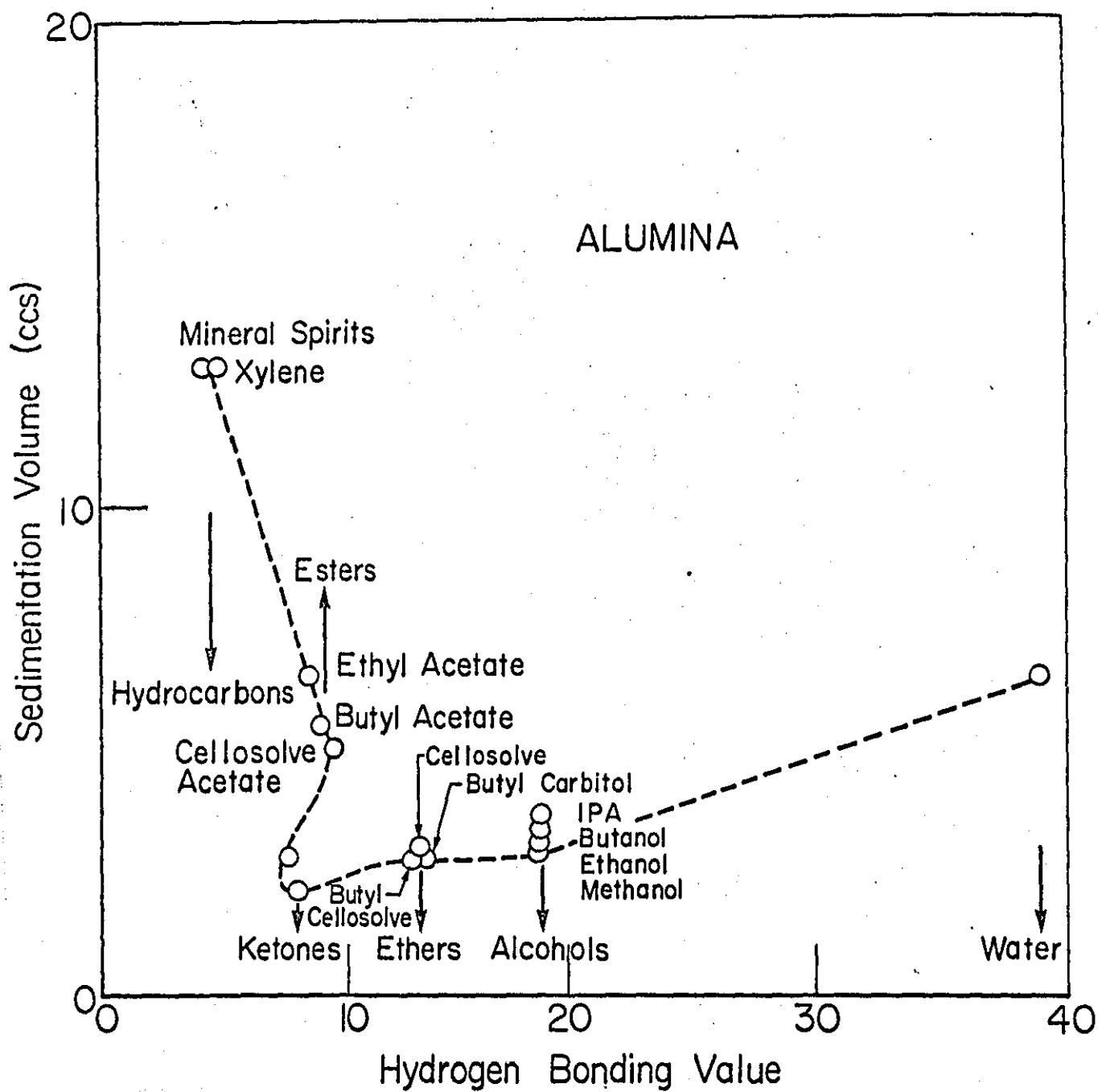


Figure 18

Sedimentation Volume Vs Hydrogen-Bonding Value for Alumina

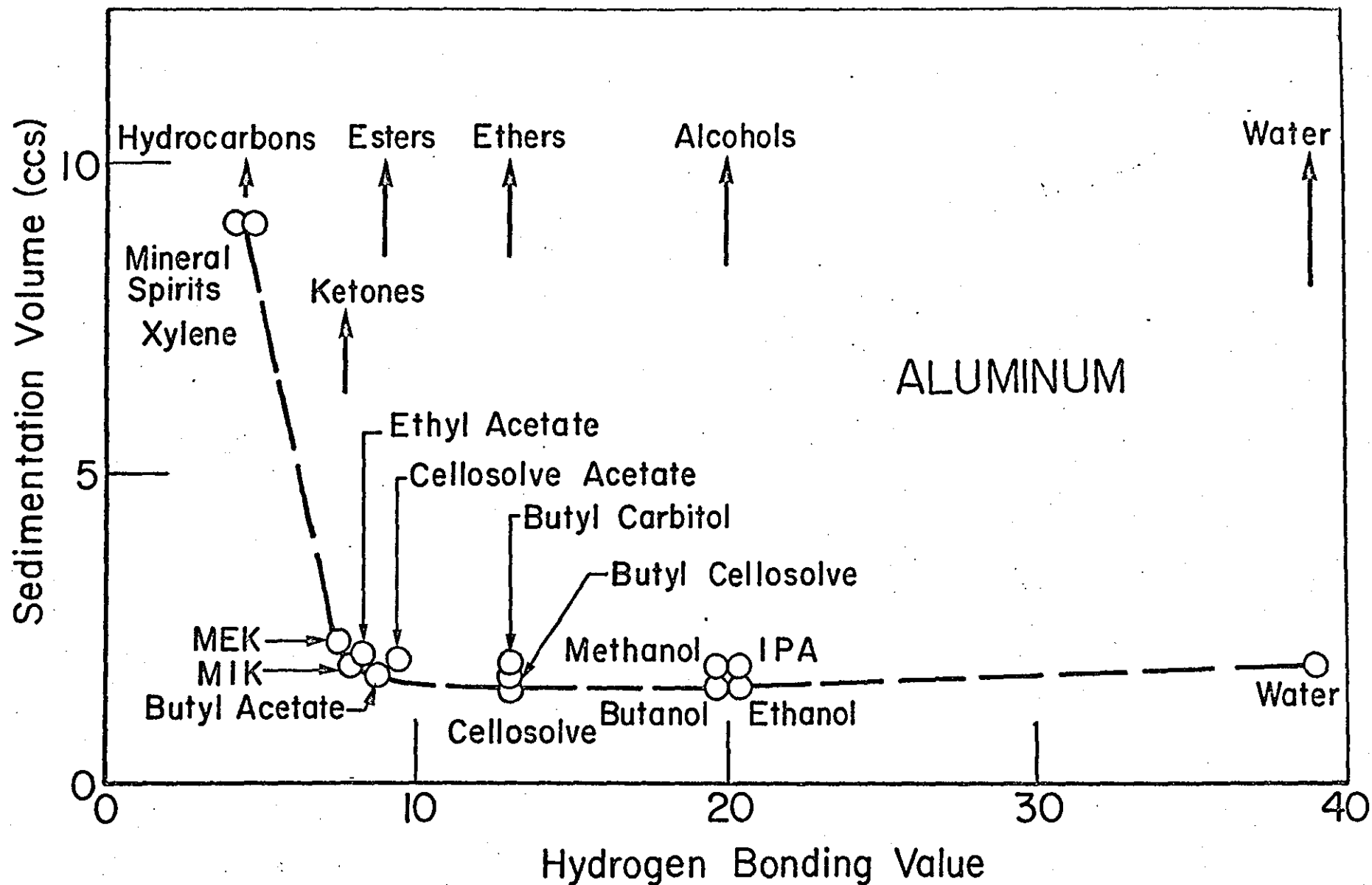


Figure 19 - Sedimentation Volume Vs Hydrogen-Bonding Value for Aluminum Metal

aluminum metal showed a minimum with butanol and cello-solve over a range of 13.0-18.9 units, showing a preference for moderate to strong hydrogen-bonding solvents. The four curves are, however, seen to demonstrate an irregularity insofar as a distinct bulge is obtained between solvents of hydrogen-bonding values of 8-10. This should not occur as there should be one minimum and two slowly increasing series of values on each side of it. In consequence, a second series of solvents was introduced to investigate this phenomenon, and the four materials were subjected to the same experimental process again. The series of solvents used for this investigation is shown in Table 6. These range from 6-8 hydrogen-bonding units. The curves for the four powders are shown in Figures 20-23. From these curves, it can be seen that the narrower range of hydrogen-bonding solvents resolved the projection into a discontinuity showing a maximum between two minima and, in fact, showing that the projection was a false one. In Figure 24, it can be seen that the discontinuity occurs at the series of values associated with esters.

The anomalous behavior of the four materials with esters suggests that perhaps the hydrogen-bonding value assigned to each ester was an erroneous one. A preliminary thought was that the esters may be exhibiting isomerism, and either the "keto" or "enol" form may predominate. In Gordy's experiments, if the esters had greater

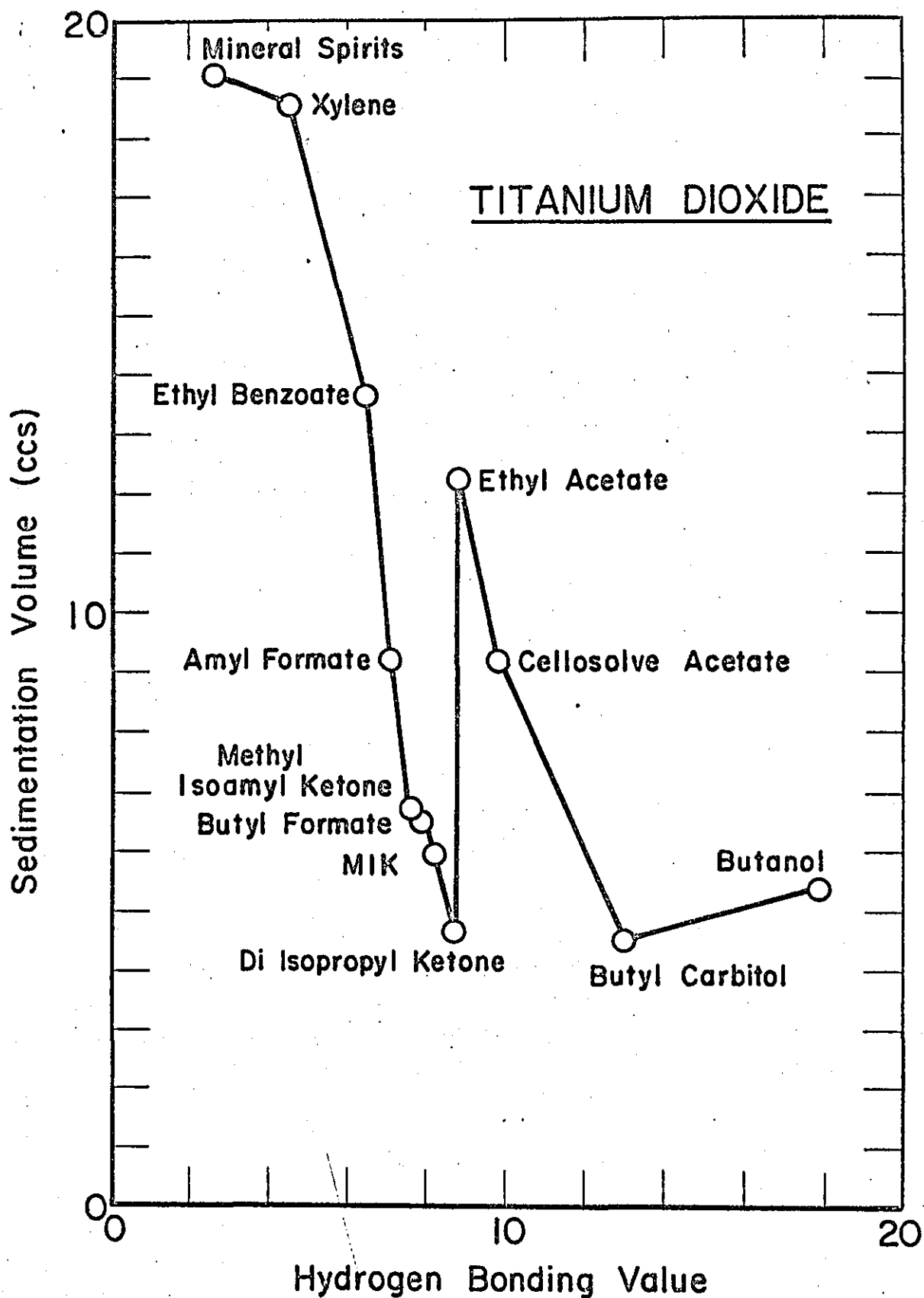


Figure 20

Sedimentation Volume Vs Hydrogen-Bonding Value for
Titanium Dioxide Using Specific Solvents

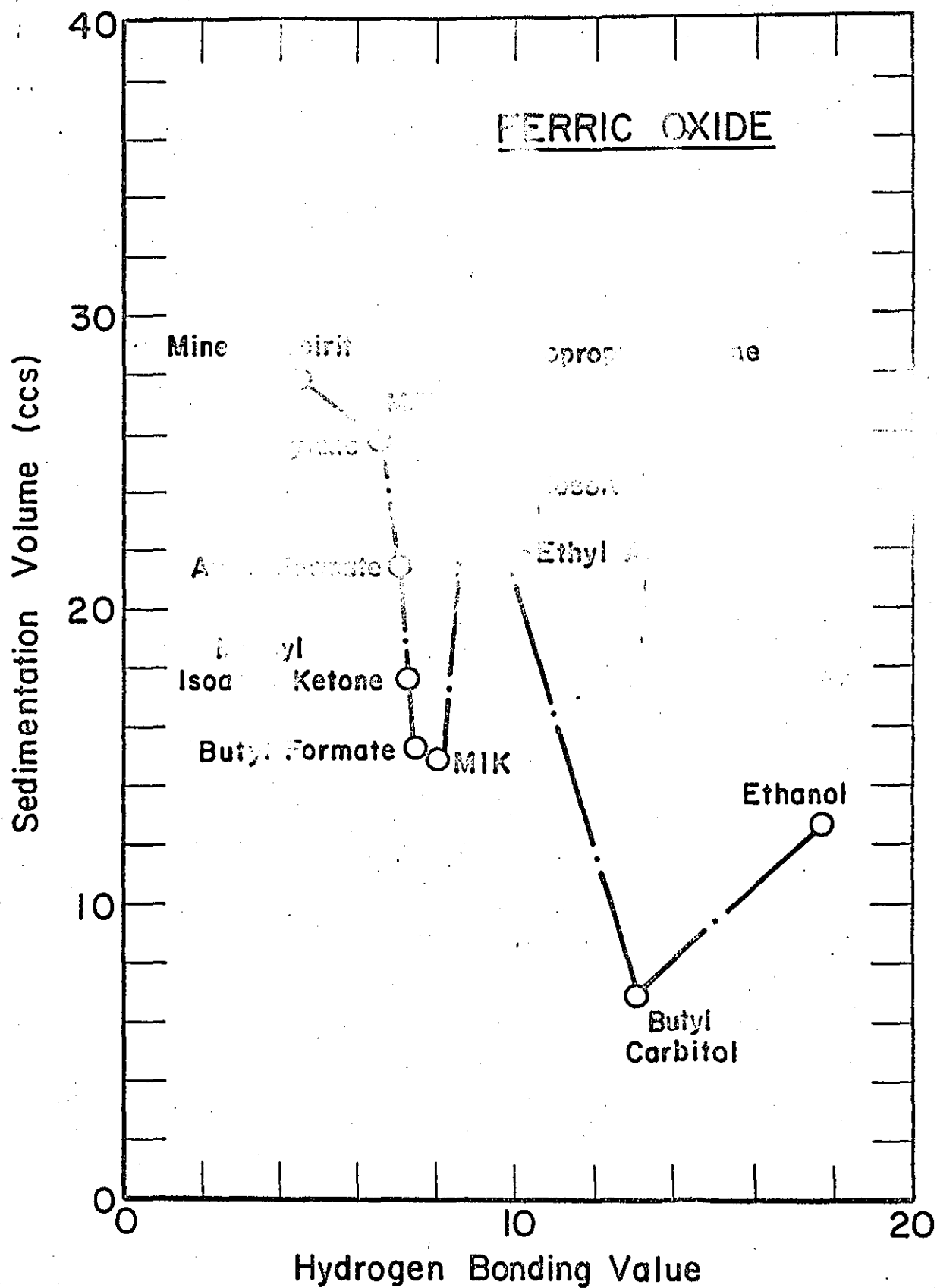


Figure 21

Sedimentation Volume Vs Hydrogen-Bonding Value for Ferric Oxide Using Specific Solvents

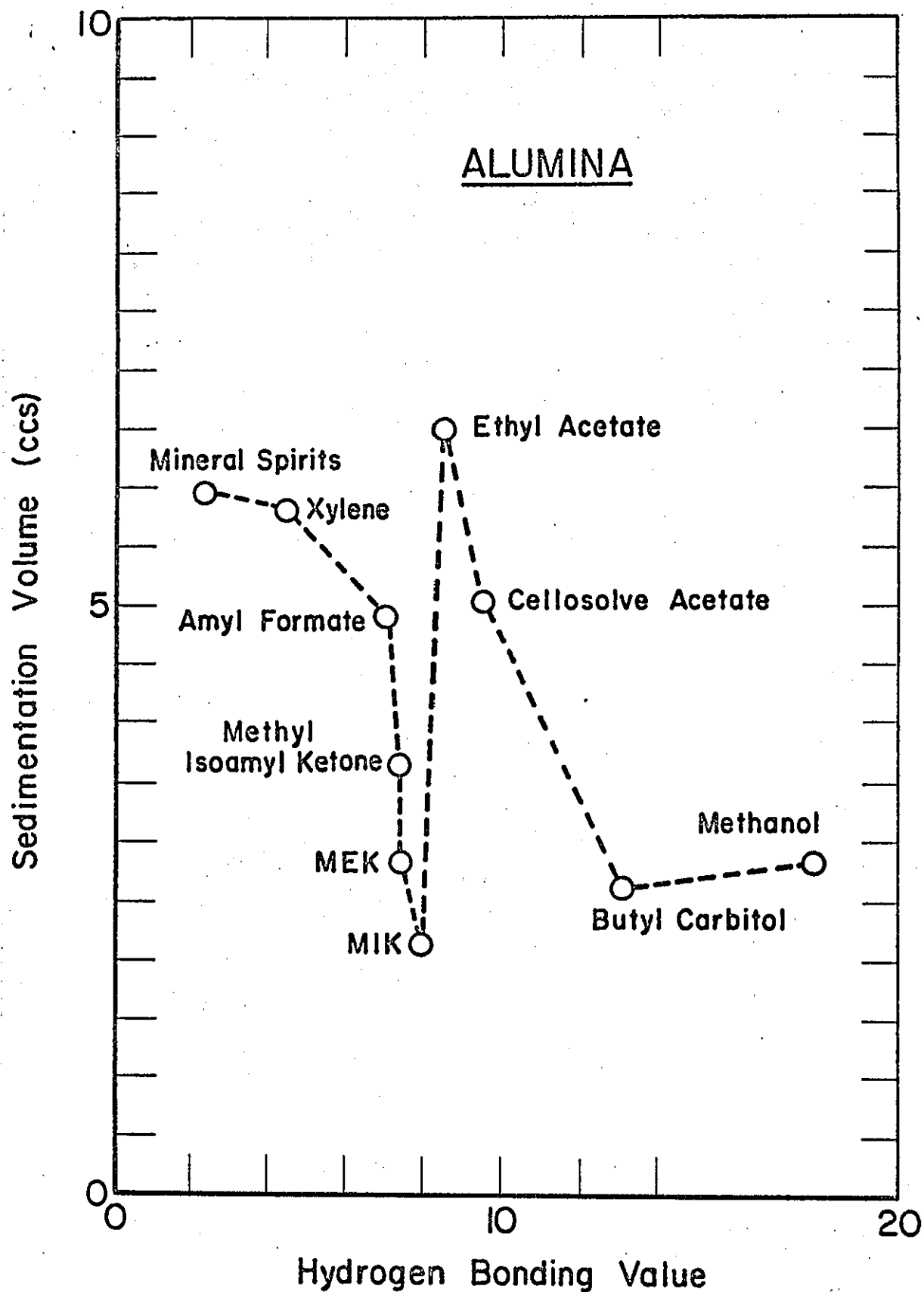


Figure 22

Sedimentation Volume Vs Hydrogen-Bonding Value
for Alumina Using Specific Solvents

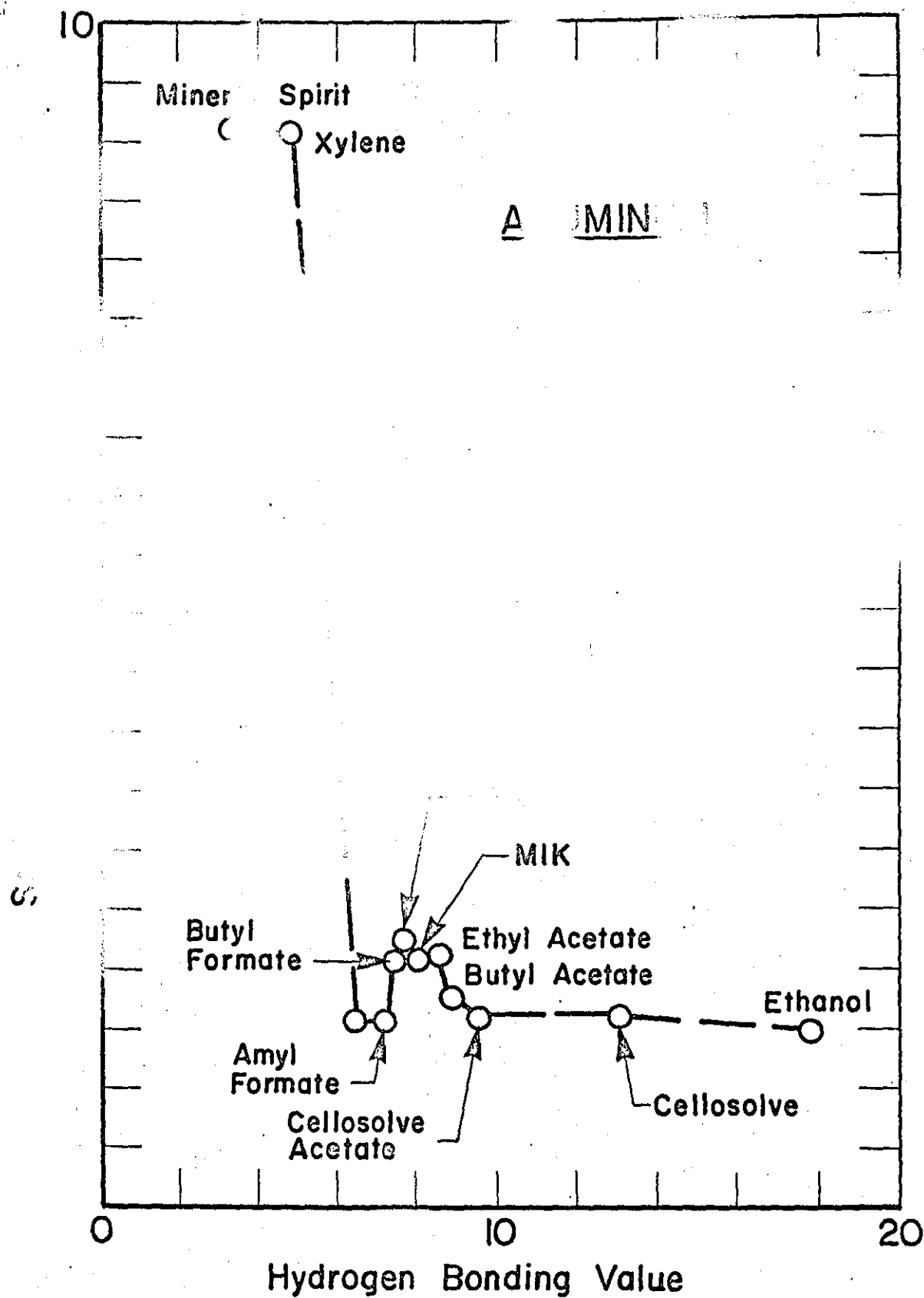


Figure 23

Sedimentation Volume Vs Hydrogen-Bonding Value
for Aluminum Using Specific Solvents

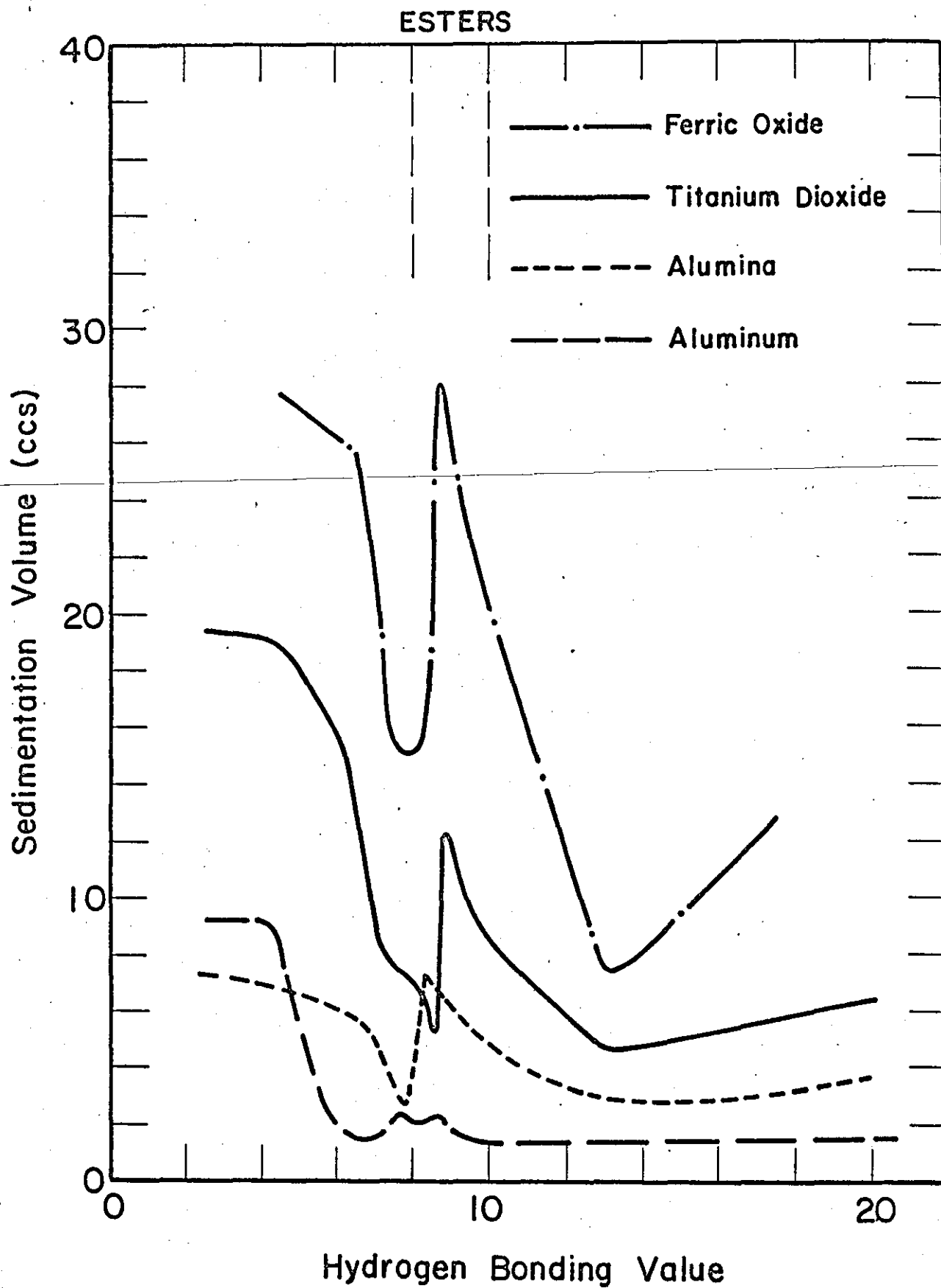


Figure 24

Relationship Between Sedimentation Volume and Hydrogen-Bonding Value for the Four Powders

TABLE 6

HYDROGEN BONDING SERIES OF TRUDGIAN AND PRIHODA¹⁴⁴


	<u>Formula</u>	<u>Lieberman H.B.P.</u>	<u>Gordy H.B. Value</u>
Water	H-OH	1.7	39.0
Methanol	CH ₃ ·OH	1.7	18.7
Ethanol	CH ₃ ·CH ₂ OH	1.7	18.7
Butanol	CH ₃ (CH ₂)CH ₂ CH ₂ OH	1.7	18.7
Isopropanol	(CH ₃) ₂ CH·OH	1.7	18.7
Cellosolve	(C ₂ H ₅ O)CH ₂ ·CH ₂ OH	1.3	13.0
Butyl Cellosolve	(C ₄ H ₉ O)CH ₂ ·CH ₂ OH	1.3	13.0
Butyl Carbitol	(C ₄ H ₉ O)CH ₂ ·CH ₂ OCH ₂ CH ₂ OH	1.3	13.0
Cellosolve Acetate	C ₂ H ₅ OCH ₂ CH ₂ ·OOCCH ₃	1.23	9.4
Ethyl Acetate	CH ₃ COOC ₂ H ₅	1.0	8.4
Butyl Acetate	CH ₃ COOC ₄ H ₉	1.0	8.8
Methyl Iso- propyl Ketone	CH ₃ ·CO·CH(CH ₃) ₂	1.0	8.0
Methyl Ethyl Ketone	CH ₃ ·CH ₂ ·COCH ₃	0.8	7.7
2 Nitro Propane	CH ₃ ·CH(NO ₂)CH ₂	0.3	4.5
Xylene	CH ₃  CH ₃	0.3	4.5
Mineral Spirit	-	0.3	2.5

TABLE 7

ADDITIONAL HYDROGEN-BONDING SERIES
(p. 137, Line 12)

Ethyl Benzoate	$C_6H_5CO \cdot OC_2H_5$	6.3
Amyl Formate	$H \cdot CO \cdot O(CH_2)_4CH_3$	7.0
Methyl Iso-Amyl Ketone	$CH_3 \cdot CO \cdot (CH_2)_2CH(CH_3)_2$	7.4
Butyl Formate	$H \cdot CO \cdot O \cdot C_4H_9$	7.5
Methyl Ethyl Ketone	$CH_3CH_2 \cdot COCH_3$	7.7
Methyl Isopropyl Ketone	$CH_3 \cdot CO \cdot CH(CH_3)_2$	8.0
2.4 Di Isopropyl Ketone	$(CH_3)_2CH \cdot COCH(CH_3)_2$	8.4
Ethyl Acetate	$CH_3CO \cdot OC_2H_5$	8.4

percentages of the "enol" form, the hydrogen-bonding value assigned would have been too high. Alternatively, the esters in use in these experiments could have been predominantly "keto" in form and behaved as if their hydrogen-bonding value was in the order of 7 instead of 9 units.

From this data, several conclusions can be drawn. The hydrogen-bonding demand of TiO_2 was found to be greater than that of Fe_2O_3 , which, in turn, was found to be greater than that of Al_2O_3 . In comparison, the sedimentation volume of the aluminum metal powder was fairly constant over the range of 10-25 hydrogen-bonding units, showing that its demand was higher than for the aluminum oxide. This was unexpected as the metal is known to have a thin film of oxide on its surface. In addition, it was found that some solvent types were more effective when their chain lengths were short, e.g., methanol was a better dispersant than isopropanol. This suggested that the key to the behaviour was in the electron configuration and charge effects between the solvent molecules and the surface. This finding could form the subject for a study in itself, but in this thesis, the effect was not investigated further. Instead, the data were only used to illustrate one important point. No one organic solvent was found to be useful for conditioning and dispersing the range of oxide types employed, and for the purpose of this thesis, this was a serious disadvantage.

In consequence, the search for a more comprehensive conditioning agent was continued, and this led to a study on the use of phosphates and silicates. Imamura and Tokiwa¹⁷¹ had reported that a pyrophosphate of formula $\text{Na}_6\text{P}_3\text{O}_{11}$ had the best potential for conditioning oxides as it produced the highest zeta potential on iron oxide. Though repeated efforts were made to obtain this phosphate, no manufacturer could be found to supply it. In consequence, the next lower phosphate in the pyrophosphate series $\text{Na}_4\text{P}_2\text{O}_7$ was used. This phosphate, tetrasodium pyrophosphate, was known to produce only a slightly lower zeta potential than the former.

To study the advantages of this phosphate over other phosphate types, a group of six materials was selected. Five phosphates and one silicate were used in the investigation. These were monobasic sodium phosphate, $\text{Na}_3\text{PO}_4 \cdot 12\text{H}_2\text{O}$; dibasic sodium phosphate, $\text{Na}_2\text{HPO}_4 \cdot 12\text{H}_2\text{O}$; tribasic sodium phosphate, $\text{NaH}_2\text{PO}_4 \cdot \text{H}_2\text{O}$; sodium pyrophosphate, $\text{Na}_4\text{P}_2\text{O}_7$; sodium hexametaphosphate, $\text{Na}(\text{PO}_3)_6$; and sodium metasilicate, Na_2SiO_3 . Each compound was prepared in solutions containing 1 mg of PO_3 or SiO_3 /ml and 10 mg of PO_3 or SiO_3 /ml. These were termed the standard phosphate and silicate solutions.

The volume concentration of each oxide in water was kept constant at 2 percent, and dispersion of the powder in the liquid was performed using the ultrasonic probe at 100 watts for 60 seconds. A total volume of 200 mls of

suspension was prepared in each case, which was sufficient to permit the determinations of pH, zeta potential, and sedimentation volume at each concentration.

The first powder analyzed was the TiO_2 , and a summary of the results obtained is given in Figure 25. It can be seen that the lowest sedimentation volume was obtained with both sodium silicate and tetrasodium pyrophosphate solutions. This occurred at a zeta potential of 80 mV, a pH of 10 to 11, and a phosphate concentration of 20 mg PO_3 .

The data for alumina are shown in Figure 26. As before, the lowest sedimentation volume occurred with tetrasodium pyrophosphate, but at a pH of 10, a zeta potential of 60 mV, and a phosphate concentration of 20 mg PO_3 .

Finally, the data for ferric oxide are shown in Figure 27. Again the lowest sedimentation volume was obtained with tetrasodium pyrophosphate, but at a pH of 8, a zeta potential of 98 mV, and a phosphate concentration of 100 mg PO_3 .

Hence, tetrasodium pyrophosphate was indeed the best phosphate of the series tested, and more importantly, was the best agent for use with all the oxides. However, distinct differences in the pH requirement were found.

To compare the relative effectiveness of organic solvents and phosphates for dispersing the oxides, Table 8 shows the sedimentation volumes obtained at the optimum

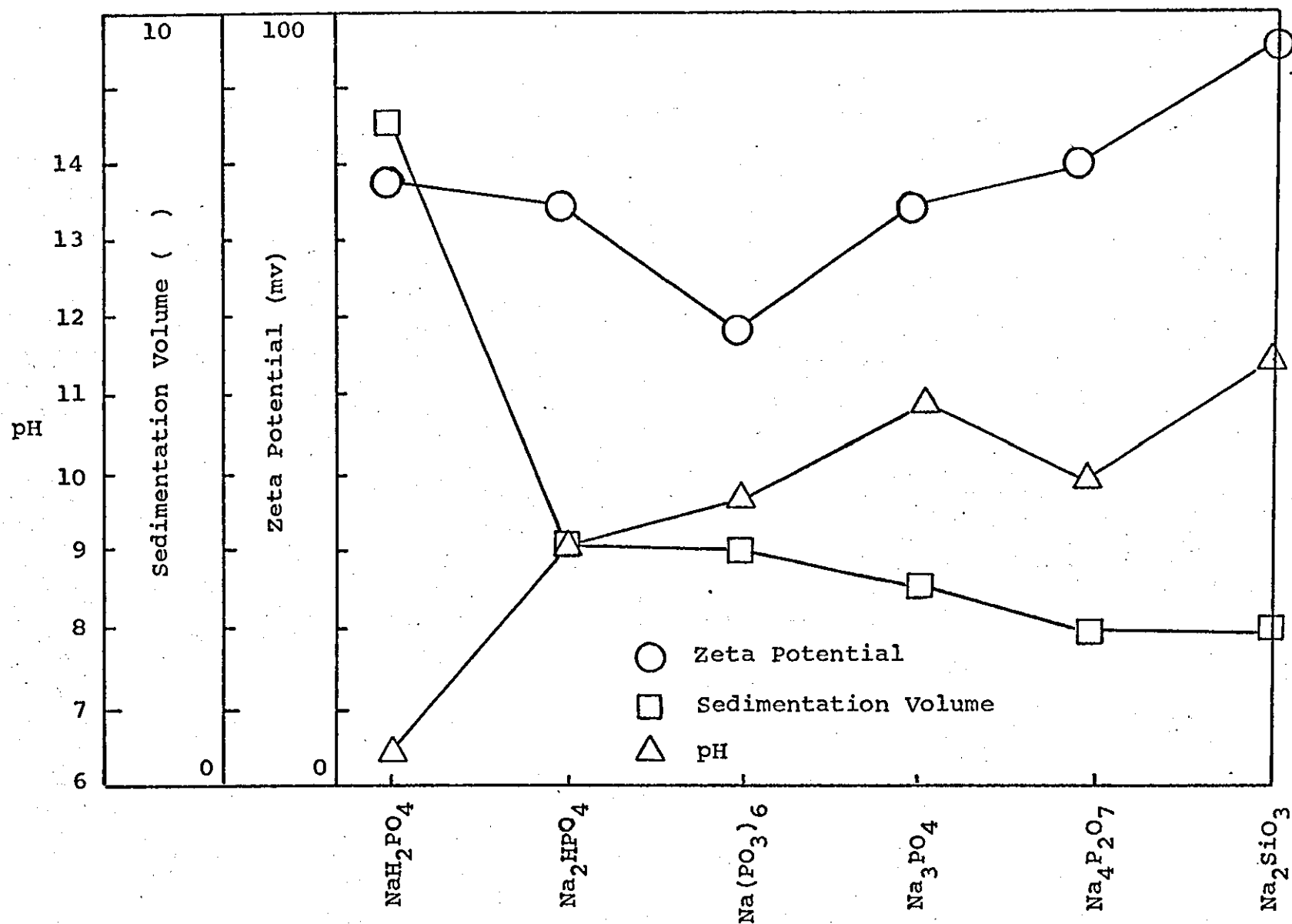


Fig. 25 - Relationships Between pH, Sedimentation Volume, and Zeta Potential for TiO_2

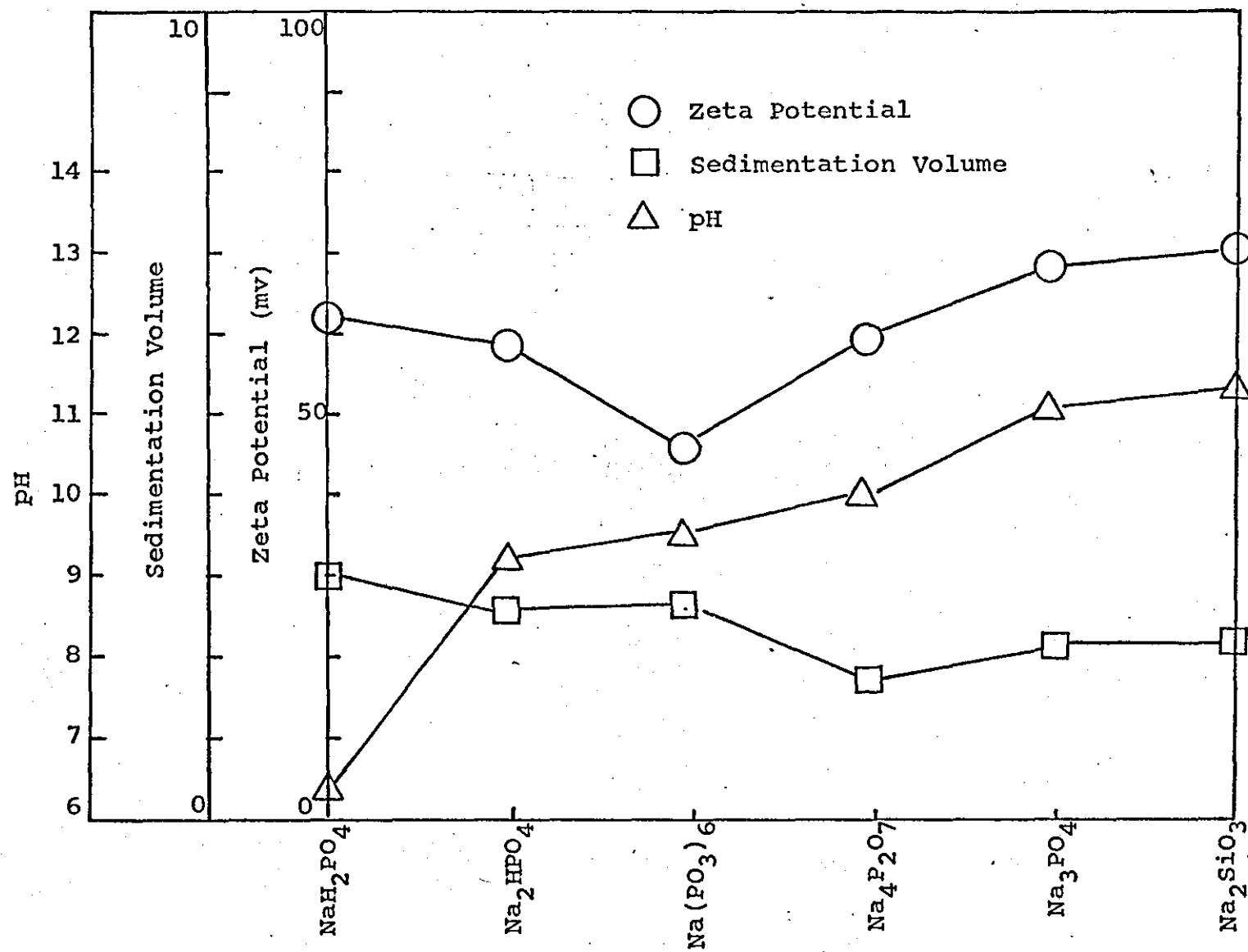


Fig. 26 - Relationships Between pH, Sedimentation Volume, and Zeta Potential for Alumina

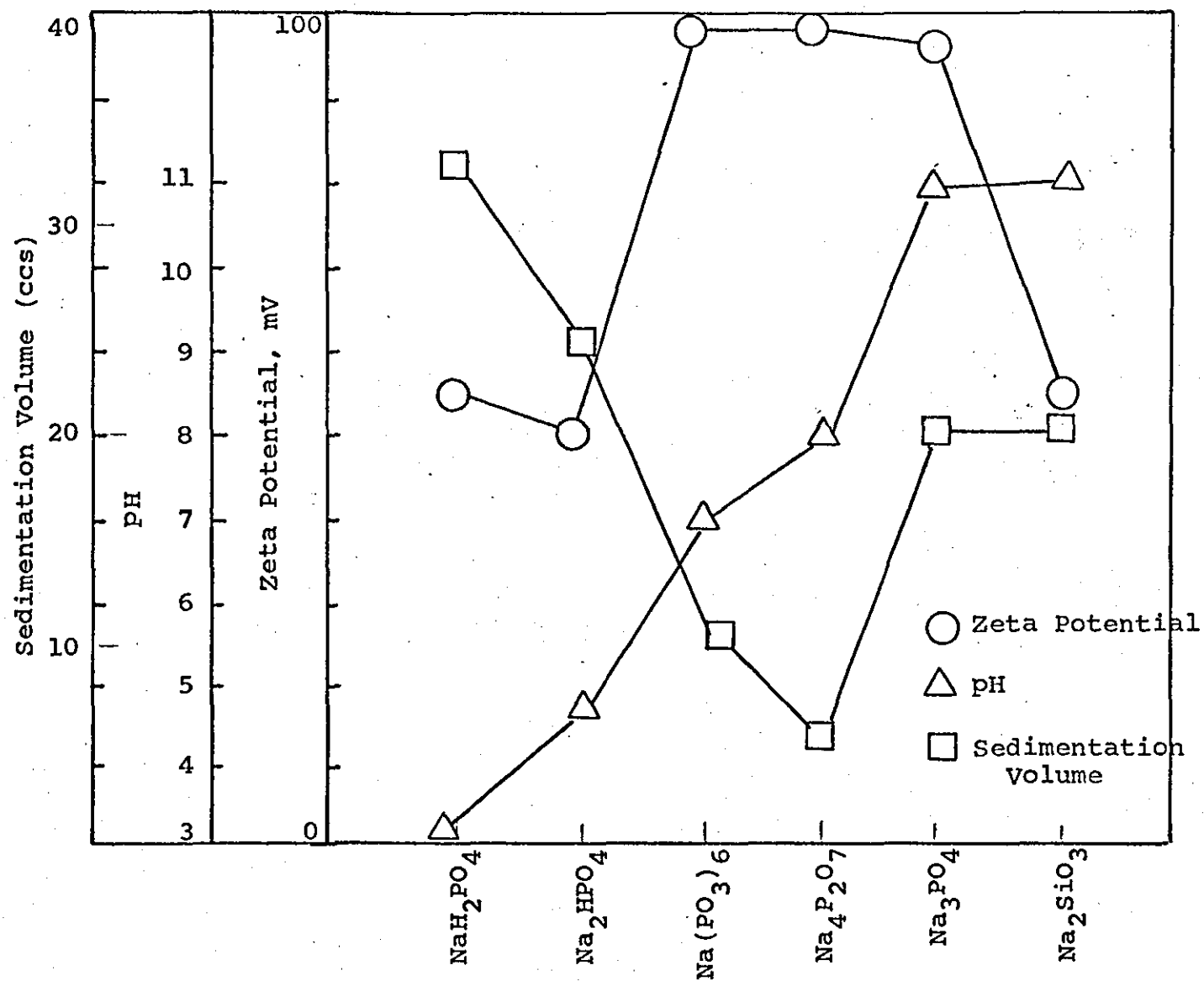


Fig. 27 - Dispersion of Ferric Oxide in Aqueous Solutions of Phosphates and Silicates -- Relationships Between pH, Mean Particle Size, and Zeta Potential

conditions for dispersion in both the solvent and phosphate series. In every instance, aqueous phosphate solutions produced a lower sedimentation volume than the corresponding solvent. This meant that phosphate solutions produced the better particle dispersion. To relate the sedimentation volume data to actual size distribution data, the oxides in tetrasodium pyrophosphate were next diluted 10:1 and size analyzed on the Joyce Loeb1 disc centrifuge. For these analyses the spin fluid was 10 percent sucrose, and during the analysis, no streaming was observed. It is important here to point out the effect that the method of dilution had upon the size distribution obtained.

To demonstrate this effect, one powder was selected for study. This was TiO_2 . The powder was dispersed in $\text{Na}_4\text{P}_2\text{O}_7$ according to the method previously described, and Figure 28 shows the size distribution of the powder after various treatments.

Firstly, the size distribution after dispersion in the presence of 1 mg PO_3 is presented. A mean size of $5.5 \mu\text{m}$ was obtained and obviously this represented an agglomerated condition and a poor degree of dispersion. After ultrasonication* in the presence of 20 mg PO_3 , a mean size of $0.37 \mu\text{m}$ was obtained. This was found to be the best degree of dispersion possible under the experimental conditions.

*"Ultrasonication" or "sonication" is a term coined by the U.S. Air Force to describe the application of ultrasonic energy from a Branson magnetostrictive ultrasonic device termed a Sonifier - Sonifer being the trade name. In this thesis, the word is used, for want of a better expression, to describe this procedure.

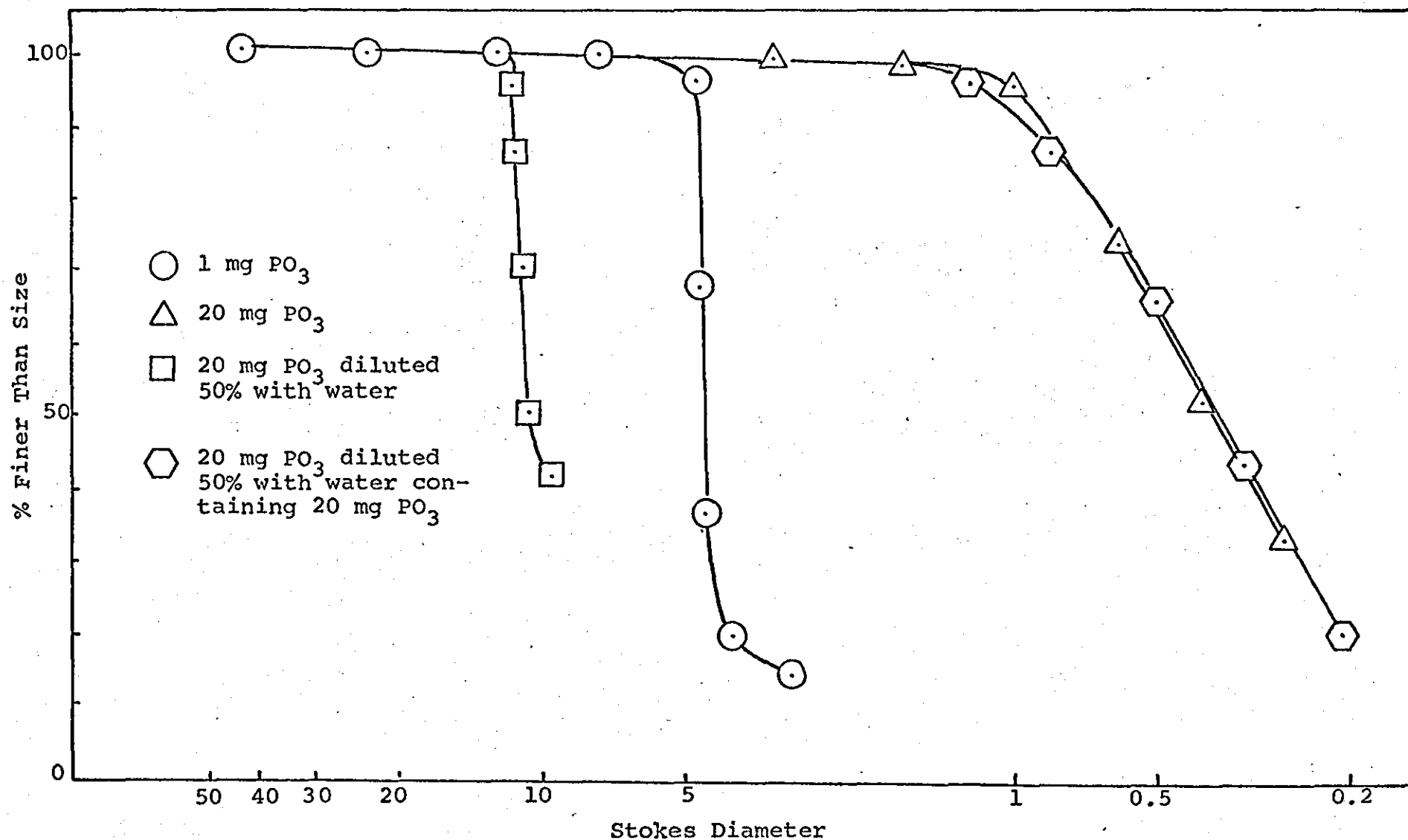


Fig. 28 - Effect of Dilution on Titanium Dioxide Size Data

TABLE 8

COMPARISON OF SEDIMENTATION VOLUMES IN AQUEOUS AND
NON-AQUEOUS MEDIA

	<u>Sedimentation Volume in Aqueous Systems</u>	<u>Sedimentation Volume in Non-Aqueous Systems</u>
TiO_2	2.0 cc	4.5 cc
Al_2O_3	1.6 cc	2.1 cc
Fe_2O_3	5.0 cc	7.5 cc

At this point, two dilution methods were tried. One involved a 50 percent dilution of the suspension with distilled water, and the other involved a 50 percent dilution with a solution of 20 mg PO_3 in distilled water. The results were significantly different. With water, immediate agglomeration occurred. This was so severe that the resultant size distribution was coarser than that of the powder originally dispersed in water with 1 mg PO_3 in solution. In fact, a mean of approximately 12μ was observed. This indicated the presence of a different form of agglomeration, usually termed "flocculation". The two terms are used here, not synonymously, but rather as two separate forms of particle interaction phenomena. The form of agglomerate present in the initial suspension has a more closely packed structure, while that of the latter has a chain-like structure. This effect was also observed in the sedimentation volume curves in the organic solvents. The values on the left-hand side of each minimum showed much higher sedimentation volumes than those on the right-hand side, indicating the presence of different interparticle structures. Examination of these structures under the microscope showed the presence of networks in those from the left-hand side and the absence of networks in those from the right-hand side.

When one now observes the data taken after dilution with the 20 mg PO_3 solution, no change in size distribution is

seen. Hence, in preparing dispersions for analysis, it is very important to remember that if dilution is necessary before analysis, it must be performed with a solution of the dispersant at the identical concentration to that used in the initial dispersion.

This technique was then used for alumina and ferric oxide and the mean sizes obtained were: TiO_2 - 0.37μ , Al_2O_3 - 0.38μ , and Fe_2O_3 - 0.5μ . Hence, tetrasodium pyrophosphate was a highly effective conditioning agent for the three oxides. However, although the use of tetrasodium pyrophosphate was highly effective with the oxides, a final class of conditioning agents was still investigated to make sure that no better system existed.

A comparison of the effectiveness of surfactants was briefly made. A series of anionic, cationic, and non-ionic dispersing agents was compiled. For reference to the basic differences between these categories, see Parfitt⁴⁷. The ones selected were as shown in Table 9. Due to the hydroxylated nature of the oxides, a predominance of cationic amines and amides was selected. These had been shown to be effective with metal oxides in the literature survey in Chapter 2. The surfactants were viewed as 0.5 percent active solutions, and sufficient surfactant was added to each suspension to give a concentration of 0.1 percent by weight. For simplicity, only titanium dioxide was used for this study, and the relationship of the mean sizes obtained relative to the surfactant

TABLE 9

SURFACE ACTIVE AGENTSAnionic

Sodium Stearate	$C_{17}H_{35}COO^-Na^+$
Sodium Lauryl Sulphate	$C_{12}H_{25}OSO_3^-Na^+$

Cationic

Arquad C50	$C_{13}H_{27}N(CH_3)_3^+Cl^-$
Arquad HT50	$C_{17}H_{35}N(CH_3)_3^+Cl^-$
Arquad 2HT	$(C_{17}H_{35})_2N(CH_3)_2^+Cl^-$
Arquad 2C	$(C_{13}H_{27})_2 \cdot N \cdot (CH_3)_2^+Cl^-$
Armeen 2HT Hydrochloride	$(C_{17}H_{35})_2 \cdot NH_2^+Cl^-$
Armeen 2C Hydrochloride	$(C_{13}H_{27})_2 \cdot NH_2^+Cl^-$
Armeen C Hydrochloride	$C_{13}H_{27} \cdot NH_3^+Cl^-$
Armeen HT HY Hydrochloride	$C_{17}H_{35} \cdot NH_3^+Cl^-$

Hyamine 1622 -
Quaternary Ammonium Salt
Salt

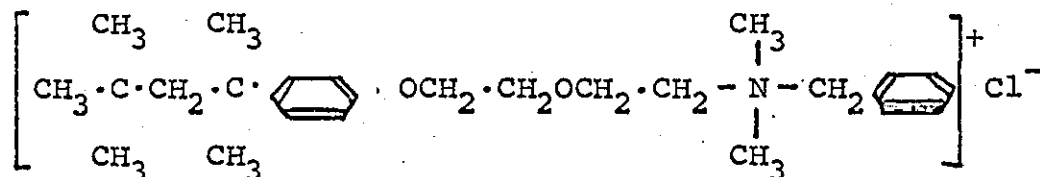


TABLE 9 (Cont.)

Non-Ionic

Tergitol 15-S-7 $C_{15}H_{30}O(CH_2 \cdot CH_2O)_7$

Tergitol 15-S-9 $C_{15}H_{30}O(CH_2 \cdot CH_2O)_9$

Tergitol 15-S-12 $C_{15}H_{30}O(CH_2 \cdot CH_2O)_{12}$

The above surfactants were received from the manufacturer at 98% purity, and were used at this purity level.

composition used is shown in Figure 29. For convenience, the mean sizes of titanium dioxide in methanol and in aqueous tetrasodium pyrophosphate are also included in these data.

The data show that the tetrasodium pyrophosphate solution remained the best conditioning agent for the powder, although Armeen 2HT and Armeen 2C were only slightly inferior. These were both branched chain amines which hydrogen bonded strongly to the hydroxyl surface. The data for the anionic agents are not shown, as these did not disperse the oxides at all.

Hence, from the data presented so far, it is seen that tetrasodium pyrophosphate is the best conditioning agent for metal oxides and should therefore be used in the studies to screen the separating devices.

It is perhaps worth emphasizing here that the selection of ultrasonics to disperse the oxides in this section was an arbitrary choice as any method could have sufficed, providing that it was strictly controlled and reproducible. This was true because only the relative differences in the data due to surfactant effects were sought, and for this purpose, ultrasonics was a satisfactory choice.

Before concluding this section on conditioning agents, one further conditioning system should be introduced as it will be seen extremely valuable in later studies. From the literature survey, interest was stimulated in the

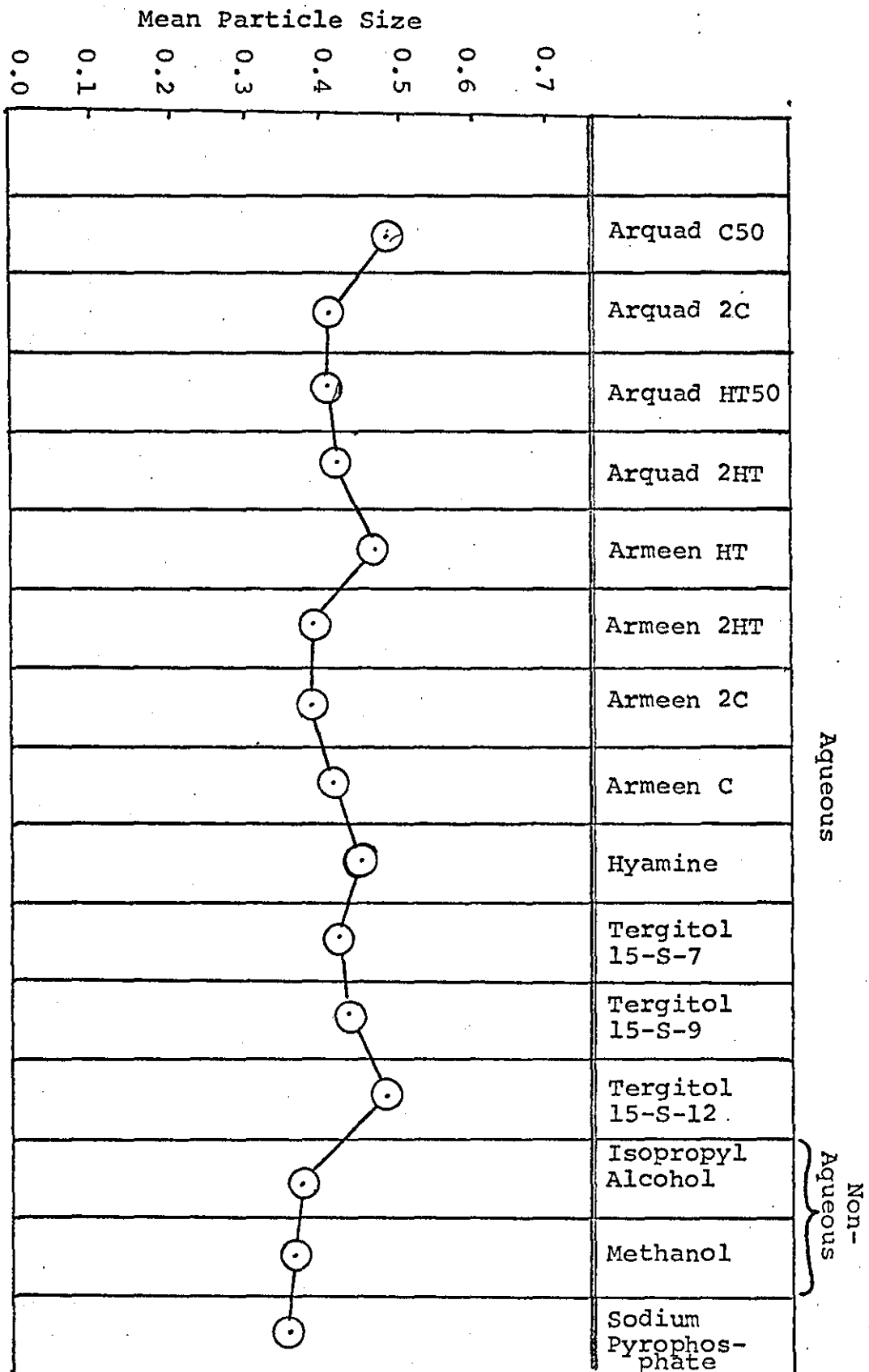


FIG. 29

Mean Particle Sizes of Titanium Dioxide in Various Solvents

work performed by Kaiser¹⁹⁶ at AVCO Corporation who had reported on the success of mixtures of fluorinated hydrocarbons as dispersing agents. Fluorinated compounds are recognized for their ability to strongly hydrogen-bond onto surfaces, and hence they appeared to be a good choice for the dispersion of metal oxides. Kaiser reported that such compounds as magnetite and uranium dioxide had been stabilized by a mixture of high molecular weight fluoro-polyacids. In particular, Krytox® 137 dissolved in Freon® E-3 solutions were prohibitively expensive for general testing on the metal oxides in this thesis. However, they did offer one potential advantage over aqueous systems if they proved as effective. They were inert solvents in which water-soluble particles were insoluble. Hence, they could be useful for separating the total water-soluble and water-insoluble atmosphere aerosol particle population. This had to be investigated. Due to their high cost considerations, the testing of this mixture of fluoro-polyacids for this purpose was left until the final stage of the thesis when small quantities of atmospheric particulates were being separated. For these small-scale tests, the costs incurred of using fluoro-polyacids were reasonable. In the meantime, tetrasodium pyrophosphate was selected as the prime conditioning agent for the screening of the potential separating devices.

3.1.3 The Measurement of the Force of Adhesion Between Metal Oxides and Surfaces

3.1.3.1 Introduction

In the literature survey, the force of attraction between particles in liquid media was shown to comprise of mechanical and Van der Waals forces. By adjusting the pH, ionic strength and dielectric constant of the liquid, the electrical double layer force of repulsion could be maximized with the result that the total force of adhesion between the particles could be reduced to a minimum.

Under these conditions, the amount of mechanical force required to physically separate the particles was also at a minimum. To apply such a force, a mechanical device had to be selected. The literature survey showed that the choice of devices was quite wide, but that the force available for application from the devices depended on the physical method of separation involved. Hence, before a potential separating method could be selected, some estimate of the force of adhesion between the particles had to be made under the optimum conditions developed in 3.1.2.

In this present section, the force of adhesion between metal oxides and various surfaces is measured. The details of this work, which already have been published, are reported in Reference 225.

3.1.3.2 Method of Approach

The literature survey indicated that a centrifuge method was best for the measurement of the force of adhesion between submicron particles and substrates. In consequence, a method similar to the one used by Boehme²⁹ and Krupp¹⁷⁶ was used. Commercially available centrifuges were investigated for the study, and a series capable of speeds from 0-70,000 rpm was assembled. These are specified in Table 10. The upper limit of speed for commercial centrifuges in the U.S.A. was 70,000 rpm, and though it will be seen that higher speeds would have been an advantage, no unit was available capable of extending this 0-70,000 rpm range.

Figure 30 shows a sketch of a typical rotor of the centrifuges used. A special holder was designed to fit into this steel rotor tube. This is shown in Figure 31. The design permitted complete filling and emptying of the tube after each run, and the holder contained a platform normal to the centrifugal field force for the mounting of a selected surface. For these experiments, a series of 4/40 stainless steel screws was selected as suitable surfaces for the deposition of particles.

With the very high-speed Beckman unit, a smaller rotor tube, and hence a smaller holder, had to be designed. This was identical in shape to that shown in Figure 31 but was of smaller dimensions.

TABLE 10

SUMMARY OF THE CAPACITIES OF VARIOUS CENTRIFUGES

<u>Manufacturer</u>	<u>Model</u>	<u>Type</u>	<u>Speed Range (rpm)</u>	<u>Speeds Used</u>	<u>Loading</u>
Sorvall	SS-1	Benchtop	0-16,850	5,000	2,588 g
				10,000	10,354 g
				16,850	29,400 g
Sorvall	RC2-B	Superspeed	0-20,000	19,600	39,780 g
<hr/>					
Spinco (Beckman)	"L"	Preparative	0-50,000	49,500	195,000 g
Spinco (Beckman)	L275	Preparative	0-70,000	-	503,000 g

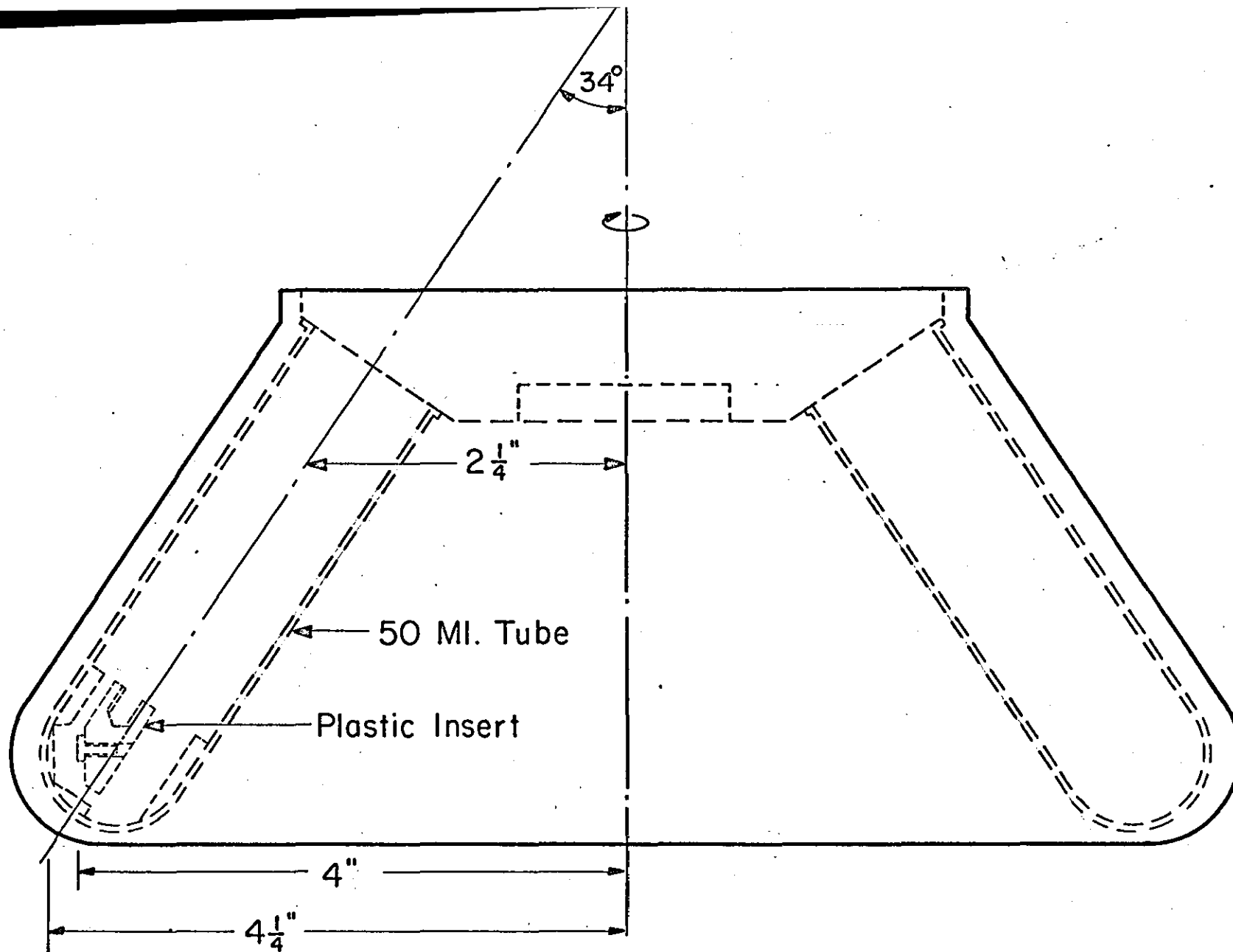
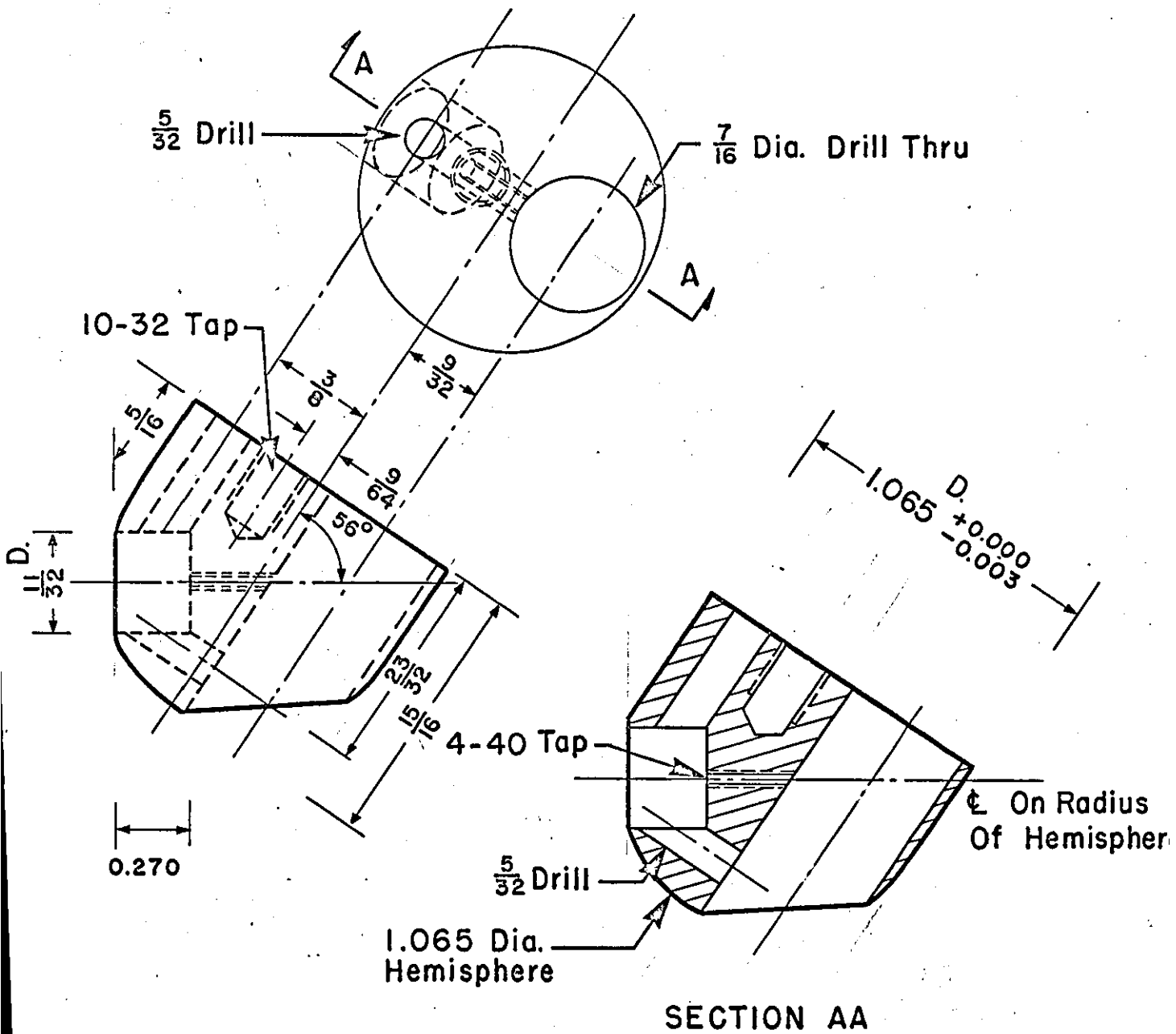


Figure 30
Sorvall SS-1 Rotor with Tube



Material

Cadco $1\frac{1}{8}$ Dia.
1103 Delrin Rod

Figure 31
Plastic Insert

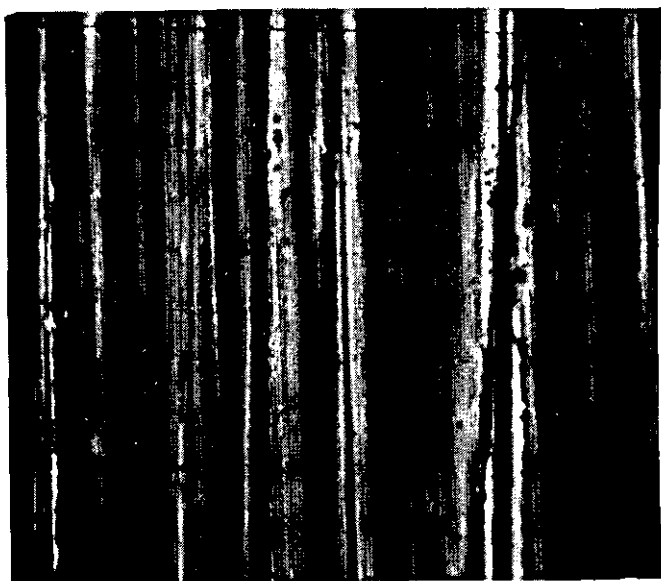
The 4/40 stainless steel screw heads were next prepared in various ways. For the experimental program, it was decided to use the Fe_2O_3 powder only and to treat the screw-head surfaces so that various particle-surface combinations could be studied. The literature had shown that surface roughness was a parameter of great importance for larger particles, and so this variable was selected for investigation. Three roughness values were selected, and the screw heads were prepared by polishing with 240-grit, 600-grit, and metallographic polish. The resulting surfaces were termed rough, medium rough, and smooth.

Surfaces having the three roughness values are depicted in Figures 32 and 33. Because the experimental program involved extensive SEM analysis, which involved coating each surface with a gold film, many of these surfaces had to be prepared in order to complete the experimental program. This raised the question of "how reproducible the surface polishing technique in fact was", and consequently this question had to be resolved before any experimentation could begin. This was done by image analysis of the SEM photomicrographs.

These surfaces were characterized by examination under the computerized scanning electron microscope facility at Pennsylvania State University. The raw data representing the width of the grooves is presented in Figure 34. The data was processed and characteristic parameters,



Figure 32
Surface of Rough Stainless Steel (240 Grit)



a) 600 Grit



b) Metallographic Polish

Figure 33
Surfaces of Medium Rough and Smooth Stainless Steel

such as fractional area occupied by the grooves, and distribution of the width of the grooves, was obtained. The reproducibility of surface preparation by different techniques is shown in Figure 34 where the broken lines represent duplicate analyses.

The depth of the grooves on the surface was estimated by taking stereoscopic pictures of the surfaces using the SEM at IITRI and analyzing the high and low regions by a parallax technique. The average depth of the grooves was $0.4\text{ }\mu\text{m}$ for the coarse and medium rough surfaces and less than $0.1\text{ }\mu\text{m}$ for the metallographically polished surface. This data showed that the surfaces could be prepared to be very reproducible and well within the requirements of the test program.

Several techniques were then considered for preparing surfaces with different chemical compositions but identical roughnesses. These included 1) the use of hollowed screw heads into which powders could be compacted before the screw face was polished, 2) gluing crystals or particles of the chemical composition required onto the screw head before polishing, 3) vacuum depositing surface films of the composition required onto the screw heads already polished to the roughness required, and 4) oxidizing the polished surface to produce a ferric oxide layer.

After experimentation, the latter two were chosen as being the most reproducible and reliable techniques.

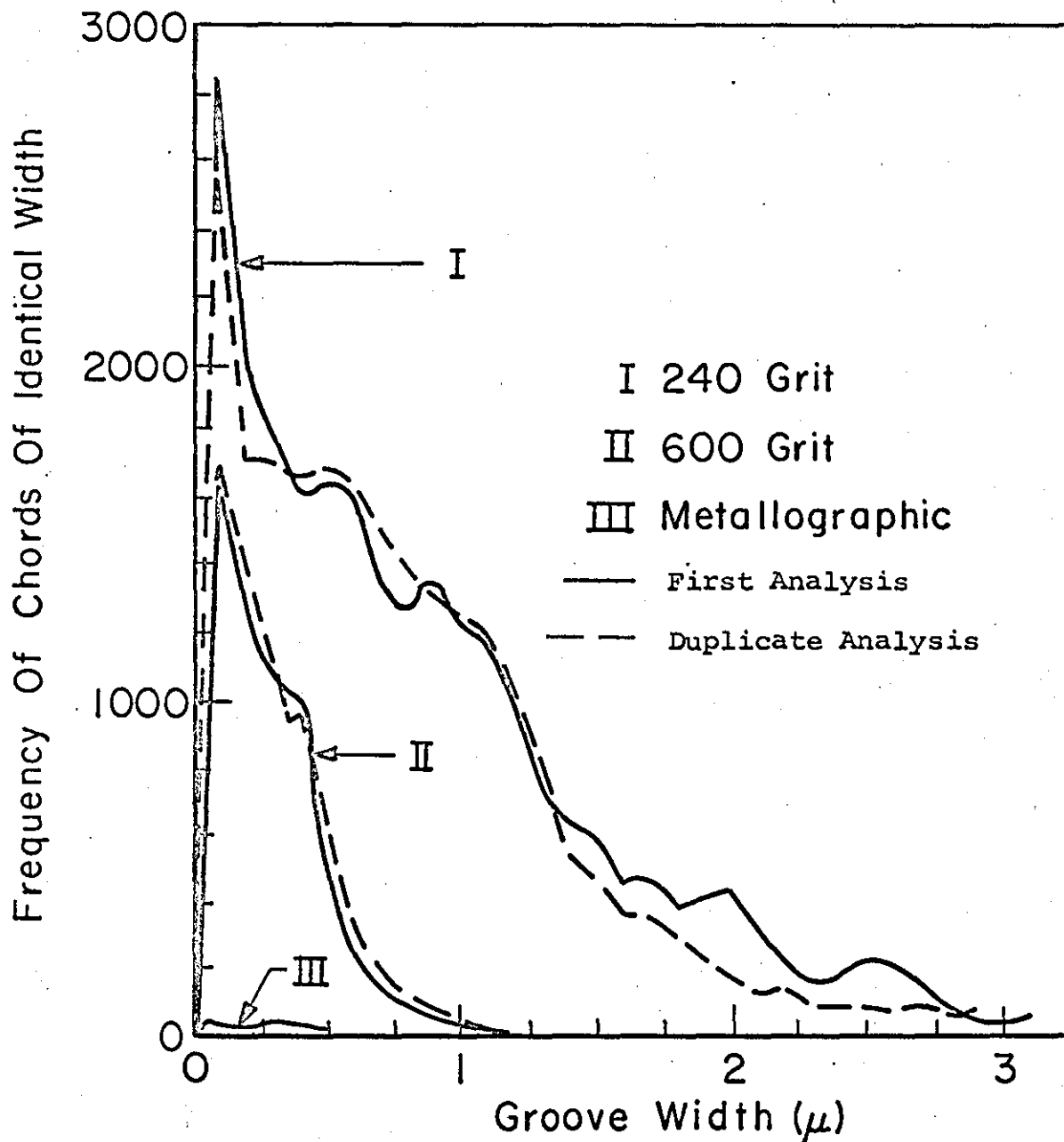


Figure 34

Surface Characterization of the
Stainless Steel Screw Heads

Consequently, films of carbon and silica were vacuum evaporated onto the polished screw heads to a film thickness of 50 Å, and it was found that this did not significantly change the surface roughness values. Also, some screw heads were oxidized in moist air at a temperature of 400°C for one hour to produce the ferric oxide surfaces required. Hence, the particle/surface combinations of ferric oxide to ferric oxide, carbon, silica, and steel could be interchanged to study the agglomerate and conglomerate forces of adhesion.

The next phase of the study involved an investigation into the methods of uniformly depositing particles of ferric oxide onto these surfaces so that adhesion measurements could be performed. Ideally, single particles were required on each surface with an interparticle distance of several diameters. This was necessary because the force of adhesion at a single particle contact was required. If agglomerates or particle layers were present, erroneous data would be generated.

Three techniques were tried for particle deposition. These included thermal precipitation, electrostatic precipitation, and diffusion.

The first two techniques were eliminated as a result of extensive agglomeration being present on the surfaces after deposition. Diffusion was selected as the best technique as fewer agglomerates were observed. A deposition chamber, such as the one shown in Figure 35, was used for the deposition experiments.

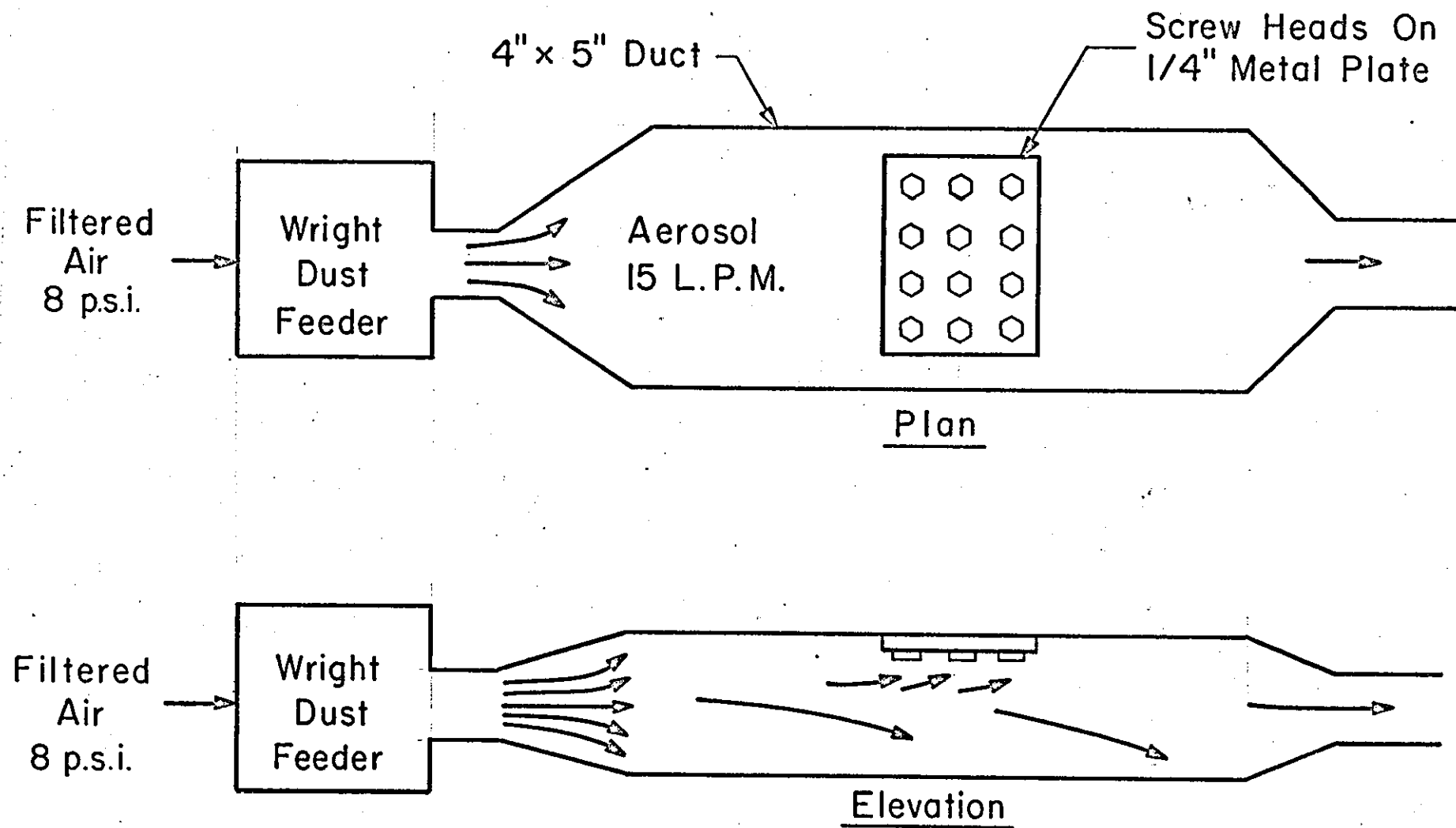


Figure 35

Apparatus for the Deposition of Particles onto the
Surfaces of the Screw Heads

A Wright Dust Feeder was employed to disperse the powder, and the resultant aerosol passed into a 4 in. x 5 in. duct. A metal plate holding 12 screw heads was placed "surface faces down" in the roof of the duct. In this way gravitational settling tended to remove most of the agglomerates from the air stream and many single particles were found adhering to the surface faces. A typical field of view is shown in Figure 36.

After repeated variations of the dust loading in the aerosol, followed by SEM examination of the surfaces, it was found that an aerosol concentration of 10^6 - 10^7 particles/cc was optimum. This gave a particle concentration of 10^7 - 10^8 particles/sq. cm. and an interparticle distance of 1-5 μ m. This was adequate for the accurate detection and size analysis of the deposited particles.

For these adhesion measurements at low particle concentration, it was found that lower phosphate concentrations could be used to produce the double layer stability. Measurements showed that dispersion in 1×10^{-3} mols/liter pyrophosphate yielded a zeta potential of -75 mv, which was the maximum obtained under these conditions.

To count and size the particles removed from a surface after each incremental centrifugal force application, it was necessary to locate the same fields each time. Three methods were tried to enable rapid and accurate location of the identical field of particles under the SEM. Two of these, micromesh screen overlay and chemical grid

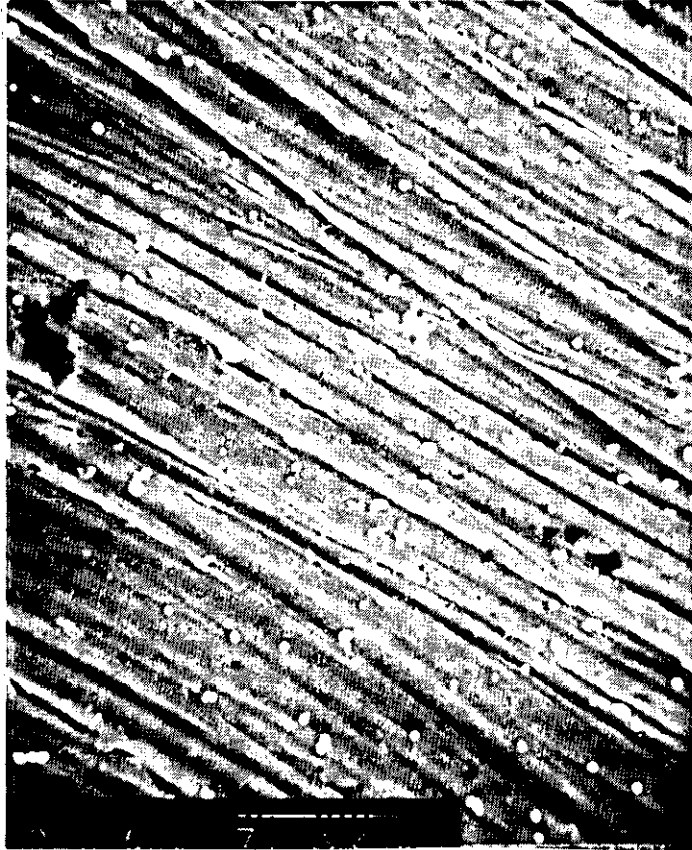


Figure 36

Surface After Deposition Showing the
Particle Distribution

etching, were not acceptable due to the problems of focusing and surface undercutting respectively. The third process involving the simple V-notching of the surface was selected even though it limited the use of the surface to one or two fields per surface.

The technique used to measure the force of adhesion was then as follows:

The polished screws were mounted on a rectangular 1/4-in. plate and submerged in Alconox solution to degrease the surfaces. Cleaning was performed in an ultrasonic bath. The screw heads were then rinsed in water, washed with acetone, and dried. The steel rotor tube and holder were cleaned and dried in an identical manner. The required number of screws were next mounted on the deposition plate in the diffusional deposition chamber and ferric oxide deposited on their surfaces in the manner and at the concentration previously established. The plate was then removed and placed in a clean petri dish under a clean hood.

One screw head at a time was selected and examined under the S.E.M. without gold coating, and a series of photomicrographs were taken in sequence starting from the V-notch location. The screw was then inserted into the centrifuge holder and the latter placed in the stainless steel rotor tube. Twenty-five milliliters of filtered sodium pyrophosphate solution of concentration equivalent to that determined in 3.1.3 was very slowly pipetted into the tube through the 7/16-in. diameter hole. The

tube was then covered with a lid and inserted into the centrifuge. The tube was allowed to stand for two hours to reach equilibrium. The lowest speed of 5000 rpm was selected and the centrifuge started. Its speed was gradually increased using a Variac so that the acceleration was smooth and even. At 5000 rpm, the centrifuge was run for 10 minutes and then its speed decreased at the same rate as it had been increased. The tube was then removed, slowly drained, and the surface and holder carefully washed by filling and emptying the tube several times with water. Finally the tube was drained and the screw head dried. The screw head was then reexamined under the S.E.M. and the identical fields of view rephotographed.

A second screw head was selected and the operation repeated at 10,000 rpm. This procedure was repeated at 10,000 rpm. This procedure was repeated for speeds of 16,850, 20,000, 50,000, and 70,000 rpm, a total of six screw heads being used for each complete run.

The photomicrographs of the fields of view were then examined and the number of single particles present, both before and after centrifuging, determined. The size distributions of particles before and after centrifuging were also measured using reticules, and the size distribution data was reported in terms of the projected area diameters. The number of particles removed was then plotted cumulatively against the force in dynes

which corresponded to each incremental speed and the force of adhesion estimated as that force at which 50% of the single Fe_2O_3 particles were removed from the surface.

The reproducibility of the force of adhesion data was investigated at 50,000 and 70,000 rpm. At the lower speed, providing that a minimum 60-100 particles were counted, reproducibility was within 10% in each case. However, when the number of particles/field fell to 20-30, the reproducibility of results deteriorated to 20%-25%. In all the 70,000 rpm work, fields containing 60-100 particles were counted, and in some cases, reproducibilities as low as 2%-3% were obtained, but the data generally fell within the 5%-10% reproducibility values.

3.1.3.3 Experimental Measurements

The preceding methods and protocols were then used, as stated, to study the effect of surface roughness, surface composition, temperature, and particle size on the force of adhesion. These measurements were made at the speeds of 5,000, 10,000, 16,850, 19,600, 50,000, 60,000, and 70,000 rpm, which corresponded to forces of 1.5×10^{-7} , 5.9×10^{-7} , 1.7×10^{-6} , 2.3×10^{-6} , 1.1×10^{-5} , 1.7×10^{-5} , and 2.5×10^{-5} dynes for Fe_2O_3 particles. The results are given in the following sections.

3.1.3.3.1 Effect of Surface Roughness

For this particular study, only the stainless steel screws were used. These were polished to the three roughness values described previously.

Ferric oxide particles were then deposited onto sets of the three surfaces, characterized for size and concentration on each surface, and centrifuged at the various speeds described above. After each speed the surface was characterized again for the size and concentration of the particles removed. No particles were removed at the first four speeds, but particle removal began at 50,000 rpm. The relative percent removed per speed is given in Table 11. From these results, it is seen that at 50,000 rpm there is some effect of surface roughness, particularly between the smooth and the other two rough surfaces. After examination of the surface, the particles removed at this speed were found to be the larger ones, that is to say, particles of 0.7 to 1.0 μm .

At 70,000 rpm there was no evidence of any effect of surface roughness, but it was indicated that the particles removed were generally of lower size than those removed at lower speeds, e.g., 0.1 to 0.7 μm . These results suggested that surface roughness was only a factor for particles of size greater than 0.7 μm . and was of no consequence for smaller sizes.

TABLE 11
EFFECT OF SURFACE ROUGHNESS

<u>Particles</u>	<u>Substrate</u>	<u>Roughness</u>	<u>% Removed at</u>		
			<u>20,000</u> <u>rpm</u>	<u>50,000</u> <u>rpm</u>	<u>70,000</u> <u>rpm</u>
Fe_2O_3	Stainless Steel	Smooth	0	0	42
		Med. Rough	0	5	42
		Rough	0	7	31

3.1.3.3.2 Effect of Surface Composition

For this study, medium rough surfaces were employed having surface compositions of stainless steel, ferric oxide, carbon, and silica. Independent batches of each surface composition had particles of ferric oxide deposited on them, and the forces of adhesion were measured at the six speeds indicated previously. The results are given in Table 12.

TABLE 12

EFFECT OF SURFACE COMPOSITION

Parti- cles	Sub- strate	Rough ness	% Removed at				
			10,000 rpm	20,000 rpm	50,000 rpm	60,000 rpm	70,000 rpm
Fe ₂ O ₃	Steel		0	0	5.4	18.5	42.0
	Fe ₂ O ₃	Med.	0	0	24.1	36.8	50.5
	Carbon	Rough	0	0	20.0	20.3	29.5
	Silica		0	0	9.5	16.5	29.5

From this table it is seen that the percent removed at 20,000 rpm was zero in all cases, and, in fact, was zero at all speeds up to 50,000 rpm. At 50,000 rpm, the percent removed from the stainless steel surfaces was significantly less than that from other surfaces; or conversely, the force of adhesion of the particles to stainless steel at 50,000 rpm was higher than it was for other particle/surface combinations. At 70,000 rpm, this effect was not observed, indicating that this may again be some particle size effect. Considering the results at 70,000 rpm, it is seen that the percent of ferric oxide removed from the ferric oxide surface was greater than

the percent of ferric oxide from any other surface. This indicated that the forces of adhesion between particles and surfaces of the same composition were lower than those between particles and surfaces of different composition. This suggested that conglomerates were more tightly bound together than agglomerates.

3.1.3.3.3 Effect of Temperature

The effect of temperature was studied using surfaces of medium rough stainless steel. Particles of ferric oxide were deposited onto individual batches of these surfaces, and the percent removed at 50,000 rpm for temperatures of 25°C and 60°C were determined. The data is given in Table 13.

TABLE 13

EFFECT OF TEMPERATURE AT 50,000 RPM

<u>Particles</u>	<u>Substrate</u>	<u>Roughness</u>	<u>Temperature °C</u>	<u>% Removal</u>
Fe ₂ O ₃	Stainless Steel	Medium	25	5.0
	Stainless Steel	Medium	60	6.0

From this data it was seen that the percent removed from the surfaces was slightly higher at 60°C. This suggested that the force of adhesion was slightly lower at 60°C than at 25°C, which confirmed the results reported in the literature for macroscopic particles.

3.1.3.3.4 Effect of Particle Size

The effect of particle size on the measurements was studied by measuring the size distributions of the

deposited particles on the surface before and after each centrifugal run. Figure 37 shows typical data obtained from the investigation.

On the left is shown the size distribution of ferric oxide on the medium rough stainless steel surface before centrifuging at 70,000 rpm. On the right is shown the size distribution of the particles removed from the surface after centrifuging. This demonstrated that the particle size distribution removed during centrifugation was deficient in fines, which suggested that there was a tendency to remove the coarser end of the size spectrum during the measurement procedure. However, a fair percentage of 0 to 0.6 μm . particles were still removed at this speed. The broad size range removed at any one speed confirmed the findings in the literature on larger particles, which was explained on the basis of variable areas of contact between particles and surfaces.

3.1.3.3.5 Determination of the Force of Adhesion for Different Particle/Surface Combinations

By definition, the average force of adhesion was that force that must be applied to removed 50% of the particles from a surface. Hence, by plotting the data in terms of the "force in dynes" versus "percent of particles removed", the force of adhesion can be determined from the 50% value of the distribution. Because of the difficulty of separating submicron particles, some data did not show a 50% removal even at 70,000 rpm. Hence, an extrapolation procedure was adopted. This was

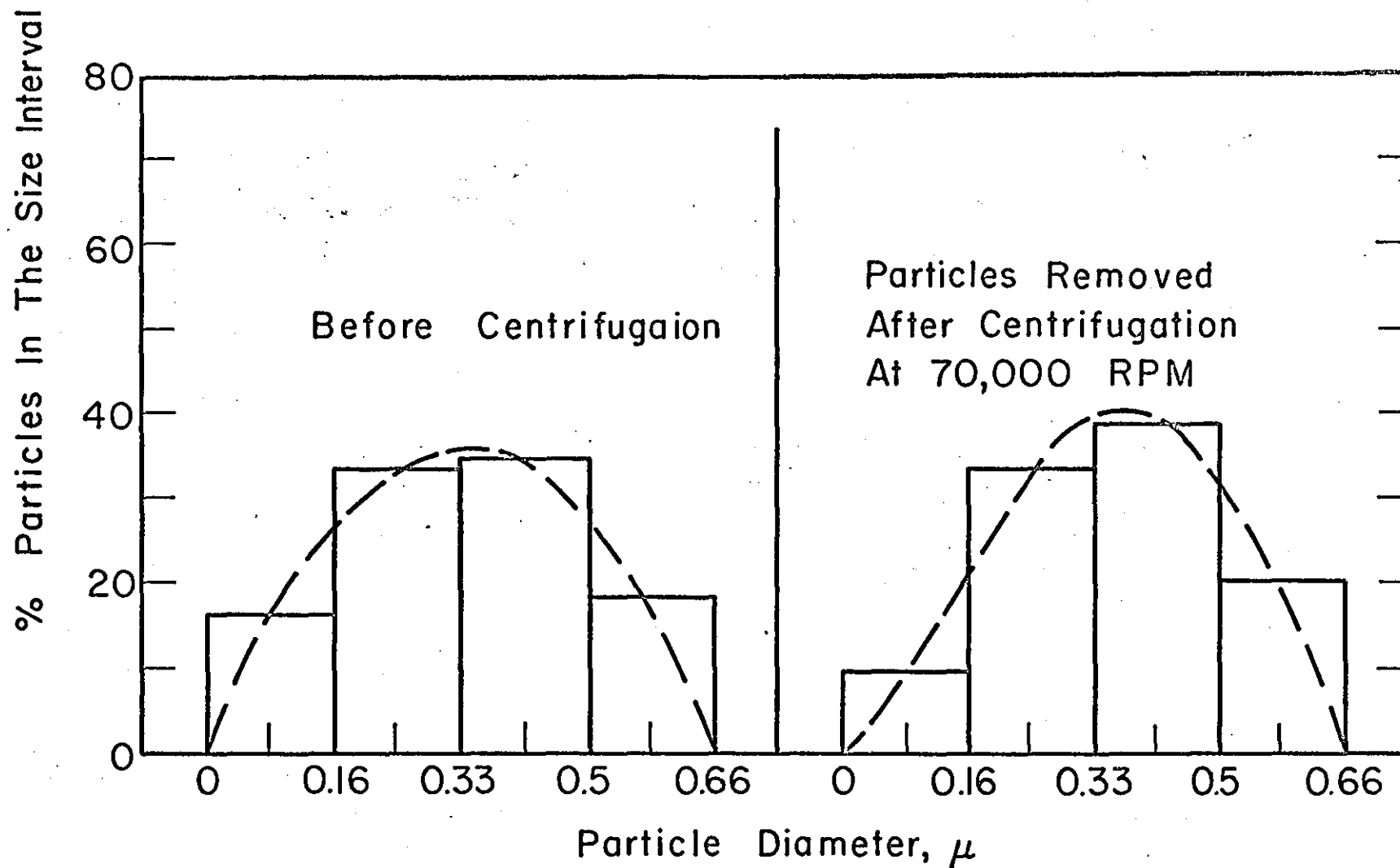


Figure 37
Effect of Particle Size

justified on the basis that much previous data on force of adhesion measurements on larger particles had shown that such a force-particle removal distribution was approximately log-normally distributed. Figure 38 shows recent data taken by Krupp¹⁷⁶ for gold spheres on polyester and cellulose plotted this way, and this demonstrates the behaviour rather well. Hence, by assuming a log-normal distribution, not only can the forces of adhesion of the Fe_2O_3 on various substrates be found, but by extrapolation to the 99.99% removed axis, an estimate of the force required to separate all particles from the surface can be obtained. The data for Fe_2O_3 on the various substrates is shown in Figure 39.

From this figure, it can be seen that the force of adhesion of Fe_2O_3 on steel, carbon, and silica is very similar and can be recorded as 3.2×10^{-5} dynes. Fe_2O_3 on ferric oxide is, however, significantly lower and is estimated at 2.1×10^{-5} dynes. This lower value indicates that the force of adhesion between similar surfaces is lower than that for dissimilar surfaces, and in consequence, the force of adhesion between agglomerates is lower than that of conglomerates. When the line of best fit for all the data was calculated and extrapolated to estimate the force required to remove 99.99% of the particles, a value of 3×10^{-4} dynes was obtained. Hence, a force of at least 10^{-3} dynes has to be applied to an agglomerate or conglomerate consisting of these particles if it is to be completely subdivided into its discrete particle population.

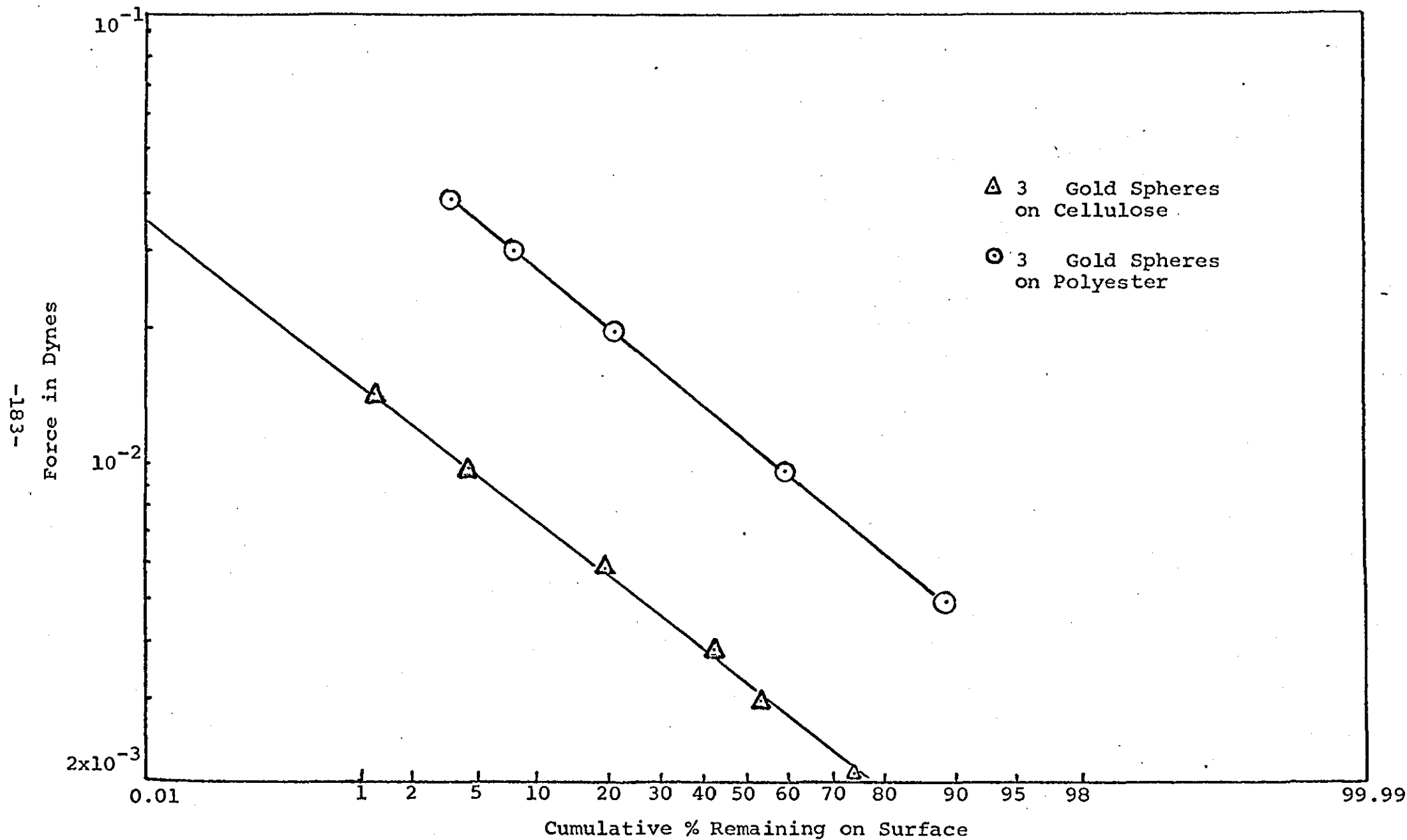


Fig. 38 - Data of Krupp for Gold Spheres on Cellulose and Polyester in Aqueous Triphosphate Solution

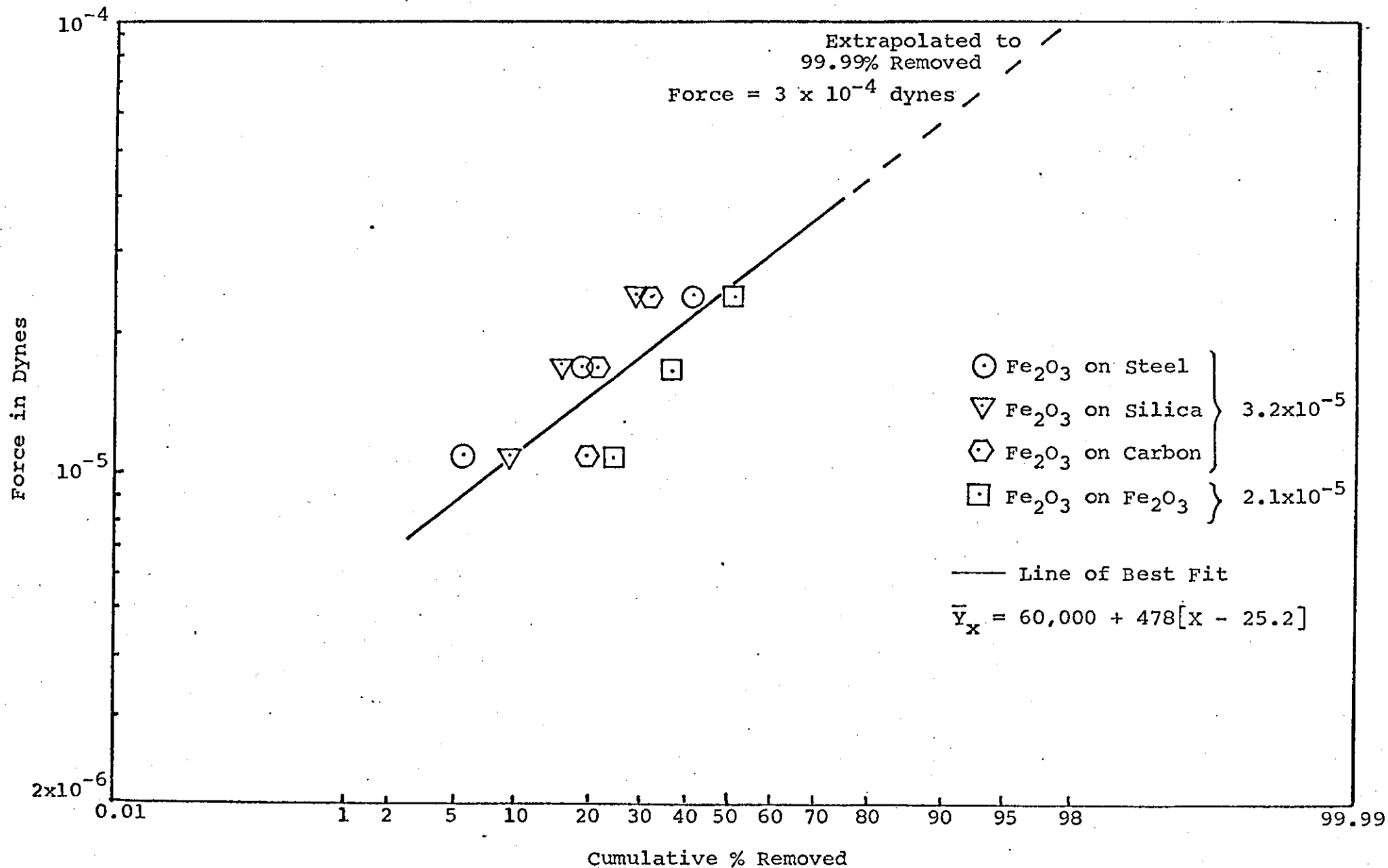


Fig. 39 - Force of Adhesion Data

3.1.3.4 Theoretical Calculation of the Force of Adhesion

The Van der Waals-London attraction energy between two spherical particles is given by

$$V_A = - \frac{Ar_1r_2}{6(r_1 + r_2)s_0}$$

where A is the Hamaker constant, r_1 and r_2 are the radii of the two particles, and s_0 is the shortest distance of separation between the two particles.

The double layer repulsion energy due to the adsorbed phosphate on the two spheres is given by Wnek¹⁷² as

$$V_R = \frac{32\pi r_1 r_2}{r_1 + r_2} \left[\gamma_1^2 e^{-2\Delta} + \gamma_2^2 e^{2\Delta} + 2\gamma_1 \gamma_2 \right] \frac{n_o K T}{k^2} e^{-ks}$$

where

γ_1 = activity coefficient for surface 1

γ_2 = activity coefficient for surface 2

$\Delta = (\zeta - 2kd)$ where ζ = zeta potential, d = separation distance

k^{-1} = thickness of double layer

K = Boltzmann constant

n_o = number of adsorption sites /cm²

The total interaction energy between the two particles is therefore obtained by addition of the two values

$$V_T = V_A + V_R$$

The net force between the two particles is given by

$$F_T = \left. \frac{dV_T}{ds} \right|_{s_0}$$

where s_0 is the minimum separation distance.

The force between a spherical particle and a flat plate was obtained by assigning a large value to the radius of one of the particles.

A computer program to calculate the attractive and repulsive components and the total interaction energy was developed. An extension to this program enabled the corresponding forces between particle and surface to be calculated. The forces of adhesion between Fe_2O_3 particles and substrates of ferric oxide and steel were calculated.

The values of the parameters used were 4.5×10^{-13} ergs for the Hamaker constant, $0.3 \mu\text{A}$ for the particle diameter, 75 mV for the zeta potential, and 0.0048 mols/liter for the ionic strength. The forces of adhesion for various values of the separation distance were plotted in Figure 40. The corresponding experimental values estimated from Figure 39 are shown as a narrow band. For theory and experiment to agree, a separation distance of 9 \AA to 10 \AA had to be present in the experimental measurements. To investigate this possibility, the literature was consulted, and it was found that distances of 4 \AA - 16 \AA had been reported, but more specifically, Bailey²²⁹ had reported distances of $7 \pm 2 \text{ \AA}$ for most materials. Hence, this confirmed that the experimental values were, in fact, in agreement with theory, and the forces of 2.1×10^{-5} to 3.2×10^{-5} dynes were a good estimate of the forces acting between agglomerates and conglomerates respectively.

To investigate this further, other experimental data was sought, but it was found that no submicron data other than this had been reported. However, an estimate of the force of adhesion for ferric oxide particles having an

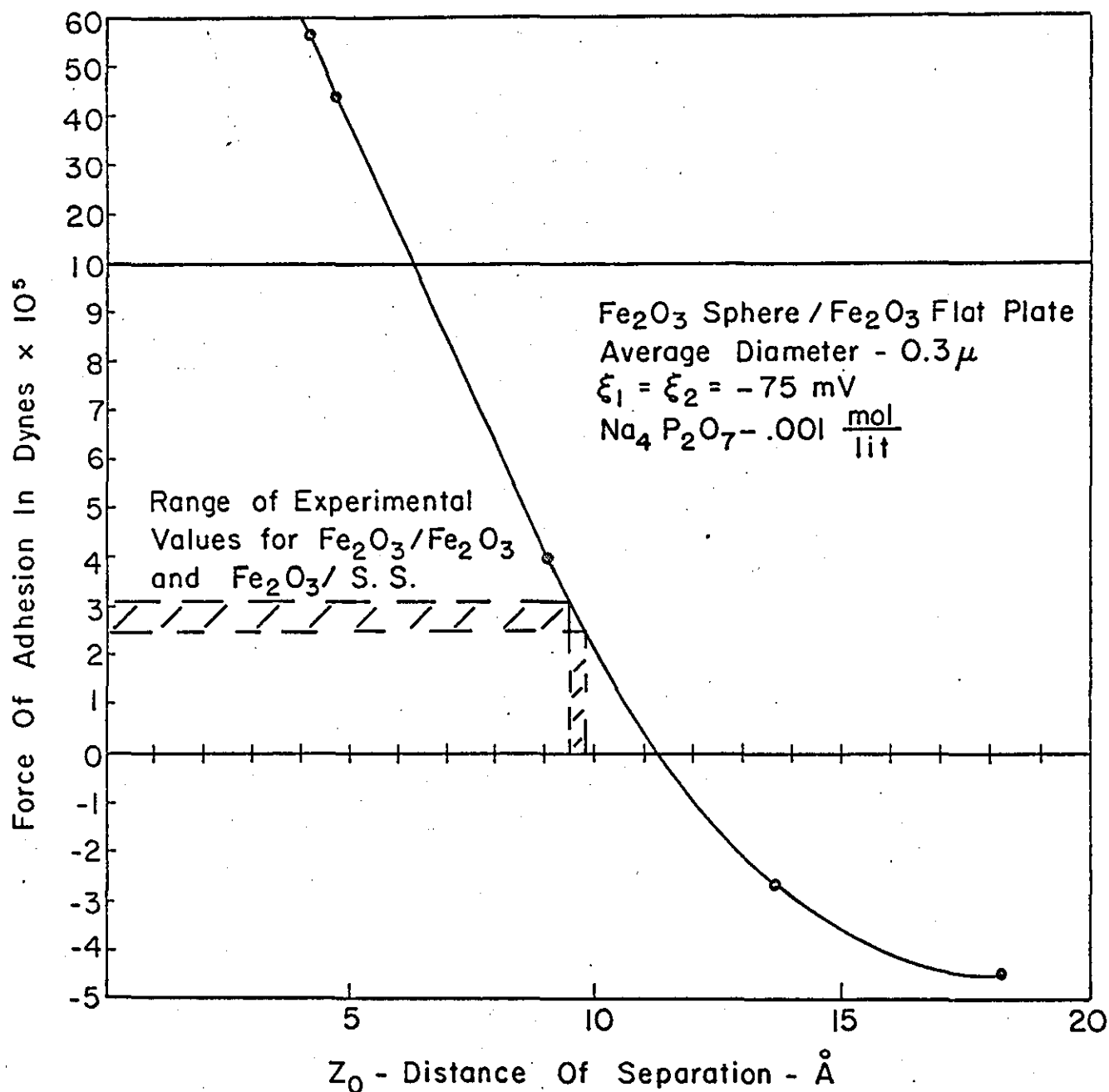


Figure 40

Calculated Force of Adhesion of Ferric Oxide
 to Surfaces Using Theoretical Models

average diameter of $0.30 \mu\text{m}$. was obtained from an extrapolation of the data of Böehme²⁹ and Beischer¹⁷⁴.

Böehme, et al.,²⁹ measured the force of adhesion between Fe_2O_3 particles (2 and $4 \mu\text{m}$. diameter) and Fe_2O_3 substrate. Beischer¹⁷⁴ allowed threads of Fe_2O_3 particles to break under their own weight. The force of adhesion was estimated from the size of the separated fragments.

The force of adhesion was assumed to depend on the particle size by the following expression:

$$F_{\text{Adhesion}} \propto d^n$$

The values of F_A calculated for $n = 1$ and 2 from the data by Böehme²⁹ showed that the actual force of adhesion was expected to lie between 1.3×10^{-4} and 2.18×10^{-5} dynes. These calculations were used only as a preliminary qualitative estimate as the extrapolation of the data was subject to errors due to differences in experimental conditions. However, once again the data showed good agreement with the experimental results obtained in this section.

3.1.3.5 Conclusion

The force of adhesion between submicron Fe_2O_3 particles and substrates of various compositions was measured. Experimental data was found to agree well with theory, and a force of 2.1×10^{-5} to 3.24×10^{-5} dynes was measured for Fe_2O_3 on Fe_2O_3 and Fe_2O_3 on carbon, silica, and steel respectively. It was estimated that a force of 1.9×10^{-4} to 4.5×10^{-4} dynes was, however, required

to remove 99.99% of particles from the substrates. Hence, allowing for errors and instituting a safety margin, a force of 10^{-3} dynes should be sufficient to separate all the particles from each other in agglomerate and conglomerate systems.

It was also found that the roughness of the surface had no effect on the force of adhesion for particles of size less than $0.7\mu\text{m.}$, but some effect was found for particles of larger size. Temperature also had a slight effect, the force of adhesion being slightly lower at 60°C than at 25°C .

Hence, for the separation studies, a force of 10^{-3} dynes applied in aqueous pyrophosphate solution at a zeta potential of 75 mV, a pH of 9.5, and a temperature of 60°C should be adequate to separate submicron particle agglomerates and conglomerates.

3.1.4 Selection of the Potential Separation Devices Based on the Force Available for Application

The force of adhesion required to remove 50% of the particles from the surfaces was shown to range from 2.1×10^{-5} dynes to 3.2×10^{-5} dynes, and the force estimated to remove all the particles from the surface was shown to be 1×10^{-3} dynes. As these forces were measured normal to the surface, they represented the tensile strengths between the particles and the surface. To estimate the shear stress that must be generated by a device to separate agglomerates and conglomerates

bound by this force, some value for the particle-to-surface contact area has to be used. Such a value was impossible to experimentally measure on the submicron particles, and so a value had to be assumed for the calculation. The problem of measuring this area proved even too difficult for larger particles of size 50-100 μm ., as Rumpf and Herrmann²³⁰ reported. These authors assumed a value of 1 μm . for the diameter of the contact area between spheres but reported no substantial reason to support such an estimate. Further, no literature reference was found in which estimates for 0.3 μm . particles were reported, and so a value had to be selected based on the following assumption. The surface roughness grooves of the medium rough surfaces were shown to have depths greater than the mean diameters of the particles, and so many particles would be within these grooves. The particles would therefore tend to have proportionally larger contact areas than those particles reported by Rumpf and Herrmann.²³⁰ Hence, as Rumpf and Herrmann reported a contact area diameter to particle diameter ratio of 1:50 or 100, a higher value of 1:10 was assumed for the submicron particles. This yielded a contact area diameter of 0.03 μm for a 0.3 μm particle. Using this value, a contact area of approximately $7 \times 10^{-12} \text{ cm}^2$ was estimated between the particle and the surface, and for a force of 1×10^{-3} dynes, a stress of 0.15×10^8 dynes/sq cm was found to be required to separate all the particles.

When equipment is now reviewed for the application of this stress, the choice is fairly narrow. For example, assuming that separation is to be performed in aqueous phosphate solution, Rumpf and Raasch²³⁴ showed that the maximum shear stress that could be applied by impellers and homogenizers was 1 Kgm/sq cm, which was equivalent to 1×10^6 dynes/sq cm. Although this was considerably lower than the value of 0.15×10^8 dynes/sq cm necessary to remove all the particles, it was fairly close to the value of 3×10^6 dynes/sq cm necessary to remove 50% of iron oxide particles from iron oxide. Hence, impellers and homogenizers should separate some of the particles in such a system, but should not separate them all. However, if one wishes to increase the liquid viscosity, then higher shear stresses could naturally be generated.

If one now calculates the shear stress that can be generated in an aqueous suspension of particles in a sand mill, it is found that higher stresses are available to separate the particles. Bosse²¹² calculated the shear stress generated in a sand mill in which 0.7 mm sand was agitated by disc impellers. The discs were assumed to produce a shear of 0.5 psi, and the stress generated on a 7 μ m agglomerate was found to be 3.5×10^8 dynes/sq cm. For 3 mm quartz sand, the stress generated on the same 7 μ m particle was shown by Engels²³¹ to be 1.7×10^{10} dynes/sq cm. Hence, forces in excess of that required to separate submicron particles are possible using a sand mill.

Finally, if one considers the use of cavitation from an ultrasonic source as a means of separation, even higher stresses are potentially available. Accurate estimates of this are not readily available in the literature, but an estimate can be obtained from a measurement of the force required to form pits in a metal surface. For example, if an aluminum plate is exposed to cavitation so that the plate becomes pitted, it is possible to calculate the diameter of the bubble that had produced the given pit. Knapp²³² showed that providing you assume that the work done on the surface by a collapsing bubble is the same as that done by a Vickers diamond pyramid hardness tester to form a pit of the same size, then an estimate can be made. For an 850 μm bubble, the work done in pit formation was estimated to be 6×10^5 cm dynes, and for a 2500 μm bubble, it was 6×10^6 cm dynes by this method. Further, Knapp²³² showed that if you assume that the work done by a fluid during bubble collapse is equivalent to the collapse energy, if surface tension is neglected, and if complete collapse of an empty bubble is assumed, then the work done in the collapse of the bubble will be the ambient pressure in the region of collapse multiplied by the initial volume of the bubble. From these assumptions, it was calculated that for an 850 μm bubble, the work done in the bubble collapse was 55×10^5 cm dynes, and for a 2500 bubble, 23×10^7 cm dynes. If this work could be done uniformly over the perimeter of a 0.3 μm particle, a force of 55×10^{10} and 23×10^{12} dynes would

be available from the collapse of an 850 μm and 2500 μm bubble respectively. Such forces are seen to be capable of separating chemical bonds in the metal plate and are in excess of those required for particle separation. However, Knapp shows that this force diminishes rapidly with distance from the bubble surface and only one bubble in 30,000 produces a damaging blow to the aluminum surface. In addition to this, Egorov¹⁹⁰ showed that by use of pressurized ultrasonics, even higher forces can be generated. Hence, these crude calculations show that ultrasonics and sand milling are capable of producing forces in excess of those required for agglomerate separation, and care must be taken to inspect particles for possible fracture after separation by these techniques.

3.1.5 Preliminary Screening of Separation Devices

The three types of separating devices discussed in the previous section were screened for their effectiveness in separating metal oxides. These were ultrasonics at variable pressures, micromedia milling, and high-speed impeller mixing.

These methods were studied by Davies and Ranade for the separation of alumina in aqueous media.²²⁵ In this study, a Branson 500-watt sonifier, a Virtis micromedia mill, and a Waring blender were studied. It was found that the micromedia mill was unsuitable for the separation of the oxide, as size reduction of the media continually occurred, and this changed the size distribution of the alumina to a coarser size.²²⁵ In consequence, it was decided to eliminate this method from the experimental studies in this thesis and to present data only on the performance of the two remaining devices. For information on the micromedia milling study, consult reference 225.

An apparatus capable of applying ultrasonic energy at high pressure to an aqueous suspension of metal oxides in aqueous media was assembled using a commercially available Branson 500-watt sonifier and a specially designed separation cell.²²⁵ A similar apparatus was used in this thesis. This is shown in Figure 41.

The sonifier unit consisted of a power supply, watt meter, converter, booster, and horn. The power supply was the Model 160, which had a power requirement of 8 amperes and was run from a 115 v 50/60 Hz supply. The maximum output

power in electrical watts transmitted to the converter was 700 watts. The converter was the Model 102, and it was claimed that this unit converted this maximum power into 670 mechanical watts. This converter consisted of a lead zirconate titanate electrostrictive element which expanded and contracted under an alternating voltage. The frequency output of the unit was 20 Hz, but its amplitude was variable, depending on the booster used. Two boosters were purchased with a coupling bar. The boosters were the Models 101-149-044 (Blue) and 101-149-012 (Black).

The coupling bar, Model 101-149-011 (Green) had an amplitude ratio of 1:1 and generated the typical amplitude that was emitted from the Branson horns. The black and blue boosters, when interchanged with the green coupling bar, generated different amplitudes. The black booster generated an amplitude $2\frac{1}{2}$ times greater than that considered typical, while the blue booster generated an output with one-half the amplitude considered typical.

The converted power was then transmitted to the particles through a titanium horn. The intensity of the transmitted power depended on the area of the horn tip. Two horns were purchased, one having a 1-in. diameter circular tip and the other a $\frac{1}{2}$ -in. diameter circular tip.

Finally, the electrical power transmitted to the converter was monitored by the Model W-3 wattmeter. According to Branson, the actual mechanical power being transmitted

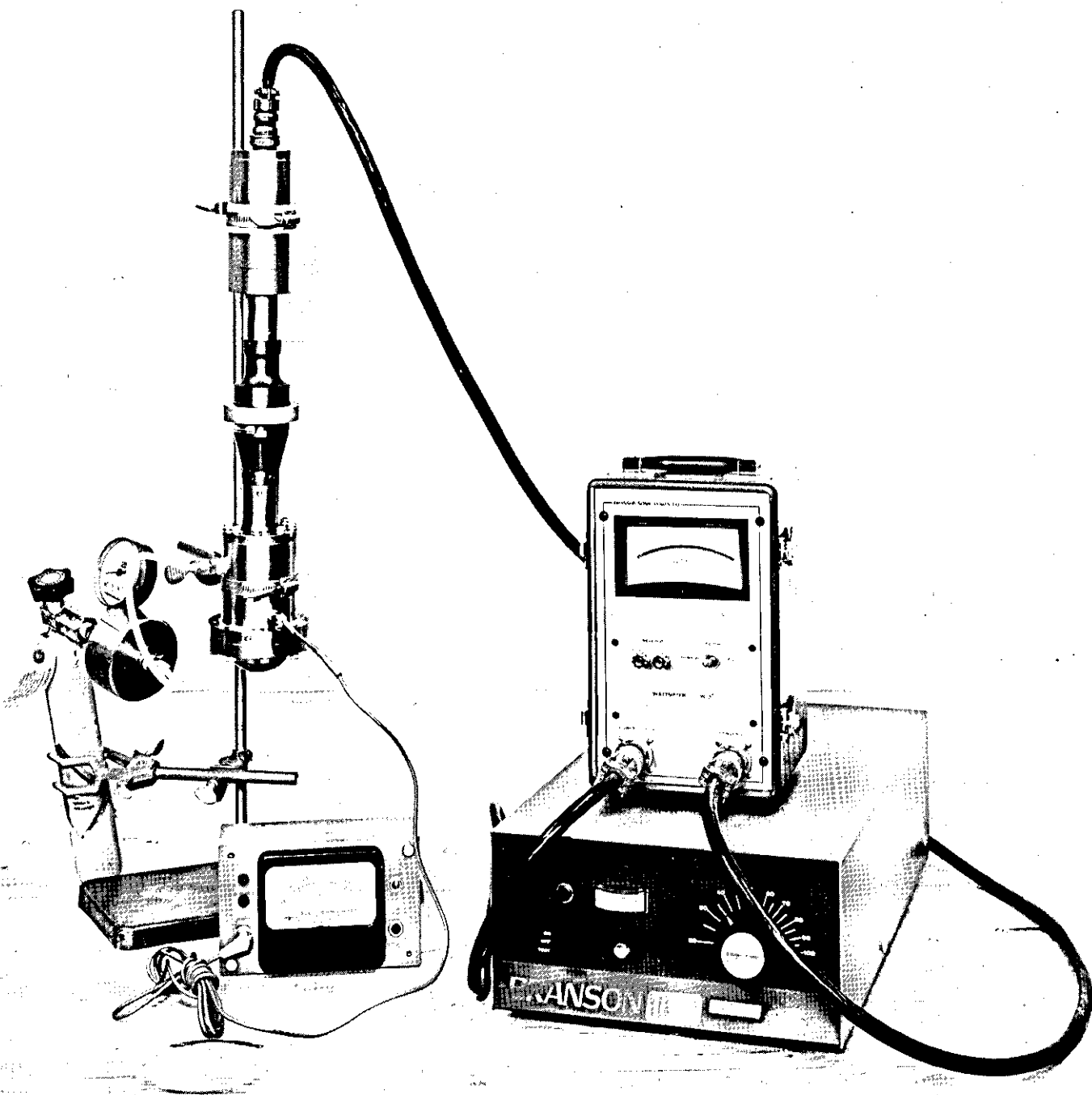


Fig. 41 - Completely Assembled Separation Unit

to the particles was then 95 percent of the electrical power reading on this wattmeter. The assembled sonifier probe system is shown in Figure 41.

The separation cell was constructed of 1/4-in. titanium metal and was designed to withstand pressures greater than 15 atmospheres. During ultrasonication, the temperature of the suspension was controlled by the use of a cooling bath. With the bath, the cell could be completely immersed during sonication, and this gave a satisfactory temperature control. To monitor the temperature, a tubular stainless steel thermistor probe attached to a telethermometer gauge was employed. The thermistor probe was sealed into the wall of the cell so that the tip was immersed in the suspension during sonication.

To measure the pressure, a 0-600 psig 2-1/2 in. stainless steel pressure gauge was mounted on the 1/2-in. diameter outlet tube. This was, in turn, connected to a nitrogen cylinder fitted with a reduction valve.

The sonifier and separation cell are shown assembled in Figure 41. The unit is mounted on a drill stand, and when the temperature bath is in position, the assembly stands 3 ft high and occupies a bench area of 3 ft square. The whole unit was placed in an acoustically insulated box during sonication to minimize the noise level. After assembly, the unit was tested for compliance with the manufacturer's specifications. During the preliminary

trials, it performed satisfactorily, and some preliminary data were obtained on its operating characteristics.

Figure 42 shows the relationship between the power in watts and the pressure in psig for the different boosters using the 1-in. diameter horn. Figure 43 shows similar data for the 1/2-in. horn. From these curves, it is seen that the blue booster, tuned with the 1-in. horn, offers the widest range of operating pressure and power. With this device, several independent or controlled variables could be studied. Four were investigated, and these were input power, pressure, temperature, and time. An evaluation of the device was performed and reported in reference 225, and the results of this study are now presented.

A statistically designed experiment was used to study the influence of the four variables selected. This design is shown in Tables 14 and 15.

The first two variables had three levels in the experiment, while the last two variables had only two. The actual levels were exactly as given, and their number was fixed. The input power was controlled by joint variation of the equipment power setting and the booster ratio. The power setting and booster ratio used were recorded for each level of input power.

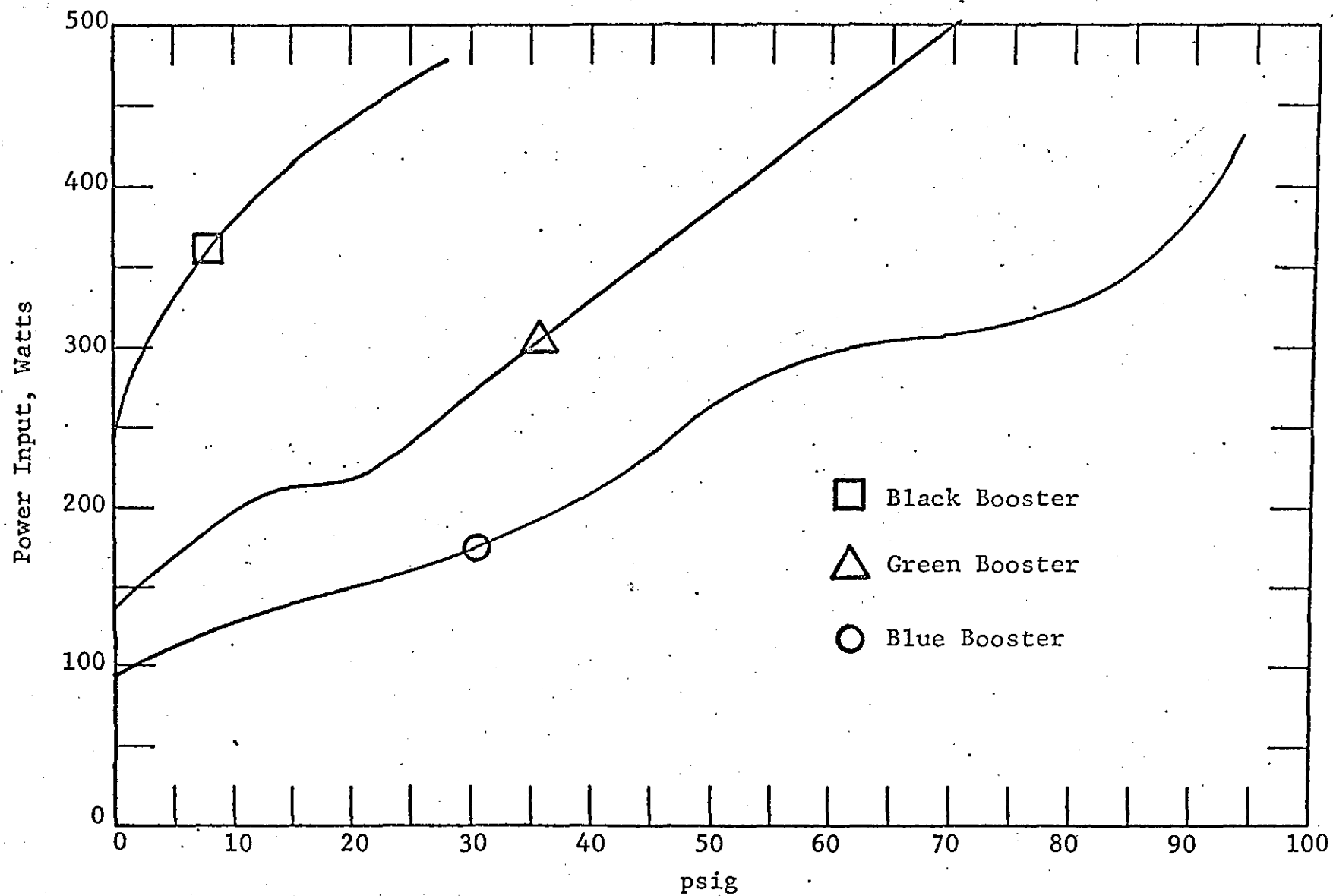


FIG. 42 - POWER SUPPLY CALIBRATION CURVES OF 1-IN. DIAMETER HORN DONE IN WATER AT ROOM TEMPERATURE

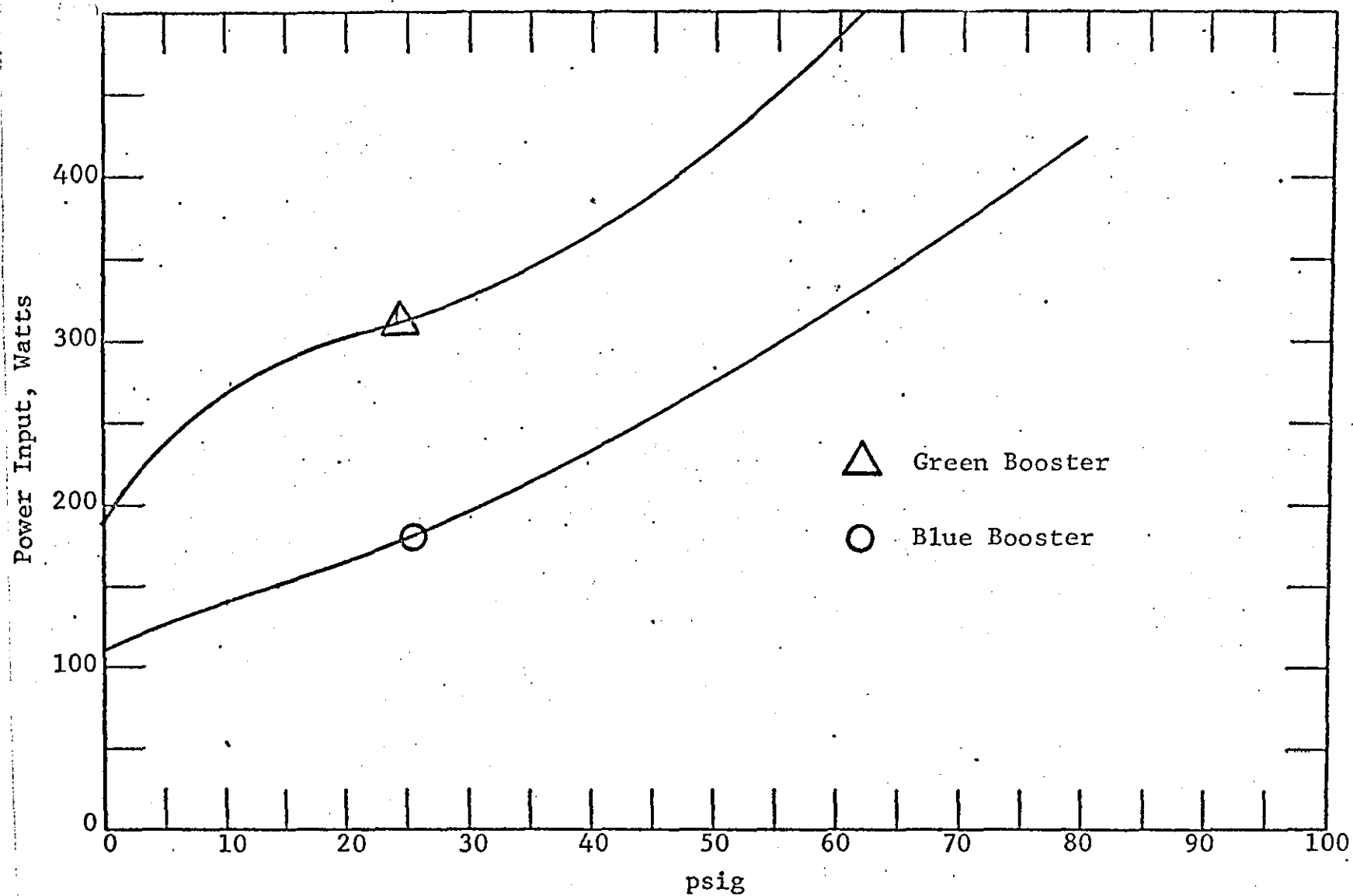


FIG. 43 - POWER SUPPLY CALIBRATION CURVES OF 1/2-IN. DIAMETER HORN DONE IN WATER AT ROOM TEMPERATURE

The principal dependent variables, i.e., measures of performance, were the observed changes in the mean and variance of the particle size distributions due to the application of the ultrasonic particle separation technique. These are discussed more fully later.

The actual design of the experiment is given in Table 15. There were 18 different combinations of levels of the independent variables. This was one-half of a complete factorial, which would have $2^2 \times 3^2 = 36$ combinations. The particular 18 combinations selected constituted a well balanced design, i.e., for each independent variable, the frequency of occurrence was the same for all levels; further, for all pairs of variables the frequency of occurrence of the 4, 6, and 9 combinations of levels was as nearly equal as possible; and so on for the variables taken three and four at a time.

Each combination in Table 15 was specified by the indices of the levels as they were defined in Table 14.

The multiplicity associated with each combination was the number of tests made with that combination. As the design stands, there were duplicate tests of three combinations, providing information on the pure experimental error (or repeatability) of the system.

The random sequence (last column of Table 15) is the order in which the combinations were run, so far as practicable.

TABLE 14

INDEPENDENT VARIABLES AND TENTATIVE LEVELS USED
IN THE EXPERIMENTAL DESIGN OF THE TESTING PROGRAM

<u>Variable</u>	<u>No. of Levels</u>	<u>Levels</u>
X ₁ , Input Power	3	(1) 100, (2) 300, (3) 500 watts
X ₂ , Pressure	3	(1) atmospheric = 14.7 (2) 50, (3) 100 psi
X ₃ , Temperature	2	(1) room, (2) 60°C
X ₄ , Time	2	(1) 5, (2) 15 minutes

TABLE 15

EXPERIMENT DESIGN OF THE TESTING PROGRAM

<u>Combi- nation</u>	<u>Multi- plicity</u>	<u>Levels of Controlled Factors</u>				<u>Random Sequence</u>
		<u>Power</u>	<u>Pressure</u>	<u>Temperature</u>	<u>Time</u>	
1	1	1	1	1	1	1
2	1	1	1	2	2	5
3	2	1	3	1	3	15
4	2	1	2	2	1	7
5	1	1	3	1	1	4
6	1	1	3	2	2	6
7	1	2	1	1	2	16
8	1	2	1	2	1	13
9	1	2	2	1	2	2
10	1	2	2	2	1	3
11	2	2	3	1	1	17
12	2	2	3	2	3	8
13	2	3	1	1	1	18
14	2	3	1	2	2	11
15	1	3	2	1	2	10
16	1	3	2	2	1	12
17	1	3	3	1	2	14
18	1	3	3	2	1	9

For these studies, the size distributions were measured using the Joyce Loebel disc centrifuge. Aluminum oxide only was used to test the device, and the conditions of phosphate, pH, zeta potential, etc., were as stated in 3.1.2.

The size distributions were plotted on logarithmic-probability paper and their geometric means read off at the 50 percent probability point. The standard deviations were measured by taking the ratio of the $\frac{84.1\%}{50\%}$ values on the size distribution plots.

The data are summarized in Table 16. It can be seen immediately that an unforeseen problem of horn erosion occurred. This introduced instant concern about the usefulness of the method as erosion introduced contamination in the form of metal alloy particulate. Of prime concern was the introduction of the particulate contamination into the sample, and of secondary concern was the problem of a short horn life. The reasons for this erosion were thought to be the application of excessive force by cavitation, and certain observations were made. Firstly, the degree of erosion was a function of the pressure applied. At atmospheric pressure, no erosion occurred at low power, but as the pressure increased, erosion became progressively worse. Secondly, the erosion was a function of the power applied. At atmospheric pressure and at a power of 100 watts and 220 watts, no erosion occurred, but at atmospheric pressure and a power of

The Joyce Loebel disc centrifuge method of size analysis is based on the work of Atherton, Cooper and Fox.²³⁹ The original instrument consisted of a disc, a sample injection apparatus, a sample collection unit and an electronic control system. The method of size analysis employed the line start or two-layer technique, whereby 1 ml of the suspension was injected onto the surface of a known volume of sedimentation fluid rotating in the disc. The particles within the dispersion then passed through the sedimentation fluid according to Stokes Law. The Stokes diameters of the particles were calculated by the following equation

$$D^2 = \frac{6.299 \times 10^9 \eta}{N^2 (p_p - p_F) T} \cdot \log_{10} \frac{R_2}{R_1}$$

where: T = centrifuge time in minutes

d_p = density of particle in ml.

d_{SF} = density of sedimentation fluid in g./ml.

N = centrifuge speed in rev./min.

η = viscosity of sedimentation fluid in poise

D = equivalent spherical diameter of particle in microns

R_2 = radius reached by a particle of diameter D after time (T)

R_1 = radius of the surface of the sedimentation fluid (determined by the volume).

At a calculated, preset time (T) a sampling probe is automatically activated to remove the sedimentation fluid to a known depth (R_2). All particles with Stokes' diameter less than D were automatically removed and transferred to a volumetric flask.

The particles were diluted to volume and the cumulative weight per cent was determined by chemical analysis of the contents of the flask.

In the experiments conducted in this thesis two important variations in this technique were used. Firstly, the buffered line-start procedure was employed. Normally, when particles are injected onto the sedimentation fluid they form a stable thin layer on the surface, free from turbulence or streaming. In some instances, this does not occur, and instability of the injected layer is seen. Instability is observed as clusters of particulates which rapidly spiral through the sedimentation fluid, making size analysis impossible. To eliminate this effect a buffered line-start procedure is adopted.²⁴⁰ This technique physically modifies the interface between the injected sample and the sedimentation fluid. For example, 1 ml. of fluid of lower density than the sedimentation fluid, is injected onto the surface of the sedimentation fluid, and the interface between the two liquids diffused by sharply increasing the speed of the rotating disc.

Use of such a technique ensures that, upon injection, the particles move into the sedimentation fluid through a smooth density gradient which, for most systems, eliminates instability and streaming.

In the experiments reported here, 1 ml. of distilled water was used as the buffer and 20 mls. of a 10% v/v glycerine/water solution was used as the sedimentation fluid.

Secondly in these studies the samples were not extracted and chemically analysed, as the Mark IV centrifuge fitted with an optical sensing mechanism was employed. In this device, the optical density of the sedimentation fluid at R_2 was automatically and constantly measured by use of a white light source and a photocell. Prior to the injection of a sample the optical density of the fluid was measured and recorded as the zero baseline of an X-Y recorder. Upon injection the optical density remained constant until the largest particles reached R_2 . At this time a change in optical density was recorded. By measuring the optical density from the time of injection to the time at which the smallest particles passes R_2 , a continuous optical density curve is obtained. By the use of a simple computer program the complete size distribution was calculated.

DATA FROM THE EXPERIMENTS USING ULTRASONIC ENERGY

Test No.	Sonication Time, min.	Temperature, °C	Pressure, psi	Power, watts	Booster	Size Distribution Mean, μ m	Geometric Standard Deviation	Remarks
1	5	Room	Atmos	100	1:1 Green	0.36/0.35	1.58/1.56	No Erosion
2	15	60	Atmos	100	1:1 Green	0.34	1.74	No Erosion
3	15	Room	50	100	1:1 Green	0.36/0.35	1.72/1.76	Slight Erosion of Horn
4	5	60	50	100	1:1 Green	0.37	1.65	Slight Erosion of Horn
5	5	Room	100	100	1:1 Green	0.54	1.57	Moderate Erosion of Horn
6	15	60	100	100	1:1 Green	0.42	1.73	Moderate Erosion of Horn
7	15	Room	Atmos	220	1:2.5 Black	0.36/0.36	1.67/1.67	No Erosion
8	5	60	Atmos	220	1:2.5 Black	0.33	1.67	No Erosion
9	15	Room	50	220	1:2.5 Black	0.38	1.71	Slight Erosion of Horn
10	5	60	50	220	1:2.5 Black	-	-	Severe Erosion - Sizing Impossible
11	5	Room	100	220	1:2.5 Black	-	-	Severe Erosion - Sizing Impossible
12	15	60	100	220	1:2.5 Black	-	-	Severe Erosion - Sizing Impossible
13	5	Room	Atmos	500	1:1 Green	-	-	Severe Erosion - Sizing Impossible
14	15	60	Atmos	500	1:1 Green	-	-	Severe Erosion - Sizing Impossible
15	15	Room	50	500	1:1 Green	-	-	Severe Erosion - Sizing Impossible
16	5	60	100	500	1:1 Green	0.39	1.59	Severe Erosion - Sizing Unreliable
17	15	Room	100	500	1:1 Green	0.41	1.70	Severe Erosion - Sizing Unreliable
18	5	60	100	500	1:1 Green	0.38	1.62	Severe Erosion - Sizing Unreliable
19	15	Room	Atmos	100	1:1 Green	0.35	1.66	No Erosion
20	15	Room	28	100	1:1 Green	0.37	1.76	No Erosion
21	15	Room	50	100	1:1 Green	0.35	1.71	No Erosion

500 watts, erosion took place. An observation of the suspension when erosion was present showed the liquid to be very turbid after sonication due to the presence of tiny gas bubbles. The action of these bubbles under intense cavitation most probably was the cause of the erosion effect. The effect was manifested by a severe pitting of the horn tip, and it was found to be more severe on the 1/2-in. probe tip than on the 1-in. probe tip. In consequence, the 1-in. probe tip was used exclusively to generate the data in Table 16. To try to resolve some of these difficulties, the manufacturer was contacted for suggestions on how to minimize the effect. He could not offer any constructive way of reducing the erosion in aqueous media but commented that in his experience the use of non-aqueous media usually minimized the erosion effect. This was a variable not taken into account in the experiments because the literature had indicated that aqueous media containing phosphate was the best separation medium to use. Of course, the basis for the selection of the aqueous phosphate solution was the double layer model, which showed a greater repulsion effect between submicron particles in phosphate solutions. It could obviously not predict the effect of cavitation on the probe tip. In consequence, the separation technique in aqueous media was a matter of compromise.

For the minimum erosion and contamination on aqueous media, a maximum of 220 watts applied at atmospheric pressure to the aqueous suspension was all that could be tolerated.

To give some idea of the extent of this erosion, the weight loss was estimated from a measure of the pit depths and diameters and a measure of the metal density. A weight loss of approximately 40 mg/hour was obtained for the high pressure tests, and this compares reasonably well with the value of 10-30 mg/hour reported by Knapp for ambient pressures.

In order now to examine the effect of the variables of power, temperature, pressure, and time on the separation of alumina, multiple regression equations were generated from existing computer programs in IIT Research Institute's Statistics Department.

Two multiple regression equations were developed that were constructed from the data of Table 16. The dependent variables of the two equations were the geometric means and the geometric standard deviations of the resulting particle size distributions.

The data are given in Table 17 and are seen to consist of 18 tests. (The additional six tests that were run are omitted from this data base because severe erosion made accurate particle sizing impossible.)

The regression analyses were made in terms of the natural logarithms of the four independent and two dependent variables (Table 18). The four independent variables were candidates for inclusion in each of the two equations.

TABLE 17

EXPERIMENTAL DATA FROM WHICH REGRESSION EQUATIONS WERE DEVELOPED

<u>Test No.</u>	<u>Generation Time, minutes</u>	<u>Temperature, °C</u>	<u>Pressure, psi</u>	<u>Power, watts</u>	<u>Geometric Mean Particle Size, microns</u>	<u>Geometric Standard Deviation, microns</u>
1	5	22	14.7	100	0.36	1.58
2	5	22	14.7	100	0.35	1.56
3	15	60	14.7	100	0.34	1.74
4	15	22	50.0	100	0.36	1.72
5	15	22	50.0	100	0.35	1.76
6	5	60	50.0	100	0.37	1.65
7	5	22	100.0	100	0.54	1.57
8	15	60	100.0	100	0.42	1.73
9	15	22	14.7	220	0.36	1.67
10	15	22	14.7	220	0.36	1.67
11	5	60	14.7	220	0.33	1.67
12	15	22	50.0	220	0.38	1.71
13	5	60	100.0	500	0.39	1.59
14	15	22	100.0	500	0.41	1.70
15	5	60	100.0	500	0.38	1.62
16	15	22	14.7	100	0.35	1.66
17	15	22	28.0	100	0.37	1.76
18	15	22	50.0	100	0.35	1.71

TABLE 18

LOGARITHMIC VARIABLES FOR LINEAR EQUATION CONSTRUCTION

<u>Variable</u>	<u>Definition</u>
<u>Candidate Independent</u>	
X_1	Ln (Time)
X_2	Ln (Temperature)
X_3	Ln (Pressure)
X_4	Ln (Power)
<u>Dependent</u>	
Y_1	Ln (Geometric Mean Particle Diameter)
Y_2	Ln (Geometric Standard Deviation of Particle Diameter)

The equations were constructed by a stepwise least-squares multiple regression procedure.

Equation A was:

$$Y_1 = -1.3030 + 0.08868 X_3$$

where X_3 , the logarithm of the pressure, was the single independent variable. The coefficient of X_3 was positive; hence, the predicted mean log particle diameter, Y_1 , increases as log pressure increases.

Equation B was:

$$Y_2 = 0.2610 + 0.06828 X_1 + 0.02794 X_2$$

The two independent variables in the equation were X_1 , the logarithm of the generation time, and X_2 , the

logarithm of the temperature. Both coefficients were positive; hence, the predicted standard deviation of log particle diameter, Y_2 , increased as log generation time increased and as log temperature increased.

These results showed that as applied pressure, temperature, and sonication time were increased, so the mean size and standard deviation increased. This meant that the particle size distribution was becoming coarser and wider in range with increasing power, pressure, temperature, and time. The increase in mean size was thought to be due to either less effective separation, the presence of coagulation, or large particle contamination from erosion sources. The latter was thought to be the prime reason for the effect, but whatever the cause, the effect precluded the use of high pressure, power, temperature, and time in the separation of particles in aqueous media.

Hence, in later experiments, the conditions of 100 watts, atmospheric pressure, 30°C for five minutes were used for the aqueous media separations.

The alternate method of separation using a Waring blender was then investigated. Only two variables were investigated. These were the blender speed and the blending time. The blender used had only three speed settings, and so two experiments were run. The first was to investigate the effect of blending time upon

separation, and the second, to investigate the effect of the blending speed.

The time dependent study was performed with the blender at high speed using the identical volume concentrations of alumina and the identical chemical conditions of the media as used in the sonication experiments. The temperature was monitored during these experiments and recorded with the data. These are tabulated in Table 19 and shown graphically in Figure 44. The size data were again obtained using the Joyce Loebel disc centrifuge.

The data show that there was no change in the ultimate particle size with blending time until a temperature of 35°C and a blending time of 20 minutes were reached. With longer blending times and higher temperatures, the mean size fell to a value lower than that achieved with the ultrasonic separation device in its restricted mode. This suggested that the separation in the blender was more effective. Of course, it must be realized that the blender was prone to leakage and loss of particles, and it generally required a greater sample volume on which to operate. In addition, it required 60 minutes of operation to reduce the mean size of the suspension to its minimum value. Neglecting these factors, the separation efficiency was better than the ultrasonic unit in its restricted mode.

A second experiment was then run to show the effect of the blender speed. Three identical suspensions of

TABLE 19

EXPERIMENTAL DATA WITH THE WARING BLENDER

<u>Time</u>	<u>Temperature</u>	<u>Pressure</u>	<u>Mean Size</u>	<u>Standard Deviation</u>
5	26	Atmos	0.35	1.70
10	30	Atmos	0.35	1.66
15	33	Atmos	0.35	1.57
20	35	Atmos	0.35	1.57
40	41	Atmos	0.30	1.66
50	44	Atmos	0.29	1.55
60	45	Atmos	0.28	1.54

TABLE 20

EXPERIMENTAL DATA WITH THE WARING BLENDER
FOLLOWED BY ULTRASONICS

<u>Blender Time, min.</u>	<u>Sonication Time, min.</u>	<u>Temp, °C</u>	<u>Pressure, psi</u>	<u>Power, watts</u>	<u>Mean Size</u>	<u>Standard Deviation</u>
5	15	60	Atmos	50	0.31	1.70
5	5	60	Atmos	100	0.27	1.55
5	5	60	Atmos	100	0.28	1.57
5	5	Room	Atmos	220	0.35	1.54
5	5	60	Atmos	220	0.30	1.47
5	60	60	Atmos	220	0.34	1.47
5	15	Room	Atmos	50	0.34	1.59

TABLE 21

COMPARABLE EXPERIMENTAL DATA FROM SONICATION
AND BLENDING EXPERIMENTS

<u>Blender Time, min.</u>	<u>Sonication Time, min.</u>	<u>Temp, °C</u>	<u>Pressure, psi</u>	<u>Sonic Power, watts</u>	<u>Mean Size, m</u>
none	5	60	Atmos	220	0.33
5	5	60	Atmos	220	0.30
none	15	60	Atmos	100	0.34
5	5	60	Atmos	100	0.28
60	none	45	Atmos	none	0.28
none	60	30	Atmos	220	0.35

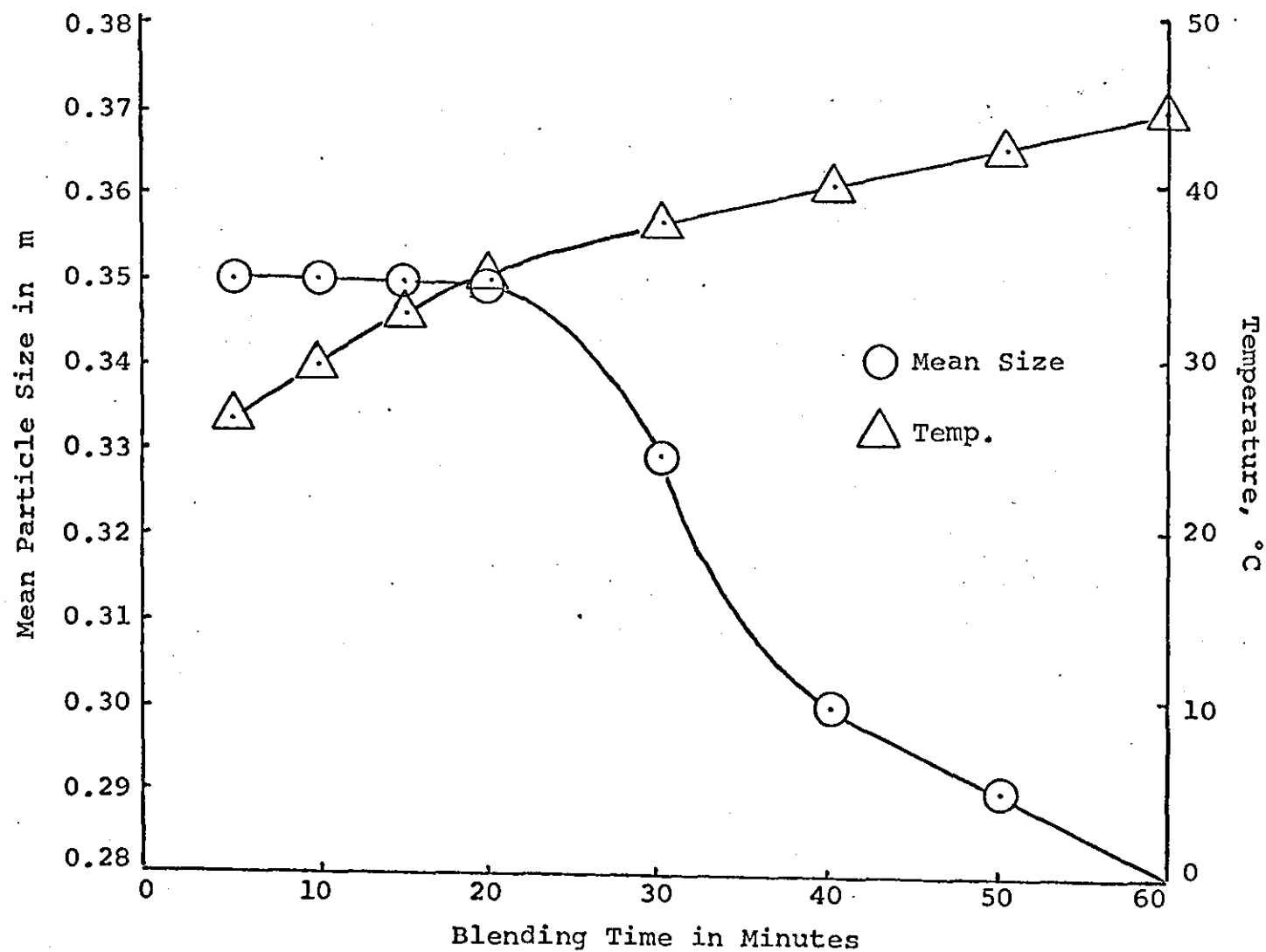


Fig. 44 - Relationship Between Mean Particle Size, Blending Time, and Temperature

alumina in tetrasodium pyrophosphate were employed, but this time one was blended for 20 minutes at high speed (setting 2) and one for 20 minutes at low speed (setting 1). The results are given in Figure 45. It is seen that the high-speed setting was by far the best speed to use as it produced the lowest particle size distribution in the same time span.

An experimental program was next performed using the blender as a preliminary separation step and following this with sonication in the restricted mode. The results are shown in Table 20.

From these data, it can be seen that a preliminary 5 minutes' agitation in the blender, followed by sonication at 60°C and at 100 watts, produced a suspension of particles of mean size 0.28 μm . Without the preblending, a mean of 0.34 μm was obtained. The mean of 0.28 μm resulting from preblending and sonication was identical to that obtained after 60 minutes in the blender with no sonication. Other interesting correlations are also shown in Table 21.

For example, 60 minutes of sonication in the restricted mode yielded a suspension of mean size 0.35 μm in comparison to 0.28 μm after 60 minutes of blending. A similar result was obtained with a five-minute sonication at 220 watts and a 60°C temperature. With no preliminary blending, a mean of 0.33 μm was obtained.

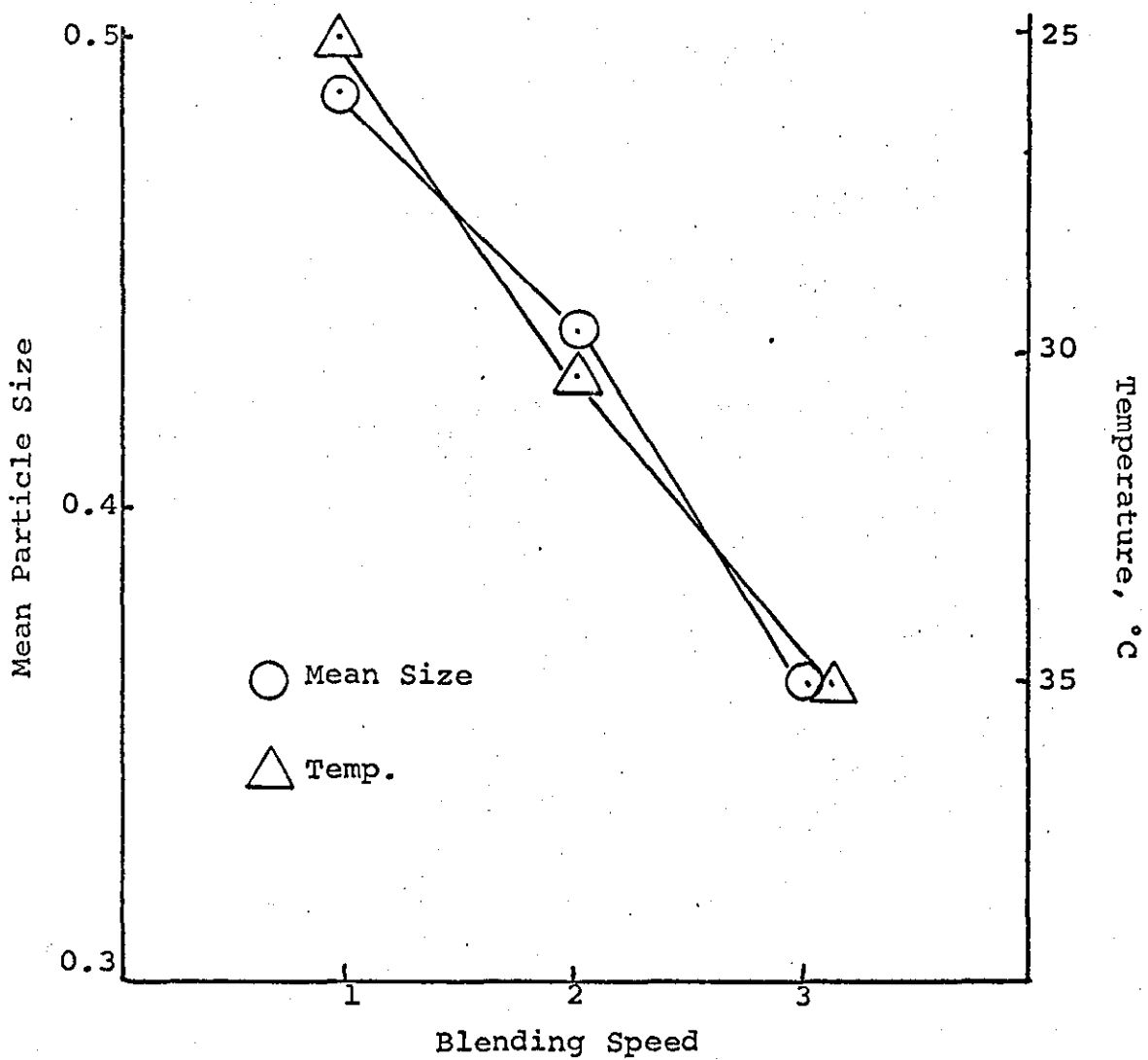


Fig. 45 - Effect of Blender Speed on the Mean Size of an Alumina Slurry

With a five-minute preliminary blending, the mean was reduced to $0.30\text{ }\mu\text{m}$. From these results, several conclusions can be drawn.

Firstly, the blending of alumina in aqueous phosphate solution can produce a suspension of mean size $0.28\text{ }\mu\text{m}$, but good separation of the particles is only achieved after 60 minutes of blending.

Secondly, sonication alone in the restricted mode of 220 watts and atmospheric pressure cannot produce a suspension of mean size lower than $0.33\text{ }\mu\text{m}$. Thus, sonication is inferior to blending under these conditions. However, by using a preblending period of five minutes followed by five minutes' sonication, a mean of $0.28\text{ }\mu\text{m}$ can then be produced. In addition, the standard deviation of the blended suspension is lower than that of the sonicated suspension, indicating less spread in the particle size distribution. This suggests the presence of less agglomerates.

The number and size of the agglomerates may, in fact, be the key to explaining the behavior of the two separating devices. Perhaps the mechanism by which energy is applied in a blender is more efficient than sonication, in breaking down the large agglomerates. This could happen if the mechanism by which sonic energy is applied in the cell does not propel the large agglomerates through the high energy-focussed field as

efficiently. If this were taking place, the larger agglomerates would then remain in suspension longer, thus effectively broadening the standard deviation and indicating a larger mean size. In a similar manner, perhaps sonication is more efficient than a blender in separating small agglomerates.

It has been shown that blending takes five minutes to produce a suspension of mean size $0.35\ \mu\text{m}$ but a further 55 minutes to reduce this size to $0.28\ \mu\text{m}$. However, when coupled with ultrasonics, this mean size is achieved in 10 minutes. This latter mode of operation supports the theory that the two separation methods are each effective in different agglomerate size ranges. When the suspension is blended for five minutes, the large agglomerates are broken down in size, producing a suspension having small agglomerates and discrete particles. When this is fed to the sonifier, it rapidly reduces the small agglomerates to discrete particles and produces a mean size of $0.28\ \mu\text{m}$.

Though not positive, this appeared to be a logical explanation for the results. Hence, in summarizing the results obtained on the screening of the two separation devices, it was found that the introduction of erosion limited the use of high power pressure, temperature, and time with the ultrasonic device, and limiting conditions of 100 watts, atmospheric pressure, 30°C for five minutes, produced useful separation in aqueous

phosphate media. The Waring blender used at high speed for 60 minutes produced a suspension with a better degree of separation, but the time of 60 minutes was extremely long. However, the use of the blender in conjunction with the ultrasonic device appeared to be the best solution to particle separation in aqueous media as five minutes' blending, followed by five minutes' ultrasonication, produced the best degree of separation in aqueous tetrasodium pyrophosphate solutions.

It must be remembered, however, that this result was obtained with a powder sample, and no data were yet taken on whether the combination of separation mechanisms could be applied to atmospheric emission particles.

The problem envisioned here was that atmospheric samples are usually collected on filters or plane surfaces, and before the agglomerates can be separated, they have to be removed from the surface. Blending could cause problems on filter shredding and surface comminution, and so the results above had to be treated with caution until this possibility was investigated.

3.1.6 Summary of Preliminary Experiments

The preliminary experiments had shown that for the best separation of metal oxide powders, tetrasodium pyrophosphate in water was the most suitable conditioning agent. This was based on zeta potential, sedimentation volume, and particle size measurements.

The force of adhesion between submicron Fe_2O_3 particles and substrates of various compositions was next measured. Experimental data was found to agree well with theory, and a force of 2.1×10^{-5} to 3.2×10^{-5} was measured for Fe_2O_3 on Fe_2O_3 and Fe_2O_3 on carbon, silica, and steel respectively. It was estimated that a force of 1.9×10^{-4} to 4.5×10^{-4} dynes was, however, required to remove 99.99% of particles from the substrates. Hence, allowing for errors and instituting a safety margin, a force of 10^{-3} dynes was estimated to be sufficient to separate all the particles from each other in agglomerate and conglomerate systems.

Using this data, it was estimated that ultrasonic energy and micromedia milling would produce sufficient forces on the particles to completely separate them, but that impeller mixing would only separate a proportion of them.

On the basis of these results, the three separating devices were investigated. Ultrasonics at various pressures, micromedia milling, and high-speed impeller mixing were considered. Ultrasonics and high-speed blending were eventually selected and screened for the effect of several operating variables. A statistical experiment was conducted to study the effect of pressure, power, temperature, and time on ultrasonic separation in aqueous media. It was shown that cavitation occurred at pressures of 220 watts and 50 psi. This became worse at

higher pressures and temperatures. It was suggested that the use of organic media would eliminate the cavitation problem, but this would produce a more inferior double-layer repulsion force.

The high-speed impeller system, typified by a Waring blender, was next investigated, and it was found to give a better separation of the powder, but the separation time was extremely long.

However, it was found that blending for five minutes, followed by low-pressure ultrasonics, separated the powder extremely well, and this method appeared to be the best for submicron powders.

One problem that was envisioned was the disintegrative nature of the blender, which would make it unsuitable for removing particles from filters and surfaces.

One obvious weakness in the preliminary experiments was that the possibility of particle comminution had not been investigated. However, it was decided to leave this investigation until the following section, when S.E.M. examination of the particles could be made.

The method suggested for testing with an actual foundry effluent was therefore a combination of blending and ultrasonics. This method is explored in the following section.

3.2 Experimental Separation of Atmospheric Aerosols Taken Downwind of an Iron Foundry

3.2.1 Aerosol Sampling

The final experimental phase of the thesis was designed to study the effect of the previously described separation methods on an atmospheric aerosol taken downwind from an iron foundry. It was decided to sample the air by two techniques involving filtration and sedimentation and to investigate the effect of weathering* on the degree of particle separation attainable on the device. Samples were taken at a rooftop site downwind of the plant, and two types of collection methods were used to cover some of the above variations. Firstly, a method employing a Hi-Vol sampler was used to collect the aerosol on a fibrous filter. Secondly, a method employing gravity sedimentation was employed to collect other aerosol as it settled onto a flat glass petri dish.

The Hi-Vol sampler used was manufactured by the Bendix Environmental Science Division, and in the experiments, a Whatman No. 52 filter paper was used as the collection surface. During the sampling period, the sampling rate was 50 liters/minute and the instrument was programmed to run unattended during the daylight hours. This time

*Here weathering is taken as being the effect of long exposure to outside weather conditions.

period corresponded to 8:30 to 16:30 hours, Monday through Friday. A clean filter paper was used every morning, and at the end of each day, the filter was removed from the filter housing, sealed in a closed glass petri dish, and stored until needed for the separation phase.

In contrast, the sedimentation procedure collected particles 24 hours per day, Sunday through Saturday, and the collection surface was openly exposed to weathering conditions for a period of one month. The sedimentation surfaces employed were open glass petri dishes, which were placed flat on the roof in a 20-in. x 20-in. high-sided box to minimize side wind contamination.

The nature of the particles collected on the Whatman No. 52 filter paper using the Hi-Vol sampler is shown in Figures 46 and 47. Figure 46(a) shows relatively low power SEM photomicrographs of the collected aerosol. It is seen that the large fibers of the filter generally collected particles of 1 to 3 μm in size, while the fine interstitial fibers collected clusters of submicron particles around their surfaces. Low power was used here to illustrate this behaviour, but it did not satisfactorily show the morphology of the collected particles. This is shown better in Figure 46(b), where high power was used. The particles are clustered in the form of spherical agglomerates or aggregates and show some tendency for chain formation. Many particles are discrete and rounded and have sharply defined boundaries.

In contrast, Figure 47 shows the particles collected on the glass petri dishes by sedimentation. The low power photomicrograph (a) shows the highly concentrated coverage of the aerosol on the surface. From this field, an area was selected and magnified to 10,000X. Here one can see the effect of particle weathering. The particles no longer appear discrete and sharply defined but appear to have been "plasticized" and to have flowed to form smooth contours with the glass surface. In Figure 47(b), one can observe a family of small discrete amorphous particles of size 0.1 to 0.2 μ m. which are magnified to 30,000X to show their structure. The particles appear as "stalagmites" rising out of the glass surface and have large areas of contact with the surface.

These photomicrographs show a distinct difference in the appearance of the samples collected by the two methods. The particles on the filter have more angularity and sharper edge definition than the sedimented particles and should be easier to separate. In contrast, the particles on the glass surface are very amorphous in nature, appear bonded to the surface, and could be much more difficult to separate.

3.2.2 Preparation of Test Samples

The Whatman No. 52 filter papers were removed from their sealed petri dishes and specimen samples cut from the filter. A sample 1 cm² in area was found to be of adequate size for the experiments conducted.



(a) 1 = 0.3 cm



(b) 1 = 3 cm

Fig. 46 - Photomicrographs of the Foundry Effluent
Collected on Whatman No. 52 Filter Paper



(a) 1 = 0.3 cm



(b) 1 = 3 cm

Fig. 47 - Photomicrographs of the Foundry Effluent
Collected on the Glass Surface

To prepare samples of reasonable uniformity for the investigation of the several variables, the following method was used. A strip, 3 cm wide, was cut through the filter paper and a square, 9 cm^2 , removed from the center portion. This square was then subdivided into nine 1 cm^2 areas for use in the experiments. These were stored in a sealed petri dish until used. Similar sizes of collection media were used with the glass surfaces. In these instances, the base of each petri dish was first covered with adhesive tape and then cleanly broken by the sharp tap of a mallet. Pieces of $1\text{-}2\text{ cm}^2$ were removed from the tape and used in the experiments.

3.2.3 Study to Show the Effect of the Blender on the Removal of Particles from Filters and Glass Surfaces

One of the 1 cm^2 pieces of filter paper was placed in a Waring blender and mixed at high speed in aqueous phosphate solution. The filter was extracted, washed, mounted on an S.E.M. stub, coated with gold, and viewed under the S.E.M. Photomicrographs of similar fields before and after blending are shown in Figure 48. Some particles were certainly removed from the larger fibers, but few particles were removed from inside the filter.

A similar method was used for pieces of the glass surfaces, and the result was the same. Many particles remained on the surface after blending.

Examination of the separated particles showed the presence of a few fibers from the filter, but no glass particles were observed. Hence, blending did not separate the particles well enough for the purpose in hand.



(a) Filter Before Blending



(b) Filter After Blending

Fig. 48 - Effect of Blending on the Removal of Foundry Particles from a Filter

The results showed that the method was not suitable for particles collected on filters and surfaces, and so the method of ultrasonics alone was investigated.

3.2.4 Studies to Show the Effect of Power and Pressure Upon the Efficiency of Removing Particles from the Filter

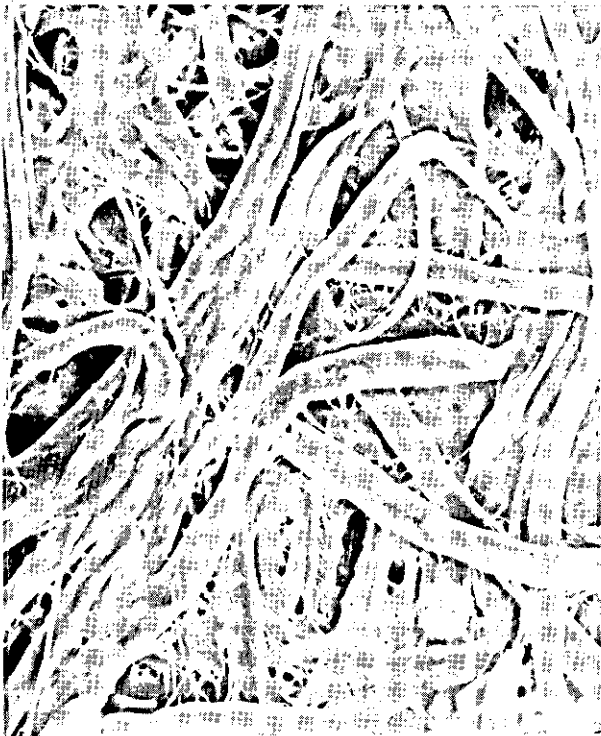
Another of the 1 cm^2 areas was removed from the dish and placed in the clean separation vessel. An aliquot of 160 ml of the filtered solution of pyrophosphate in water was added and the cell attached to the sonifier horn. The green booster was employed to give a 1:1 amplitude ratio with the 1-in. diameter horn. From the calibration curves, the power supply setting to provide 50 watts of power at atmospheric pressure was selected. The cell was submerged in the constant temperature bath at 30°C and the power applied for five minutes. After this time, the power was cut off, the cell removed from the bath, separated from the horn, and the filter paper removed from the suspension. This was washed, dried, mounted on a SEM stub, coated with gold, and viewed under the SEM. A similar procedure was then used for the application of 100 watts. However, because of the potential of erosion at higher powers, no higher power was applied in this study.

Figure 49 shows views of the Hi-Vol filter paper before and after treatment with ultrasonics. In each example, the filter paper was slowly scanned for uniformity of appearance, and random fields were selected and



(a) Filter As Received
from Hi-Vol Sampler

(b) Filter after Application
of 50 Watts for Five
Minutes at Atmospheric
Pressure



(c) Filter after Application
of 100 Watts for Five
Minutes at Atmospheric
Pressure

Fig. 49 - Effect of Sonic Power
on the Separation of
Foundry Effluent
Particles from Filters

photographed. The results showed that 50 watts of power left many particles remaining on the filter, while after 100 watts, the filter was relatively clean. However, isolated fields containing some particles were found. The particles remaining appeared to be contained within the structure of the filter, but there was an occasional field in which particles still adhered to surface fibers.

These results showed that separation from the filter was certainly a function of the applied power, but that 100 watts at atmospheric pressure in aqueous media was inadequate to completely remove the collected particles.

The experimental procedure above was repeated using 100 watts for five minutes at 30°C, but this time the pressure was varied from atmospheric to 100 psi.

Figure 50(a) shows the filter paper as received, and Figure 50(c) shows the effect of these conditions on the separation of particles at atmospheric pressure.

Figure 50(b) shows the added effect of applying this power at 50 psi pressure in the cell. Very few particles were seen adhering to the filter after the application, and removal efficiencies of greater than 99%* were achieved. After the application of the power at 100 psi, even better results were obtained. Hardly any particles could be found on the filter paper, and separation was excellent. The application of pressure did, however, cause corrosion of the horn. Pressure, therefore, improved the efficiency of separating particles from the filter, and its

*This removal efficiency is on a number basis.



(a) Filter Paper As Received



(b) After Application of 50 psi



(c) After Application of 100 psi

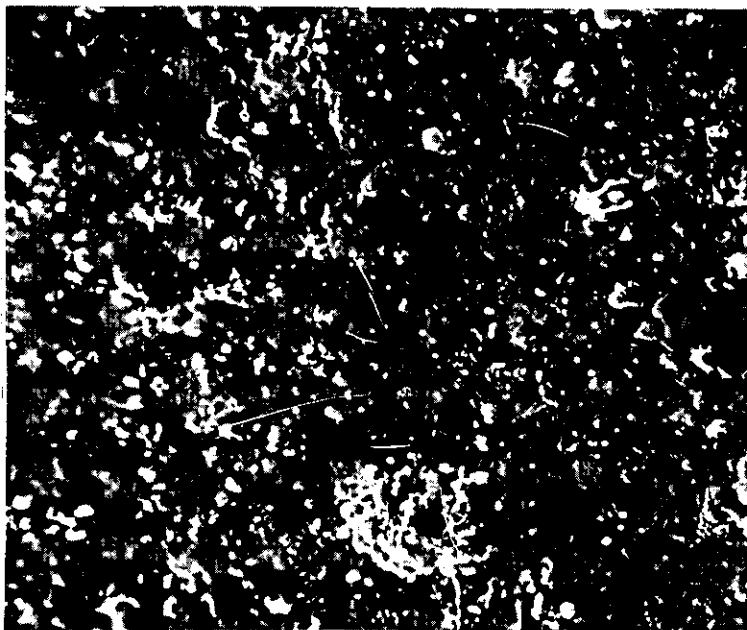
Fig. 50 - Effect of the Application of Pressure on the Separation of Foundry Effluents from Filters

use would be desirable if the erosion problem was encountered.

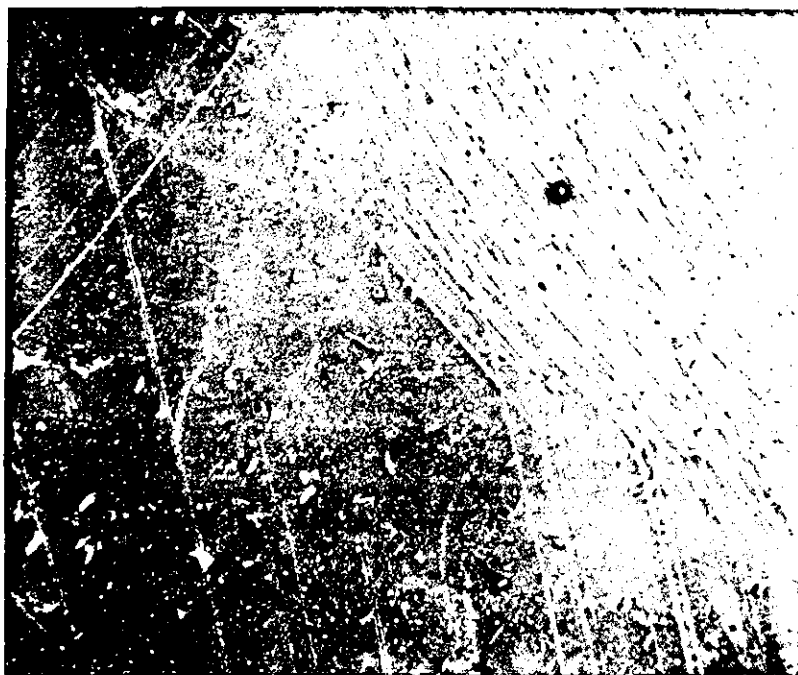
3.2.5 Experimental Studies to Show the Effect of Power and Pressure on the Removal of Sedimented Particles from the Glass Petri Dish

For this study, it was assumed that the effect of power on separation had been adequately demonstrated in the filter experiments. With the glass surface, the conditions of 100 watts, 100 psi, five minutes' sonication, and 30°C only were employed. The sonication was performed in aqueous phosphate solution.

In the experiment, the glass surface was added to the separating cell in aqueous phosphate solution and treated in exactly the same manner as the filter papers. After sonication, the surface was extracted, mounted on a stub, gold coated, and examined under the SEM. The field scans showed that the particle removal efficiency was excellent. The glass surface was found to be free of particles, Figure 51. From these results, the morphological differences between the particles on the filter and the glass surface had no adverse effect on the separation efficiency in aqueous media. The appearance of the particles on the as-received glass surface suggested that some plasticity and contouring had occurred. The lack of any residual particles on the surface after sonication suggested that the substance responsible for this effect was either water soluble or had a low adhesional nature. Such water-soluble material would



(a) Field of Foundry Particles on the Glass Surface



(b) Field of Surface after Sonication

Fig. 51 - Effect of 100-Watt Power and 100-psi Pressure on the Removal of Foundry Particles from the Glass Surface

be washed through the filter during precipitation and so would not be expected to be present around the particles on the filter surface.

In conclusion, the study showed that sonication at high pressure and power was excellent for removing particles from both filters and surfaces, and as far as particle removal efficiency was concerned, atmospheric weathering had no influence on the result. Both weathered and non-weathered particles were removed at 100 watts and 100 psi.

3.2.6 Experimental Studies to Show the Effect of Sonic Power and Applied Pressure on the Separation of Particles Removed from Filter Surfaces

3.2.6.1 Collection and Presentation of Separated Particles

In the previous experiments, only the removal efficiencies of particles from the two types of surfaces were discussed, and no mention of the state of subdivision of the separated particles was made. In this section, the condition of the particulate phase is the prime consideration. In each of the previous experiments in which pressure and power were varied, it was explained that the filter papers were removed from the suspension of separated particles and subjected to analysis. At the same time, however, the separated particles were filtered and recollected as uniformly as possible on a new filter surface. Three types of filter media were tested for use as this collecting surface, and the Nuclepore 0.1 μm . filter was eventually selected. This filter was used because it had a very smooth surface which was ideal for the recollection and subsequent microscopic analysis of the particles. When the particles had

been collected on this filter, it was mounted on a SEM, gold coated, and observed under the SEM. The general state of uniformity of the particles was first observed by scanning the whole filter at low magnification. Random fields were then selected and photographed at magnifications of 1,000X, 3,000X, 10,000X, and 30,000X.

3.2.6.2 Measurement of Particle Size Distribution and the Separation Efficiency

The measurement of these parameters was only performed on photomicrographs at 10,000X. All other magnifications were used for general observation only. A magnification of 10,000X was selected because it presented a large number of particles per photomicrograph, and particles of size $0.05\ \mu\text{m}$ and above could easily be detected. At lower magnifications, resolution of particle doublets, triplets, etc., was very difficult and any comment on particle separation statistics would be of little value. At higher magnifications, e.g., 30,000X, the images were generally rather blurred and difficult to assess. Also, too few particles appeared in each frame, and many more photomicrographs would have had to be scanned to permit a fair size distribution measurement to be made.

During the quantitative assessment of the photomicrographs, the images were classified, counted, and sized in a critical manner. The images were classified as "discrete" and "non-discrete" particles. Discrete

particles were single entities standing alone on the surface of the filter, while non-discrete particles were considered as any image in which two or more particles were seen to be in contact. This class of images needs further comment. Past experience has shown that when the particle area coverage of a surface rises above a value of 4 percent, the probability of two particles being in contact by random chance becomes significant.²³³ The two particles then appear as a non-discrete image, despite the fact that they have been separated and have no attractive forces between their surfaces. These would then be one form of a non-discrete particle reported in the data. On the other hand, non-discrete particle images may be present in which the particles really have maintained an attractive force for each other both during and after sonication. It has been shown that there are three types of particle systems having these properties: the "agglomerate", which is a statistically defined group of particles of the same chemical composition, held together by physical forces only; the "conglomerate", which is defined similarly except that the chemical compositions of particles in the group are different; and the "aggregate", which is defined as a statistically defined group of particles of any composition, held together by chemical bonds. Unfortunately, from the observation of a photograph, there is no certain way of differentiating between the three types of bonded systems and the statistically oriented system. The proportion

of the latter can be minimized by preparing fields of low-particle concentration in which the area coverage is no higher than 4 percent. In the current experimental studies, the use of 1 cm² of filter paper produced a field of particles having an average area coverage of 1 to 4 percent. Hence, the number of statistically oriented groups of particles was at a minimum.

Consequently, the data presented in the following sections reflect the number of discrete and non-discrete particles in the field. The number of non-discrete particles includes statistically oriented, agglomerated, conglomerated, and aggregated groups of particles. No further breakdown was made in this category. The size distribution of the discrete particles and the non-discrete particles were determined independently by measuring their projected area diameters using reticules, and the size distributions were plotted in a histogram form.

Finally, the separation efficiency under each particular set of operating variables was determined from the count data and was defined as:

$$\frac{\text{the number of discrete particles/field}}{\text{the sum of the number of discrete and non-discrete particles/field}} \times 100\%$$

3.2.6.3 Effect of Power on the Separation Efficiency

The particles collected after sonication at 50 watts for five minutes at 30°C and atmospheric pressure were observed and were found to be very poorly separated.

Under these conditions, the particle separation efficiency was 40 percent. No sizing was performed on this sample. A typical field is shown in Figure 52. At 100 watts, with all other conditions being the same, a separation efficiency of 64.3 percent was obtained. A typical field is again shown in Figure 53. The discrete and non-discrete particle size distributions of this sample were measured and are shown in Figure 54. The size distributions of the discrete particles ranged from 0.1 μ m to 1.0 μ m, the major portion being in the 0.05 to 0.25 μ m size range. Most non-discrete particles had sizes of 0.25 to 0.5 μ m, and they contained 2 to 3 particles in their structures. These results showed that an increase in power improved the separation efficiency in aqueous media but that this was far from ideal.

3.2.6.4 Effect of Pressure

Examination of the particles collected after sonication at 100 watts, 50 psi, 30°C, for five minutes showed that marked erosion had taken place, and the erosion products were seen as fine particles on the filter. This was confirmed by non-dispersive X-ray scans of the filter. A non-dispersive X-ray scan of a filter, which had collected particles at atmospheric pressure when no erosion had occurred, was used as the base data. A second scan of the filter after sonication at 100 watts and 50 psi showed a marked increase in the titanium level. This was interpreted as the presence of erosion products.

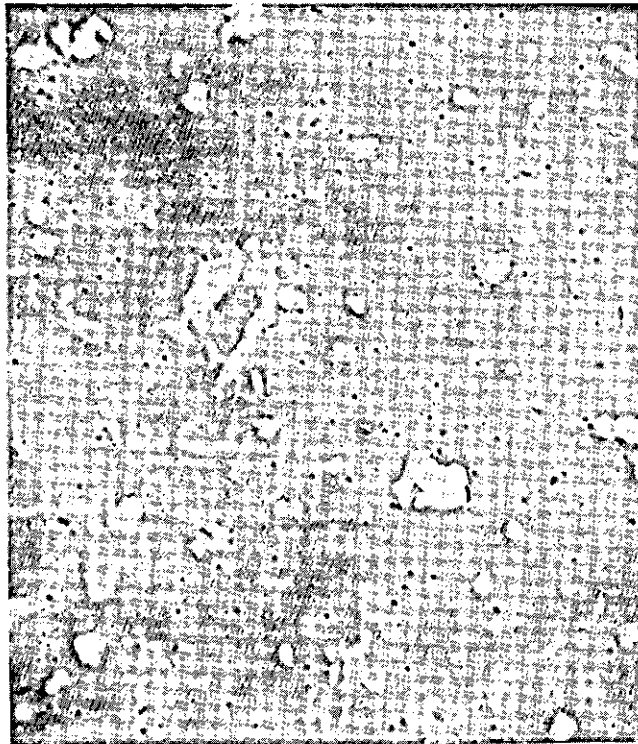


Fig. 52 - Typical Field of Foundry Particles
Separated in Aqueous Phosphate at
50 Watts at Atmospheric Pressure



Fig. 53 - Typical Field of Foundry Particles
Separated at 100 Watts at Atmos-
pheric Pressure

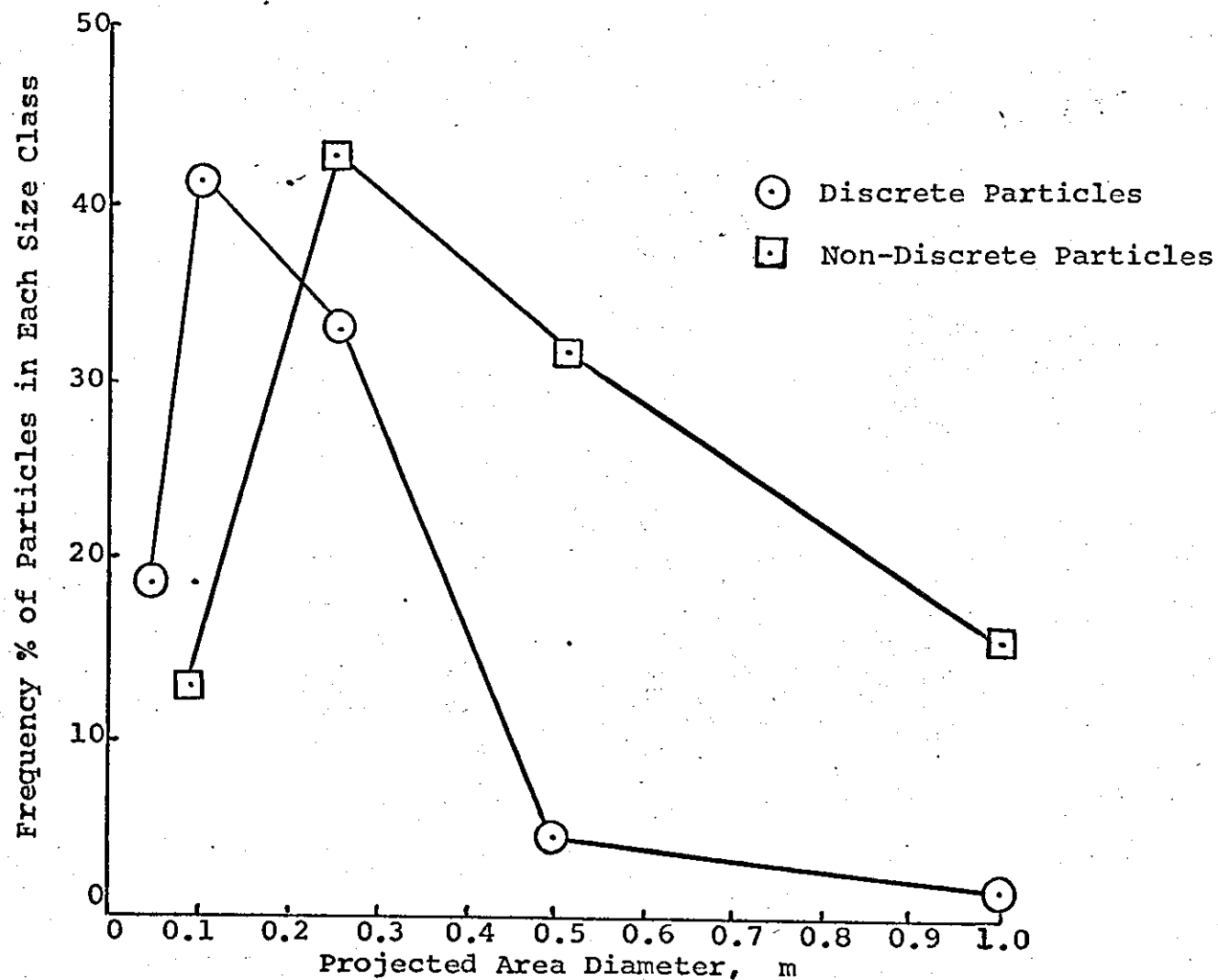


Fig. 54 - Size Distributions of Foundry Particles Separated at 100 Watts, 30°C, Atmospheric Pressure for Five Minutes in Aqueous Pyrophosphate Solution

Quantitative measurements showed the separation efficiency to be 61.8 percent, which was slightly worse than that at atmospheric pressure.

This decrease in efficiency was thought to be due to the increase in statistically oriented particles as a result of the increased particle loading of the filter after erosion.

The size distributions of the particles are shown in Figure 55. There was a general coarsening of the size distributions at this pressure, and this was, again, no doubt due to the particulate erosion products. In aqueous media then, pressure appeared to have no advantage as erosion products masked the character of the atmospheric particle phase.

3.2.7 Experimental Studies to Show the Effect of Sonic Power and Pressure on the Separation of Particles Extracted from Glass Surfaces

In the previous experiments, the efficiency of removing particles from the glass surface was qualitatively discussed. In this section, the degree of subdivision of the actual particles after removal is investigated.

In aqueous phosphate solution, a power of 100 watts for five minutes at 30°C was used at 50 psi pressure, and the particles were collected and analyzed in exactly the same manner as described earlier. Typical fields of view are shown in Figure 56. In general, the particles were not as well separated as those from the filter

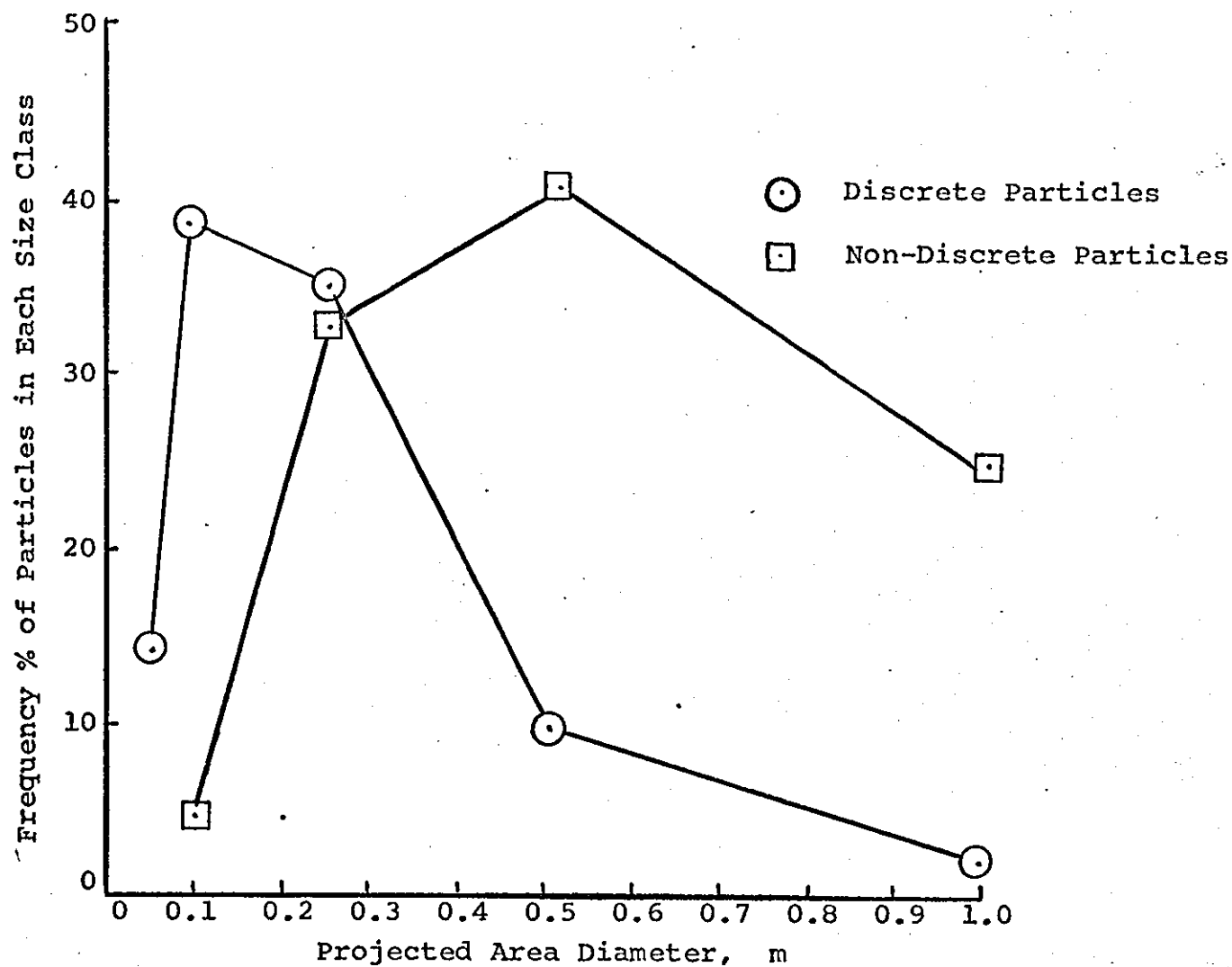
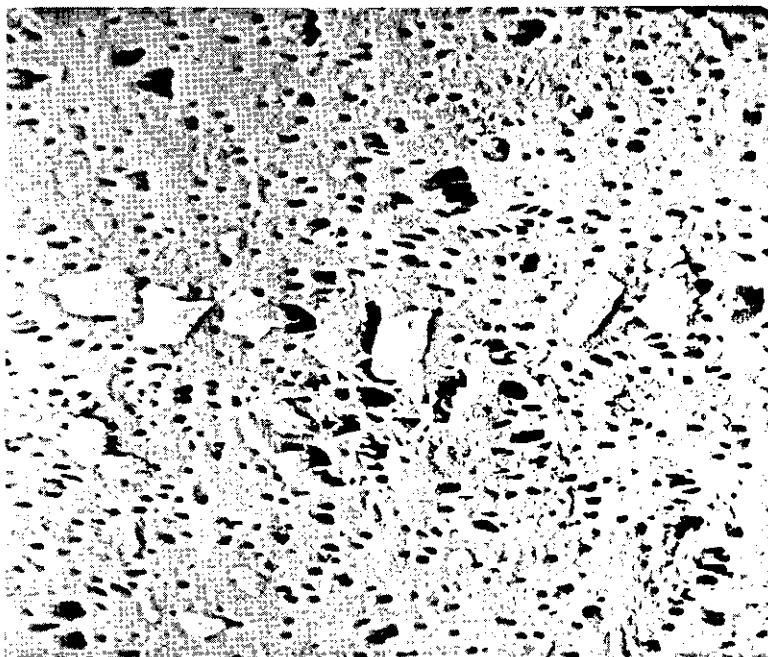
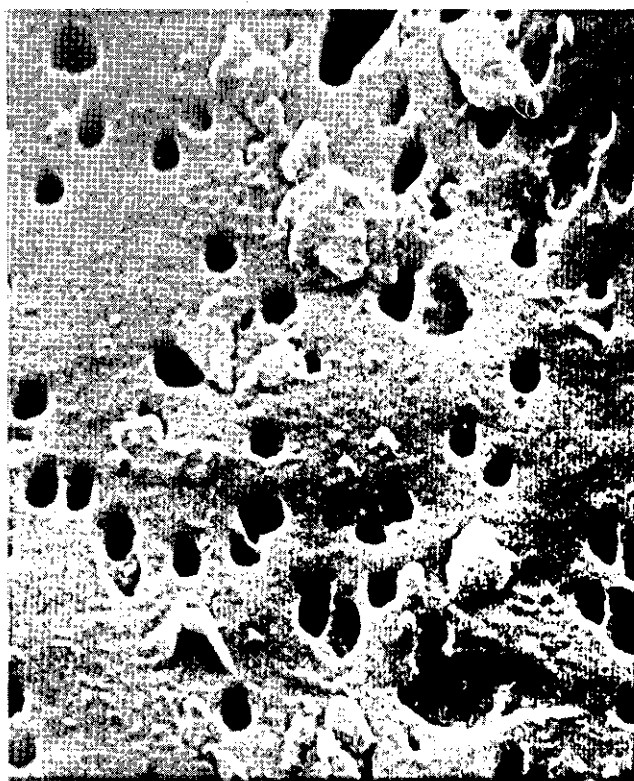


Fig. 55 - Size Analysis of Particles Separated from Filters at 100 Watts, 50 psi, 30°C, for Five Minutes in Aqueous Pyrophosphate Solution



(a) $1\mu\text{m} = 3\text{ mm}$



(b) $1\mu\text{m} = 1\text{ cm}$

Fig. 56 - Nature of Foundry Particles Separated from Glass Surfaces Using Ultrasonics at 100 Watts at Atmospheric Pressure in Aqueous Phosphate Solution

surfaces. Considering the non-discrete particles first, the ones from the glass surface were larger in size than those from the filter. Large clumps of particles were seen to be present, and 30 percent by number were greater than $1\text{ }\mu\text{ m}$ in size. In comparison, only 13 percent of the non-discrete particle population was greater than $1\text{ }\mu\text{ m}$ when removed from the filter. In comparing the total size distributions, the mean size and standard deviation of the non-discrete particles from the filter were $0.45\text{ }\mu\text{ m}$ and 1.9, while from the glass, they were $0.58\text{ }\mu\text{ m}$ and 2.5. This shows the particle size distribution of the non-discrete particles from glass to be coarser and wider in range than those from the filter. An opposite effect was seen in the discrete particle size distributions, where the mean and standard deviation of the distribution from the filter was $0.22\text{ }\mu\text{ m}$ and 2.1, and that from the glass was $0.16\text{ }\mu\text{ m}$ and 2.0. It is felt that the lower mean size of $0.16\text{ }\mu\text{ m}$ from the glass was largely due to the reduction in the population of particles to form the non-discrete particle structures and did not represent a better separation. The separation efficiency for these conditions was 55.5%.

As a result of the somewhat disappointing data with ultrasonic separation in phosphate solution, one further series of experiments was conceived. This employed fluoropolyacids as the separation solvent.

It had been suggested that one approach to overcome the erosion problem was to use non-aqueous media. Kaiser had

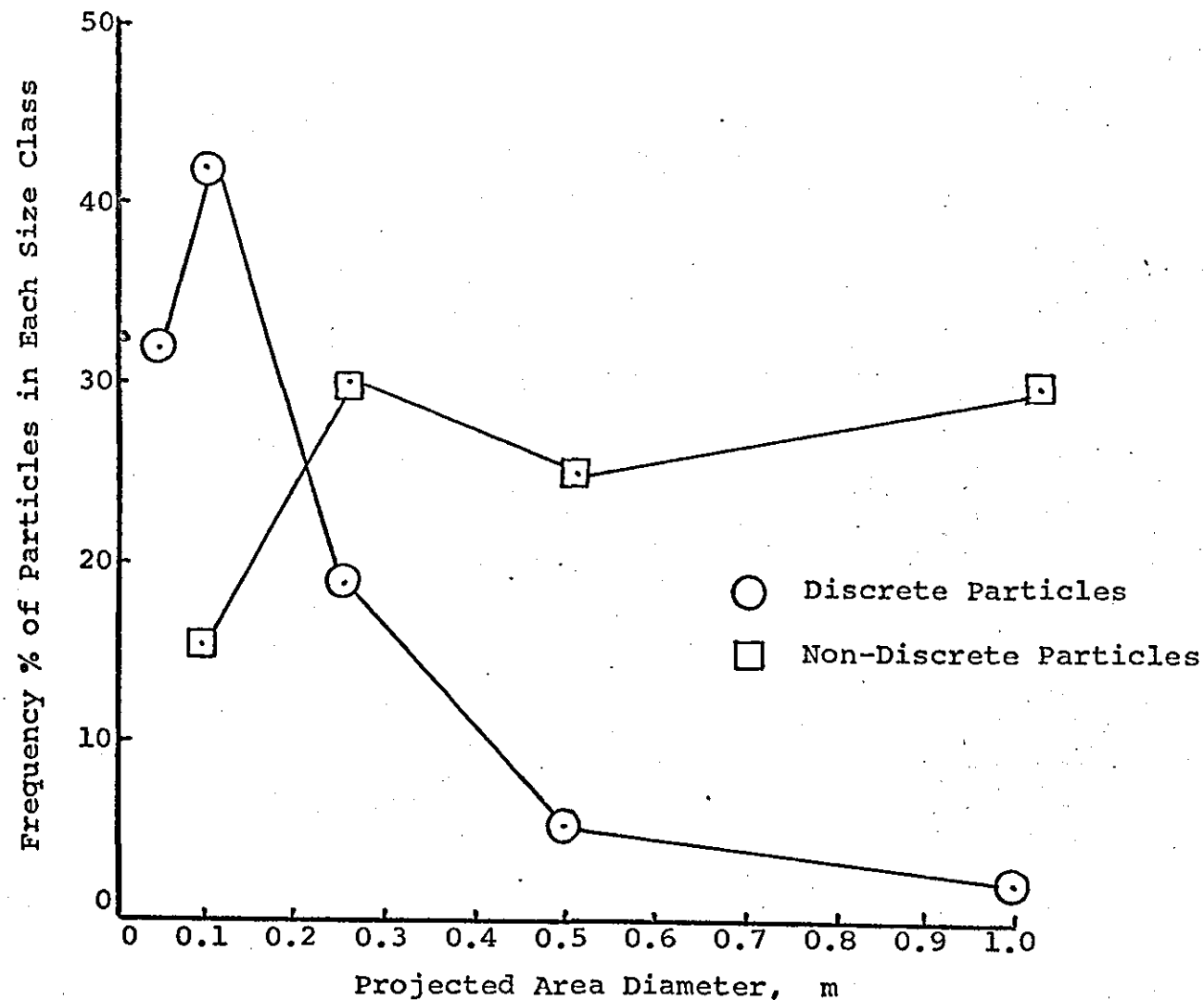


Fig. 57 - Size Distributions of Foundry Particles Removed from the Glass Surface at 100 Watts, 50 psi, 30°C, for Five Minutes in Aqueous Phosphate Solutions

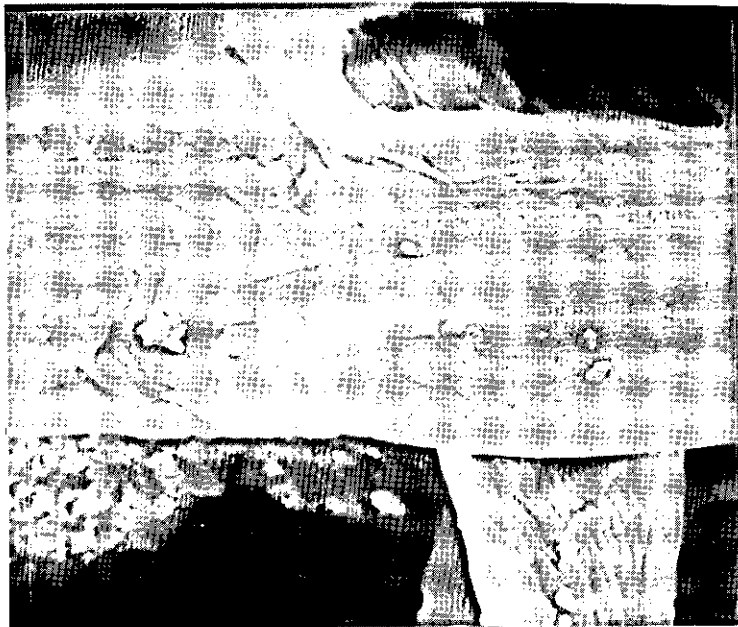
reported success in separating particles in 1 percent Krytox®* 157 in Freon®** E-3 solution, so this medium was used for this series of experiments.

3.2.8 Experimental Studies to Show the Effect of Sonic Power and Pressure on the Removal of Particles from Filters in a 1 Percent Krytox® 157 in Freon® E-3 Solution

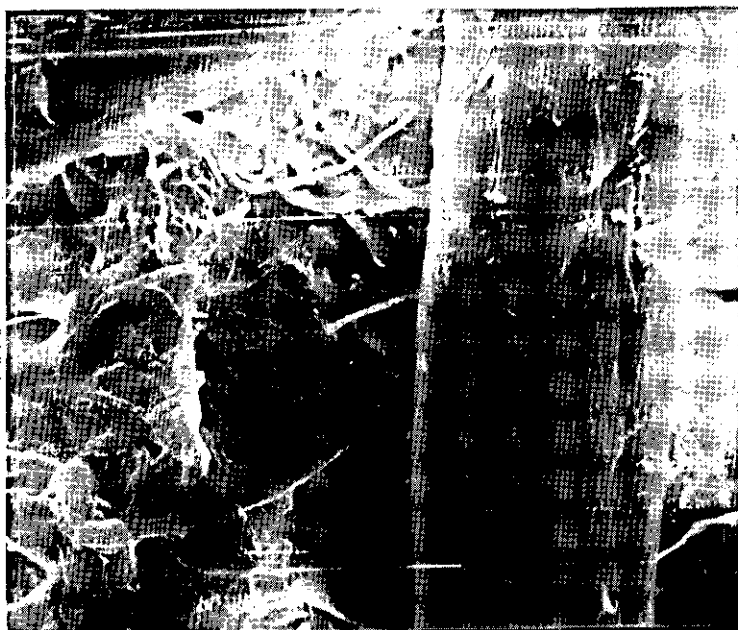
These were very limited in scope due to the cost of the Krytox® 157 and Freon® E-3 solutions. Preliminary tests were conducted first to study the extent of erosion in this solvent. Sufficient Krytox®-Freon® was purchased to permit five separation experiments to be conducted. The first sonication was performed at 100 watts, 30°C, 50 psi, for five minutes. The second was performed at 100 psi, all other conditions being the same. Filter scans showed slightly inferior removal efficiencies with Freon® than with aqueous media at 50 psi, but the filter was relatively clear of particles at 100 psi (Figure 58). More importantly, horn erosion was completely absent at 50 psi and was very slight at 100 psi. In consequence, it appeared that the use of the Krytox®-Freon® solvent did minimize the erosion problem experienced in aqueous phosphate solutions, while at the same time, produced a comparable degree of separation at 100 psi.

* Du Pont's registered trademark for fluorocarbons

** Du Pont's registered trademark for fluorinated oils and greases



(a) 50 psi
Scale: $1 \mu\text{m} = 3 \text{ mm}$



(b) 100 psi
Scale: $1 \mu\text{m} = 3 \text{ mm}$

Fig. 58 - Filter Paper after Sonication in Freon®

3.2.9 Experimental Studies to Show the Effect of Sonic Power and Pressure on the Separation Efficiency of Particles Removed from the Filter in a 1 Percent Krytox® 157 in Freon® E-3 Solution

Data were taken in only two experiments to enable

1) comparisons to be drawn between aqueous and organic solvent dispersions at 50 psi and 2) the effect of pressure at 50 and 100 psi to be established in organic media. Typical photomicrographs of the particles separated at 50 psi, 100 watts, 30°C, for five minutes in Krytox®-Freon® are shown in Figure 59. A separation efficiency of 82.8 percent was obtained under these conditions, and the size distributions obtained are shown in Figure 60.

In general, the size distribution of the discrete particles was slightly finer in Krytox®-Freon® than in aqueous phosphate, but this was not highly significant. The mean and standard deviation of the former was 0.19 μ m and 2.2, and that of the latter, 0.22 μ m and 2.1. This suggested that the size distributions of the particles once separated into discrete form were quite similar, but the major difference was in the marked increase in the separation efficiency and the lower degree of erosion.

At 100 psi, however, a marked reduction in the particle size distribution was seen. Typical photomicrographs of the separated particles are shown in Figure 61 and their size distributions in Figure 62. Here the mean size of the discrete particles was 0.085 μ m and the standard



Fig. 59 - Field of View Showing the Degree of Separation of Foundry Particles Separated at 100 Watts and 50 psi in Krytox® 157-Freon® E-3 Solution

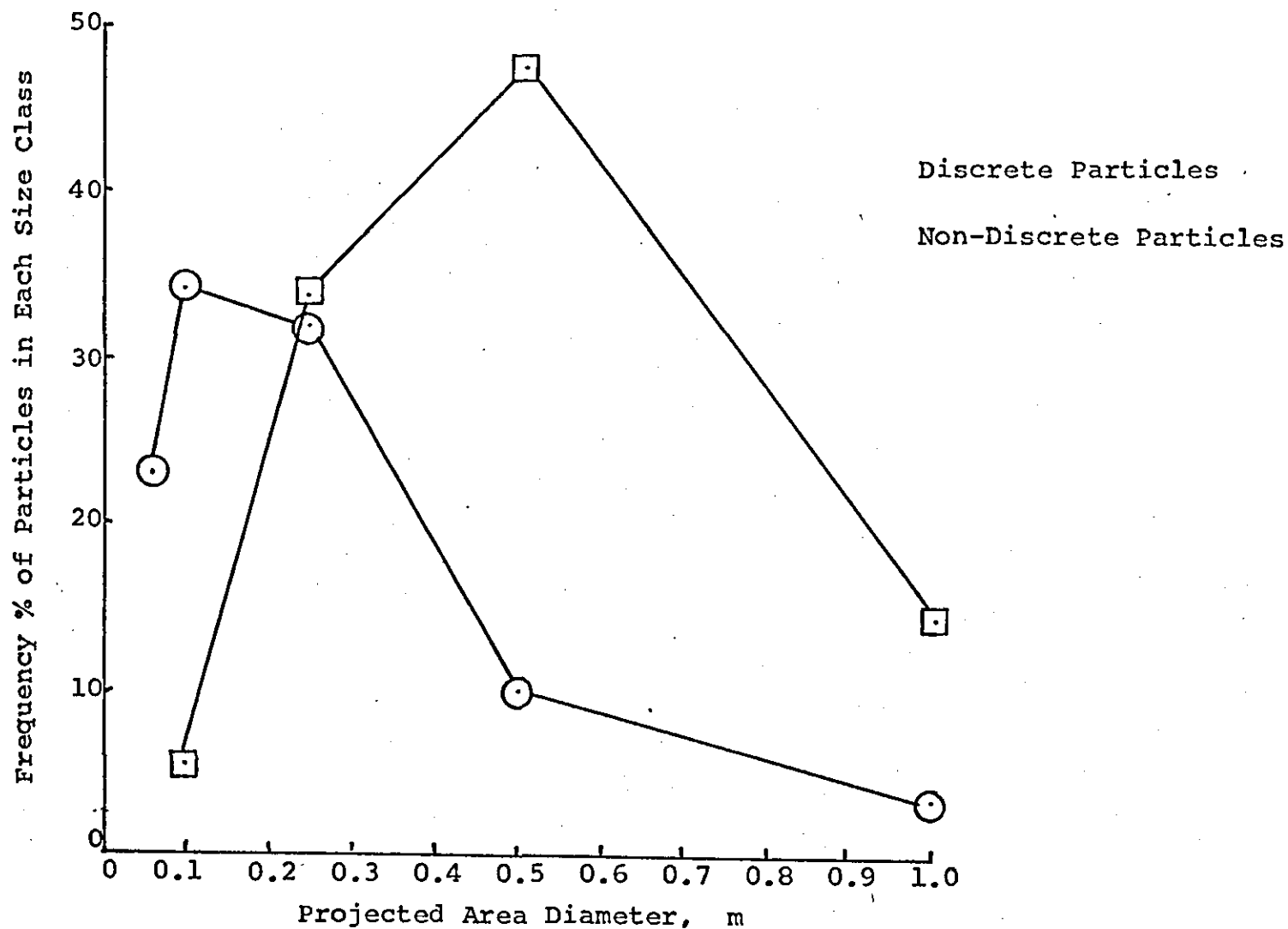


Fig. 60 - Size Distributions of Particles Separated at 100 Watts and 50 psi in Krytox[®]-Freon[®] Solution

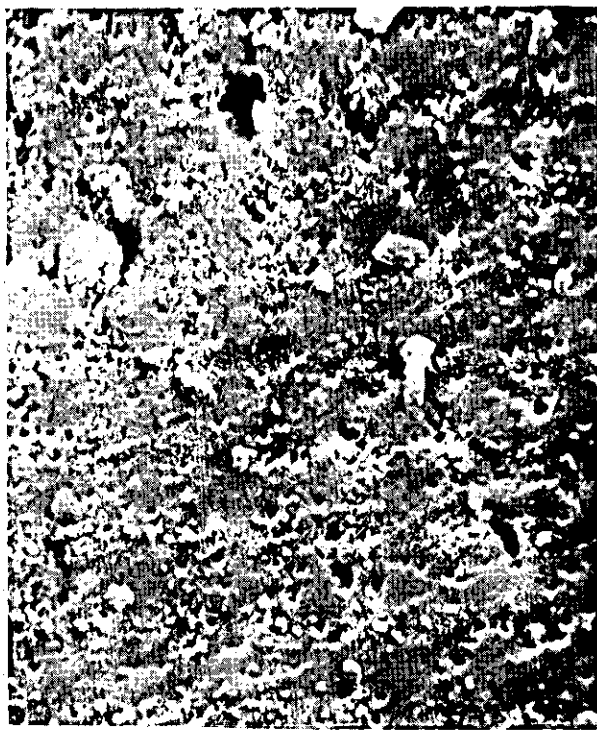


Fig. 61 - Typical Field Showing the Degree
of Separation of Foundry Particles
at 100 Watts and 100 psi in
Krytox® 157-Freon® E-3 Solution

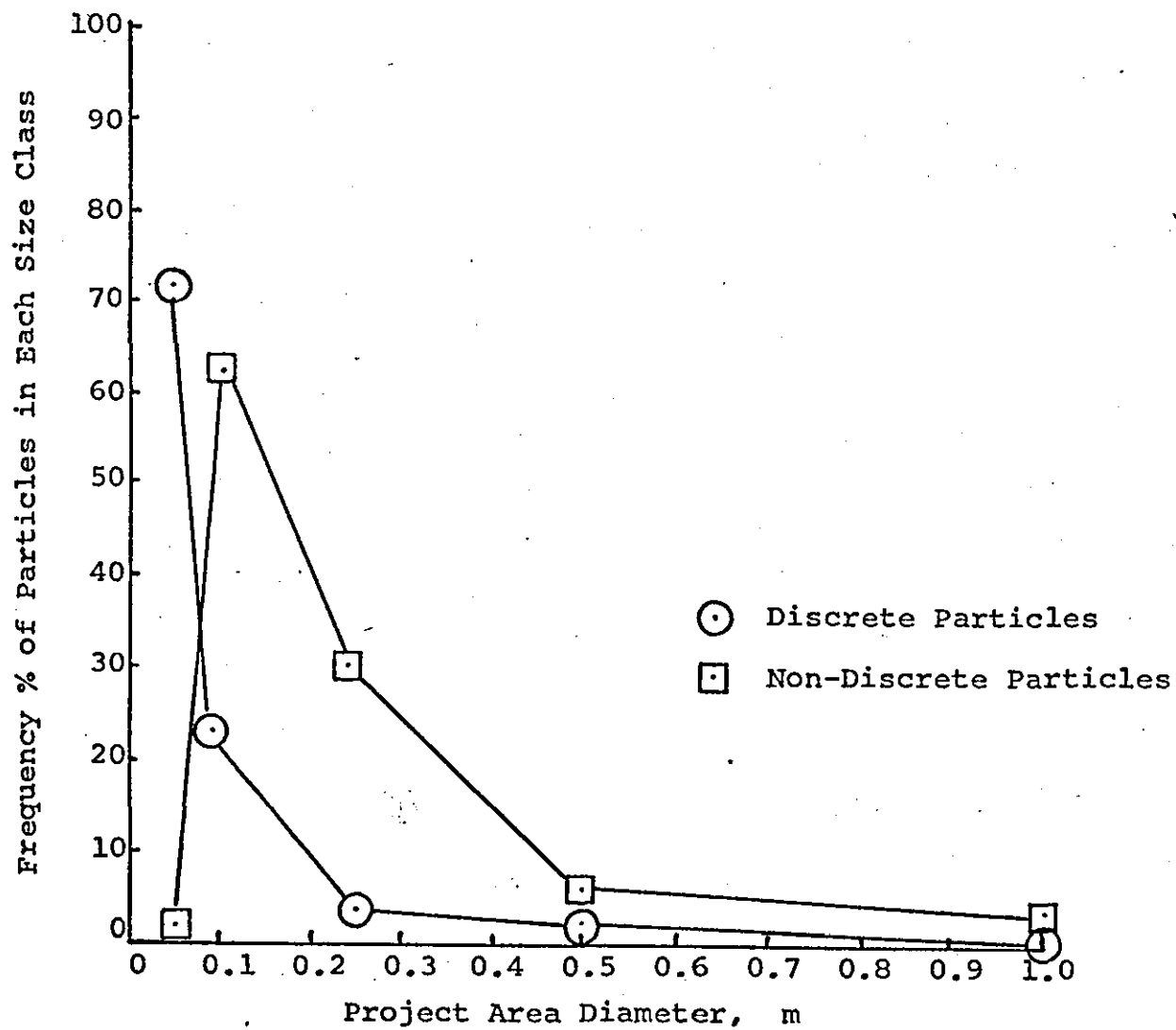


Fig. 62 - Size Distributions of Foundry Particles Separated at 100 psi and 100 Watts in Krytox[®]-Freon[®] Solution

deviation, 1.5. Under 100 psi pressure, the separation efficiency was increased to 85.9 percent, and most discrete particles appeared in the 0.05 to 0.1 μ m range as well separated images.

Very slight erosion was observed on the horn tip, but apparently this did not adversely affect the sample. The effect of the solvent then was to reduce the erosion potential to a minimum and enable higher pressures to be applied during sonication. This capability significantly improved the separation efficiency of the ultrasonic device. Sonication at 100 watts and 100 psi produced a very finely divided discrete particle population with extremely good separation characteristics.

3.2.10 Experimental Studies to Show the Effect of Sonic Power and Pressure on the Separation Efficiency of Particles Removed from the Glass Surface in a 1 Percent Krytox® 157-Freon® E-3 Solution

In Krytox®-Freon®, the separating conditions were 100 watts, 100 psi, 30°C, for five minutes, and typical photomicrographs are shown in Figure 63. With these conditions, a separation efficiency of 68.4 percent was obtained. This was distinctly worse than the value of 85.9 percent obtained under the same conditions but using the filter sample. Once again, there were large clumps of non-discrete particles present, which were not present among the particles collected from the filter. The size distributions of the discrete and non-discrete particles are shown in Figure 64, and these support this



(a) $1\mu\text{m} = 1\text{ mm}$



(b) $1\mu\text{m} = 2\text{ cm}$

Fig. 63 - Typical Field of Foundry Particles Separated from the Glass Surface at 100 Watts, 100 psi, in 1 Percent Krytox® 157-Freon® E-3 Solution

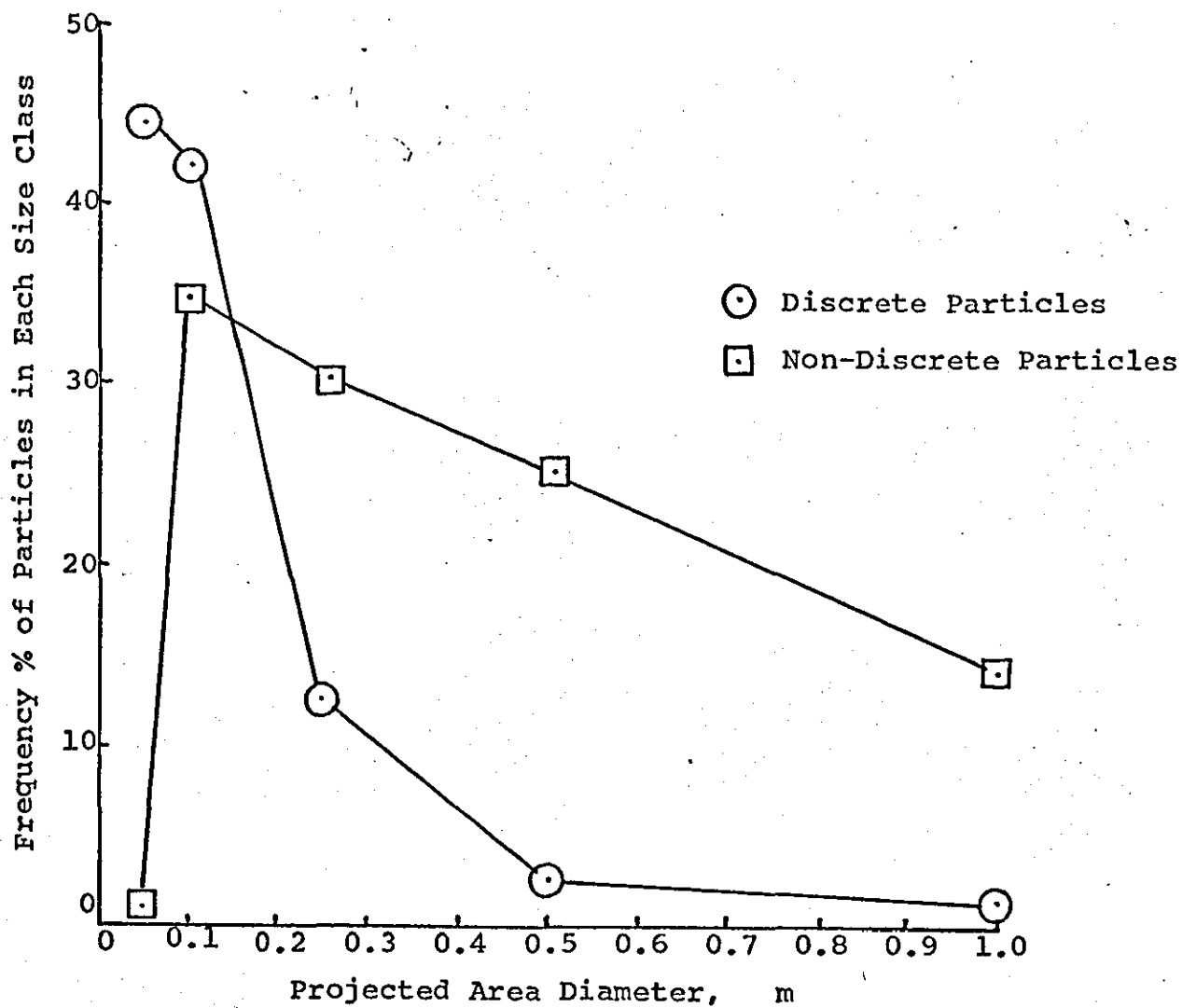


Fig. 64 - Size Distributions of Foundry Particles Separated from the Glass Surface at 100 Watts, 100 psi, 30°C, for Five Minutes in Krytox®-Freon® Solution

observation. By comparing Figures 62 and 64, the mean and standard deviations of the non-discrete particles were $0.40\ \mu\text{m}$ and 2.1 from glass and $0.21\ \mu\text{m}$ and 1.5 from the filter. Similarly, the mean and standard deviations of the discrete particles were $0.16\ \mu\text{m}$ and 2.0 from glass and $0.08\ \mu\text{m}$ and 1.5 from the filter. These results again show that the separation of particles from the filter is more efficient and more effective than from the glass.

In summary, the results show that the separation efficiency and degree of separation of particles in aqueous phosphate at 100 watts, atmospheric pressure, 30°C , for five minutes were much lower than in Krytox®-Freon® at 100 watts, 100 psi, 30°C , for the same time of sonication. In addition, the separation efficiency and degree of separation of particles removed from the glass surfaces were much lower than those of particles removed from the filter surface. Qualitative observation of the photomicrographs is also believed to indicate a higher degree of aggregation between particles from the glass surfaces than from the filter. This is supported by the general morphology of the non-discrete particle groups which appear more amorphous and flaky. It is further supported by the fact that as the particle concentrations in Figures 61 and 63(a) were similar, one can assume that the probability for random juxtaposition of particles in each field was the same, and as the separating

conditions were identical, one can assume that the particles were subjected to the same sonic energy. Hence, to satisfy the conditions for a wider size range and coarser size distribution, it appears reasonable to assume that many non-discrete particles on the glass surface were more tightly bound together. This was a reasonable assumption, as weathering and aging of the aerosol could explain this result.

3.3 Discussion of the Experimental Results

The preliminary experiments showed that the inorganic oxides of iron, aluminum, and titanium could be separated best in aqueous sodium pyrophosphate solution. Measurements of the force of adhesion between iron oxide and various surfaces showed that at the maximum zeta potential, the force of adhesion varied from 2.1×10^{-5} dynes to 3.2×10^{-5} dynes. The former value was obtained for the separation of iron oxide particles from an iron oxide surface, and the latter value was obtained for the separation of the same oxide particles from surfaces of silica, carbon, and steel. The lower force needed to separate chemically similar solids suggested that agglomerate systems consisting of chemically similar particles would be easier to separate than conglomerates consisting of chemically dissimilar particles. This result was surprising, and, in fact, no logical explanation can be given to explain it. The experimental data were found to agree closely with theory and also were found to agree closely with the extrapolated data of other workers. However, no data could be used to directly compare the results with those of other workers as no force of adhesion data had previously been published on sub-micron particulates. Although this difference in adhesion between similar and dissimilar particle and surface combinations was extremely interesting and worthy of further study, it was not considered necessary for the purposes of this thesis. The reason was that an estimate of the

maximum force needed to separate all particles from every surface was the prime requirement, and providing that this could be found from the experimental data, no further measurements were necessary. By examination of the extensive force of adhesion data generated by Krupp for larger particles, it was found that the "force applied" versus "particle removal efficiency" data were log-normally distributed. In consequence, a good estimate of the maximum force required could be made by simply extrapolating the straight line through the data to the 99.99% particle removal point and reading off the value of the force. This was done using the highest force of adhesion data, i.e., for iron oxide on carbon, steel, and silica, and so the maximum force value of 10^{-3} dynes obtained was more than enough to separate iron oxide particles from iron oxide surfaces.

Using a value of 10^{-3} dynes, (the total force needed to separate all submicron particles), an attempt was next made to calculate the stress that must be applied to separate the particles, and then to estimate the ability of various separating devices to generate this stress. The calculations made had to rely on many assumptions. Firstly, to measure the stress needed to separate particles, an interparticle contact area had to be assumed. Past literature provided no assistance in selecting such an area as the value depended on the particle form and surface texture. A particle contact area diameter to particle diameter ratio of 1:10 was eventually

selected based on a limited knowledge of both the particle size and surface roughness parameters. Using this value, a stress of 0.15×10^8 dynes/sq cm was estimated as being necessary to separate them. In comparing this to the shear stresses that could be generated by various devices, including impellers, homogenizers, sand mills, and ultrasonic sources, further difficulties were encountered. Extensive studies by Rumpf and Raasch²³⁴ provided good data on the shear stress available from impellers and homogenizers, but good data on sand mills and ultrasonic generators were not available. This was due to the complexity of the system. In sand mills, for example, shear is generated by the rotating discs and the moving sand. However, shear is not the only mechanism acting on the particles. Impaction of the media occurs constantly, and the probability of an agglomerate being sandwiched between two impacting grains is very high.²¹² In consequence, literature references relating the force actually applied in sand mills to the mill performance were very few, and the ones available were subject to much doubt. With ultrasonic energy, and specifically cavitation, the situation was even worse. No known theory relating the available force was found to exist, and the subject is so little understood that standard text books hesitate to suggest probable values.¹³² Hence, calculations on cavitation forces can only be considered as rough estimates and cannot be regarded with much confidence. However, the calculations showed

that if the values were even approximately correct, sand milling and cavitation could produce forces so much in excess of those required to separate submicron particles in agglomerates that actual comminution of discrete particles and aggregates could occur. Of course, this assumption was made on the basis that the maximum shear stress generated by a device could be actually applied to the agglomerate or aggregate system. It is known that devices have zones of maximum shear and minimum shear. Maximum shears are found at the surfaces of impellers and collapsing bubbles, but this shear is rapidly reduced with increasing distance from the shear source. Consequently, depending on the mixing efficiency of the device, there is a probability that an agglomerate or aggregate will never enter the maximum shear zone and will therefore experience less shear than anticipated. Calculations on the probability of this occurring are extremely difficult to make, and no reference could be found to even suggest an approximate value. The only sure measure of the ability of a device to apply sufficient force for separation was to experimentally test it with a known system and measure the degree of separation attained. This was done during preliminary experiments using a Waring blender impeller mixer, a Virtis micromedia mill, and a Branson magnetostrictive ultrasonic probe. Calculations had predicted that the impeller mixer would generate less shear than the latter two devices, and the experiments showed this to be fairly true. Large

agglomerates were quickly separated by the device, but smaller agglomerates were separated only after long separation times and at higher temperatures. This was thought to be due to the available amount of shear, the probability factor described above, and the additional effect of impaction. To explain such a statement, let us consider the example of separating one large agglomerate. During blending, this one large particle will be agitated within the fluid flow field and will have a tendency to strike the walls and blades of the impeller. Such a behaviour can be demonstrated practically by simply adding sand to a blender and listening to the impacts of the particles on the container walls. As the particles become smaller and their mass decreases, this effect diminishes. Submicron particles begin to follow the fluid flow patterns in the container and are subject to less impaction. Under these circumstances, they are further reduced in size only in the high shear zone of the impeller. However, as their number has now increased, each agglomerate has a lower probability of being in the shear zone at any one time, so the separation occurs progressively more slowly until the shear stress from the device equals the shear stress necessary to separate the small agglomerates. At this point, no further separation occurs. However, in studies on collected aerosols the agglomerates that have to be separated are not in powder form but are attached to surfaces. In consequence, the ability of the blender to separate particles from

filters and plane surfaces was next investigated. Though shown to be quite good as a separating device for dispersed agglomerates, the device proved unsatisfactory in its ability to remove particles from surfaces. This limited its use as a potential device for atmospheric tracer studies. The results did show, however, that the blender applied insufficient shear to fracture a glass surface on which the particles were supported but had sufficient shear to separate some of the fibers from a filter on which a duplicate particle sample was residing. This supported the previous theoretical shear stress estimate, which predicted that insufficient shear was available for comminution in impeller devices. However, this calculation did not include any estimate on the effect of impaction, which is now thought to be a factor in large agglomerate separation in impeller mixers.

Studies on the micromedia mill were next conducted. Two hundred μm glass beads were used as the media, with alumina agglomerates as the test powder. It was found that during milling in aqueous pyrophosphate solution, the size distribution increased with time and did not decrease as expected. Examination of the separated particles showed the presence of large glass particles which had originated from the media. Impaction of the glass beads was thought to be the mechanism responsible for this effect. In industrial practice, e.g., disperse dye milling, the same behaviour has been reported. In this process, the fractured media is removed by cartridge

filtration, the $< 0.2 \mu\text{m}$ dye particles passing through the filter where they are collected. For the purpose of this thesis, such a filtration procedure could not be applied as the particles of interest spanned the size range of 10^{-3} to $10^2 \mu\text{m}$. As the glass particles appeared in the range $1\text{--}10^2 \mu\text{m}$, micromedia milling was considered an impractical method for the separation of foundry particle agglomerates. However, the results did confirm the theoretical predictions that particle comminution could take place with this type of separating method.

The final device tested was the Branson ultrasonic probe. Experimental studies conducted with alumina in aqueous phosphate solution showed that the variables of power, pressure, temperature, and time had to be critically controlled to prevent erosion of the probe tip. As these variables were increased, erosion became so severe that 40 mg of metal was eroded from the probe per hour of use. This was thought to be the result of cavitation. It is known that various types of cavitation can be defined. These include travelling, fixed, vortex, and vibratory cavitation.²³² All types except the latter have the common feature that a given element of liquid passes through the cavitation zone only once.²³² Vibratory cavitation, on the other hand, is the one type in which a given element of liquid is exposed to many cycles of cavitation.²³¹

During cavitation, the forces that cause bubbles to form and collapse are thought to be generated by a continuous series of high amplitude, high frequency pressure

pulsations. Also, the bubbles are only thought to be formed when the amplitude of the pressure variation is great enough to cause the pressure to fall to or below the vapour pressure of the liquid.²³² Such pressure variations are generated by all submerged surfaces which vibrate at high frequency normal to their forces.²³² The Branson ultrasonic probe is typical of such a device: During cavitation, the magnitude of the force applied to a probe tip is thought to be dependent on several factors, which include the applied pressure, the bubble size, and the interfacial tension.²³² In a vibrating system, there can also be chemical changes which can induce corrosion of the probe material. For example, a protective oxide film can be stripped from a metal surface, exposing the bare metal to chemical attack. In addition, thermal effects can increase the severity of such an attack.²³²

Hence, during the ultrasonic treatment of the alumina agglomerates, it appeared that high cavitation forces had indeed been applied to the probe tip and were of sufficient magnitude to fracture the metallic bonds. Such a force would also have been sufficient to fracture discrete particles and aggregates if it had been applied to the particle surface. This possibility is discussed later. The fact that increased power and pressure increased the magnitude of cavitation in aqueous phosphate solution was unfortunate as an increase in these parameters was found to improve the efficiency of removing particles from filters and plane surfaces.

To circumvent the erosion problem, a mixture of Krytox® 157 and Freon® E-3 was employed. This fluorohydrocarbon mixture had two important properties. The liquids had a high hydrogen-bonding potential as a consequence of the fluorine atom in the molecule. This was desirable to stabilize the metal oxides after separation. The liquids also had low surface tensions and low vapour pressures. These properties induced good wetting of the agglomerates and permitted cavitation bubbles to form at lower pulse amplitudes. The use of the fluorohydrocarbon mixture appeared to be sufficient to minimize the erosion of the horn, while at the same time yielding good separation and stabilization properties. Also using this mixture, it was found that power and pressure could be considerably increased before erosion was detected. For example, the most successful separation was obtained on the filter sample in the fluorohydrocarbon mixture using 100-watt power, 100 psi pressure, 30°C temperature, and a treatment time of five minutes. This produced a separation efficiency of 85.9% with negligible erosion. The term "separation efficiency" requires some discussion at this point because its meaning is slightly obscure.

The separation efficiency was defined as:

$$\frac{\text{the number of discrete particles/10,000X field}}{\text{the sum of the number of discrete and non-discrete particles/10,000X field}} \times 100\%$$

Such a definition can be misleading, particularly if such factors as erosion, aggregation, and comminution are not taken into account. For example, if every particle

collected was an aggregate, then providing no chemical bonds were broken, a separation efficiency of 0% would be obtained. Hence, this low value could be misinterpreted as meaning the device was inefficient and not that the particles were too tightly bound. Alternatively, if the condition of cavitation were such that marked erosion took place, the separation efficiency could appear to be lower, simply as a consequence of the presence of more particles on the filter. In this event, the probability of interparticle contact would increase with the increase in concentration, and the probability of finding more non-discrete particles would increase as a result. In this event, the separation efficiency would fall. However, if the force applied was sufficient to comminute aggregates, but not erode the metal horn, then comminution and separation could not be distinguished from each other by a measure of the separation efficiency. Both processes would yield finer size distributions and higher separation efficiencies. In consequence, the separation efficiency has to be interpreted carefully, if meaningful data are to be generated.

For example, Table 22 contains all the relevant data reported on the separation efficiencies in Section 3.2. Considering the phosphate solution first, it is seen that an increase in the pressure from atmospheric to 50 psi reduced the efficiency of separating the particles from the filter from 64.3% to 61.8%. This

TABLE 22

SUMMARY OF SEPARATION DATA

<u>Substrate</u>	<u>Liquid</u>	<u>Power (Watts)</u>	<u>Pressure (psi)</u>	<u>Separation Efficiency (%)</u>	$\frac{\sum nd}{\sum n}$ (μm)	$\frac{\sum nd^4}{\sum nd^3}$ (μm)
Glass	Phosphate	100	50	55.5	0.30	0.93
Filter	Phosphate	100	50	61.8	0.30	0.86
Filter	Phosphate	100	Atmos.	64.3	0.26	0.82
Glass	Freon®	100	100	68.4	0.18	0.86
Filter	Freon®	100	50	82.8	0.24	0.81
Filter	Freon®	100	100	85.9	0.09	0.71

All data were taken at 30°C for five minutes' sonication.

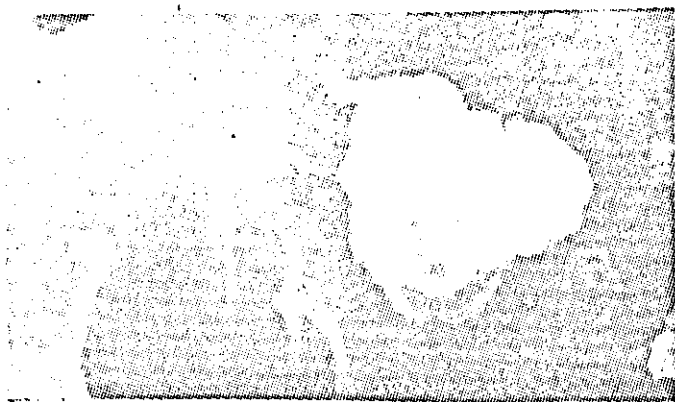
was not due to a less efficient separation, but due to the presence of erosion products, which increased the population of non-discrete particles on the final filter. Such a conclusion was only possible after an examination of the filter and could not be obtained solely from the value of the separation efficiency.

If the separation efficiencies obtained for the filter and the glass surfaces are now compared, a different conclusion can be reached. It is seen that for the identical conditions of separation in phosphate solution, the separation efficiency is higher for the filter sample than for the glass. An even greater difference is observed when separation is performed in Freon®, but the result was eventually the same. From an observation of the scanning electron micrographs of the four samples prior to separation, it was seen that the nature of the particles on glass was different from the nature of particles on the filter. Those on glass were amorphous, rounded, and appeared to have melted and flowed onto the surface. In contrast, those on the filter were more angular, distinct, and sharp. The areas of contact of the particles on glass appeared to be larger, and there appeared to be cement bridges between the particles and the surface. Size data revealed that after separation the discrete particles and aggregates from glass were also larger in size. This was interpreted to mean that the particles on glass were more aggregated and had higher tensile strengths; hence, for the same amount of energy, a

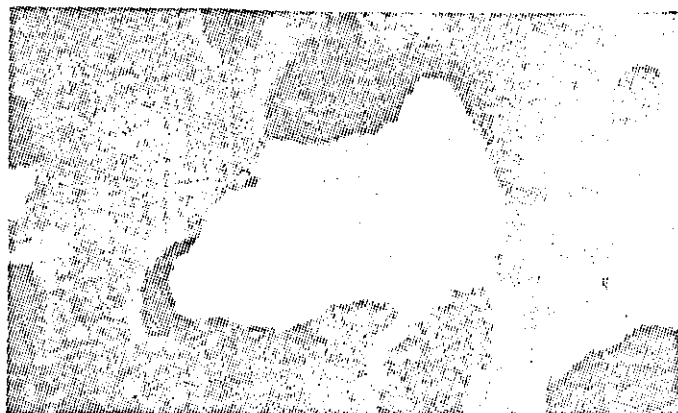
lower separation efficiency was obtained. The only conceivable reason to account for the differences in separation efficiency and appearance was that the particles on the glass surfaces had been exposed to the ambient air for three winter months during the sampling stage, while those on the filter had been exposed for only eight hours. Hence, exposure or "weathering" appeared to have caused a significant increase in the tensile strength between the particles and the glass surfaces. It is conceivable that this could have arisen through the presence of water-soluble compounds or volatile organic trace elements which could have undergone chemical reactions during the continuing cycles of freezing, thawing, rainfall, and evaporation. In this event, such compounds would tend to remain with the particles on the glass surfaces but would be washed through the filter surfaces, leaving the water-insoluble inorganic particulates retained on the filter relatively free of them. By such a mechanism, particles on glass would tend to have higher tensile strengths and be more aggregated than those on a filter. Hence, it is thought that for tracer studies on foundry effluents, it would be more advantageous to collect samples of particles on filters rather than on glass surfaces and subject them to a minimum amount of exposure. In this way, they would be collected relatively free of volatile organic and water-soluble components, which would prevent the formation of aggregates after particle collection. This would make

particle separation easier but, more importantly, would increase the accuracy of tracer studies by preventing the detection of aggregates which were not present in the atmospheric aerosol.

If one finally compares the data between the particles on filters separated 1) in phosphate at atmospheric pressure, 2) in Freon® at 50 psi, and 3) in Freon® at 100 psi, separation efficiencies of 64.3%, 82.8%, and 85.9% were measured respectively. It can be argued that the increases in separation efficiency in Freon® are not due to a more efficient separation, but due to comminution. To investigate such a possibility, scanning electron micrographs of the samples were scrutinized for evidence of fracture planes, severed cement bridges, etc. Particles were observed at 30,000X and typical examples are shown in Figure 65. No evidence of fracture was found, although the particle in Figure 65(f) does have a rather unusual angularity. No better method of investigating this phenomenon was thought to be available. On this evidence, it was concluded that virtually no comminution had taken place. When this hypothesis is combined with the fact that erosion of the probe was minimal in Freon®, it seems logical to assume that particle fracture would also be unlikely. Hence, the separation of particles in Freon® at 100 watts, 100 psi, at 30°C, for five minutes appeared to be a highly satisfactory separation method to use for the preparation of samples in tracer studies.



(a)



(b)



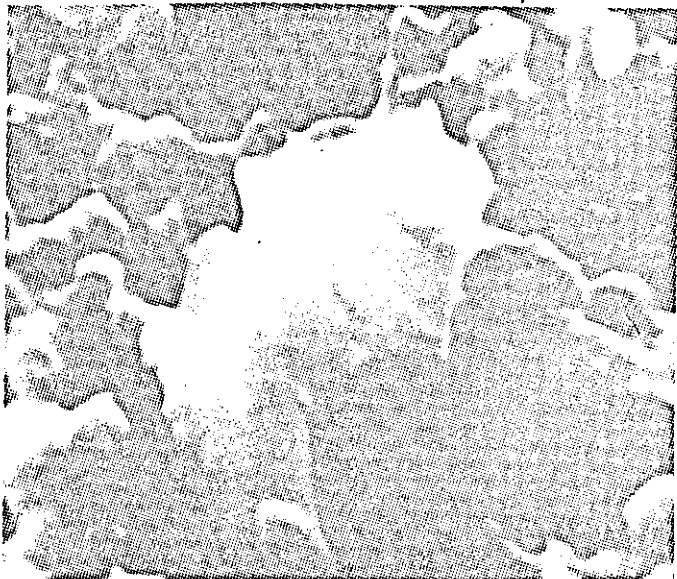
(c)



(d)



(e)



(f)

FIGURE 65

Typical Scanning Electron Micrographs of
Separated Particles Viewed at 30,000X

As a final comment, some prediction of the validity of the method for tracer studies would be beneficial. No extensive microprobe or X-ray measurements were made on the recollected particles on the filters as the real purpose of the thesis was to devise a satisfactory separation method to permit tracer studies to be performed. Such studies would contain sufficient work to be presented as a thesis in itself. However, fortunately, a very recent paper appeared in the journal "Atmospheric Environment", which was devoted to this subject.²³⁵ Gatz reported on the relative contributions of different sources of urban aerosols in the Chicago area, where incidentally the samples for this thesis were taken. To measure these contributions, two kinds of information were required: 1) the detailed chemical composition of each emission and 2) the detailed chemical composition of the urban aerosol. Such data were obtained by the chemical analysis of filter samples, not by individual particle analysis, but by total chemical elemental analysis of the whole filter.

Gatz suggested that the percent P_i of any element i in the aerosol was given by

$$P_i = \sum_j \alpha_{ij} \cdot p_{ij} \cdot C_j$$

where p_{ij} = % of element i in particulate matter emitted from source j

C_j = fraction of the aerosol sample contributed by source j

α_{ij} = coefficient of fractionation

Six main sources of man-made aerosols were listed for the Chicago area:

- 1) Coal burning
- 2) Coke production
- 3) Fuel oil burning
- 4) Automotive fuel burning
- 5) Iron and steel manufacture
- 6) Cement manufacture

Only iron and steel manufacture is of interest to this thesis on the basis of a foundry effluent study, so only this will be discussed.

The element Fe was selected as the tracer element for the iron and steel industry effluents, and from published data in the literature, the source coefficient C_j was estimated to be 3.9%. This meant that the iron and steel industry contributed 3.9% of the iron to the Chicago urban aerosol. To follow the path of any plume from the steel industry, a series of filter samples were taken at various locations in the Chicago metropolitan area and the elemental iron determined. Figure 66 shows the distribution of the source coefficient for iron. The variation of the coefficient had a range from 3% at Station C to 8% in the central shaded location, but a rather uniform distribution was seen to extend over the remainder of the city. The sampling site for the filter and glass samples analyzed in this thesis is shown on this figure.

Although the purpose of the work reported in this thesis was to develop and test a separation method for agglomerated aerosols and not to conduct tracer studies, it appeared logical to test the procedure so as to demonstrate that it can be applied in practice as an essential preliminary to tracer studies. An X-ray scan of one filter was therefore performed under the SEM. Only elemental iron was detected, but it was detected particle by particle over a total of 50 particles. The results are given in Table 23. It was found that traces of iron were present in every particle, but that large amounts were found in approximately one in nine particles. Finally, the total iron content of the particles on the filter was measured and found to be 4.1% of the total particulate mass. In comparing this to the data of Gatz²³⁵, it was found that the iron content was considerably lower than the figure of 7.1% reported for the same sampling location, but, meteorological differences could account for these variations. In consequence, the data show that the separation method is useful to prepare particles for tracer studies and, moreover, has distinct advantages over the method reported by Gatz²³⁵. For example, to predict the source coefficients, Gatz reports that the background aerosol composition and elemental analysis have to be accurately known. However, sudden wind changes can increase the wind-blown soil content of an aerosol, which will increase the elemental iron content of the sample. This could not be accounted for by total filter sampling, with the result that the tracer study would indicate an erroneous value for the iron emission. By use of a particle separation method, followed by a particle by particle scan, this background can be constantly

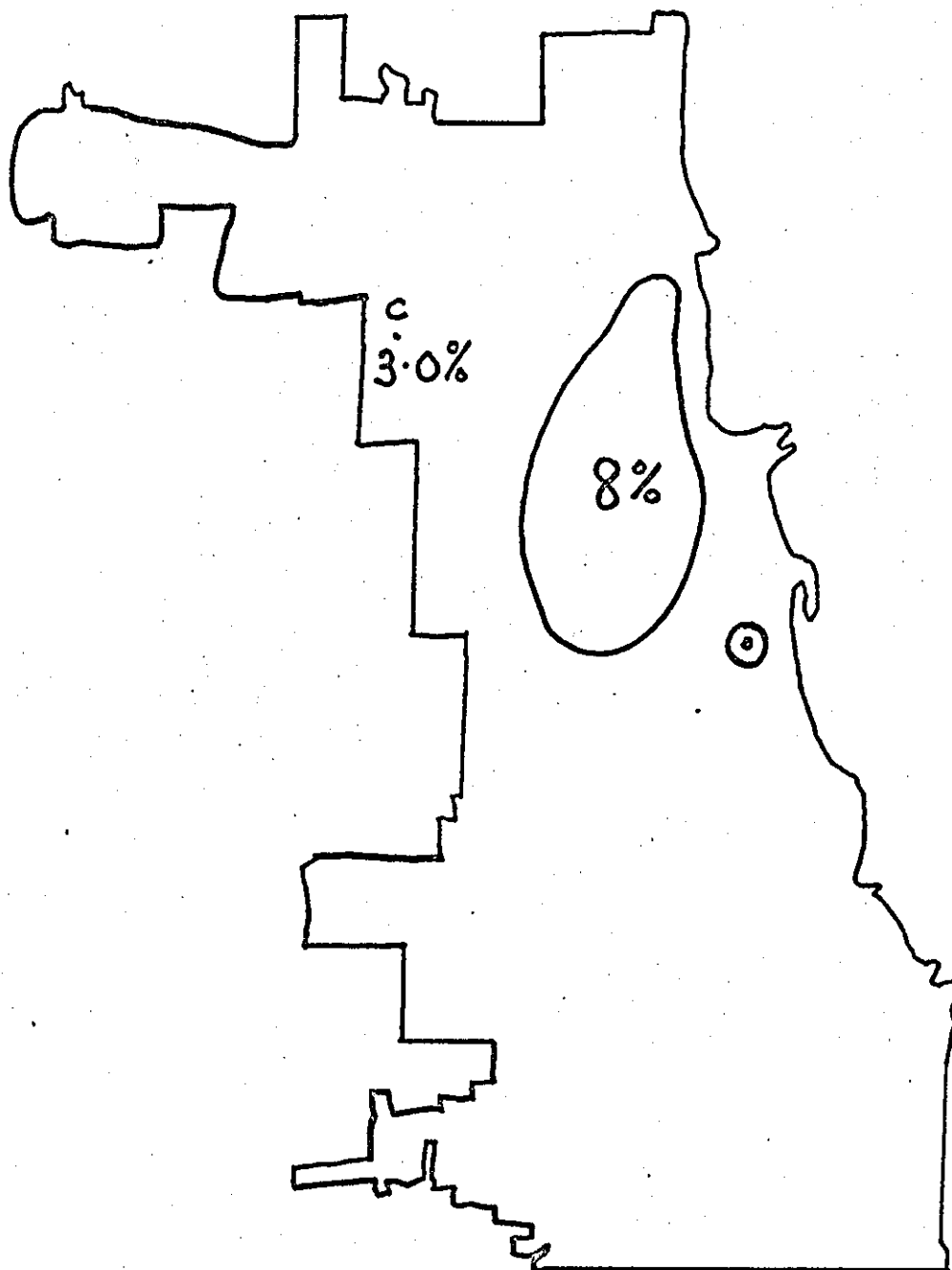


Fig. 66 - Distribution of Elemental Iron in the
Chicago Metropolitan Area (Gatz²³⁵)

⊙ Sampling Station

eliminated by use of a combination of tracer elements. For example, foundry emissions consisting of iron oxide particles would exhibit a high iron content in each particle and low concentration of other elements. Wind-blown soil would be rich in silica, alumina, iron, and other elements, which should enable an analyst to distinguish such soil from nonoxide particles. Hence, particle by particle scans would be superior to filter sampling for the purpose of particle tracer studies. However, such particle scans would be impossible without good separation procedures, and for the above reasons, it is felt that tracer studies would be more accurate using particle by particle scans and the separation procedure developed in this thesis will enable such studies to be performed.

4. SUMMARY AND CONCLUSIONS OF THE THESIS

4.1 Summary

On the average, about 1.6 billion tons of particulates are emitted or formed in the atmosphere each year as a result of both natural and man-made discharges. Of these, wind-blown soil, sea salt, sulphur, nitrogen and hydrocarbon complexes, ammonium sulphate and nitrate, carbonaceous matter, biological debris, metal oxides, trace metals, and extraterrestrial magnetic and radioactive compounds are the most common particulates present. (Chapter 2, Section 3)

During the last century, particles from man-made sources were emitted in such large quantities that they began to adversely affect animal and plant life. This induced the formation of, first, national, and, more recently, global, air pollution monitoring programs. To study the effect of world-wide pollution on the biosphere, and to prevent the discharge of potentially dangerous effluents from any location in the world, was no easy task. It demanded a knowledge of every conceivable source and its emission factor, the formation of a series of emission standards for every discharge, a method capable of measuring deviations from these standards, a method of tracing and locating any unsatisfactory emission, and a system of punishing any offender. (Chapter 1)

For the purpose of global monitoring, particulates offered the best potential for use as permanent tracers

of the pollution sources, and because of their permanence, they could be used more effectively than gases to fingerprint an emission for an agency.

Unfortunately, the very processes which naturally cleansed the atmosphere of its particulate burden, i.e., rainfall, snowfall, gravitational settling, also cleansed the atmosphere of the tracer particles needed to fingerprint the emission. Further, when collected at ground level, the resultant particles appeared physically and chemically bonded into agglomerate, conglomerate, and aggregate structures which contained many discrete particles. Consequently, if one wished to use these particulates effectively as tracers, it was necessary to physically separate them into their independent particle units prior to analysis and identification. This was no simple matter as the agglomerates were held together by strong physical forces. No accepted method was available for this task, and so there was a distinct need for such a method if atmospheric tracer studies were to be effective. (Chapter 1)

The purpose of this thesis was, therefore, to develop a method of physically separating particulates into their discrete and aggregate populations for atmospheric tracer studies. However, the task of devising a method for the total and very complex atmospheric aerosol was considered beyond the scope of one thesis, and so a simpler particulate model was sought. An emission from a metals casting plant or foundry was investigated as one alternative. It

was found that if one simply considered the separation of the particles of a permanent nature, e.g., submicron water-insoluble metal oxides, then the foundry effluent was a good substitute for the atmospheric aerosol for the purposes of this thesis. (Chapter 2, Section 2.3.3)

However, it was also found that to separate an agglomerate consisting of such small particles it demanded a knowledge of the nature and magnitude of the forces binding the particles together. Then, from this knowledge, a method of applying a force equal to or greater than the binding force could then be devised and applied. Literature studies showed that the forces that bound small particles together were dependent on the size, shape, surface, and chemical composition of the particles. They also depended upon their areas of contact, surface roughness, surface temperature, and surface cleanliness. The attractive forces acting at any one time in air could be mechanical, Van der Waals, capillary, electrical, or valency and were dependent on the nature and conditions of the fluid in which they were suspended. (Chapter 2, Section 2.2)

For example, it was found that the interparticle attractive forces were significantly lower in liquids than in air. This was because strongly charged ions could be adsorbed into the particle or liquids producing a strong repulsive force; hence, by the use of conditioning agents, which supplied these ions, particles could be separated by relative low energy applications. (Chapter 2, Section 2.2)

With such particle fluid systems, separation methods including impeller mixing, micro-media milling and ultrasonics appeared to have potential applications (Chapter 2, Section 2.4.3).

Using the above findings, a multiphase experimental program was performed to investigate a suitable method of separation for the submicron foundry particles (Chapter 3).

First, the potentially useful conditioning agents were screened for suitability. An aqueous sodium pyrophosphate solution was found to be superior to organic solvents and surfactants and, in fact, other phosphate and silicate compositions (Chapter 3, Section 3.1.2). For this purpose, the use of such a conditioning agent, produced the highest surface charges, and the minimum force of adhesion values.

A quantitative measurement of the actual forces between submicron particles and surfaces was next obtained using a centrifugal technique.

The forces between iron oxide particles and surfaces consisting of nonoxide, silica, carbon and steel were determined. It was found that the force of adhesion between iron oxide particles and an iron oxide surface was lower than that between iron oxide particles and other surfaces, suggesting that agglomerates consisting of chemically similar particles should be easier to separate than conglomerates consisting of chemically dissimilar particles. These forces which were equivalent to 2.1×10^{-5} dynes

and 3.2×10^{-5} dynes respectively, represented the forces required to separate 50 percent of the particles from the respective surfaces, but it was estimated that a force of 10^{-3} dynes was required to separate 99.99 percent of the particles from all the surfaces (Chapter 2, Section 3.1.3).

Using this value, it was calculated that potential separation equipment would have to supply a stress of 0.15×10^8 dynes/cm² to the agglomerates in order to separate them. Impeller mixers were shown to supply slightly less shear than this, but sand-mills and ultrasonic probe devices were shown to be capable of supplying shear forces far in excess of this value (Chapter 3, Section 3.1.4).

Experimental measurements on the separation of alumina powder in aqueous pyrophosphate solution using these devices confirmed the above predictions. Impeller mixers were shown to separate large agglomerates of powder fairly well, but were later shown to be inefficient in separating submicron particles from filters and surfaces. As this was the principal method in which particles were collected from the atmosphere, impeller mixing was considered impractical for tracer studies.

Micro-media milling was also found to be impractical, but for a different reason. Fracture of the media occurred during separation and the resulting particles were found to have sizes comparable to the upper size range of the

atmospheric aerosol. In consequence, fractured particles would interface with any tracer studies performed on this upper size fraction.

The final device tested was a magnetostrictive ultrasonic probe. It was found that in phosphate solution, severe erosion of the probe occurred by cavitation.

This became more severe with an increase in pressure, power, temperature, and time. To circumvent this erosion, a mixture of Krytox® 157 and Freon® E-3 was used. This eventually proved to be the best media for separating submicron inorganic metal oxides. (Chapter 3, Section 3.2.6)

Actual atmospheric aerosol samples were then taken downwind of an iron foundry, and the particles collected on fibrous filters and plane glass surfaces. The particles on the fibers were exposed to ambient conditions for a maximum of four hours, while those on the glass were exposed for three months. (Chapter 3, Section 3.2.1)

Experimental measurements of the effect of ultrasonic power, applied pressure and liquid composition were made on these samples. Increased power and pressure was shown to improve the removal efficiency of particles from filters and glass surfaces, but in aqueous pyrophosphate solution they also increased the degree of erosion of the ultrasonic probe. In the Krytox® 157 - Freon® E-3 mixture, the removal efficiencies were slightly lower than in phosphate solution, but the

the erosion of the probe was significantly less (Chapter 3, Section 3.2.6). The particles removed from the filters and glass surfaces were examined for their degree of separation, by recollecting them in a 0-1 mm nucleopore filter and observing them under the SEM. An expression termed the separation efficiency was devised to compare the relevant degrees of separation of the particles.

This was defined as:

$$\frac{\text{Number of Discrete Particles/10,000X Magnification Field}}{\text{Sum of the Number of Discrete and Nondiscrete Particles /10,000X Field}} \times 100\%$$

(Chapter 3, Section 3.2.6)

Here a discrete particle was categorized as a unit particle free from any contact with neighboring particles. Conversely, a non-discrete particle was categorized as two or more particles in contact either by random chance or by interparticle physical or chemical forces.

The results were summarized in Table 22 (Chapter 3, Section 3). Firstly, it was found that higher separation efficiencies were obtained with particles from the filter than from glass. This was true in both phosphate and Freon® media. The particles on glass were observed to be more amorphous, larger in size, more aggregated and less separated than those in filter, and their lower separation efficiency was thought to be a consequence of their long exposure to the atmosphere during the sampling period. Filtration was thought to collect particles relatively free of volatile organic and water soluble

components which were thought to be the source of the cement bridges in the aggregate structure. Hence for inorganic oxide particle tracer studies, filtration with a minimum exposure to the atmosphere was thought to be the better method of particle collection (Chapter 3, Section 3).

Secondly, separation in Freon® was superior to separation in phosphate, as erosion of the ultrasonic horn was suppressed. Cavitation was thought to be the cause of the erosion, and the properties of the Freon® liquid minimized the cavitation attack (Chapter 3, Section 3).

Thirdly, when the data between the particles on the filters separated at increasing power and pressure in both phosphate and Freon® were compared, the separation efficiency increased to a maximum under the conditions of 100 psi, 100 Watts, 30°C, for five minutes in Freon®. Examination of the particles separated under these conditions showed no indication of comminution, so it was confirmed that only physical bonds had been separated by the process. This meant that only agglomerates had been separated, and further that they had been separated with an efficiency of 85.9%.

Brief tests were finally made to indicate the usefulness of the separation method for tracer studies. A particle-by-particle scan of a foundry effluent separated under the above conditions showed that one in nine particles

contained high concentrations of iron, and that the total iron content of the filter was 4.1%. Though slightly lower than the reported figure for the same location in Chicago, the value of 4.1% could be accounted for by changes in wind direction. As a result, it was suggested that the method of separation followed by a particle-by-particle scan appeared not only satisfactory for tracer studies, but appeared superior to the method reported in the literature. This was because particle-by-particle scans provided a means of continually correcting for fluctuations in the background aerosol nature and composition which chemical analyses of filters could not do. (Chapter 3, Section 3)

Further, the method of separation in Freon® offered the potential for separation not only inorganic water insoluble particles, but water-soluble particles also. This was not investigated but was suggested as a topic for future study.

4.2 Conclusions

1. Atmospheric aerosols are a complex mixture of natural and man-made particles.
2. Worldwide pollution control of man-made sources requires a knowledge of every particulate source, its emission factor, the development of a series of international emission standards, a method capable of measuring deviations from these standards, a method of tracing and locating unsatisfactory emissions and a system of punishing each offender.

3. Particulates offer the best potential for use as permanent pollution traces for man-made sources.
4. When collected at ground level, particulates include a wide range of compositions and unfortunately appear in the agglomerated state.
5. For effective tracer studies these agglomerates have to be physically separated by species prior to chemical and physical analysis.
6. Here separation involves the removal of the agglomerates from the collection surface, their break-up into discrete particles and aggregates, their stabilization to prevent reagglomeration, and their recollection in the separated state in such a manner that an analyst can chemically identify each particle and measure its physical characteristics.
7. The purpose of this thesis was to develop a separation method for submicron inorganic oxide particles found in iron foundry emissions.
8. It was found that such particles could be collected at ground level by high volume filtration and gravitational sedimentation. However, when subjected to severe exposure to the winter climate, the particles became more aggregated and difficult to separate.
9. It was found that the collected agglomerates could be best removed from these surfaces by the application of ultrasonic energy in a mixture of Krytox® 157 - Freon E-3, the most suitable conditions being 100 watts 100 psi 30° for 5 minutes.

10. These conditions were found to physically break-up the agglomerates into their discrete and aggregate populations without evidence of comminution.
11. The samples collected on the filter under the conditions of minimum exposure to the winter climate, yielded the highest separation efficiency of 85.9%.
12. This efficiency was determined from a count of the discrete and nondiscrete particles after their re-collection on a 0.1 μ m Nuclepore filter.
13. This specific filter was found to be highly suitable for the measurement of the physical and chemical properties of the particles; and is recommended for particulate tracer studies.
14. Size analysis was simply performed by particle count on a series of scanning electron photomicrographs of the filter at 10,000X magnification, and, with the sample under the S.E.M., chemical analysis was performed using a scanning x-ray source.
15. A particle by particle scan of the filter was easily performed using the element iron as the tracer element. One in nine particles revealed a high concentration of iron in its structure, and the total iron content of the whole filter was found to be 4.1%. This agreed fairly well with past total iron compositions reported for the Chicago Metropolitan area.

16. Such a scan was also shown to be superior to past techniques, because fluctuations in the background aerosol composition can be continually accounted for.
17. Hence, the method of collection, separation, recollection and analysis developed in this thesis was shown to be a most suitable technique for particulate tracer studies.

5. RECOMMENDATIONS FOR FURTHER WORK

5.1 Hydrogen-Bonding Series

The work begun to investigate the dispersion of different oxides in pure solvents showed that significant differences in behaviour occurred with each oxide. It appeared that surface charge or the degree of hydroxylation of the oxide could account for some of the variations. This should be studied further. In addition, the anomalous behaviour of esters was not explained conclusively. This too should be studied. Such an investigation could lead to a successful classification of powders by their hydrogen-bonding potential. The results of such a classification could be useful in particle size analysis, paint technology, and, in fact, any process in which particle dispersion is a factor.

5.2 Cavitation

The study on the behaviour of ultrasonic power in aqueous phosphates and fluorohydrocarbons should be extended. Explanations for the degree of erosion observed in aqueous phosphate solutions should be sought. It is thought that if cavitation can be reduced, for example, by the development and use of stronger metal alloys for the probe material, that better separation could be obtained in phosphate media.

5.3 Extended Fluorohydrocarbon Studies

The controlled study of the effect of power, pressure, temperature, and time on the separation of a metal

powder should be repeated using Krytox® 157-Freon® E-3 instead of aqueous phosphate. For the limited experiments conducted in this thesis, 100 Watts and 100 psi were adequate, but they can possibly be exceeded without erosion to yield even higher separation efficiencies than 85.9 percent. This should be investigated.

5.4 Studies with Water-Soluble Particles

A controlled study of the effectiveness of separating water-soluble particles by the method above should be investigated. Particles such as submicron nitrates and sulphates should be studied. Very recently, there has been growing interest in the role of ammonium sulphate in atmospheric chemistry. The separation method offers the potential of investigating both the concentrations of the compound in man-made emissions and its rate of formation and concentration in the atmosphere. In addition, the method could be used for investigating the behavior of larger water-soluble particulates such as chlorides and bromides.

5.5 Studies with Other Emissions

Tracer studies should now be extended to different emission, and x-ray data taken to identify each species. For example, Gatz²³⁵ suggested that the obvious choices for tracer elements for the auto, cement, and fuel oil emissions are lead, calcium, and vanadium respectively. Lead makes up 40% of the auto emission, and calcium 44% of the cement industry emission. Bromine is also suggested as an alternate for lead in auto emission tracer studies, as this is specific for this discharge.

Vanadium, on the other hand, makes up only 2.5% of its source emission, but it has the advantage that fuel oil is its only major source. ²³⁵ In selecting iron as a tracer for the foundry and steel mills emissions (having a 39% abundance), Gatz concedes that it is a major constituent of other sources, and perhaps manganese should be coupled with iron as a steel mill emission tracer. However, for most purposes; iron is satisfactory.

The most difficult selection of tracers is for the coal and coke industry. Aluminum is abundant in ash, but is likewise abundant in windblown soil. However, potential elements such as Potassium, Lanthanum and Scandium have possibilities as specific soil tracer elements.

It may be that certain emissions will be best fingerprinted by a specific series of tracer elements, and that emission monitoring will then depend on a form of pattern recognition.

It is obvious that there is much work needed in the development of tracer particles for emission identification, and investigations in this field certainly promise to be highly interesting and rewarding.

5.6 Studies with an Atmospheric Aerosol

The studies should be finally extended to actual atmospheric aerosols and be used to separate and identify the above species in various geographical locations.

With the potential of separating and analysing both water soluble and water insoluble species, the particulate nature of various geographical locations can be studied.

Tracer studies of this kind would be beneficial not only in global pollution monitoring, but in atmospheric research too.

6. ACKNOWLEDGEMENTS

I wish to thank Professor D. C. Freshwater for his encouragement and guidance during this investigation. In addition, I wish to thank Professor D. T. Wasan, my external supervisor, for his many helpful discussions during the past three years.

The fundamental ideas behind this thesis were developed during the fulfillment of a recent U. S. Air Force contract, F33657-71-C-0859, on which I was Project Leader. The experience gained on this contract and the separation device developed were crucial to the performance of this work, and the Project Officer, Major R. N. Park, is acknowledged for his assistance and guidance on this contract.

Further, I acknowledge the assistance of Madhav B. Ranade both in the design and operation of the centrifuge during the force of adhesion studies and in the design of the separating unit. I also wish to thank J. Puretz for taking some of the raw data during the separation studies.

Dr. Om Johari is acknowledged for his SEM work, and Dr. F. Bock is acknowledged for the statistical design and analysis of the data in the controlled experiment.

Finally, I wish to thank Helen Brown for typing the final manuscript, because without this there would have been no thesis.

7. REFERENCES

1. Ross, S. R., Chemical Engineering Deskbook, May 1972
2. White, L. J., Chemical Engineering Deskbook, May 1972
3. Lee, R. E., Goranson, S. U.S.E.P.A. Publication No. AP-108, 1972
4. Lee, R. E., Science 178 (4061) 567, 1972
5. Anon, U.S.E.P.A. Report PB 227-059, 1973
6. Anon, Pollution Control Technology, Research & Education Association, New York, NY, 1974
7. Burchard, J. K., J. Air Pollution Control Assoc. 25 (2) 99, 1975
8. McLellan, A., U.S.E.P.A. Report 650-74-116, Contract 68-02-1308, 1974
9. Davies, C. N., Atmospheric Environment, 8 1069, 1974
10. Morgan, G. B., Bretthausen, E. W., Melfi, S.H., Instrum. Tech. 21 (2) 27, 1974
11. Environmental Sci & Technol, 9 (3) 207, 1975
12. Lundholm, B., Svenson, S., Bulletin 10, Swedish National Research Council, 1970
13. Wallen, C.C., Environ Sci & Technol, 9 (1) 31, 1975
14. Lee, R. E., Caldwell, J., Akland, G.G., Atmos. Environ., 8 1095, 1974
15. Georgii, H. W., Berichte d. Dt. Wetterd., 14 (100) 23, 1965
16. Lieberman, A., Hydraulics and Pneumatics, October 1974
17. Davies, R., et al, Bull. Parenteral Drug Assoc. March 1975
18. Draftz, R., Graf, J., Proc. Air Pollution Control Association Meeting, Denver, CO, 1974
19. Gerstner, W. J., Oil & Colour Chem. Assoc., 49 954, 1966
20. Rumpf, H., "Agglomeration", "Strength of Granules and Agglomerates", Editor - W. A. Knepper, J. Wiley & Sons, 1962

21. Davies, R., USAF Report A005-1, Literature Survey, Contract 33657-71-C-0859, October 1971
22. Zimon, A. D., Adhesion of Dust & Powder, Plenum Press, New York, 1969
23. Green, H.L., and Lane, W.R., Particulate Clouds, Dusts, Smokes, and Mists, VanNostrand, 1957
24. Allen, T., Particle Size Measurement, Chapman & Hall, Ltd., 1968
25. Herdan, G., Small Particle Statistics, Butterworth Press, 1960
26. Corn, M., Adhesion of Particles, Aerosol Science, Acad. Press, 1966
27. Deryaguin, B.V., Zimon, A.D., Kolloid, Z., 23 544, 1961
28. Kordecki, M.C., Orr, C., Amer. Med. Assoc. Archives, Ind. Health, 1 (1) 1960
29. Böehme, G., et al, Z. Angew. Phys. 16 (6) 486, 1964
30. Davies, R., Powder Technology, 12.(2) 111, 1975
31. Meldau, R., Handbuch der Staubtechnik 1., Dusseldorf, 1956
32. Zimon, A.D., Volkova, T.S., Kolloid, Z., 27 (3) 365, 1965
33. Corn, M., J. Air Pollution Control Assoc., 11 523, 1961
34. Corn, M., J. Air Pollution Control Assoc., 11 566, 1961
35. McFarland, J., Tabor, D., Proc. Royal Soc., A220 (1069) 224, 1950
36. Howe, P.L., et al, Canadian J. Chemistry, 33 (9) 1375, 1955
37. Gregg, S.J., Surface Chemistry of Solids, Chapman & Hall, 1965
38. Seitz, F., Theory of Solids, McGraw Hill, 1940
39. Mott, N.F., Jones, H., Theory of Metals and Alloys, Oxford Univ Press, 1940
40. Stone, F.E., Chemistry of the Solid State, Butterworth Press, London, 1955

41. Gray, T.J., The Defect Solid State, Interscience Publishers, 1955
42. Wright, D.A., Semiconductors, Methuen Press, 1958
43. Cottrell, A.H., Dislocation and Plastic Flow in Crystals, Oxford Univ Press, 1953
44. Reid, T.A., Dislocation in Crystals, McGraw Hill, 1953
45. Ross, S., Oliver, J.P., Physical Adsorption, Interscience Publishers, 1964
46. Gregg, S.J., Sing, K.S.W., Adsorption, Surface Area and Porosity, Academic Press, 1967
47. Parfitt, G.D., "Dispersion of Powders in Liquids", Elsevier Press, 1969
48. Krzyt, H., Colloid Science, Volumes 1 & 2, Elsevier Press, 1949
49. Verwey, E.J.W., Overbeek, T.G., Theory and Stability of Lyophobic Colloids, Elsevier Press, 1948
50. Bowden, V.P., Tabor, D., Friction and Lubrication in Solids, Clarendon Press, 1964
51. Krupp, H., "Particle Adhesion, Theory and Experiment", Advances in Colloid and Interface Science, Edition 1, J. Wiley & Son, 1967
52. Zimon, A.D., Deryaguin, B.V., Kolloid, A., 25 (2) 159, 1963
53. Fuks, G.I., et al, Doklady, Akad, Nauk, SSSR 65 (3) 307, 1959
54. Zimon, A.D., Kishin, N.G., Kolloid, Zh., 27 (5) 685, 1965
55. Taylor, A., Wood, F., Trans Farad Soc., 53 (4) 523, 1956
56. Junge, C.E., Air Chemistry and Radioactivity, Academic Press, New York, 1963
57. Goldberg, E.D., Gross, M.G., Atmospheric Dust - The Sedimentary Cycle & Men, Geophysics Earth Sciences
58. Robinson, E., and Robbins, R.E., Emissions, Concentrations and Rate of Particulate Emissions, Final Report SCC-8507, Stanford Research Institute, 1971

59. Peterson, J.T., and Junge, C.G., Sources of Particulate Matter in the Environment, MIT Press, 1971
60. Hidy, G.M., and Brock, J.R., Assessment of Global Resources of Tropospheric Aerosols, Ind. Int. Clean Air Congress, Washington, DC, 1970
61. Mitchell, J.M., Global Effects of Environmental Pollution, Reidel Publishing Co., 1970
62. Hidy, G., Assessment of Airborne Particles, C.C.Thomas, Springfield, IL, 1972
63. Shannon, L.J., et al, Assessment of Small Particle Emissions, Midwest Research Institute Report No. 425, 1970
64. Israel, H., Israel, G.W., Trace Elements in the Atmosphere, Ann Arbor Science, 1974.
65. Davies, C.N., Aerosol Science, Academic Press, London and New York, 1966
66. Reist, P.C., Small Particles in the Atmosphere, AIChE Symposium Series 70 (137) 262, 1974.
67. Sheasley, D.C., et al., Proceedings of Symposium on the Environment in Amazonia, Part I, Measurement of Particles in the Non-Urban Atmosphere, Instituto Nacional de Pesquisas de Amazonia, Manaus, Brazil, 1970
68. Sood, S.K., and Jackson, M.R., Proc. Symposium on Precipitation Scavenging, US Atomic Energy Commission, Richland, WA, 1970
69. Kerker, M., et al., Scavenging of Aerosol Particles by a Falling Water Drop and Calculation of Washout Coefficients, Proc. Symposium on Precipitation Scavenging, US Atomic Energy Commission, Champaigne, IL, October 1974
70. Houghton, H.G., Compendium of Meterology, Edited by T. Malone, Boston American Meterol. Soc., 1951
71. Goetz, A., Pueschel, R., Atmos. Environ., 1 287, 1967.
72. Sears, P.B., American Scientist, New Haven, 52 (1) 1-15, March 1964
73. Flanigan, D.F., DeLong, H.P., Applied Optics, 10 (1) 51, 1971
74. Prospero, J.M., Bonatti, E., J. Geophys. Res. 74 3362, 1969

75. Fergusen, W.S., et al, J. Geophys. Res., 75 (6) 1137, 1970
76. Kashina, V.I., Akademia Nauk Kazakhskoi SSR, Alma-Ata Astrofizicheskii Institut, Trudy 3. 115, 1962
77. Prospero, J.M., et al, Earth Planet Sci. Letters, 9 (3) 287, 1970
78. Friend, J.P., 162nd Natl. ACS Meeting, Washington, DC, April 1970
79. Cadle, R.D., Allen, E.R., Science, 167 243, 1970
80. Urone, P., Schroeder, W.H., Environmental Science and Technology, 3 (5) 436, 1969
81. Heard, M.J., and Wiffen, R.D., Atmos. Environ., 3 337, 1969
82. Lodge, J., and Frank, E., Journal de Recherches Atmospheriques, 140, 1966
83. Good, A., and Thynne, J.C.J., Trans Farad Soc., 63 (11) 2708, 1967
84. Quon, J.E., et al, Intl. Clean Air Congress, Washington, DC, 1970
85. McKay, H.A.C., Atmos. Environ., 5 (1) 7, 1971
86. Kimura, K., et al, Rodo Kagaka, 41 (10) 501, 1965
87. Goetz, A., Pueschel, R., Atmos. Environ, 1 287, 1967
88. Smith, B.M., Wagman, J., Environ. Science and Technology, 3 558, 1969
89. Urone, P., et al, Environ. Science and Technology, 2 611, 1968
90. Lodge, J. and Pate, J., Science, 153 408, 1966
91. Junge, C., Scheich, G., Atmos. Environ, 5 165, 1971
92. Eggleton, A.E.J., Atmos. Environ, 3 (3) 355, 1969
93. Dingle, A.N., Joshi, B.M., Atmos. Environment, 8 1119, 1974
94. Pate, J.B., et al, Symposium on Environment in Amazonia, III, June 1971
95. Stephens, E.R., Advances in Environmental Science, 1. 119, 1969

96. Went, F.M., Proc. Nat. Acad. Sci. 46 212, 1960
97. Went, F.M., Tellus, 18 (2) 549, 1966
98. Spengler, C., Haupt, G., Erdoel Kohle (Hamburg), 22 (11) 679, 1969
99. Semenov, A.D., et al, Doklady Akad Nauk SSR, 173 (5) 1185, 1967
100. Tabor, E.C., Trans N. York Acad. Sci., 28 569, 1966
101. Stanley, C.W., et al, Environ. Science and Technology, 5 430, 1971
102. Niki, H., et al, Mechanisms of Smog Formation, Advances in Chemistry, ACS No. 113, 1972
103. Whitby, K.T., Air Pollution Control Office Publication No. A PTD-0630, November 1970
104. Harris, F.S., Paper 70-146, Air Pollution Control Assoc. Meeting, St. Louis, MO, 1970
105. McPhee, R.D., Bokian, A.H., J. Air Pollution Control Assoc., 17 580, 1967
106. Murthy, Gh, V.R., et al, Proc. Int. Conf. on Cloud Physics, Tokyo & Sapporo, 67, 1965
107. Laamanen, A., Work. Environ. Health, 6 (1) 23, 1967
108. Kneip, T.J., et al, J. Air Pollution Control Assoc., 20 (3) 144, 1970
109. Junge, C.E., Large Scale Distribution of Micro-organisms in the Atmosphere, Proc. Atmos. Biological
110. Akerman, H., Rev. Canadian Biol. 27 (1) 61, 1968
111. Reifferschied, H., Deutscher Wetterdienst Berichte, 12 (91) 92, 1963
112. Reddi, C., Acta Allergol 25 (2) 189, 1970
113. Wright, T.J., et al, Viable Organisms in Urban Atmospheres, Proc. 61st APCA Symposium, Univ. of Minnesota, June 1968
114. Lee, R.E., VonLehmden, D.J., J. Air Pollution Control Association, 23 (10) 853, 1973
115. Burt, R., Thomas A., Phil. Trans. Series Math & Phys. Sciences, 307 (1489) 183, 1968

116. Yamate, G., US EPA Contract 68-02-0641, Final Report, 1973
117. Atkins, P.R., J. Air Pollution Control, 19 (8) 591, 1969
118. Daines, R.H., et al, Environmental Science and Technology, 4 (4) 318, 1970
119. Jepson, A.F., Proc. 162nd Natl. ACS Meeting, Washington, DC, 1971
120. Kothny, E.L., Proc. 162nd Natl. ACS Meeting, Washington, DC, 1971
121. McMullen, T.B., et al, J. Air Pollution Control Assoc., 20 (6) 369, 1970
122. Hasagawa, T., et al, Proc. 10th Annual Meeting of Japan Society of Air Pollution, 1969
123. Rancitelli, L.A., et al, Proc. Symposium of Precipitation Scavenging, Richland, WA, 1970
124. Rosinski, J., J. Atmos. and Terr. Physics, 32 805, 1970
125. Marchesani, V.J., et al, J. Air Pollution Control, 20 (1) 19, 1970
126. Bashforth, G.R., Manufacture of Iron and Steel, Chapman & Hall, 1948
127. Teichert, E.J., Introduction to Ferrous Metallurgy, McGraw Hill, 1944
128. Begeman, M.L., Foundry Practice, Manufacturing Processes, 4th Edition, Wiley & Sons, NY, 1957
129. Particulate Pollutant Systems Study, US E.P.A. Reports, I, II, III on Contract CPA-22-69-104, 1969
130. DeGarmo, E.P., Materials and Processes in Manufacturing, MacMillan Press, NY, 1974
131. Gould, D.G., American Foundryman's Dictionary, AFS Society, Des Plaines, IL, 1968
132. Engels, G., Weber, E., Cupola Emission Control, Gray and Ductile Iron Founders Society, Cleveland, OH, 1967
133. Air Pollution Engineering Manual, Public Health Service Publication 999-AP-40, 1967
134. Foundry Air Pollution Control Manual, AFS, DesPlaines, IL, 1967

135. Kane, J.M., Foundry, November 1968
136. McIlvaine, R.W., J. Air Pollution Control Assoc. 17, August 1967
137. Shaw, F.M., Foundry Trade Journal 217, August 1956
138. Muller, W.C., Proc. 3rd International Clean Air Conf. Dusseldorf, 1973
139. Engels, G., Giesserei, 60 (9) 597, 1973
140. Weber, J.H., J. Air Pollution Control Assoc., 20 (2) 67, 1970
141. Woodcock, K.R., Barrett, L.B., J. Air Pollution Control Assoc., 20 (2) 72, 1970
142. Campbell, D.S.E., Cathcart, D., and Giles, C.H., J. Soc. Dyers and Colorists, 73, 546, 1957
143. Long, J.S., et al, Official Digest, 11, January 1963
144. Trudgian, L., Prihoda, H., Official Digest, 1211, November 1963
145. Burrell, H., Official Digest, 726, October 1955
146. Lieberman, E.P., Official Digest, 30, January 1962
147. Gardon, J., J. Paint Tech., 38 (492) 43, 1966
148. Crowley, J. D., Teague, G.S., and Lowe, J.W., J. Paint Tech., 38 (496) 269, 1966
149. Crowley, J.D., Teague, G.S., and Lowe, J.W., J. Paint Tech., 39 (504) 19, 1967
150. Hansen, C.M., J. Paint Tech., 39 (505) 104, 1967
151. Hansen, C.M., J. Paint Tech., 39 (511) 505, 1967
152. Lee, L.H., J. Paint Tech. 42 (545), 365, 1970
153. Eissler, R.L., Zgol, R., and Stolp, J.A., J. Paint Tech. 42 (548), 483, 1970
154. Every, R.L., Wade, W.H., and Hackerman, N., J. Phys. Chem., 65 937, 1971
155. Wade, W.H., and Hackerman, N., J. Phys. Chem. 66, 1823, 1962
156. Wade, W.H., and Hackerman, N., J. Phys. Chem., 65, 1681, 1961

157. Parfitt, G.D., and Wilshire, I.J., J. Phys. Chem., 12, 3545, 1964
158. Day, R.E., and Parfitt, G.D., J. Phys. Chem., 71, 815, 1967
159. Livanova, N.M., et al, Kolloid Zhurnal, 31 (6) 875, 1969
160. Masaji, M., et al, J. Sci. Hiroshima Univ. Ser A-II, 30, 57, 1966
161. Krupskii, N.I., et al, Ionites and Ion Exchange, Nauka 139, 1966
162. Ermolaeva, T.A., et al, Lakakrasochnye Materialy i Ikh, Primenerie, (3), 14, 1964
163. Dickman, S.R., et al, Soil Science, 52, 263, 1941
164. Kelley, J.B., et al, Soil Science, 55, 167, 1943
165. Vissers, D.R., J. Phys. Chem., 72 (9) 3236, 1968
166. Low, M.J.D., and Ramamurthy, P., J. Phys. Chem., 72 (9), 3161, 1968
167. Bellamy, G., Infra Red Spectra of Complex Molecules, p. 319, J. Wiley & Son, NY, 1960
168. Wade, W.H., and Hackerman, N., J. Phys. Chem., 64 1196, 1960
169. Bakker, W.T., and Bartok, D., Am. Ceram. Soc. Bull., 45 (6) 582, 1966
170. Peri, J.B., J. Phys. Chem., 72 (8), 2917, 1968
171. Tokiwa, F., and Imamura, T., J. Am. Oil Chem. Assn., 46, 572, 1969
172. Wnek, W., PhD Thesis, Illinois Inst Tech., 1973
173. Schubert, H., and Wibowo, W., Chemie Ingenieuer-Technik, 42 (8) 541, 1970
174. Beischer, D., Kolloid-Z., 89 (2): 214, 1939
175. McFarlane, J., and Tabor, D., Proc. Roy. Soc., A220 (1069):224, 1950
176. Krupp, H., J. Colloid and Int. Sci., 24 (1):170, 1968
177. Böhme G., Krupp, H., Rabenhorst, H., and Sandstede, G., Trans. Inst. Chem. Eng., London, 40, 252, 1962

178. Böehme, G., Kling, W., Krupp, H., Lange, Sandstede, G., and Walter, G., Preprint, Intern. Congr. Surface Activity, 4th Brussels, 1964, paper B/III.16
179. Böehme, G., et al, Z. Angew, Phys., 16, 486, 1968
- 180.) Böehme, G., et al, Angew, Phys., 19, 265, 1965;
- 181.) through Phys. Abstr., 69, 48, 1966
- 182.) Krupp, H., and Angew, Z., Phys., 19, 259, 1965;
- 183.) through Phys. Abstr., 69, 4832, 1966
184. Deryagin, B.V., Toporov, Yu. P., and Aleinikov, I.N., ibid., 26, 335, 1964
185. Deryagin, B.V., Zimon, A.D., and Kolloid, Z., 23, 454, 1961
186. Corn, M., and Stein, F., Nature 211, 60, 1966
187. Fuks, N.A., and Sutugin, A.G., Generation and Use of Monodisperse Aerosols Given in "Aerosol Science", C.N. Davies, Acad. Press, 1966
188. Carlin, B., "Ultrasonics", McGraw-Hill (1949)
189. Neduzhii, S.A., Soviet Physics-Acoustics (Engl. Transl.) 7, to 221, 1962
190. Egorov, P.A., Colloid, J., USSR (Engl. Transl. 33, 696, 1971
191. Pohlman, R., Werden, B., Marziniak, R., Ultrasonics, 10, 156, 1972
192. Fridman, V.M., Ultrasonics, 10, 162, 1972
193. Brodov, et al, Poluch Svoistra Primen Tonkikh. Metal. Porosch Dokl., Vses Conf., 113, 1970, C.A. 76, 116809, 1972
194. Holl, P., Proc. Int. Symp. Particle Technol., IITRI, August 1973
195. Satoh, T., Yamane, I., Nippon Dojo-Hiryogaku Zasshi, 43, 41, 1972
196. Kaiser, R., "Particle Dispersion Studies". Final Report on USAF Contract F33657-72-C-0388, August 1973
197. Agabal'yants, E.G., et al, Dopov. Akad. Nauk Ukr. RSP. Ser. B, 32 (9) 813, 1970
198. Lowe, L.E., and Parasher, C.G., Can. J. Soil Sci. 51 (1) 136, 1971
199. Hislop, T., Ultrasonics, 8, 88, 1970

200. Cozzens, S.L., NPIRI Project Report 44, Lehigh Univ., 1960
201. Guggenheim, S., Official Digest, 30 (402), 729, 1958
202. Schlieser, R.H., et al, Official Digest 265, March 1962
203. Wade, W.G., and Taylor, B.A., Paint Manuf., 30, 355, 1960
204. Ensminger, R.I., Official Digest 71, January 1963
205. Dowling, D.G., J. Oil & Col. Chem. Assoc., 44, 188, 1961
206. Armstrong, W.G., J. Paint Tech., 41 (530) 179, 1969
207. Weisberg, H.E., Official Digest, 1261, November 1964
208. Daniel, F.R., J. Oil Col. Chem. Assoc. 54 84, 1971
209. Daniels, F.K., Natl. Paint Varnish Lacquer Assoc. Sci. Sect. Cir. 744, 1950
210. Shurts, R.B., Natl. Paint Varnish Lacquer Assoc. Sci. Sect. Cir. 745, 1950
211. Fischer, E.K., Colloidal Dispersions, J. Wiley & Son, NY, 1950
212. Bosse, D.G., Official Digest, 30 (398), 251, 1958
213. Brownlie, G., J. Oil & Col. Chem. Assoc. 43, 1960
214. Vavra, J., (FR) Efficiency of Dispersion in a Ball-Mill. Chim. Ind. GC 103 358 70 NO R N3 F5668
215. Mölls, H.H., and Hörnle, R., Third European Symp. on Comminution Cannes, 1971; Dechema Monograph 69, 1972
216. Garrett, M.D., and Hess, W.M., J. Paint Tech. 40 (524), 367, 1968
217. Weisberg, H.E., Official Digest, 1155, November 1962
218. Princen, L.K., Official Digest, 766, July 1965
219. Dintenfass, L., J. Oil & Colour Chem. Assoc., 41 125, 1958
220. Yashiro, Y., Nagoya & Kogyo, 9, 261, 1957
221. Matthews, V.A., Rhodes, C.T., J. Coll. & Int. Sci, 32 (2), 332, 1970

222. Sennett, P., Olivier, J.P., I&E.C., 57, 32, 1965
223. Riddick, T.M., Zeta Meter Inc., New York, 1968
224. Davies, R., Ranade, M.B., Werle, D., Proc. of 49th Int. Colloid Symposium, Clarkson Coll. of Technol., June 1975
225. Davies, R., Final Report, IITRI, C6239-A008 on USAF Contract F33657-71-C-0859, June 1974
226. Gordy, W., J. Chem. Physics, 7, 93, 1939
227. Gordy, W., J. Chem. Physics, 9, 204, 1941
228. Davies, C.N., Aerosol Science, 5 293, 1974
229. Bailey, A.L., et al, Friction & Lubrication of Solids III, Oxford Press
230. Rumpf, H., Herrmann, W., Aufbereitungs Technik, 11 (3) 117, 1970
231. Engels, K., Farbe und Lack, 71 375-385; 464-472, 1965
232. Knapp, R.T., Cavitation, McGraw Hill, 1970
233. Zerlaut, G., et al, Thermal Control Coatings for Space Vehicles, NASA Report 1967
234. Rumpf, H., Raasch, J., Proc. Env. Symposium on Comminution, p. 151, 1962
235. Gatz, D. F., Atmos. Environ., 9, 1-18, 1975
236. Koglin, B., Chem. Ing. Tech., 41, 1926, 1969
237. Wade, W.H., Hackerman, N., J. Phys. Chem., 64, 355, 1960
238. Every, R.L., Wade, W. H., Hackerman, N., J. Phys. Chem., 65, 937, 1961
239. Atherton, E., Cooper, A.C., Fox, M.R., J. Soc. Dyers & Colour, 80, 521, 1964
240. Beresford, J., J. Oil Colour Chem. Assoc., 50, 594, 1967

